Using conditioned media from adipose tissue derivatives and adipose-derived stromal cells to induce vascularisation for soft tissue wound healing

Alejandra Peñuelas Alvarez

Thesis submitted to the University of Sheffield for the degree of Doctor of Philosophy

Department of Material Science and Engineering

University of Sheffield

Abstract

Although different skin engineering strategies have been developed to help wound healing, crucial obstacles such as vascularisation have yet to be overcome. Fat-derived stromal cells have been shown to aid in wound healing through their ability to drive angiogenesis, increase protein production, and reduce inflammation. Whole adipose tissue can also be emulsified by passing it between two syringes to rupture adipocytes prior to reinjection, reducing the degree of adipocyte apoptosis and necrosis *in vivo*. If the emulsified fat is filtered and centrifuged to remove the oils, SVF-gel is generated. SVF-gel is easily handled and can be reinjected subcutaneously with small-bore needles. The regenerative potential of adipose tissue and its stromal cells may come from their derived secreted products. In this thesis, we tested and compared the pro-vascularisation properties of media conditioned using human adipose tissue, emulsified fat, SVF-gel, and cultured adipose-derived stromal cells (ADSC).

In order to study the angiogenic properties of adipose tissue, emulsified fat, SVF-gel and ADSC, it was important to characterise each of the formulations. Studying how processing affects adipose tissue structure, cell density and viability was essential to understand how the adipose tissue angiogenic properties varied with each formulation. DNA isolation and quantification were performed to approximately determine cell numbers were in each of the samples. Also, fluorescent staining of lipids, cell membrane, nuclei and endothelial cells, in combination with light sheet and confocal imaging were performed to study in detail the cellular structure of each formulation. It was possible to distinguish that, as adipose tissue was processed, more the disruption to its structure increased, while cell viability decreased.

Conditioned media from adipose tissue, emulsified fat and cultured ADSC were obtained after 3 days of culture. Human microvascular endothelial cells (HMEC-1 and HDMEC) were used to analyse the pro-vascularisation properties of the conditioned media. MTT reduction to formazan by viable cells was used to test if the conditioned media promoted endothelial cell proliferation; while a migration assay was used to study if conditioned media was also able to stimulate cell migration. LDH levels were measured in measured in conditioned media from each group to determine the level of cell death during its cultivation. Whilst these results did not show significant effects from the investigated tissue or ADSC on endothelial cells, further investigation was needed to measure the pro-vascularisation on more complex angiogenic models. In addition, it was also important a study of the factors released by the adipose tissue and its derivatives into the conditioned media was required.

In vitro pro-angiogenic potential of the conditioned media from adipose tissue, emulsified fat, SVF-gel and ADSC in a 3D environment was shown using endothelial

tube formation. SVF-gel exhibited improved pro-angiogenic properties compared to the other studied groups. Then, to test the conditioned media in a more complex model, *ex ovo* the chick embryo chorioallantoic membranes (CAM) were used to observe new blood vessel formation. Likewise, the chick aortic rings were used to study tubular structure formation promoted by conditioned media from adipose tissue and ADSC. In both cases, adipose tissue and SVF-gel conditioned media promoted a significant increase in angiogenesis. Finally, the secreted growth factors in each conditioned media were investigated using a cytokine array. Adipose tissue showed the highest growth factor profile with factors mainly related to inflammation, and promotion of cell survival. Emulsified fat presented a similar profile but in lower intensity than adipose tissue, followed by SVF-gel. In contrast ADSC secreted growth factors related to extracellular matrix remodelling. Our results illustrate the relative contributions direct and paracrine factors have on angiogenesis *in vitro* and demonstrate that adipose tissue and ADSC have the potential to improve vascularisation in future tissue engineered treatments.

Oral Presentations

“Using adipose tissue derivatives and adipose-derived stromal cells conditioned media to induce vascularization and soft tissue wound healing”. Future Investigators of Regenerative Medicine Conference 2019, Costa Brava, Spain

Poster presentations

“Effect of conditioned media from adipose-derived stromal cells, adipose tissue and emulsified fat on endothelial cells”. Tissue and Cell Engineering Society Conference 2019, Nottingham, UK.

“Using adipose-derived stromal cells and tissue to induce vascularization and soft tissue wound healing”. Tissue Engineering and Regenerative Medicine International Society World Conference 2018, Kyoto, Japan.

“Study of adipose-derived stromal cells and tissue to induce vascularization in soft tissue wound healing”. Tissue and Cell Engineering Society Conference 2018, Keele, UK.

Acknowledgements

I would like to thank my supervisors Vanessa Hearnden and Joey Shepherd for their guidance and support during this project. I feel grateful to be part of the Biomaterials Department and had the opportunity to work with Sheila McNeil, Anthony Bullock, Victoria Workman, and Sabiniano Roman that supported me and taught me so much during these years. Thanks to Katherine Fish for helping me find the motivation to write this thesis.

I present my gratitude to the National Council of Science and Technology of Mexico (CONACyT) and the University of Sheffield for their funding to make this project possible. Thanks for all those patients that donated their tissue through the Sheffield Hospital Directorate of Plastic, Reconstructive Hand and Burns Surgery.

To all my friends that became my family during these years. You made these years amazing in Sheffield. To my Red Deer family and my Kroto family for always being there for me. I'm especially grateful to Gaby, Sam, El Niño, Pablito, Anita and David for your special friendship and support.

To my family for their love and support despites the distance. To my brother to be always an inspiration and a role model for me. This thesis is for you Papá, Mamá and José Antonio.

Abbreviations

ADSC	Adipose Derived Stromal Cells
AIe	Adipose Liquid Extract
Ang 1	Angiopoietin 1
BCN	Biocomponent Polymer Network
bFGF	Basic Fibroblast Growth Factor
CAM	Chorioallantoic Membrane
CM-CSF	Granulocyte-macrophage colony-stimulating factor
ECM	Extracellular Matrix
EGF	Epithelial Growth Factor
ELISA	Enzyme Linked Immunosorbent assay
EMA	European Medicine Agency
ESCs	Embryonic Stem Cells
EthD-1	Ethidium homodimer-1
EUTCD	European Union Tissue and Cells Directive
FDA	Food and Drug Administration
FE	Cell Free Extract
FSC-A	Forward Scatter High
GM-CSF	Granulocyte Macrophage Colony Stimulating Factor
HDMEC	Human Dermal Microvascular Endothelial Cells
HGF	Hepatocyte Growth Factor
HIF-1	Hypoxia-inducible Factor 1
HMEC-1	Human Microvascular Endothelial Cells
IGL-1	Insulin Like Growth Factor 1
IL-6	Interleukin 6
iPSC	Induced Pluripotent Stem Cells
MHC-II	Histocompatibility Complex II
MHRA	Medicine and Health Care Products Regulatory Agency
MMPs	Metalloproteinases
MSCs	Mesenchymal Stem Cells
MTT	(3-(4,5-dimethylthiazol-2-yl)-2,5-diphenyltetrazolium bromide)
NADH	Nicotinamide Adenine Dinucleotide
NIH	National Institute of Health
PDGF	Platelet Derived Growth Factor
PLGF	Placental Growth Factor
SHH	Sonic Hedgehog Homolog
SSC-A	Side Scatter Area
SVF	Stromal Vascular Fraction
SVF-gel	Stromal Vascular Fraction Gel
TGF- β1	Transforming Growth Factor Beta
TSP	Thrombospondin
TIMP-1,2	Tissue inhibitor of metalloproteinases 1,2
VEGF	Vascular Endothelial Growth Factor

Table of contents

Chapter 1 Literature Review 15
1.1 Skin anatomy and wounds 15
1.1.1 Pressure, shear and friction ulcers 16
1.1.2 Diabetic ulcers 17
1.1.3 Burns 18
1.2 Normal wound healing process 18
1.2.1 Angiogenesis 20
1.3 Current treatment and challenges 23
1.3.1 Ideal scaffold design 24
1.3.2 Engineering vascularised tissue 25
1.3.3 Stem cells 26
1.4 Adipose-derived Stromal cells 27
1.4.1 Adipose-derived Stromal Cells and Angiogenesis 27
1.4.2 Adipose-derived stromal cell challenges and regulation 28
1.5 Stromal Vascular Fraction 30
1.5.1 SVF in regenerative medicine 32
1.6 Adipose tissue 35
1.6.1 Adipose tissue in regenerative medicine 37
1.7 Emulsified fat 38
1.7.1 Emulsified fat in regenerative medicine 39
1.8 Stromal Vascular Fraction-gel 40
1.8.1 SVF-gel in regenerative medicine 41
1.9 Conditioned Medium 42
1.10 Summary of adipose related treatments 45
1.11 Angiogenesis assays 45
1.11.1 In vivo assays 45
1.11.2 Ex ovo assay 48
1.11.3 In vitro angiogenesis assays 50
1.11.4 Ex vivo angiogenesis assays 54
1.12 Summary 56
1.13 Hypothesis, aims, and objectives 57
Chapter 2 Processing and characterising adipose tissue 58
2.1 Aim 58
2.2 Introduction 58
2.3 Materials and Methods 61
2.3.1 Cell culture 61
2.3.2 Cell culture medium preparation 61
2.3.3 Cell passaging and counting 63
2.3.4 Cell cryopreservation and thawing cells 64
2.3.5 Adipose tissue processing 64
2.3.6 Emulsified fat protocol 65
2.3.7 SVF-gel protocol 65
2.3.8 ADSC isolation from adipose tissue 66
2.3.9 Experimental design and samples 67
2.3.10 Flow cytometry on ADSC 68

2.3.11 QIAzol DNA isolation from adipose tissue, emulsified fat, SVF-gel, and ADSC 70
2.3.12 Macherey-Nagel NucleoSpin DNA isolation from ADSC 71
2.3.13 DNA quantification 72
2.3.14 Correlation between weight-volume for each sample 72
2.3.15 Lightsheet imaging of adipose tissue, emulsified fat, SVF-gel, and ADSC 72
2.3.16 Confocal imaging of adipose tissue, emulsified fat, SVF-gel and ADSC 73
2.3.17 Live/dead imaging of adipose tissue, emulsified fat, SVF-gel, and ADSC 74
2.4 Results 74
2.4.1 Tissue processing 74
2.4.2 ADSC characterisation 75
2.4.3 DNA isolation and quantification using QIAzol 78
2.4.4 DNA isolation and quantification using NucleoSpin columns 80
2.4.5 Correlation between weight-volume for each sample 81
2.4.6 LightSheet imaging 81
2.4.7 Confocal imaging 85
2.4.8 Live/Dead imaging 87
2.5 Discussion 89
Chapter 3 Study of conditioned media from adipose tissue and derivatives in 2D models of angiogenesis 100
3.1 Aim 100
3.2 Introduction 100
3.3 Methods 101
3.3.1 Conditioned media 101
3.3.2 Experimental design and samples 102
3.3.3 LDH assay 103
3.3.4 Endothelial migration assay 104
3.3.5 Endothelial metabolic activity assay 105
3.3.6 Free lipid effect on endothelial cells 106
3.3.7 Statistical analysis 106
3.4 Results 107
3.4.1 Generation of conditioned media 107
3.4.2 LDH cytotoxicity assay 108
3.4.3 Endothelial (HMEC-1) migration assay 110
3.4.4 Metabolic activity using MTT on HMEC-1 112
3.4.5 Endothelial (HDMEC) migration assay 114
3.4.6 Metabolic activity using MTT on HDMEC 115
3.4.7 Free lipid effect on endothelial cells 116
3.5 Discussion 117
Chapter 4 Study of conditioned media on endothelial tube formation assay, ex vivo and ex ovo models 127
4.1 Aim 127
4.2 Introduction 127
4.3 Materials and Methods 128
4.3.1 Experimental design and samples 128
4.3.2 Endothelial tube formation 129
4.3.3 Chick aortic ring 130

4.3.4 Chick Chorioallantoic Membrane (CAM) Assay 131
4.3.5 Human angiogenesis antibody array 132
4.3.6 Statistical analysis 134
4.4 Results 135
4.4.1 Tube formation assay 135
4.4.2 Aortic ring assay 139
4.4.3 CAM assay 141
4.4.4 Cytokine array 143
4.5 Discussion 146
Chapter 5 Conclusions and Future work 161
Chapter 6 Appendix 166
Chapter 7 References 169

Table of figures

Figure 1.1 Skin structure is composed of three main layers: Epidermis, Dermis and Hypodermis..... 15

Figure 1.2 Skin wound healing diagram with the three main phases: inflammatory, proliferation and remodelling 19

Figure 1.3 Schematic diagram detailing the angiogenesis process starting with a hypoxic environment that promotes the degradation of the ECM allowing cell migration and capillary formation to end up in vessel maturation..... 21

Figure 1.4 Schematic diagram showing adipose tissue composition and lipoaspiration of subcutaneous fat (A) after enzymatic digestion and centrifugation displaying the different layers obtained (oil, adipose tissue, a layer composed mainly of red blood cells and plasma and stromal vascular fraction) (B). And isolation of ADSC for their plastic adherence characteristic (C)..... 31

Figure 1.5 Schematic diagram illustrating different protocols to process adipose tissue for skin regenerative medicine..... 36

Figure 1.6 Diagram of dorsal skinfold chamber assay 46

Figure 1.7 Chicken embryo after 7 days of incubation highlighting CAM membrane 49

Figure 1.8 Schematic diagram illustrating endothelial cell migration assay by scratching.... 53

Figure 1.9 Schematic diagram illustrating chick aortic ring assay.. 55

Figure 2.1 Photographs showing adipose tissue processing for conditioned media where the whole tissue (A) is minced mechanically (B). 65

Figure 2.2 Photographs showing how to produce emulsified fat from minced adipose tissue. 65

Figure 2.3 Photographs illustrating protocol to produce SVF-gel from emulsified fat. 66

Figure 2.4 Images of whole adipose tissue (A), lipoaspirate (B), minced adipose tissue (C), emulsified fat (D), SVF-gel (E), and cultured ADSC (F)..... 75

Figure 2.5 Flow cytometry histograms (A) illustrating analysis carried out using different cell markers. 77

Figure 2.6 Cells side scatter area (SSC-A) vs forward scatter area (FSC-A) (A), and forward scatter area (FSC-A) vs forward scatter high (FSC-H) (B). Two parameter density plots for different markers to identify ADSC population using CD73 vs CD 90 (C), CD34 vs CD105 (D), CD45 vs CD73 (E), and CD146 vs CD90 (F)..... 78

Figure 2.7 DNA quantification in µg of DNA per gram of sample of ADSC, adipose tissue, lipoaspirate, emulsified fat, and SVF-gel. 79

Figure 2.8 DNA quantification from 10,000, 30,000, and 50,000 ADSC using NucleoSpin DNA Lipid Tissue kit (A). DNA quantification in µg of DNA per gram of sample of lipoaspirate, unwashed SVF-gel and washed SVF-gel. 80

Figure 2.9 Correlation between weight and volume for adipose tissue (A), lipoaspirate (B), emulsified fat (C), and SVF-gel (D). 81

Figure 2.10 ADSC and adipose tissue imaged using BODIPY (yellow), CellMask (green), Hoechst (blue) and Isolectin stains (red) (A) compared to samples stained only with CellMask (B). 82

Figure 2.11 ASDC, adipose tissue, lipoaspirate, emulsified fat, and SVF-gel stained using Isolectin (endothelial cells in red), Hoechst (nuclei in blue), and BODIPY (fatty acids in yellow). Images taken using LightSheet microscopy. 84

Figure 2.12 Confocal imaging of adipose tissue (A), emulsified fat (B), and SVF-gel (C) using MemBrite™ Fix dye (cell membrane in green), DAPI (nuclei in blue), and BODIPY (fatty acids in red). 86

Figure 2.13 Image of SVF-gel showing the different layers formed after centrifugation (A). Confocal imaging of whole SVF-gel (B), SVF-gel yellow layer or fat layer (C), and SVF-gel pellet (D). Samples were stained with MemBrite™ Fix dye (cells membrane in green), DAPI (nuclei in blue), and BODIPY (fatty acids in red). 87

Figure 2.14 Live/dead imaging of adipose tissue (A), lipoaspirate (B), emulsified fat (C), SVF-gel (D), and unstained adipose tissue (E)..... 88

Figure 3.1 Schematic diagram illustrating endothelial migration assay using silicone stoppers 105

Figure 3.2 Schematic diagram illustrating MTT assay of endothelial cells after 48 hr of culture in conditioned media. 106

Figure 3.3 Photographs showing differences in the appearance of media conditioned using 0.13 g adipose tissue per ml of media (A), 0.13 ml of emulsified fat per ml of media (B), and 0.036 ml of SVF-gel per ml of media (C). 107

Figure 3.4 Lactate dehydrogenase (LDH) content of conditioned media from ADSC (50,000 cells/cm^2), adipose tissue (0.1 g/ml media), emulsified fat (0.13 ml/ml media), SVF-gel (0.03 ml/ml media) after 3 days of co-culture (A), and LDH accumulation over time with three different concentrations of adipose tissue in conditioned media (B). 108

Figure 3.5 LDH analysis of media conditioned with adipose tissue or emulsified fat for different incubation times (A). Metabolic activity (B) and migration (C) of endothelial cells (HMEC-1) using the conditioned media from adipose tissue and emulsified-fat with a change of media after 1 hr of culture or without any media change.. 110

Figure 3.6 Migration of endothelial cells (HMEC-1) after 24 hrs cultivated in conditioned media from ADSC (A), adipose tissue (B), emulsified fat (C), and SVF-gel (D). 112

Figure 3.7 Metabolic activity of endothelial cells (HMEC-1) after 2 days cultivated in conditioned media from ADSC (A), adipose tissue (B), emulsified fat (C), and SVF-gel (D).. 113

Figure 3.8 Migration of endothelial cells (HDMEC) after 24 hrs cultivation in conditioned media from ADSC (A), adipose tissue (B), emulsified fat (C), and SVF-gel (D)..... 115

Figure 3.9 Metabolic activity of endothelial cells (HDMEC) after 2 days cultivation in conditioned media from ADSC (A), adipose tissue (B), emulsified fat (C), and SVF-gel (D). 116

Figure 3.10 Effect of lipids in the media on migration (A) and metabolic activity (B) of HDMEC 117

Figure 4.1 Light microscope image (A) showing HDMEC endothelial tube formation assay analysis using ImageJ to identify all the tubular structures in the image to produce the map of segments identified (B).. 130

Figure 4.2 Light microscope image of vessels grown from chick aortic ring (A), and after measuring the five longest branches coming from the ring (in red) using ImageJ (B).. 131

Figure 4.3 Images of the chicken embryo development (A-E). Finally, CAM assay image analysis using ImageJ (F-H)..... 132

Figure 4.4 Schematic diagram illustrating how the angiogenesis cytokine array functions.. 134

Figure 4.5 Number of tubes formed on endothelial tube formation assay using conditioned media from ADSC (A), adipose tissue (B), emulsified fat (C), and SVF-gel (D). 136

Figure 4.6 Total segment length on endothelial tube formation assay using ADSC (A), adipose tissue (B), emulsified fat (C), and SVF-gel (D) FGF (100 ng/ml) was used as a positive control while MV media without supplements, was used as negative control. 137

Figure 4.7 Images showing endothelial tube formation using conditioned media from ADSC (50,000 cells/cm^2) (A), adipose tissue (0.13 g/ml media) (B), emulsified fat (0.13 ml/ml media) (C), and SVF-gel (0.036 ml/ml media) (D) conditioned media.. 138

Figure 4.8 Chick aortic rings after 4 days culture using ADSC (50,000 cells/cm^2) (A), adipose tissue (0.13 g/ml media) (B), emulsified fat (0.13 ml/ml media) (C), and SVF-gel (0.036 ml/ml media) (D) conditioned media. FGF (100 ng/ml) (E) was used as a positive control and MV media without supplements (F) as negative control..... 140

Figure 4.9 Average sprout area on chick aortic ring assay using ADSC (50,000 cells/cm^2), adipose tissue (0.13 g/ml media), emulsified fat (0.13 ml/ml media), and SVF-gel (0.036 ml/ml media) conditioned media. FGF (100 ng/ml) was used as a positive control and MV media without supplement as negative control. 141

Figure 4.10 Vascular area change on CAM between day 7 and 13 of culture. Mean with error bars showing standard deviation. 142

Figure 4.11 Angiogenic cytokine array after incubation with conditioned media from ADSC, adipose tissue, emulsified fat, SVF-gel, and non-conditioned media (A). Map of the different cytokines studied on the array (B), and analysis of mean pixel density for all the samples (C). 144

Figure 4.12 Relative expression levels (A) angiogenin, (B) IL-6, (C) TIMP-2, (D) bFGF, and (E) PLGF in conditioned media from ADSC, adipose tissue, emulsified fat, and SVF-gel.. 145

Table of Tables

Table 1.1 Growth factors involved in vascularisation 22

Table 1.2 Cell yield from adipose tissue..... 32

Table 1.3 Different methods for producing conditioned media highlighting different seeding densities and incubation times. 44

Table 2.1 ADSC media composition..... 61

Table 2.2 MCDB 131 medium composition for HMEC-1 62

Table 2.3 Dulbecco's modified Eagle's Medium composition 62

Table 2.4 Growth medium MV for HDMEC 63

Table 2.6 Tissue and formulation batches used in the different experiments. 68

Table 2.7 Fluorophores used for the seven different CD markers used for ADSC characterisation..... 69

Table 3.1 Cell and tissue quantities used for conditioned media..... 102

Table 3.2 Tissue and formulation batches used in the different experiments. 103

Table 4.1 Tissue and formulation batches used in the different experiments. 129

Table 4.1 Conditions to produce conditioned media 138

Table 4.2 Summary of results obtained from different angiogenic assays on this chapter using conditioned media from ADSC, adipose tissue, emulsified fat, and SVF-gel. 142

Chapter 1 Literature Review

1.1 Skin anatomy and wounds

Skin is the biggest organ in the body, and it is the barrier between our internal bodies and the environment. Skin can be divided into three main layers: epidermis, dermis and hypodermis (Figure 1.1). The epidermis is the outer layer and is mainly composed of keratinocytes that are arranged in a multilayer structure. Then, the dermis is the underlying layer of fibrous tissue mainly composed of collagen and reticular fibres produced by fibroblasts. This layer also contains hair follicles, blood vessels, nerves and sweat glands. Finally, the hypodermis is composed mainly of adipose tissue, blood vessels and nerves with the main function of regulating body temperature and to separate the dermis from the underlying muscular fascia (Saladin, 2008).

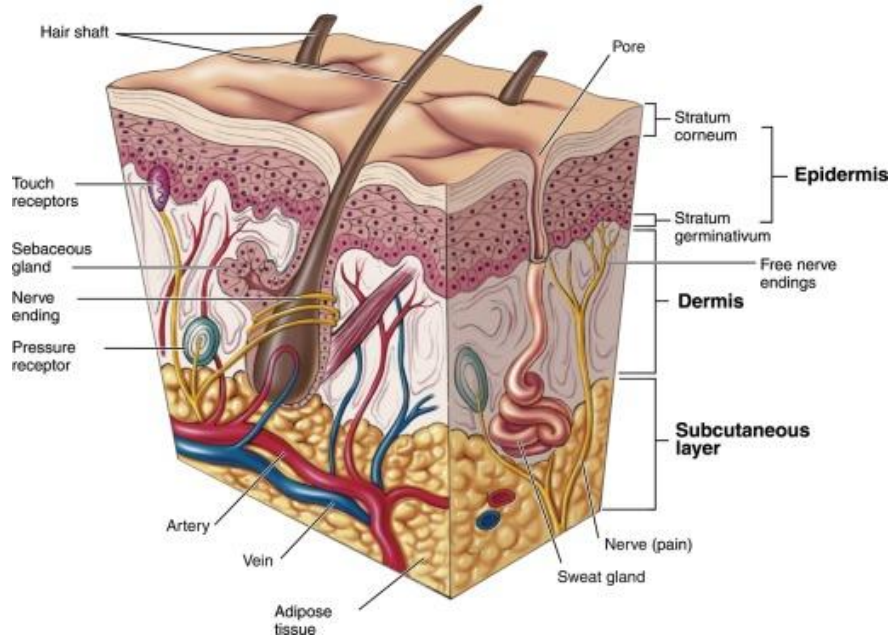

Figure 1.1 Skin structure is composed of three main layers: Epidermis, Dermis and Hypodermis (Reproduced by the permision of Krapohl and Shaw, 2015).

When skin is damaged there is a risk of infection by microorganisms, that can penetrate into the body, or harm to adjacent tissues as the barrier is damaged. Depth, extent, location and signs of infection determine the severity of the skin wound and they can be classified into lacerations, rupture injuries, punctures, abrasions,

penetrating wounds, burns and ulcers (Tissue), 2018). When an injury has failed to heal through an orderly and reparative process by 4 weeks, it can be considered a chronic wound (Frykberg and Banks, 2015). Chronic wounds generate extensive economic and social burdens around the world. It was estimated that in the UK wound care services cost up to £2,165 million in 2014, and it is predicted to rise to £2,377 million by 2019 (Morgan, 2015). In addition, in developed countries around 1-2% of the population are expected to experience a chronic wound during their lifetime since they are associated with obesity, diabetes mellitus and advancing age, which are all increasing in incidence in developed countries leading to a dramatic rise in cost over time (McDaniel and Browning, 2014). The most common chronic wounds are pressure ulcers, diabetic ulcers, and burns that frequently present difficulties to heal alone (Sen *et al.*, 2010).

1.1.1 Pressure, shear and friction ulcers

An ulcer is a skin wound that can be caused by pressure, shear, or friction. This type of wound is highly preventable: however, they are very common in hospitals and care homes, locations where people are immobile in bed for weeks making them a global healthcare problem. Pressure ulcers are generated during prolonged and excessive compression on the lymphatic and vascular network of a specific skin area. When the pressure obstructs the blood flow in capillaries, oxygen and nutrients cannot be supplied to that specific tissue area resulting in ischaemia, acidosis and necrosis (Flanagan, 2013). Pressure is the most common factor to generate a skin ulcer but shearing and friction can also damage the skin. Sheer stress is commonly generated by sliding or pulling over a surface. This force on the skin can produce distortion of the tissues leading to deformation of the transverse plane of the tissue (Flanagan, 2013). On the other hand, friction ulcers occur when skin is rubbed on a rough or wrinkled surface. This action results in skin blisters or abrasion. In general, pressure, sheer and friction forces may be combined to injure the skin. The population with highest risk of suffering these kinds of wounds are elderly people as they have skin with reduced elasticity which is easily deformed with less force applied. This kind of wound

generates pain and discomfort in patients. The best approach is to prevent these types of injuries by not allowing a person to be in the same position for long periods of time by repositioning and using adequate support surfaces that do not generate sheer and friction forces. One of the main complications of pressure ulcers are infections that can increase the wounded area complicating the healing process (Flanagan, 2013).

1.1.2 Diabetic ulcers

Diabetes is a metabolic disorder characterised by high blood glucose due to insulin deficiency (type 1) or insulin resistance (type 2) (Dennis L. Kasper, Anthony S. Fauci, Stephen L. Hauser, Dan L. Longo, J. Larry Jameson, 2016). Poor control of diabetes can lead to peripheral artery disease, microvascular abnormalities and neuropathy that in conjunction can result in poor wound healing. Normally, blood flow is increased in an injured area because high metabolic rate is needed in the healing process. However, in diabetics hyperglycaemia leads to modification of proteins and enzymes resulting in dysfunction. This occurs in the basement membrane of capillaries which become thicker, decreasing the capacity of vasodilation and altering their permeability and nutrient delivery (Yang *et al.*, 2015). As a result, there is a mismatch of blood supply and demand in wounds (Chadwick *et al.*, 2013). These factors combined can lead to the development of diabetic ulcers, which commonly develop on the foot. Diabetic ulcers are open sores in the skin with thick borders that result in the complete loss of the epidermis and sometimes in the loss of dermis and even hypodermis. Unfortunately, approximately 10 percent of diabetic people will have a diabetic ulcer in their life, at an estimated cost of £650 million to the NHS (Health and Social Care Information Centre, 2016). In addition, diabetes affects peripheral nerves causing insensitivity in patient limbs, consequently when a person has an injury in one of their extremities, he/she does not feel any pain thereby underestimating the severity of the wound (Chadwick *et al.*, 2013).

1.1.3 Burns

Burns are damage to the skin characterised by red skin, blisters, swelling and white or charred skin caused by heat, chemicals, sunlight, electricity or radiation (Lyons and Ousley, 2014). Burns are classified according to the severity of damage to the skin. First degree burns are those in which the damage occurs to the epidermis resulting in a red appearance, slightly swollen affected areas and tolerable pain such as sun burns. Second degree burns affect not only the epidermis, but also the dermis causing blisters, soreness, blotchiness and they can be dry or moist. Finally, third degree burns are those in which the three layers of skin (epidermis, dermis and hypodermis) are damaged. The tissue left is pale or blackened, but if some skin remains it is dry and white, brown or black with no blisters and lack of sensitivity to touch (National Burn Care Review Committee, 2001; Lyons and Ousley, 2014). These types of wounds are extremely dangerous because the body's natural barrier has been destroyed leaving the patient vulnerable to infections and dehydration. Usually, skin grafts are used to help the healing process, but since tissue regeneration starts at the injury edges, sometimes this process is not rapid enough to cover all the injured area risking the patient's life (Lyons and Ousley, 2014). Also, in third degree burns even if a skin graft is placed on the wound, there is no blood supply to it because the blood vessel network in the zone has been destroyed resulting in graft failure (MacNeil, 2008).The wound healing process is complex and to improve existing treatments understanding is needed in order to be able to enhance them.

1.2 Normal wound healing process

Wound healing is a multifaceted and dynamic process that historically has been divided into four main stages: hemostasis, inflammatory, proliferation and remodelling (Figure 1.2) (Korrapati *et al.*, 2016). Although, some authors add haemostasis as a inciting phase (Jeffrey E. and Bridget, 2014). Haemostasis happens in the moment an injury is created, damaging the vascular endothelium leading to bleeding and platelet activation followed by clotting and the release of growth factors. Then, the inflammatory phase is responsible for preventing infections during the healing process,

taking place during the first 1 or 2 days. During this time, the necrotic tissue is degraded and there is further signal activation for wound healing. Through this stage, neutrophils and monocytes are recruited into the injured area by vasodilatation and fluid extravasation; followed by the late inflammatory response in which the macrophages arrive at the zone (Jeffrey E. and Bridget, 2014; Rowan *et al.*, 2015).

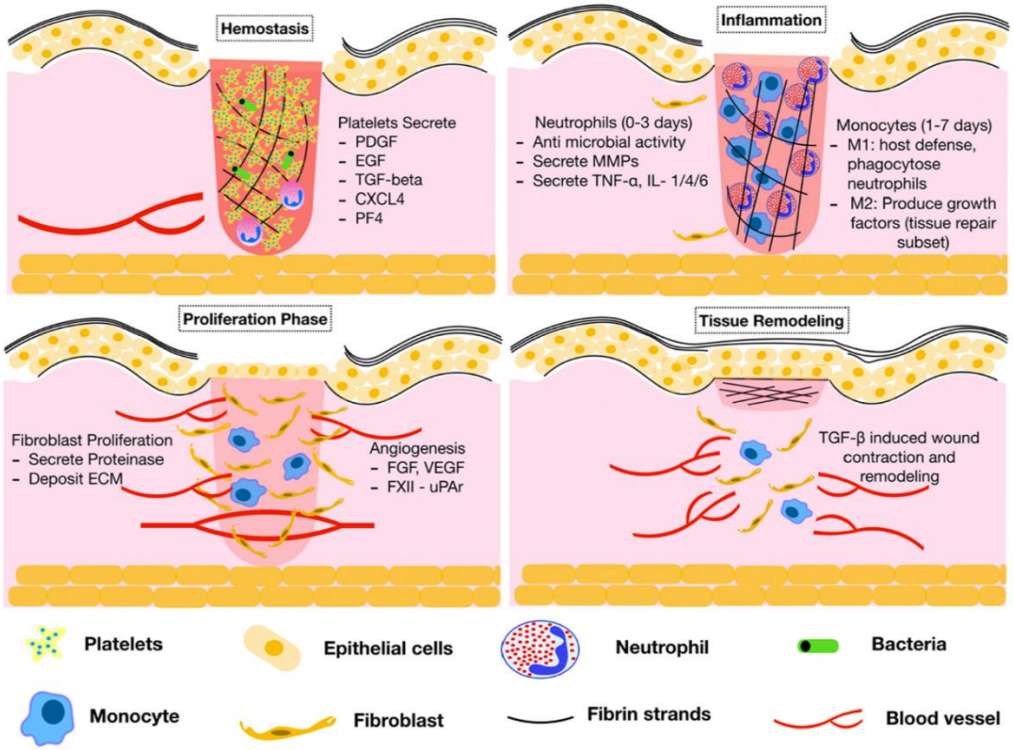

Figure 1.2 Skin wound healing diagram with the four main phases: hemostasis, inflammatory, proliferation and remodelling (Reproduced with permission Opneja, Kapoor and Stavrou, 2019)**.**

The proliferative phase takes place when macrophages begin the development of granulation tissue and the secretion of growth factors such as fibroblast growth factor (FGF), epithelial growth factor (EGF), transforming growth factor beta (TGF-β) and platelet derived growth factor (PDGF) (Korrapati *et al.*, 2016). Epithelisation is stimulated by EGF promoting keratinocyte migration and proliferation to resurface the wound area (Yang *et al.*, 2015). Simultaneously, platelets secrete vascular endothelial growth factor (VEGF) and FGF to promote the proliferation of endothelial cells to initiate the angiogenesis which is vital for wound healing. Fibroblasts are recruited after

24 hours of the injury and activated by TGF-β and PDGF to change their phenotype into myofibroblasts and create an extracellular matrix (ECM). They require adequate oxygen supply for elastin and collagen production along the edges of the wound to facilitate wound closure (Jeffrey E. and Bridget, 2014; Rowan *et al.*, 2015).

Finally, the remodelling process, which overlaps with the proliferative phase, results in the maturation of scar tissue by the synthesis and continuous remodelling of collagen and elastin. The granulation tissue is replaced by collagen and elastin fibres saturated with proteoglycans and glycoproteins (Korrapati *et al.*, 2016). Overall, an increase in collagen formation is seen after 4 to 5 weeks after the injury indicating wound strengthening (Jeffrey E. and Bridget, 2014). During this process, there must be a balance between ECM production and degradation by fibroblasts, smooth muscle cells and stem cells. If the ECM production and degradation is not balanced, abnormal healing can lead to excessive accumulation of ECM (Jeffrey E. and Bridget, 2014). Keloids and hypertrophic scars are the most common type of excessive healing that create disfiguring masses disturbing the structural and functional integrity of the tissue, which can result not only in physical problems, but also in psychological trauma to patients (Korrapati *et al.*, 2016). Vascularisation is also a key element for wound healing. Delayed vascularisation during wound healing may produce chronic wounds in which the main problem is capillary damage and slow, neovascularisation impeding the wound healing process (Korrapati *et al.*, 2016).

1.2.1 Angiogenesis

In all body tissues except the cornea (which receives oxygen by direct diffusion), blood vessels provide the supply of oxygen and nutrients for individual cells. The oxygen diffusion limit is around 100-200 μm (Laschke *et al.*, 2006; Rouwkema, Rivron and van Blitterswijk, 2008); if a tissue grows beyond this distance from a capillary network, new blood vessels are needed. Angiogenesis is the formation of new capillaries from pre-existing blood vessels. The blood vessel formation process can be divided into three stages: vasculogenesis, angiogenesis and arteriogenesis (Tahergorabi and Khazaei, 2012). Vasculogenesis takes place when endothelial cells differentiate and proliferate within avascular tissue creating a nascent capillary network. Then, angiogenesis is the

process in which the existing capillary network is remodelled to become a more complex structure (Figure 1.3). The endothelial cells degrade the surrounding ECM by secreting metalloproteinases (MMPs) to allow cell migration into the gaps and proliferation creating capillary buds. Finally, arteriogenesis takes place to remodel and enlarge the existing arterioles into larger vessels (Park *et al.*, 2013). Vessel maturation is important in vascularisation because if vessel growth is not completed, the result is a disorganised, leaky and haemorrhagic blood vessel that can cause regression. To avoid this, pericytes (mural or perivascular cells that wrap around blood vessels to control blood flow) and smooth muscle cells migrate to the abluminal surface to stabilise vessel structures and stop endothelial cell growth (Distler *et al.*, 2003).

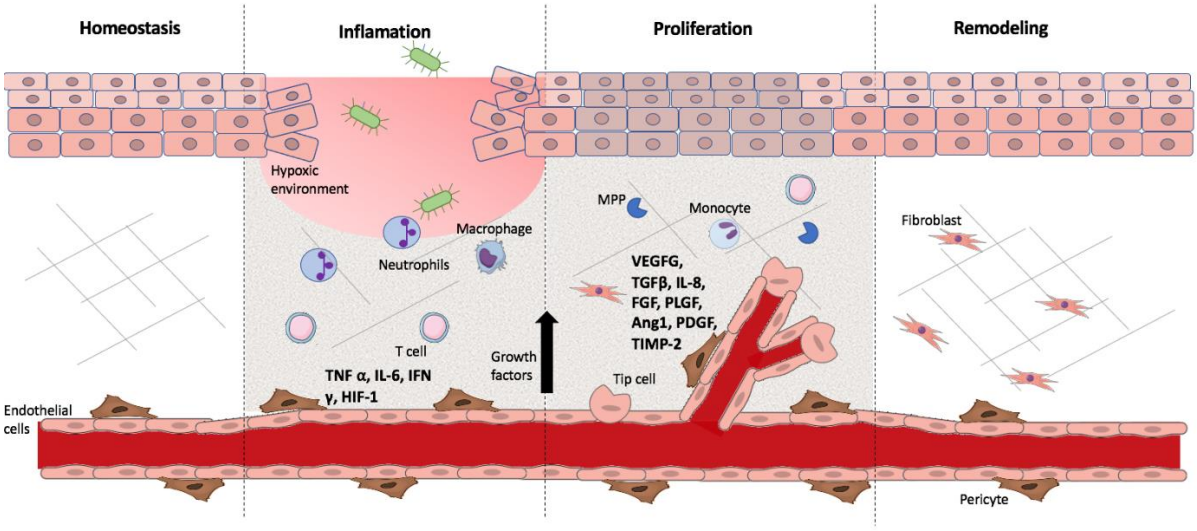

Figure 1.3 Schematic diagram detailing the angiogenesis process during skin wound healing. When there is a damage in the tissue a hypoxic environment is generated and an immune response is started as part of the inflammation phase. This promotes the degradation of the ECM to allow different types cell to migrate to the injured zone. During the proliferation phase new capillaries and collagen fibres are formed while re-epithelisation takes place to close the wound. Finally, the new collagen fibres are remodelled maturated and vessel maturation takes place to complete the wound healing process.

Vascularisation is a complex process in which different cells (fibroblasts, endothelial cells, pericytes) participate and need to be coordinated at different times by a variety of signals as shown in Figure 1.3. There are well known factors that promote and support vascularisation (Table 1.1) that can be classified into two main groups: direct and indirect factors. Direct growth factors promote the formation of vessels directly;

while indirect factors promote vascularisation by stimulating cells close to the vascularisation site to secrete vascularisation factors.

Table 1.1 Growth factors involved in vascularisation

Growth factors	Function	Reference
VEGF	Induces local extravasation of proteases and matrix components for the recruitment, proliferation of endothelial cells for tube formation.	Hirota and Semenza, 2006
bFGF	Promotes the mobility and recruitment of endothelial cells.	Hirota and Semenza, 2006
Granulocyte macrophage colony stimulating factor (GM-CSF)	Increases circulation population and differentiation of haematopoietic progenitor cells, myeloid lineage cells and non-haematopoietic cells such as bone marrow stromal cells and endothelial cells.	Ribatti *et al.*, 2001
PDGF	Stabilises the new blood vessels by bringing in smooth muscle cells and pericytes.	Hirota and Semenza, 2006
TGF- β	Promotes ECM production and correct interaction between endothelial cells and mural cells.	Hirota and Semenza, 2006
Angiopoietin 1 (Ang1)	Paracrine growth factor that interacts with endothelial cells for the maturation and stabilisation of the new vessels.	Tahergorabi and Khazaei, 2012
Hepatocyte growth factor (HGF)	Participates in the motility, migration, growth and morphology of endothelial cells, melanocytes and epithelial cells for the formation of new blood vessels.	Nomi *et al.*, 2002
Sonic hedgehog homolog (SHH)	Signals interstitial mesenchymal cells to produce VEGF and angiopoietins-1 and -2 resulting in highly organised, mature vessels.	Rouwkema, Rivron and van Blitterswijk, 2008
Hypoxia-inducible factor 1 (HIF-1)	Directly or indirectly induces the production of different angiogenic factors and cytokines within endothelial cells such as VEGF, PDGF-B, PLGF and angiopoietins.	Hirota and Semenza, 2006
Angiostatin	Suppresses proliferation, migration and differentiation of endothelial cells inhibiting vascularisation.	Distler *et al.*, 2003
Endostatin	Inhibits endothelial cell migration and proliferation.	MacDonald *et al.*, 2001; Tahergorabi and Khazaei, 2012
Thrombospondin (TSP)	Inhibits endothelial cell migration and proliferation and blocks tube formation.	Jiménez *et al.*, 2000; Tahergorabi and Khazaei, 2012
Angiogenin	Promotes endothelial cell proliferation and migration.	Efimenko *et al.*, 2014
Interleukin-6 (IL-6)	Pro-inflammatory cytokine that helps to regulate angiogenesis process.	Dong *et al.*, 2013; Pu *et al.*, 2017
Placental growth factor (PLGF)	Promotes proliferation and migration of endothelial cells.	Xu *et al.*, 2018
TIMP-2	Inhibits MMPs and capillary endothelial cell proliferation to allow vessel maturation.	Fernández *et al.*, 2003

One of the problems of vascularisation in wounds is that vascularisation ingrowth is limited to several tenths of micrometres per day meaning that to vascularise a complete wound of several millimetres, would take days or weeks (Rouwkema, Rivron and van Blitterswijk, 2008). Moreover, if the area that is wounded is large and the regeneration process is limited due to a pathology as in diabetes (section 1.1.2), this could lead to a poor vascularisation process creating chronic wounds. As mentioned before (see sections 1.1.1 - 1.1.3), in dermal chronic wounds the main issue that interferes with the healing process is a poor vascularisation process. As a result, new treatments need to overcome these challenges in order to guarantee wound healing. Currently, there are different strategies in skin engineering to improve vascularisation within the injured tissue to help accelerate the healing process, which are detailed below.

1.3 Current treatment and challenges

In the last 25 years, medical treatments have improved, nevertheless there are still 300 deaths in UK hospitals each year caused by burns alone (National Burn Care Review Committee, 2001). However, those patients that survive live with the aftermath for the rest of their lives such as disfigurements, restriction in motion, and disability, and in some cases psychological recuperation is needed to overcome depression, anxiety, appearance insecurity, sleep disruption and stress (Wood, Bellis and Atherton, 2010).

Skin grafting is the most used technique used in clinic to treat large wounds. It is necessary to take a split-thickness skin graft (epidermis and part of the dermis) or full-thickness skin graft (epidermis and entire dermis) to place into the wounded area. Slip-thickness grafts could be autografts, homograft, allografts or xenografts (Braza and Fahrenkof, 2020). Skin grafts provide a barrier to the wounded area from the environment, pathogens and water loss. Nevertheless, skin grafts are not vascularised and rely on the vascularisation on the wounded area. This is the biggest disadvantage since chronic wounds frequently lack this vascularised bed that lead into graft failure (Braza and Fahrenkof, 2020). In addition, an extra wound area is created in order to

harvest the graft, difficulties for an aesthetic match (colour and texture), and prolonged wound care for the donor site and wounded area. As a result, there is a necessity to create new treatments for chronic wounds that not only allow patients to heal, but also help scar formation in a more aesthetic way to improve patient's physical and psychological recuperation.

Different skin engineering strategies have been developed to help wound healing. A variety of scaffolds are currently used in clinics. These scaffolds are typically made of biopolymer fibres that can degrade in the host body and support cell growth and migration. Even when these scaffolds create a barrier between the wounded tissue and the environment and promote wound healing. There are still some obstacles to overcome such as graft contraction, scar formation, time required to produce skin engineered treatments and delayed vascularisation. In all these cases, there is not yet a treatment available to treat chronic wounds with good aesthetic outcomes. Regardless of the type, according to Papuga and Lukash (2015) skin wound treatments should cover a variety of features including:

- Non-antigenicity
- Skin compatibility
- No permeability
- Inhibition of exogenous microorganisms
- Sufficient adhesion to the wound surface
- Elasticity
- Biodegradability
- Extensive lifetime
- Simplicity of storing
- Low cost
- Usability for medical staff
- Shortened time of wound healing
- Resistance to linear shift deformations

Although many skin grafts have most of these properties, vascularisation is still a challenge because even when some skin substitutes allow vascularisation, it is not rapid enough to maintain long-term survival and integration of the wound bed resulting in treatment failure. There are multiple approaches to help the vascularisation in wound healing including modification of structural and physiochemical properties of dermal scaffolds, integration of growth factors, generation of pre-vascularised skin substitutes, and use of stem cells. In the following sections these approaches will be discussed in more detail.

1.3.1 Ideal scaffold design

For tissue engineered treatments for soft tissue wounds including skin chronic wounds, scaffolds are essential to support cell attachment, proliferation and differentiation. The scaffold must be selected to provide a suitable structure for cell survival, as the environment can be severe for cells as a result of poor nutrient and oxygen supply. The focus of scaffold design is to create an adequate structure to allow and promote vascularisation in skin wounds once the graft is implanted into the host body.

Porosity is one of the most significant characteristics that can affect vascularisation within the grafts. Zhang and Suggs (2007) used *in vitro* and *in vivo* studies to show that pore sizes larger than 300 μm and increased numbers of pore interconnections increased vascularisation significantly within the scaffold. Another technique to improve vascularisation is angiogenic factor delivery. Richardson *et al.*, (2001) described how growth factors were integrated into biodegradable polymer scaffolds to deliver localised and sustained growth factor release. Growth factors such as VEGF, bFGF, PDGF and TGF-β have been integrated into different scaffolds made of gelatin, fibrin, collagen, PLGA/PEG (poly(lactic-co-glycolic acid/Polyethylene glycol) or alginate to promote blood vessel growth and maturation (Frueh *et al.*, 2016).

Also, indirect factors such as sonic hedgehog homolog (SHH) have been used to stimulate cells adjacent to the wound to produce angiogenic factors including VEGF and angiopoteins-1 and -2, improving vessel formation when this approach was combined with growth factors delivered within the graft (Rouwkema, Rivron and van Blitterswijk, 2008). Bai *et al*., (2018) developed a scaffold incorporating three different growth factors (VEGF, FGF, and PDGF) with a different release rate for each of them. This was possible to achieve by encapsulating the growth factors in different types of polymers within the scaffold. Each polymer had a different degradation rate making it possible to control the release rate. It was reported that the scaffold with VEGF, FGF and PDGF enhanced endothelial cell angiogenesis *in vitro* and chorioallantoic membrane angiogenesis *in vivo* (Bai *et al.*, 2018). Even though several growth factors

have been combined and integrated into scaffolds used for tissue engineering, vascularisation requires a vast number of different cytokines at different times during the healing process (Nomi *et al.*, 2002). In addition, these growth factors have a short half-life and instability. Also, it is hard for them to penetrate into the wounded area in concentrations high enough to have an effect. As a result, this strategy is a good option to improve vessel growth, however it does not solve the main problem (Edwards *et al.*, 2014; Cai *et al.*, 2019). In addition, in optimal conditions graft vascularisation takes around 14 days and can be delayed in case of patients with vascular insufficiency (Shepherd *et al.*, 2006).

1.3.2 Engineering vascularised tissue

In vivo and *in vitro* pre-vascularisation methods aim to create grafts with blood vessel already in place to accelerate their integration to the host body once they are implanted at the wound site (Polzer *et al.*, 2014). *In vivo* pre-vascularisation starts when the graft is implanted, connecting it to an artery or wrapped in an axial vascularised tissue like muscle. Then, the graft is left for several weeks to allow the production of a microvascular network around the scaffold. Once the construct is ready, it is harvested with the microvascular structure and the supplying artery present thus allowing it to be re-implanted at the wound site (Rouwkema, Rivron and van Blitterswijk, 2008; Polzer *et al.*, 2014). This techniques' advantage is that after the implant is placed in its final location, it becomes immediately perfused by surgical anastomosis. The disadvantage is that two surgeries are required, and it takes a couple of weeks to produce this kind of construct (Shepherd *et al.*, 2006). In contrast, *in vitro* pre-vascularisation consists of adding endothelial cells to the tissue culture, skin in this case, in order to produce a pre-vascular network within the tissue. The vascularisation time is reduced from weeks to days in which the host body vascularises the area surrounding the implant to connect the blood vessels of the implanted tissue with the circulatory system (Shepherd *et al.*, 2006). This strategy can help incorporate the graft into the host, but there could be some complications in finding culture conditions that are suitable both for endothelial cells and the tissue culture at the same time (Shepherd *et al.*, 2006).

1.3.3 Stem cells

The use of autologous stem cells is gaining attention for their promising use in the generation of new tissues. Stem cells are undifferentiated cells that have the capacity to self-renew and differentiate into different cell types. They also release cell signalling factors which drive effects in surrounding tissues. There are three main classifications for stem cells: embryonic stem cells (ESCs), multipotent adult stem cells and induced pluripotent stem cells (iPSCs). ESCs appear to be the most useful stem cells types due to their potential and pluripotency. Nevertheless, there are ethical issues and technical obstacles to their clinical application. iPSCs are generated when mature somatic cells, such as skin fibroblasts, are re-programmed. They have the same differentiation capability as ESCs, but they require the induction of exogenous transcription factors that can affect the stability of the cell lines and produce carcinogenesis, limiting their use in human trials (Bunnell *et al.*, 2008).

Adult mesenchymal stem cells (MSCs) evade many of the ethical and technical difficulties associated with ESCs as they can be obtained from a wide variety of adult tissues such as bone marrow and adipose (Hasegawa and Ikeda, 2015). Adult stem cells can be found in small populations localised in niches in adult tissues. They are multipotent, meaning they have the capability to differentiate into mesodermal, endodermal and ectodermal cells according to their origins. In addition, mesenchymal stem cells can be used as an allogeneic treatment since they lack the histocompatibility complex II (MHC-II) and express low quantities of MHC-I (Bateman *et al.*, 2018). Ideally, stem cells used in regenerative medicine must meet certain criteria. They should be found in high quantities (millions of cells) and it should be easy to collect them with a minimally invasive harvesting procedure. In addition, they should have the potential to differentiate into multiple cell lineage pathways in a reproducible manner and have safe and effective procedures to transplant them to the host body (Bunnell *et al.*, 2008). MSCs have been proved to promote angiogenesis due to the variety of secreted pro-angiogenic factors and their interaction with endothelial cells to stimulate tubular-like structures *in vitro* (Pill *et al.*, 2015).

1.4 Adipose-derived Stromal cells

Adipose-derived stromal cells (ADSCs) are the most easily harvested in large quantities (200- and 400-fold higher than mesenchymal stromal and mononuclear cells derived from bone marrow) (Jin *et al.*, 2017) of all the adult stem cells with multipotency (Hasegawa and Ikeda, 2015). ADSCs can be obtained from the subcutaneous adipose tissue of the abdomen, arms and thighs by lipoaspiration, which does not affect ADSC viability (Tsuji, Rubin and Marra, 2014). It has been suggested that ADSCs niches are in the vasculature or perivascular zones of adipose tissue (Yoshimura, Sato, Aoi, Kurita, Hirohi, *et al.*, 2008; Tsuji, Rubin and Marra, 2014). This localisation allows ADSCs to be in contact with the inner endothelium and help initiate stable vascularisation during angiogenic responses, which is necessary to restore the microenvironment for tissue remodelling in skin regeneration (Natesan *et al.*, 2011).

In order to isolate ADSC from adipose tissue, it is necessary to use an enzymatic digestion with collagenase, to break the tissue. Then, a series of washes are necessary to remove any remaining traces of the enzyme, lipid, connective tissue, and other cells present (Bunnell *et al.*, 2008). ADSCs are easily cultured and expanded *in vitro* and can be used for soft tissue wound healing thanks to their multipotency, the facility to obtain them and their capability to promote regeneration and angiogenesis (Tsuji, Rubin and Marra, 2014; Klar, Zimoch and Biedermann, 2017).

As a result, ADSC are easy to harvest and expand making them a promising tool for regenerative medicine. Apart from the differentiation potential of ADSC, it has been reported that stromal cells can modify the microenvironment of a wounded tissue by secreting soluble factors which contribute to its regeneration (Pu *et al.*, 2017). As a result, they can regulate other cells such as fibroblasts, monocytes, macrophages and endothelial cells; which are all part of wound healing process (Chung *et al.*, 2015).

1.4.1 Adipose-derived Stromal Cells and Angiogenesis

Eke *et al*., (2017) develop ADSC loaded bicomponent polymer network (BCN) hydrogels using gelatin and hyaluronic acid. They tested the ADSC loaded BCN

hydrogels on chick aortic ring and CAM assay. It was suggested that the hydrogels induced an increased sprouts on the aortic ring and angiogenesis on the CAM assay due to ADSC paracrine activity (Eke *et al.*, 2017). Nakagami *et al.,* (2005) tested the paracrine molecules secreted by ADSC using their conditioned media on endothelial cells. They reported that ADSC conditioned media increased significantly the viability and tube formation on endothelial cells (Nakagami *et al.*, 2005). Tomaszewski *et al.,* (2019) studied the secreted factors by ADSC in 2D and 3D cultures. They found that the molecules secreted by ADSC are dependent on the physical environment and period of time of culture (Tomaszewski *et al.*, 2019). However, it has been reported that ADSC secrete pro-angiogenic factors when they are cultured in 2D, such as VEGF, FGF, PLGF, ANG, IL-6, and HGF (Efimenko *et al.*, 2014; Li *et al.*, 2014; Pu *et al.*, 2017).

1.4.2 Adipose-derived stromal cell challenges and regulation

In the future, a standardised cell line of ADSCs could be a promising tool for skin engineering, taking advantage of ADSCs low antigenicity and potent immunomodulatory effect (Klar, Zimoch and Biedermann, 2017). However, one of the challenges for ADSCs clinical application is their transplantation into the host. Selecting the correct scaffold or vehicle to deliver ADSC is a critical step in taking ADSCs into clinic as a wound healing treatment because cells must survive until effective angiogenesis occurs.

Moreover, to isolate ADSC an enzymatic treatment is required, which could introduce biological contamination. In addition, ADSC cell culture to expand the cells to have a sufficient number for treatment could take weeks and, in many cases, patients cannot wait that long for a treatment. Finally, transplantation of ADSC without any ECM to protect them into a wounded area leads to the elimination of the ADSC by the immune system (Sun *et al.*, 2017).

Another concern about stromal cell related treatments is the possibility of cancer development. Preisner *et al*., (2017) demonstrated that ADSC interact with melanoma

cells in a paracrine way, and this cross-communication led to changes in gene expression, protein secretion, and promotion of both cell migration and invasion. However, according to Bateman *et al.*, (2018) in the studies all the studies using ADSC there has not been any case of ectopic tissue formation proving they are safe cell therapy. In addition, they have been there are studies that suggest that ADSC may promote cancer cell apoptosis. Wu *et al.*, (2019) studied the effect of ADSC conditioned media in different breast cancer cell lines and non-cancerous breast cell lines. They reported that the cancerous breast cells presented DNA damage and activation of DNA damage signalling leading to apoptosis after being treated with ADSC conditioned media. While the non-cancerous breast cells did not present any damage when treated in equal conditions. Similarly, Xie *et al.,* (2018) treated liver cancer cells with conditioned media from ADSC and found a downregulation in migration and invasion signals in liver cancer cells *in vitro*. This downregulation results not only in a reduced migration, but also in an inhibition of cancer cells to proliferate, move and adhere (Xie *et al.*, 2018).

Finally, using ADSC for clinical applications involves different legal regulations and different organisations. The National Institute of Health (NIH) from USA and the Food and Drug Administration (FDA) made available a public database in 2008 with the different registered clinical trials in a wide variety of diseases (Locke, Feisst and Meidinger, 2015). Under the search “adipose stromal cells” or “adipose stem cells” it was possible to find 410 different clinical trials around the world; however, only 6 of them are for skin wound research (National Library of Medicien, 2020). It is surprising that the actual number of clinical trials on skin wounds that involve stromal cells is low. However, it is important to take into account that each country has different regulations for the research and application of these type of cells.

The Medicine and Healthcare products Regulatory Agency (MHRA) is the organisation that regulates the use of advanced therapeutic medicinal products, including those with cell therapy, in clinical trials in the UK. In the production of a medical device in the UK, it is necessary to have authorisation from the MHRA and the European Medicine Agency (EMA). Also, since 2007, any human tissue that will be used in patient treatment must have all the requirements requested from the European Union Tissue

and Cells Directive (EUTCD). These regulations are procurement, testing, processing, storage, distribution and import/export of tissue and cells used for human treatment (Human Tissue Authority, 2020). The lack of any of the approvals mentioned above could affect application for the authorisation of a medical product (Human Tissue Authority, 2020). During the enzymatic digestion of adipose tissue not only ADSC can be obtained, but different types of cells present on the tissue are isolated. These cells that form the stromal vascular fraction of the tissue are believed to support and boost the regenerative potential of ADSC. As a result, it is also important to study in more detail the stromal vascular fraction.

1.5 Stromal Vascular Fraction

Adipose tissue is mainly composed of adipocytes that not only store energy, but also, form a protective layer for inner organs and produce specific hormones to control energy homeostasis (Volz, Huber and Kluger, 2016). It is composed of a variety of cell types in which adipocytes are the highest volumetric component, but they only represent 20% of all cells in adipose tissue (Spiekman *et al.*, 2017). When this tissue is submitted to enzymatic digestion to remove adipocytes and fibrous tissue, a mixture of stromal and vascular cells known as stromal-vascular fraction (SVF) is generated (Figure 1.4). SVF is composed of blood cells, fibroblasts, pericytes, endothelial cells and adipocyte progenitors (Bunnell *et al.*, 2008). It is important to mention that approximately between 1 and 10% of the SVF are ADSC (Kilinc *et al.*, 2018).

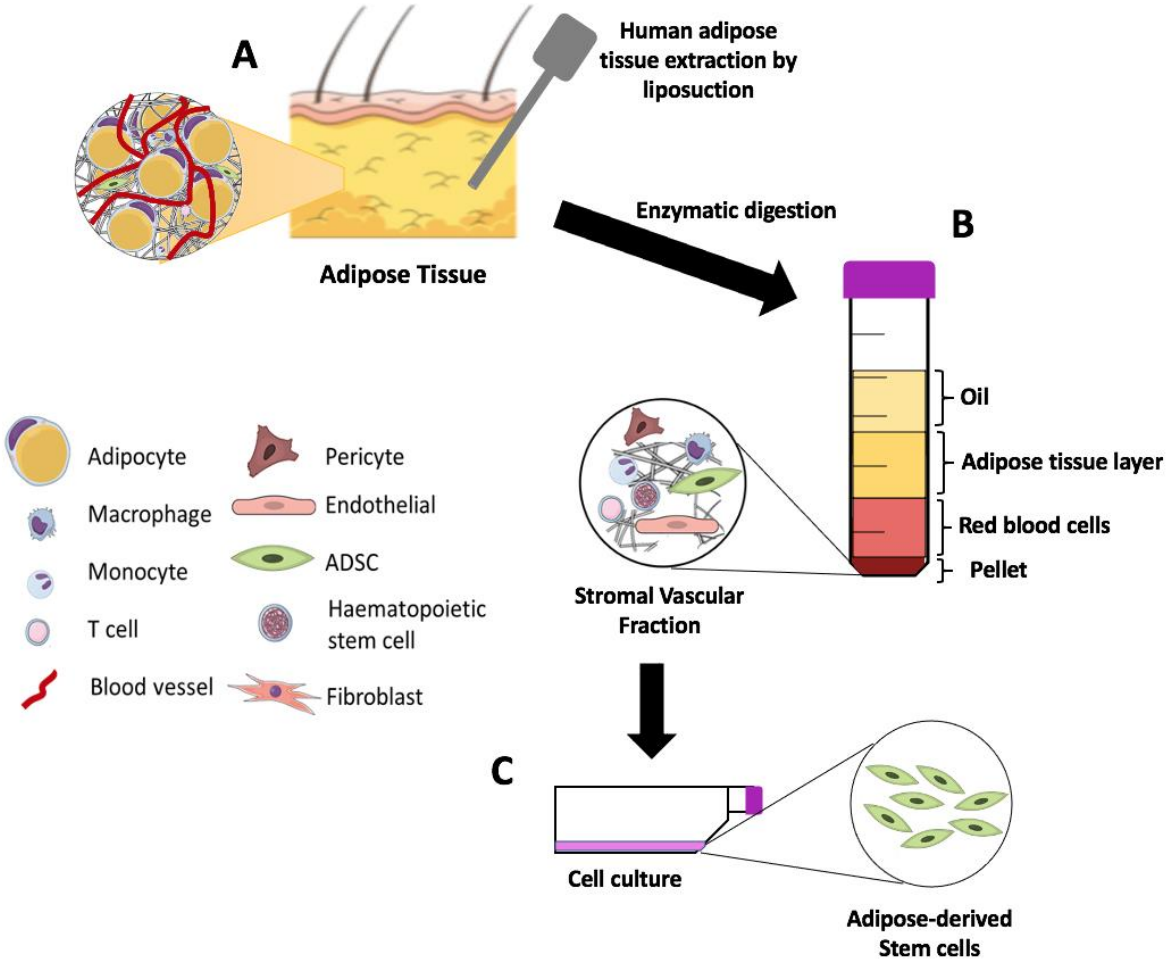

Figure 1.4 Schematic diagram showing adipose tissue composition and lipoaspiration of subcutaneous fat (A) after enzymatic digestion and centrifugation displaying the different layers obtained (oil, adipose tissue, a layer composed mainly of red blood cells and plasma and stromal vascular fraction) (B). And isolation of ADSC for their plastic adherence characteristic (C).

Different research groups have made an approximation of cell yield of adipose tissue, which is collated in Table 1.2. An advantage of freshly isolated SVF is that it can be stored frozen by cryopreservation without affecting cell viability, surface markers or differentiation potential for further use when the patient requires it, similar to an off-the-shelf products (Wittmann *et al.*, 2015). However, cultured SVF loses its initial characteristics making it hard to expand. Endothelial cell population in SVF, which play an important role in blood vessel formation, are lost during 2D cultures due to their lack of adherence to plastic, while ADSCs capacity to adhere to plastic is used to isolate them from SVF (Klar *et al.*, 2014). However, if SVF is cultured in 3D hydrogels,

it retains most of the characteristics of fresh SVF and has superior results to 2D cell cultures *in vivo* presenting a faster neovascularisation when it is implanted into the host body (Park *et al.*, 2013; Wittmann *et al.*, 2015).

Table 1.2 Cell yield from adipose tissue

Reference	Technique used to isolate cells	Number of cells in adipose tissue	Percentage of ADSC
The Regenerative Stem Cell Institute, 2017	Lipoaspirate digested by collagenase	0.5-2x10^6 cells per gram of adipose tissue (SVF only)	Between 1 to 10% of the total cells are adult stem cells (around 4x10^3-2x10^5 in quantity)
Aust *et al.*, 2004	Lipoaspirate digested by collagenase	2x10^8 nucleated cells per 100 ml of lipoaspirate	No data
Hutmacher *et al.*, 2009	No data	2x10^8 nucleated cells per 100 ml of lipoaspirate	No data
Baer and Geiger, 2012	No data	0.5-2x10^6 cells per gram of adipose tissue (SVF only)	5x10^4-2x10^5 stem cells per gram of fat (around 1-10% of the SVF)
Maijub *et al.*, 2015	Human adipose tissue digested by collagenase	1x10^6cells per gram of fat (SVF only)	No data

1.5.1 SVF in regenerative medicine

Atalay, Coruh and Deniz, (2014) describe SVF as a source of anti-apoptotic, anti-inflammatory, antioxidant, and immune-modulatory factors that act by direct immune suppression/tolerance-inducing ability that can be highly beneficial for wound healing. According to Chae *et al.*, (2017) SVF has strong wound healing potential as well as high chemotactic and epithelialisation properties. In the same way, Jin *et al*. (2017) suggest that endothelial progenitors present in the SVF boost blood vessel development, while in conjunction all the different cells present in SVF secrete crucial angiogenic factors such as Ang-1, IL-8, IGF-1, VEGF-A and PDGF-b. In their study, it was seen that high levels of Ang-1 interacting with VEGF-A stimulated micro vessel-like network formation; whilst, PDGF-b and IGF-1 might stimulate endothelial proliferation, angiogenesis or angiogenic synergism in combination with VEGF-A, FGF, IGF-1 and PDGF. Also, the endothelial cells in the SVF play an important role as paracrine mediators and regulate ADSCs by releasing PDGF (Mashiko *et al.*,

2017). The combination of cells may enhance the angiogenic properties of ADSCs making SVF a suitable alternative to promote vascularisation in skin wounds (Jin *et al.*, 2017).

A significant step to transfer SVF into clinic is to define an adequate SVF concentration to promote vascularisation in wounded tissue. Maijub *et al*. (2015) determined that SVF supported dose-dependent vasculogenesis *in vivo*. However, concentrations of 10^9 cells/ml or even higher doses are normally applied in clinical trials for cell-based technologies (Maijub *et al.*, 2015). Adipose tissue differs between patients and the place of the body from which it is extracted. As a result, it is difficult to approximate a standard cell yield from a specific amount of adipose tissue.

Kilinc *et al.* (2018) tested the efficiency of freshly isolated SVF autologous injections in patients of different ages and medical conditions (classified into orthopaedic problems, organ or tissue dysfunctions, and autoimmune diseases). The results show that patient age doesn't significantly affect SVF treatment efficiency. Also, the health condition did not make any difference in clinical outcome since patients gained similar beneficial results even when the treatment was either applied directly to the damaged area or injected into the bloodstream. In addition, they analysed the yield of adipose-derived cells according to gender, BMI, and in patients with and without cancer. They found that these factors (gender, age, physiological condition, and cancer) affected the number of isolated cells, since in cancerous patients the cell yield was lower than in healthy patients and women in general had a higher cell isolation rate than men (Kilinc *et al.*, 2018).

Zakhari *et al.,* (2018) tested the ability of adipose-derived SVF to undergo vasculogenesis (ability to form new vessels from cellular components) *in vitro*. They cultured freshly isolated SVF in Matrigel for a seven-day period. They reported that SVF has the ability not only to undergo angiogenesis, but also vasculogenesis. In this case they observed that SVF not only formed tubular-like structures, but also tip cell formation, and branching forming a complex vessel network (Zakhari *et al.*, 2018). Costa *et al.,* (2017) developed SVF-cell based sheets by culturing fresh isolated SVF at high densities under hypoxic conditions for 8 days. Then these constructs were

transplanted to a mouse hind limb ischemia model. SVF cell sheets were able to promote vascularisation in the surrounding area of the implantation area helping the regeneration of the damaged area. Similarly, Bi *et al.,* (2019) injected subcutaneously SVF in a mouse skin wound healing model. The mice treated with SVF healed significantly more rapidly than the controls. Using immunohistochemistry, they found that SVF induced fibroblasts to produce more collagen and endothelial cells to create a microvascular network in the wounded area. Both mechanisms are strongly associated with skin wound healing, so they suggest that SVF promotes skin wound healing by stimulating angiogenesis and collagen production (Bi *et al.*, 2019).

SVF is a promising tool for regenerative medicine; nevertheless, there are some concerns around using it clinically. Similar to ADSC (Section 1.4.2), tumour formation is one of the principal concerns of using SVF. However, in all the studies carried out in the last 5 years with SVF there has not been any ectopic tissue formation suggesting it is a safe cellular therapy (Bateman *et al.*, 2018). As mentioned before (Section 1.4.2), one of the problems of isolating ADSCs or SVF is that adipose tissue needs to be digested by enzymes such as collagenase, dispase or trypsin to break the fibrous matrix of the tissue. Steps that follow the enzymatic digestion include washing, centrifugation and filtration of obtained material. This protocol is far from ideal for many clinical applications even though it is useful for laboratory investigations. The main problems are endotoxin residues, other protease activities, inconsistency in enzyme activity and cell surface marker cleavage that hamper the use of enzymes. As a result, there is a necessity to develop automated systems with standardisation of the results or to avoid enzymatic use (Klar, Zimoch and Biedermann, 2017). In order to avoid the procedures required to obtain ADSC or SVF, the use of whole adipose tissue has called the attention of researchers as an alternative for new regenerative medicine treatments.

1.6 Adipose tissue

Adipose tissue is composed of large, rounded adipocytes and other, smaller, cell types, including ADSC, with a complex network of capillaries running between the adipocytes (Nishimura *et al.*, 2007; Maclean *et al.*, 2015). Adipose tissue is a dynamic and multifunctional organ. One of the main functions of this tissue is to store energy as triglyceride. Adipocytes are used for long-term storage of energy (triglyceride), and during weight gain and loss they undergo constant remodelling according to the gain or loss of stored energy (Maclean *et al.*, 2015). These changes of mass in the tissue are always accompanied with changes in the microcirculation (Rojas-Rodriguez *et al.*, 2014). As part of this process, adipose tissue plays an important role as an endocrine organ thanks to its adipocytokines or humoral factors that regulate a variety of metabolic and vascular systems (Nishimura *et al.*, 2007). Adipose tissues' angiogenic ability (change its blood vessel volume) to adapt to rapid changes of volume, plus the complex adipocytokines secreted make adipose tissue a potential tool for regenerative medicine.

In clinic is common that before re-injecting the adipose tissue the issue that was harvested (lipoaspirate in most of the cases) is centrifuged at 1200 g for 3 min to remove oils and liquid portion to obtain what is called Coleman fat (Zhang *et al.*, 2018). Nevertheless, different methods to apply adipose tissue grafts have been developed such as tissue emulsification (emulsified fat), concentrating the cells in the tissue by removing adipocytes and lipids (SVF-gel), or only using the SVF. In Figure 1.5, the different protocols in which adipose tissue can be processed are illustrated, including the isolation of ADSC. In the following sections each of them will be explained in more detail along with their importance in vascularisation of skin wound healing.

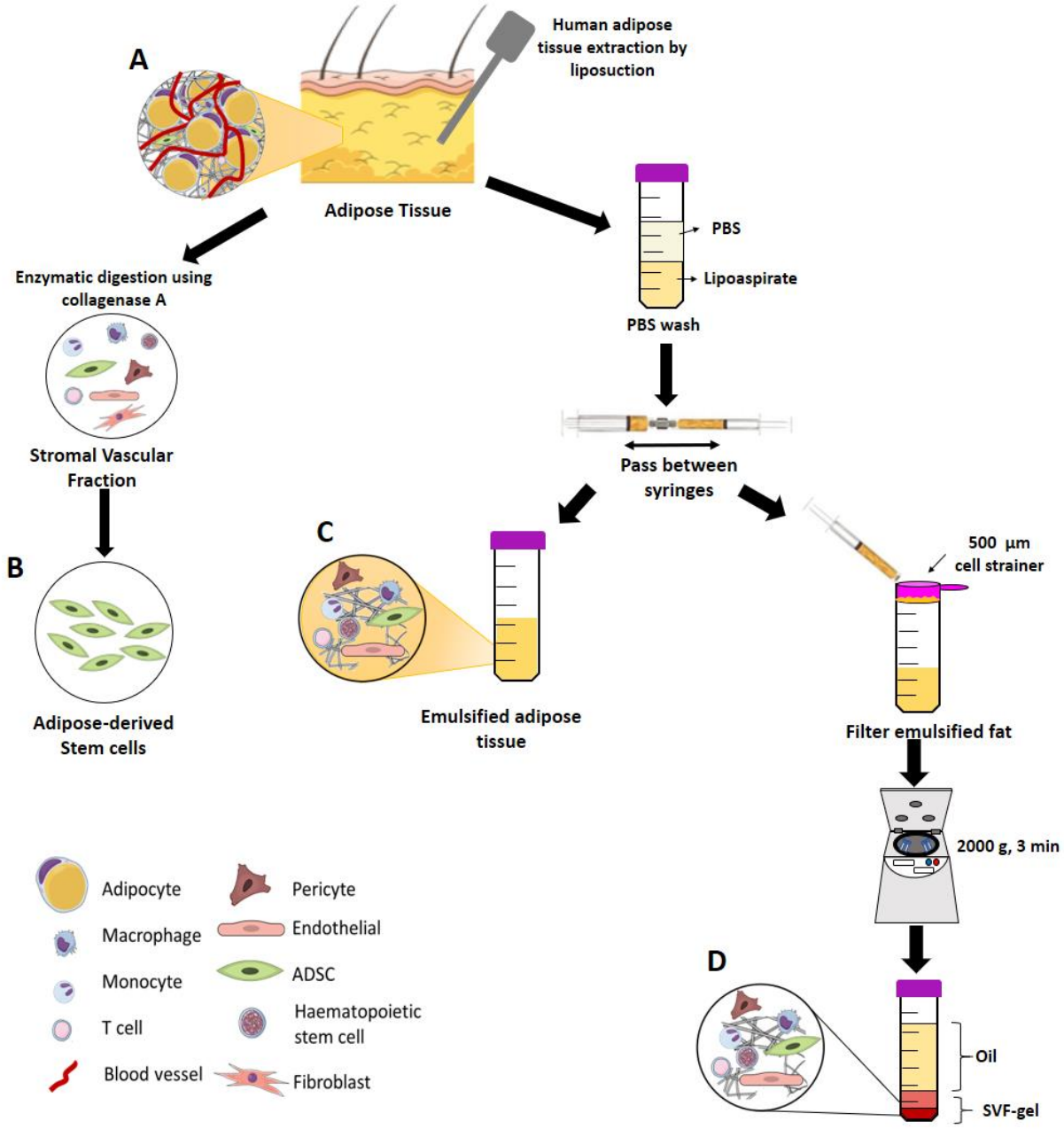

Figure 1.5 Schematic diagram illustrating different protocols to process adipose tissue for skin regenerative medicine, starting with whole tissue (A), extracted typically by liposuction. An enzymatic digestion is used to isolate ADSC from the whole tissue (B). Al Alternatively, lipoaspirate is washed with PBS before digesting it mechanically passing the sample multiple times between two connected syringes. As a result, emulsified fat is produced (C). If emulsified fat is then filtered using 500 µm cell strainer to remove the connective tissue and centrifuged at high speed. Four different phases are formed and the top oily one is removed to generate SVF-gel (D).

1.6.1 Adipose tissue in regenerative medicine

Currently, adipose tissue is used as a filler for contour deformities or volume enhancement in breast reconstruction or augmentation and facial rejuvenation. Adipose tissue is a densely vascularised organ that has low tolerance to ischemia (Zhang *et al.*, 2018). Therefore, revascularisation after adipose tissue transplantation needs to be rapid to allow the adipose tissue to survive (Wittmann *et al.*, 2015). Lipofilling has been used to improve scar appearance, making them less visible and more similar to normal skin (Spiekman *et al.*, 2017). Likewise, Maione and their team (2014) applied lipofilling in different pathological conditions such as severe burn scars, chronic ulcers and scars in the mammary region after surgical treatment. They found that treating burn scars with adipose tissue grafts improved scar formation making the tissue softer and less retracted. In patients with chronic ulcers they observed healing after lipofilling thanks to the regenerative properties of adipose tissue. Finally, they found that lipofilling improved pain control in patients that underwent surgery in the mammary region after breast cancer. They hypothesised that adipose tissue grafting induced architectural remodelling thus reducing fibrotic tissue formation and nerve scar entrapment (Maione, Memeo, *et al.*, 2014; Maione, Vinci, *et al.*, 2014)

One of the major inconveniences of lipofilling is that up to 70-100% of the initial injected tissue volume undergoes resorption as a consequence of the lack of angiogenesis, leading to apoptosis and chronic adipose tissue necrosis (Shukla, Morrison and Shayan, 2015). As a result, patients need to be submitted to several surgical procedures (liposuctions) to obtain long term results. To improve lipofilling outcomes, adipose tissue grafts should be transplanted to areas of the body with native structural adipose tissue deposits; however adipose tissue grafting is not always needed in areas with this characteristic (Alexander, 2016). One way to boost lipofilling outcomes is by combining lipofilling with isolated ADSCs or stromal vascular fraction (SVF; discussed in further detail in Section 1.5) in order to improve adipose tissue graft survival (Spiekman *et al.*, 2017). Kang *et al*. (2009) developed an aqueous silk 3D scaffold model with co-culture of human vascularised adipose tissue, adipose-derived stem cells and human umbilical vein endothelial cells. Endothelial lumens were formed after 2 weeks of the co-culture (Kang, Gimble and Kaplan, 2009).

Additionally, transplanted adipose tissue with non-cultured adipose-derived stem cells into an *in vivo* murine model improved long term graft retention containing a higher density of capillaries after 6 or 9 months of transplantation than transplantation with adipose tissue alone. This may occur as a result of pro-angiogenic growth factors secreted by adipose-derived stem cells (Tobita, Orbay and Mizuno, 2011; Baer and Geiger, 2012)

Adipose tissue grafts cannot only be enriched with ADSC, but also SVF can be added to improve lipofilling outcome. Yoshimura *et al*. (2008) tested the effect of SVF isolated from adipose tissue extracted by liposuction. Half of the harvested tissue was used to isolate the SVF and then added to the other half of the harvested tissue to generate cell-assisted lipotransfer (CAL). With this new technique, CAL, it was seen that SVF improved graft survival for 12 months with no fibrotic tissue formed. The CAL technique has also been applied to improve facial disfiguration in patients with lipoatrophy, with advantages in results over the conventional surgical methods such as lack of scarring and adaptability to be applied in the required shape of the facial defect (Yoshimura, *et al.*, 2008). One disadvantage of adipose tissue is that it can be hard to manipulate, especially if lipofilling is needed in small and superficial areas. As a result, another alternative that has been calling researchers and clinicians attention is to use emulsified adipose tissue, which requires minimal manipulation and can be carried out in a single surgical procedure, seems to have important properties for wound healing and vascularisation with a composition that is easier to handle than the whole adipose tissue.

1.7 Emulsified fat

Emulsified fat, also known as nanofat, is obtained by mechanical emulsification of adipose tissue (Tonnard *et al.*, 2013). Passing the fat between two syringes connected to each other creates a shear force that results in ECM and adipocyte rupture, while the rest of the cells, SVF, remain intact with a similar viability as adipose tissue or lipoaspirate (Figure 1.5) (Alexander, 2016; Yao *et al.*, 2017). As a result, the emulsification process can be considered an SVF /ADSC enrichment process without

an enzymatic process (Cai *et al.*, 2019). Mashiko *et al*. (2017) analysed adipose tissue and emulsified fat microscopically using different dyes for adipocytes and endothelial cells. They found that adipose tissue has compactly packed adipocytes with blood vessels; while emulsified fat presented structural damage including dead space and disrupted capillaries between cells and no large blood vessels. One of the main advantages of emulsified fat is that it is easy to handle, and it can be injected using small needles (Alexander, 2016).

1.7.1 Emulsified fat in regenerative medicine

Emulsified fat has previously been used clinically for wound healing, and anti-aging treatments with positive outcomes (Tonnard *et al.*, 2013), however the underlying mechanism is still not known (Xu *et al.*, 2018). It has been suggested that emulsification of the tissue enhances its wound healing properties thanks to the presence of SVF, including ADSC and growth factors that are released during tissue processing (Cai *et al.*, 2019). According to Yao *et al.*, (2017), ADSC are present in emulsified fat at around $1x10^4$ ADSC per ml, comparable to unprocessed adipose tissue. Moreover, emulsified fat is rich in growth factors such as VEGF, EGF, IGF, IL-6, and bFGF, which play important roles in wound healing (Alexander, 2016; Cai *et al.*, 2019).

Xu *et al.* (2018) injected subcutaneous emulsified fat and ADSC to investigate their healing properties on a photoaging skin model in nude mice. They found that the injected emulsified fat and ADSC were absorbed within 8 days after injection with an improvement in skin thickness and an increase of capillary density suggesting that both groups participated in early stages of skin wound healing. On the other hand, Tonnard *et al.* (2013) performed emulsified fat grafting on 67 different patients with a variety of skin problems, with the main goal of skin rejuvenation. In the beginning the researchers were trying to fill rhytids. Nevertheless, they found that emulsified fat grafting had a rejuvenation effect resulting in changing their main proposal to “improve skin quality”. Intradermal injections of emulsified fat may be used in small volumes to obtain a soft-tissue filling effect in which the graft is “layered more fanwise in an

intradermal level to enhance the skin quality" (Tonnard *et al.*, 2013). While the lipid found in emulsified fat provides a carrier for SVF injection there are concerns some adipocytes and oils from the adipose tissue that could induce a chronic inflammation response in the host body (Zhang *et al.*, 2018). As a result, an innovative approach has been developed to remove the oils and adipocytes thus generating SVF-gel to enhance its healing properties.

1.8 Stromal Vascular Fraction-gel

Adipose tissue grafting normally results in poor survival of the graft since adipocytes have a low tolerance for hypoxic environments. As a result, the removal of adipocytes could enhance regenerative activity in the SVF. SVF-gel is the result of removing most of the adipocytes, oil and tumescent fluid from adipose tissue without using enzymatic digestion, thus leaving a thick solution containing the ECM with SVF, called "extracellular matrix/stromal vascular fraction gel" (Yao *et al.*, 2017). To produce SVF-gel, emulsified fat is filtered through 500 µm mesh and then centrifuged for 3 min at high speed (2 000 g). The tissue is separated into 4 layers: the superior oily layer, the second fatty layer, then the third pink aqueous layer, and finally the cell pellet containing the SVF cell population (see Figure 1.5) (He *et al.*, 2019).

The final volume of SVF-gel is approximately one-tenth of the original adipose tissue volume, since adipocytes compose 90% (by volume) of adipose tissue, which means it has a high cell density greater than 4 x10^5 cell/ml (Yao *et al.*, 2017; Cai *et al.*, 2019). In addition, SVF-gel contains ECM which is rich in growth factors giving support for the SVF cell population preventing rapid migration and stem cell apoptosis (Deng *et al.*, 2017; Sun *et al.*, 2017). One of the problems of SVF-gel is that large amounts of lipoaspirate or adipose tissue are needed to produce it, which could be difficult particularly for those patients with low BMI (Zhang *et al.*, 2018). However, SVF-gel is easy to inject since it can be injected using a 27-gauge sharp needle (Yao *et al.*, 2017)

1.8.1 SVF-gel in regenerative medicine

Yao *et al*. (2017) compared the *in vivo* healing properties of SVF and SVF-gel by applying the same number of cells into cutaneous wounds in nude mice. They found that SVF-gel produced a faster healing process than SVF as a possible result of SVF-gel retaining its natural ECM, providing a native environment for the cells and thus enhancing their healing properties. Zhang *et al.* (2018) analysed retention of SVF-gel and SVF after subcutaneous injection into nude mice. They found that SVF-gel showed better long-term retention than SVF; maintaining more than the 80% of its original volume, while SVF retained only around 40%. Also, the SVF-gel did not show signs of necrosis and the SVF-gel components developed into vessel-associated structures that were assumed to be connected to the host blood supply, promoting a faster vascularisation within the SVF-gel graft. In all the cases, cytokines released by cells in SVF-gel emulsified fat, ADSC, and SVF play an important role in wound healing (Zhang *et al.*, 2018).

Zakhari *et al*., (2018) seeded SVF isolated from adipose tissue onto a Matrigel coated surface to observe its potential to generate tubular structures. They reported that the different cell populations on the SVF underwent vasculogenesis and angiogenic processes since different phases such as cell clustering, tip cell formation, stalk cell formation, branching and complex network formation were observed after 112 hr of culture. This study suggests that the angiogenic properties of the SVF are not only the secretion of growth factors, but also the potential to self-assembly to form new vessels (Zakhari *et al.*, 2018).

Sun *et al*., (2017) treated skin wounded mice with local injections of SVF-gel. The wounded area was monitored, and their results show that SVF-gel treated mice presented a faster wound closure compared to the control group. They found high levels of vascularisation around the tissue that was injured, suggesting that the SVF-gel wound healing properties are due to its ability to induce angiogenesis (Sun *et al.*, 2017). Similarly, Cai *et al.,* (2019) studied the effect of SVF-gel in a rat skin flap model by subcutaneously injecting SVF-gel. They reported that SVF-gel improved flap survival as a result of its paracrine effect. Also, they suggested that the ECM remaining

within the SVF-gel protected and gave support to the SVF cells to maintain their viability and function (Cai *et al.*, 2019). It has been suggested by different authors that the potential of ADSC, or adipose tissue and its derivatives that their wound healing properties are a result of their paracrine effect. As a result, an alternative to treat soft tissue wounds is to take advantage of cytokine secretion in order to produce non-cellular therapies to enhance wound healing. The best example of a non-cellular method to introduce cytokines is conditioned medium.

1.9 Conditioned Medium

In vitro cultured ADSC in which the cells release trophic factors into the media generates what is called conditioned medium. This medium without cells can reproduce the same regenerative effect as ADSC transplantation (Locke, Feisst and Meidinger, 2015). In addition this is a potential cell free therapy resulting in lower risk of immune response and lack of tumorigenicity (Locke, Feisst and Meidinger, 2015). Another benefit of conditioned media is that it could be produced as an off-the-shelf product that would be ready for patients whenever it is needed (Sagaradze *et al.*, 2019). Shukla *et al*. (2015) and Locke *et al.* (2015) describe that preconditioned ADSC media without cells had the same effect as immune-modulation and secretion of growth factors; which may be the path to enhance tissue regeneration making conditioned media a promising tool for regenerative medicine.

To produce conditioned media there is no specific protocol. Different research groups use different seeding concentrations and different incubation times (Table 1.3). Most of the conditioned media is produced at high seeding densities or using highly confluent cultures. Also, the incubation time is normally around 2-3 days, although there are some cases in which cultures are left for over a week or just 24 hours. In addition, the media used plays an important role and normally is the media compatible with the cells in which it will be tested. The media should have a low serum concentration to avoid the serum generating confounding or non-reproducible results, but the media itself should sustain ADSC culture to allow the cells to release cytokines into the media.

Normally, the conditioned media is collected from 2D cultures (on flat surface). However, there is a tendency to collect the media from 3D cultures (three dimensional

environment) since the cell environment could affect the expression of ADSC cytokines and 3D cultures provide a more physiologically suitable condition for cells (Kim *et al.*, 2018; Tomaszewski *et al.*, 2019). Kim *et al*. collected ADSC conditioned media from 2D and 3D cultures and analysed the cytokines released from each one. They found that different growth factors were produced by growing cells in 2D and 3D, where 3D cultures produced more cytokines related to ECM such as β-actin, collagen I and II (Kim *et al.*, 2018). In addition, Tomaszewski *et al*. (2019) found that 2D cultures produced more dynamic conditioned media over time than 3D cultures. This change in cytokine production along time in 2D cultures might be a result of ADSC differentiating over time; nevertheless, this is not the case in 3D cultures which maintain a constant cytokine production throughout the culture time (Tomaszewski *et al.*, 2019).

Table 1.3 Different methods for producing conditioned media highlighting different seeding densities and incubation times.

Type of cells	Seeding cells	Time of incubation	Media	Study
Rat adipose-derived mesenchymal stem cells	$2x10^3$ cells/cm^2 in 6 well plate ($2x10^5$ cells/well). 2D and 3D cultures using AlgiMatrix.	2 days	StemPro MSC SFM CTS medium (Gibco)	Xie *et al.*, 2018
	$2x10^4$ cells/cm^2 in 6 well plate. 2D cultures.	24 hrs	SFM (type unstated)	Huang *et al.*, 2017
Human adipose-derived mesenchymal stem cells	445 cells/cm^2 in 6 well plate ($4x10^4$ cells/well). 2D culture.	5 days	60% of DMEM-HG (Invitrogen) and 40% MCDB-201 supplemented with 2% FCS (Becton Dickinson)	Preisner *et al.*, 2017
Human adipose-derived mesenchymal stem cells	80% confluent. 2D cultures	7 days	DMEM-LG SFM	Kamalov *et al.*, 2017
	70-80% confluent. 2D cultures	2 days	Supplement-free ASCBM (Sigma-Aldrich)	Efimenko *et al.*, 2014
	70% confluent. 2D cultures	3 days	L-DMEM supplemented with 1% FBS (Gibco)	Li *et al.*, 2014
	Initial seeding density of $1x10^6$ cells/ml in siliconised spinner flasks and cultured for 3 days before changing media for conditioned media collection	2 days	α-MEM SFM (Gibco)	Kwon *et al.*, 2015
	$7.054x10^3$ cells per cm^2 in 100 mm dishes. 2D cultures	3 days	DMEM/F12 SFM (Invitrogen-Gibco-BRL)	Kim *et al.*, 2007
	0.12 ml of lipoaspirate per cm^2 (just after isolation).	3 days	DMEM-Ham's F12 medium (vol/vol 1:1) supplemented with antimycotic solution (Invitrogen) supplemented with 10% FBS	Aust *et al.*, 2004
	1.33 $x10^4$ cells per cm^2 (in T25 with 5 ml of media). 2D culture.	2 days	α-MEM and F-12 (vol/vol 1:1) (Gibco) supplemented with 1 mg/ml bovine fetuin	Tomaszewski *et al.*, 2019
	80% confluent. 2D cultures.	2 days	DMEM SFM	Jin *et al.*, 2017
	100% confluence. 2D cultures	Cultured until cells achieved confluence	DMEM supplemented with 20% Fresh Frozen Human Plasma	Noverina *et al.*, 2019
Stromal Vascular Fraction	Hyperconfluence (forming a robust cell monolayer). 2D culture	5 to 8 days	α-MEM supplemented with 10% FBS	Costa *et al.*, 2017
Human adipose tissue	~333 mg/ml	24 hrs	DMEM/F12 supplemented with 10% FCS	Klimcakova *et al.*, 2007

MSC = Mesenchymal Stem Cell Culture, SFM = serum free media, CTS = Culture media for cell Therapy Systems, DMEM= Dulbecco's Modified Eagle's Medium, DMEM-HG = High glucose DMEM, DMEM-LG = Low glucose DMEM, FCS = Fetal Calf Serum, ASCBM = Advanced Stem Cell Basal Medium, FBS = Fetal Bovine Serum, L-DMEM = Low glutamine DMEM, α-MEM = Minimum Essential Media, DMEM/F12 = Mixture of DMEM and Ham's F12 medium.

1.10 Summary of adipose related treatments

Although ADSCs in general are an encouraging tool for regenerative medicine, there are some risks in their application. ADSCs may induce cancer growth and metastasis through paracrine properties, epithelial-mesenchymal transition and immunosuppressive mechanisms (Tsuji, Rubin and Marra, 2014). Furthermore, cell isolation from patients takes some time and, in many patients, treatments are required immediately.

In summary, adipose tissues and their derivatives: emulsified fat, SVF-gel, SVF and ADSCs, have vascularisation properties that can enhance the healing process in chronic wounds. Although there have been different studies using adipose tissue, emulsified fat, SVF-gel and ADSCs, their angiogenic potential has not been compared in a single study. In this thesis, we aim to measure the ability of adipose tissue-derived ADSC, adipose tissue, emulsified fat, and SVF-gel to induce angiogenesis. There are several different assays used to study vascularisation as detailed in the next section. In order to determine the effect of fat and its derivatives on angiogenesis various assay are required. *In vitro, in vivo and ex vivo* assays offer different advantages.

1.11 Angiogenesis assays

1.11.1 In vivo assays

In vivo models allow the study of angiogenesis in a living model with all the complex processes, requiring the interaction of different cell types and an intricate balance of cytokines included, that is difficult to reproduce in the laboratory. The models to study angiogenesis *in vivo* are: chorioallantoic membrane (CAM) or chick embryo assay, dorsal skinfold chamber, matrigel plug assay, corneal angiogenesis assay and hindlimb ischemia assay. These assays will be discussed in more detail in the following sections.

1.11.1.1 *Dorsal skinfold chamber*

The dorsal skinfold chamber can be applied in rabbits, rats, nude, immunocompetent or immune-deficient mice and hamsters. Two symmetrical titanium frames are positioned on the shaved animal's dorsal skinfold making a sandwich with the double skin layer. Afterwards, a circular area with a diameter of around 15 mm of one layer of skin is removed, leaving the striated skin muscle, subcutaneous layer, and skin on the remaining tissue. This tissue is covered with a removable coverslip integrated in the titanium frame to create an observation window (Figure 1.6) (Staton *et al.*, 2004; Laschke *et al.*, 2006).

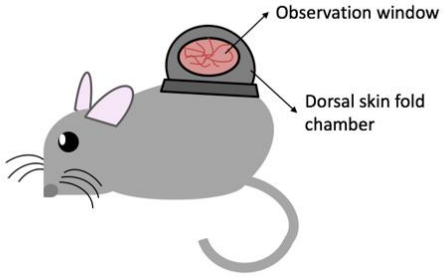

Figure 1.6 Diagram of dorsal skinfold chamber assay

This model is ideal for long term *in vivo* analysis of angiogenesis and blood vessel growth in porous biomaterials due to the fact that the observation glass can be temporarily removed. Cellular and molecular aspects can also be studied with this model such as macrophage activation, leukocyte and platelet adhesion, mast cell degranulation, vascular endothelial leakage and apoptosis or necrotic cell death (Laschke *et al*., 2006). One of the most remarkable advantages of this model is the fact that the microcirculation can be analysed over a period of 1 to 4 weeks (Staton *et al.*, 2004). The main limitation of the skinfold chamber is that the size of the construct to be implanted cannot exceed 5 mm in diameter (width and length) and 1 mm high in order to fit in the chamber (~15 mm diameter) (Laschke *et al.*, 2006). Moreover, the healing process may be affected using the skinfold chamber as the model is enclosed in a chamber limiting air exposure and keratinocyte migration and proliferation (Druecke *et al.*, 2004).

1.11.1.2 *Matrigel plug assay*

Matrigel is harvested from mouse sarcoma cells and composed of extracellular components including laminin and collagen IV with the growth factors EGF, bFGF, PDGF and IGF-1 also present. It is stored at -20ºC and is liquid at 4ºC and solidifies at 37ºC (body temperature). The final gel is implanted subcutaneously into the ventral region of a mouse. After 7-10 days, the Matrigel plug is removed and blood vessel formation can be observed within the gel and quantified by measuring the haemoglobin and histological staining. Pro-angiogenic and anti-angiogenic substances can be added into the Matrigel to test their effect (Adair and Montani, 2010).The advantage of this technique is that in the beginning of the study the Matrigel is avascular, so at the end any vessel that is formed *de novo* in the gel is easily distinguished. However, it is important to use Matrigel formulated without growth factors to avoid the gel itself promoting angiogenesis and interfering with the results. Likewise, results can also be affected by the implantation site, and the age of the mice used for the study (Tahergorabi and Khazaei, 2012).

1.11.1.3 *Corneal angiogenesis assay*

The corneal angiogenesis assay was first designed for use in rabbits, but it has been adapted for mice and rats. The test substances are placed into micro-pockets in the cornea to promote or inhibit vascularisation and the new ingrowth of vessels can be monitored daily due to the transparent nature of the tissue (Adair and Montani, 2010). The main problems of this technique are that the available space for testing substances is limited, and an inflammatory response may be created. Also, it is more expensive compared to the CAM assay (explain in section 1.11.2.1) and researchers could face ethical problems since the assay takes place in a sensory organ (Staton *et al.*, 2004). Nevertheless, the blood vessel formation can be easily observed since the cornea is an avascular tissue, and microvessel density can be distinguished using immunohistochemistry (Tahergorabi and Khazaei, 2012).

1.11.1.4 *Hindlimb ischemia assay*

The hindlimb ischemia assay is used as a mouse model of peripheral arterial disease to study vascular remodelling. The procedure starts by exposing vessels *via* an incision in the middle portion of the hindlimb, followed by ligation of the proximal and distal femoral artery, and the arteries beside side-branches are cut. This results in no blood flow creating a limb ischemia (Padgett *et al.*, 2016). New blood vessels are formed in the ischemic distal location and they can be analysed by histology or laser Doppler perfusion images, counting the capillaries per muscle fibre or capillaries per square millimetre (Tahergorabi & Khazaei, 2012). This technique is very sensitive, however, the result is highly dependent on successful surgery to create an acute hindlimb ischemia. Also, the constrictors used to block the arteries may create variability between models since their quality and shape may vary. Finally, the mice used for a study must be the same age and around the same size, otherwise inconsistent data can be generated (Padgett *et al.*, 2016).

1.11.2 Ex ovo assay

1.11.2.1 *Chick chorioallantoic membrane (CAM) assay*

The CAM assay is an *ex ovo* assay carried out on fertilised chicken eggs. It can be used to investigate aspects of the angiogenesis process including: migration, proliferation and differentiation of endothelial cells, effects of growth factors and cytokines, gene therapy and ECM changes (Adair and Montani, 2010). The CAM assay is performed on the extra-embryonic membrane which is composed of the fusion of the allantois (yolk sac's posterior wall) and the adjacent mesodermal layers of the chorion (outermost membrane around the embryo) (Naik, Brahma and Dixit, 2018). The chorioallantoic membrane characteristically has a dense microvascular network in which the vessels grow rapidly until day eight when some differentiate into capillaries (Figure 1.7).

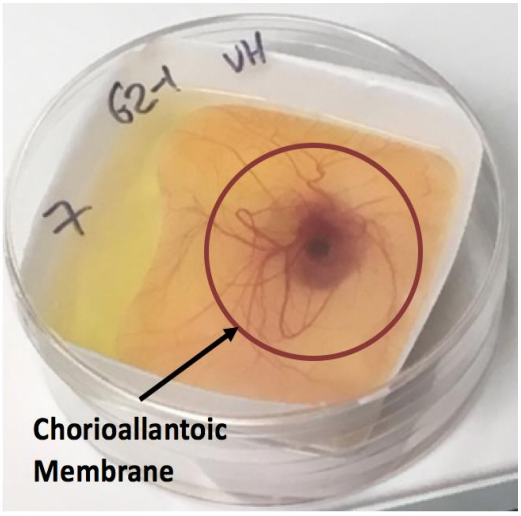

Figure 1.7 Chicken embryo after 7 days of incubation highlighting CAM membrane

Normally, vascularisation increases with the development of the embryo, meaning the CAM reaches its maximum vascularisation potential between incubation days 9 and 12. For this reason, the sample is added to the CAM on day 5 and observations are carried out between incubation days 5 and 14, thus allowing 10 days of study (Laschke *et al.*, 2006). It is important to consider that in this embryonic assay the growth factor profile is different from an adult tissue. Also, the lack of immune system in chick embryos allows xenografts without rejection, making it suitable to test with human cells.

Additionally, the most noteworthy advantages are that CAM is easy to run, low cost and has less-severe restrictions on its use than mammalian models. Finally, since CAM gives a similar response to mammalian models, this model can be used as a mammalian alternative (Mangir *et al.*, 2019). The fact that chick embryos lack a nervous system before day fourteen of gestation help the regulations around this assay since the embryos do not experience pain reducing the ethical restrictions and facilitating the approval process compared to animal assays (Kue *et al.*, 2014). On the other hand, this model has some limitations; only capillaries after maturation (bigger than 10 μm) can be studied, and the lack of immune system makes it impossible to test material for biocompatibility (Laschke *et al.*, 2006). It can also be difficult to

distinguish between actual growth of vessels and dilation of existing ones (Adair and Montani, 2010).

1.11.3 In vitro angiogenesis assays

In vitro assays provide quicker results and are simpler and cheaper than *in vivo* assays. However, in using *in vitro* assays to study vascularisation it is difficult to reproduce all the signals between the different cell types involved in the process, and to maintain cell culture conditions for all of them. Most of the angiogenic *in vitro* assays are carried out on endothelial cells since these cells are the main component of blood vessels. Nevertheless, there are different types of endothelial cells for large or small blood vessels, arteries, veins, and tumour vessels (Adair and Montani, 2010).

Important decisions to plan angiogenic *in vitro* experiments are not only to choose the best endothelial cell type, but also the use of primary cells or a cell line. A relevant model to study angiogenesis should be as close as possible to the phenotype of the primary cell of the studied tissue. In this case, primary cells are the better option. However, they are hard to isolate, have a short *in vitro* lifespan, and lose original characteristics with time (Unger *et al.*, 2002). On the other hand, a cell line is more robust to grow, even though these cells have a modified phenotype from the primary original cells (Unger *et al.*, 2002).

One of the most used cell lines in the study of angiogenesis are human umbilical vein endothelial cells (HUVEC). HUVEC are isolated from umbilical cord and are easy to culture and expand. However, as they are derived from a foetal tissue, their response during *in vitro* studies can differ from an adult endothelial cell (PromoCell, 2017). For studies on microvascular endothelial cells, one of the most commonly used are human microvascular endothelial cell (HMEC-1). This cell line has been immortalised by the transfection of a plasmid with Simian Virus 40 gene (Tat *et al.*, 2015). HMEC-1 can been grown until passage 95 without changes in their morphological and functional characteristics; which are similar to primary endothelial cells including CD31+ marker expression and the ability to form tubular-like structures in Matrigel (Tat *et al.*, 2015).

Finally, of interest to this research, primary human dermal microvascular endothelial cells (HDMEC) are the closest cell type used to study vascularisation of dermal cells *in vitro*. As mentioned before, since HDMEC are primary cells, they have a short *in vitro* lifespan. As a result, for this research it was decided to start experiments using HMEC-1, and in case another model is needed HDMEC would be the second option to create a better studied model.

Once the cell type is chosen, there are different *in vitro* assays that can be used to study vascularisation such as endothelial cell proliferation assays, endothelial cell migration assays and endothelial tube formation assays. Each assay will be discussed in more detail in the following sections.

1.11.3.1 Endothelial cell proliferation assays

Endothelial cell proliferation is necessary to develop blood vessels in living animals. Endothelial cell proliferation assays allow the measurement of effects of pro- and anti-angiogenic factors on endothelial proliferation. Some of the most commonly used techniques to quantify cell proliferation are by measuring DNA synthesis, direct cell content or metabolic activity of viable cells (Riss *et al.*, 2004; Adair and Montani, 2010). To analyse DNA synthesis, bromodeoxyuridine (BrdU), 5-ethynyl-2'-deoxyuridine (EdU), or DNA-binding dyes are used to determine cell-cycle distribution, proliferation state and apoptosis rate. BrdU and EdU compete with thymidine during incorporation into DNA during the S-phase of the cell-cycle and can be detected by immunocytochemistry, enzyme linked immunosorbent assay (ELISA), or flow cytometry (Adair and Montani, 2010; Nowak-Sliwinska *et al.*, 2018). In case of the DNA-binding dyes, the amount of dye can be measured using colourimetry and correlated to the number of cells present in the sample (Staton *et al.*, 2004).

On the other hand, net cell number can be determined with a haemocytometer using a light microscope or an electronic counter. Finally, to measure the overall cell metabolic activity MTT (3-(4,5-dimethylthiazol-2-yl)-2, 5-diphenyltetrazolium) or resazurin assays can be used. MTT reagent generates a blue/purple coloration when

crystals are formed after it reacts with nicotinamide adenine dinucleotide (NADH) (Riss *et al.*, 2004). The crystals can be dissolved in DMSO or acidified isopropanol and analysed by reading absorbance. The colouration is proportional to the cell metabolic activity that can be used to estimate cell proliferation (Tahergorabi and Khazaei, 2012). MTT assay is simple, cheap and fast. One of the disadvantages of MTT assay is that formazan crystals destroy cell integrity leading to cell death (Gilbert and Friedrich, 2017). In contrast, resazurin assay is based on the reduction of resazurin to resorufin by metabolically active cells. Resazurin is dissolved in physiological buffers and it has a blue coloration with a low intrinsic fluorescence, while its reduced form, resorufin, has a fluorescent pink coloration that is permeable through cell membranes. One of the advantages of resazurin assay is that it doesn't kill the cells and the metabolic activity can be measured at different time points throughout cell culture. However, the reaction requires hours of incubation (Gilbert and Friedrich, 2017).

1.11.3.2 Endothelial cell migration assays

Endothelial cell migration is very important during the wound healing process, making endothelial cell migration assays a good option to test angiogenic properties. There are different assays to observe/measure migration including: the modified Boyden chamber, scratch assays, and the phagokinetic track assay. A modified Boyden chamber is used to estimate/observe endothelial cell migration. Boyden chambers contain a filter with 8 µm pores coated with Matrigel, fibronectin or collagen. The endothelial cells are cultured on the filter and on the other side an angiogenic factor to be tested is placed (Adair and Montani, 2010). Cell migration occurs in the direction of the attractant substance, but in order to migrate endothelial cells secrete proteolytic enzymes to degrade the ECM barrier. This assay is rapid, reproducible and has high sensitivity to small differences in concentration gradients since it equilibrates between the different wells over time (Staton *et al.*, 2004). However, it can be difficult to maintain the trans-filter gradient for long periods of time. In addition, it is not possible to measure cell migration distance during the assay (Tahergorabi and Khazaei, 2012).

One of the most frequently used endothelial cell migration assays is scratch assay. This assay came from the idea of cells migrating to a wounded area. Endothelial cells are cultured until they form a confluent monolayer. Then with a scraping tool, or a pipette tip the cell layer is scratched in a straight line to clear that zone of cells and then analyse how cells migrate to that area using microscope images (Figure 1.8). This assay is simple and can be run for a short period of time; around 2-4 days. However, some of the problems of this technique are that the experimental samples and the control must have the same degree of confluence and the denuded area must be precise and the same size for all the samples (Staton *et al.*, 2004).

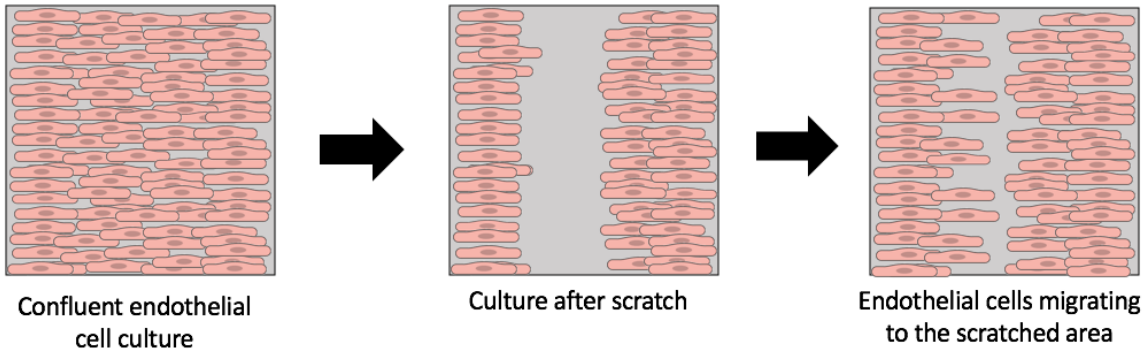

Figure 1.8 Schematic diagram illustrating endothelial cell migration assay by scratching a confluent cell layer and measuring how cells migrate into the scratched area.

An alternative to manually creating the scratch is to use stoppers to create the exclusion zone, which ensures that the denuded area is the same in all the samples (Nowak-Sliwinska *et al.*, 2018). Silicone stoppers can be placed into 96 well plates prior to seeding the cells. Then, cells are seeded in high densities that can reach a confluent monolayer in 24 hours. Stoppers are removed leaving an area without cells and the tested substance is added to the cultures. Cell migration can be studied using a light microscope (Nowak-Sliwinska *et al.*, 2018).

Finally, the phagokinetic track assay is performed on colloidal gold-plated coverslips. The 1 µm gold layer on the coverslip works as a substrate for cell migration that is displaced by cells which leave a track in the gold layer. Even when this assay can be

performed in 96 well plates, the analysis is time consuming and sometimes the interpretation is complex (Auerbach *et al.*, 2003a; Staton *et al.*, 2004). Also, endothelial cells are cultured on a “strange” substance that cannot be found *in vivo*, and a few cells are cultured per well making this model distant from their native environment (Staton *et al.*, 2004).

1.11.3.3 Endothelial tube formation assay

The endothelial tube formation assay is used to analyse the ability of endothelial cells to form tubular structures. For these assays, the matrix used is critical to the results, since the ability of the cells to create tubular structures (tubules mainly formed by tight cell-cell and cell-matrix interaction) depends on the surrounding ECM (Auerbach *et al.*, 2003a). Normally, Matrigel is considered the optimum matrix for tubular formation, which starts just one hour after cell seeding and is completed after 12 hours. On the other hand, collagen IV and V allow generation of extensive tubular formations with minimal cell proliferation; while collagen I and III allow better cell proliferation with occasional tubule construction (Segura *et al.*, 2017). Co-cultures of fibroblasts, smooth muscle cells and blood vessel explants with endothelial cells may enhance tube formation. Though, co-cultures are not well-characterised and it can be difficult to optimise conditions suitable for the different cell types (Tahergorabi and Khazaei, 2012). In general, endothelial tube formation is easy to set up, quantifiable and quick results are obtained (within hours) (DeCicco-Skinner *et al.*, 2014).

1.11.4 Ex vivo angiogenesis assays

Ex vivo assays allow the study of angiogenesis *via* organ culture methods. These reproduce the *in vivo* situation with the presence of many different interacting cell types such as pericytes, fibroblasts, smooth muscle cells and endothelial cells with a supporting matrix, forming vessels very similar to *in vivo* blood vessels (Adair and Montani, 2010). The chick aortic ring assay is one example of an *ex vivo* angiogenesis assay.

1.11.4.1 Aortic ring assay

In the first step of aortic ring assay rat assays a rat's thoracic aortas are removed and cleaned of peri-aortic fibro-adipose tissue that surrounds them. Then, the aortas are cut into 1mm thick rings that are then cultured in Matrigel. The substance to be tested is combined with the media and the microvessel outgrowth is observed for a period of 10-14 days (Eke *et al.*, 2017). There is also a modified version of the rat aortic ring assay in which the aortas are removed from 12-14 days old chick embryos. The advantages of using embryonic chick aortas are that it is quicker (the assay takes 1-3 days (Figure 1.9) instead of 7-21 days with rats), and, the aortas are derived from growing embryos that have endothelial cells with enhanced properties to form microvessel structures (Nowak-Sliwinska *et al.*, 2018). New microvessels can be visualised using fluorescein-labelled lectins and then quantified. The difficulty with both aortic assays is that the explants from different animals may produce variable results, and the tissue used is non-human that could produce doubtful applicability of the information obtained. Also, if the aortas are damaged during their extraction this can cause uneven sprouting adding variability to the experiment (Nowak-Sliwinska *et al.*, 2018). Moreover, there is a lack of blood flow that can produce regression of vessels after some time making the analysis time limited (Baker *et al*., 2012).

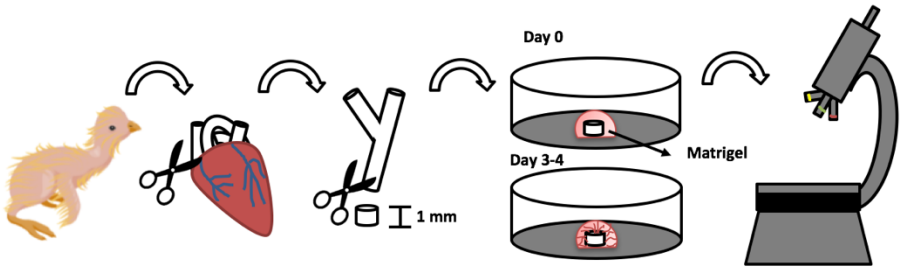

Figure 1.9 Schematic diagram illustrating chick aortic ring assay. Chicken's heart and aorta are extracted; then the aorta is cleaned from any surrounding tissue and cut into 1 mm rings which are cultured in Matrigel with the tested substance for 3-4 days to see the tubular structure formed around the ring by light microscopy.

1.12 Summary

Vascularisation is one of the main challenges in tissue engineering. There have been different strategies to enhance neovascularisation in soft tissue wounds in order to accelerate or in some cases to allow the healing process, but none of them have successfully solved the problem. ADSCs have received a lot of attention in tissue engineering due to their benefits to wound healing, such as greater vessel growth, improved scar tissue formation, a faster healing process and ease of extraction. However, there are technical regulatory and safety challenges to overcome before these can be translated to patients, for example during the adipose tissue digestion process to isolate ADSCs, enzymes and chemicals are used that potentially have harmful effects on patients. Despite this challenge, both SVF and adipose tissue have garnered the attention of the scientific community due to their promising potential use in wound healing. Adipose tissue and its derivatives have the advantage clinically of less regulations. In addition, the combination of ADSCs with other cell populations may enhance adipose tissue and its derivatives vascularisation properties in soft tissue injuries.

1.13 Hypothesis, aims, and objectives

Hypothesis: Factors secreted by adipose tissue and formulations of adipose tissue can promote angiogenesis *in vitro* and *ex vivo*.

Aim: To understand how processing adipose tissue affects its pro-angiogenic capability by comparing conditioned media from: adipose derived-stromal cells (ADSC), adipose tissue, emulsified fat, and SVF-gel in *in vitro* and *ex vivo* angiogenesis assays.

Specific objectives:

- Characterise how processing affected the adipose tissue and its components including cellular content, tissue structure and viability of cells within each formulation.
- Measure the ability of conditioned media from ADSC, adipose tissue, emulsified fat, and SVF-gel to promote cell migration and cell viability in endothelial cells *in vitro*.
- Measure the ability of media conditioned with ADSC, adipose tissue, emulsified fat, and SVF-gel to induce angiogenesis *ex vivo* and *ex ovo*.
- Determine the composition of conditioned media from different adipose formulations to compare secretion of proangiogenic and regenerative factors.

Chapter 2 Processing and characterising adipose tissue

2.1 Aim

To characterise the structure, cellular composition and viability of different formulations of adipose tissue used clinically, including emulsified fat, stromal vascular fraction-gel (SVF-gel), and ADSC.

2.2 Introduction

Mesenchymal stem cells are a key component for regenerative medicine due to their ability to differentiate into different cell types. Adipose derived stromal cells (ADSC) have become important for different cell therapies thanks to their efficacy and easy isolation (Volz, Huber and Kluger, 2016). In recent years the known role of adipose tissue itself has changed from being an energy storage and temperature regulator organ to being recognised as an important component in complex interactions with the endocrine, nervous and cardiovascular systems (Miana and Prieto González, 2018). Adipose tissue, which contains regenerative ADSCs, is being used clinically to stimulate wound healing in skin and other tissues (Pawitan, 2014). It has been proposed that many of the positive effects seen from adipose tissue therapies are as a result of cytokines and growth factors released from ADSC.

This thesis aims to compare the regenerative properties of adipose tissue compared to cultured ADSC. Uncultured adipose tissue which can be harvested and delivered in a single procedure has logistical advantages over cultured ADSCs, however cultured ADSCs have shown great promise in clinical and preclinical studies. So far, there have been very few studies that compare side-by-side the healing properties of ADSC, adipose tissue and formulations of adipose tissue.

Adipose tissue is typically used as lipofilling or lipo-injections to improve volume deformities, to stimulate skin rejuvenation and to improve scar appearance

(Yoshimura, Sato, Aoi, Kurita, Hirohi, *et al.*, 2008; Gebremeskel *et al.*, 2019). Most of the time, liposuction is the method in which adipose tissue is extracted before reinjection to the patients. Lipoaspirate conserves the structure of adipose tissue even when it has been mechanically broken during the extraction (Klar, Zimoch and Biedermann, 2017). Adipocytes represent 80% of the volume of the adipose tissue, however they are only the 20% of the total cells within the tissue (Spiekman *et al.*, 2017). The rest of the cells found in adipose tissue are within the SVF, including ADSCs, preadipocytes, endothelial cells and leukocytes (Figure 1.5). It has been identified that ADSC are located around adipocytes and ECM, especially on the surroundings of blood vessels that run through the tissue (Yoshimura, Sato, Aoi, Kurita, Hirohi, *et al.*, 2008).

One of the main challenges with lipofilling treatments is the reabsorption of the tissue resulting in volume loss between 20 to 90% of injected adipose tissue volume (Klar, Zimoch and Biedermann, 2017). Since it is believed that the regenerative potential of adipose tissue comes from ADSC, and most of the adipocytes undergo apoptosis after lipofilling, new protocols to concentrate the SVF and ADSC without an enzymatic treatment have been generated. These formulations, which have been used clinically, include emulsified fat and SVF-gel (Yoshimura, Sato, Aoi, Kurita, Hirohi, *et al.*, 2008; Xu *et al.*, 2018). Emulsified fat (also called nanofat) is produced by passing adipose tissue between two syringes to break the mature adipocytes without damaging the SVF (Sesé *et al.*, 2019). By doing this, the adipose tissue can be injected more superficially than whole adipose tissue and with smaller needles. Mostly, emulsified fat is clinically used for skin rejuvenation by interdermal injections (Xu *et al.*, 2018). Emulsified fat is composed of cellular and structural fragments with lipid droplets (Alexander, 2016; Sesé *et al.*, 2019). The free lipid in emulsified fat is a result of the lysed adipocytes and gives the final formulation a smooth, injectable consistency (Yao *et al.*, 2017).

SVF-gel is a different formulation generated by filtering and centrifuging emulsified fat to remove the lipid. As a result, the SVF cells are concentrated, conserving its fragmented ECM, but without lipid droplets (Mashiko *et al.*, 2017). The final volume of

SVF-gel is a tenth of the initial volume of adipose tissue, indicating its high cell concentration (Yao *et al.*, 2017).

Although there is some literature on the clinical description of adipose tissue, emulsified fat, and SVF-gel there is no published direct comparison of the structure of the tissue and number of cells before and after processing adipose tissue. One of the challenges of clinically using ADSC, adipose tissue and its derivatives, is the dosage. There is uncertainty regarding effective/safe dosage (Maijub *et al.*, 2015; Cai *et al.*, 2019). Understanding how the different protocols affect the structure and cell content of adipose tissue would provide the basic knowledge required to establish a therapeutic dosage. Without knowing how many and what type of viable cells are present in each formulation, it will be difficult to standardise wound healing treatments based on adipose tissue.

In this chapter, adipose tissue was processed into emulsified fat and SVF-gel using published protocols reported to be used clinically. DNA was extracted from each of the formulations and then quantified to measure the number of cells in each sample. Adipose tissue formulations and ADSCs were imaged using light sheet and confocal microscopy to study the structure of the tissue before and after processing. Finally, flow cytometry was used to characterise stromal cells isolated from the adipose tissue to confirm the proportions of cell types present.

2.3 Materials and Methods

2.3.1 Cell culture

All cell culture work was carried out in Class II biological safety cabinets (Walker Safety Cabinets, Derbyshire, UK) that were cleaned before being used with 70% (v/v) industrial methylated spirits (IMS; Fisher Scientific UK Ltd, Leicestershire, UK). All cell culture plates and flasks were bought from Costar (Buckinghamshire, UK) and Greiner Bio-one (Gloucestershire, UK). All cell cultures were incubated at 37ºC with a 5% CO_2 humidified environment.

2.3.2 Cell culture medium preparation

Different media were used according to the cell type that was cultured. Once prepared the media were stored at 4°C up to a month. To test sterility, 5 ml of media were placed into the incubator at 37°C for 24 hrs prior to use. Primary cells, ADSC and HDMEC, were used until passage 8; while HMEC-1 cell line was used until passage 21. MesenPRO RS™ basal medium supplemented with MesenPro RS™ Growth supplement was used to culture ADSC which is described in Table 2.1.

Table 2.1 ADSC media composition

Component	Stock concentration	Volume solution	Final concentration	Storage	Supplier
MesenPRO RS™ Basal medium	--	435 ml	--	4°C	Gibco, Paisley, UK
MesenPRO RS™ Growth Supplement	--	50 ml	10% (v/v)	-20°C	Biosera, East Sussex, UK

MCDB 131 medium without L-glutamine was used to culture human microvascular endothelial cells (HMEC-1). The media was purchased in 500 ml bottles and prepared as described in Table 2.2.

Table 2.2 MCDB 131 medium composition for HMEC-1

Component	Stock concentration	Volume solution	Final concentration	Storage	Supplier
MCDB 131	--	440 ml	--	4°C	Gibco, Paisley, UK
FCS	--	50 ml	10%(v/v)	-20°C	Biosera, East Sussex, UK
Penicillin/ Streptomycin	10,000 i.u./ml penicillin and 10,000µg/ml streptomycin	5 ml	100 i.u./ml penicillin and 100 µg/ml streptomycin	-20°C	Sigma Aldrich, Dorset, UK
Endothelial Growth Factor	0.2 mg/ml	200 µl	10 ng/ml	-20°C	Sigma Aldrich, Dorset, UK
Hydrocortisone	2.5 mg/ml	250 µl	1 µg/ml	4°C	Sigma Aldrich, Dorset, UK
L-Glutamine	200 mM	5 ml	2 mM	-20°C	Sigma Aldrich, Dorset, UK

Dulbecco's modified Eagle's Medium (DMEM) medium was used to produce conditioned media. Media was purchased in 500 ml bottles and prepared as described in (Table 2.3)

Table 2.3 Dulbecco's modified Eagle's Medium composition

Component	Stock concentration	Volume solution	Final concentration	Storage	Supplier
Dulbecco's modified Eagle's Medium	--	438 ml	--	4°C	Gibco, Paisley, UK
FCS	--	50 ml	10%(v/v)	-20°C	Biosera, East Sussex, UK
Penicillin/ Streptomycin	10,000 i.u./ml penicillin and 10,000µg/ml streptomycin	5 ml	100 i.u./ml penicillin and 100 µg/ml streptomycin	-20°C	Sigma Aldrich, Dorset, UK
Amphotericin B solution	250 µg/ml	2 ml	1 µg/ml	-20°C	Sigma Aldrich, Dorset, UK
L-Glutamine	200 mM	5 ml	2 mM	-20°C	Sigma Aldrich, Dorset, UK

Growth medium MV was used to culture Human dermal microvascular endothelial cells (HDMEC) (Promocell, Heidelberg, Germany). Media was purchased in 500 ml bottles and prepared as described in Table 2.4 and supplements were added as the company specifies.

Table 2.4 Growth medium MV for HDMEC

Component	Volume solution	Final concentration	Storage	Supplier
Growth medium MV	500 ml	--	4°C	PromoCell, Heidelberg, Germany
FCS	Supplement Mix (33 ml)	0.05 ml/ml	-20°C	PromoCell, Heidelberg, Germany
Endothelial Cell Growth Supplement		0.004 ml/ml		
Epidermal Growth Factor		10 ng/ml	-20°C	
Heparin		90 µg/ml		
Hydrocortisone		1 µg/ml	4°C	

2.3.3 Cell passaging and counting

When cells reached 80% confluence, they were trypsinised to detach cells from the tissue culture plastic and transferred to new flasks at lower cell density to allow cell proliferation. To passage the cells, medium was removed, and cells were washed with Phosphate Buffered Saline (PBS) (Oxoid Ltd, Hampshire, UK) to remove any remaining protein. For endothelial cell cultures, Dulbecco´s PBS without calcium chloride and magnesium chloride (Sigma Aldrich, Dorset, UK) was used for washing. Then, trypsin-EDTA (0.05% trypsin and 0.02% EDTA (0.5 g porcine trypsin and 0.2 g EDTA), Sigma Aldrich, Dorset, UK) was added to each flask and incubated for 5 min at 37ºC. In case of HDMEC, cells were incubated at room temperature for 3 min. After cells detached, medium appropriate to the cell type was added to neutralise the trypsin-EDTA. Cells were centrifuged at 150 g for 5 min. In case of HDMEC, they were centrifuged at 150 g for 3 min. Afterwards, the supernatant was discarded, and cells were re-suspended in the desired volume of appropriate cell culture media. To count cells a modified Neubauer haemocytometer (Weber Scientific International, Middlesex, UK) was used and two different 1mm^2 squares were counted to get an average count. The total number of cells was calculated by:

$$Total\ number\ of\ cells = \frac{(averaged\ cell\ count\ per\ 1mm^2)(dilution\ factor)}{10^{-4}}$$

2.3.4 Cell cryopreservation and thawing cells

For cryopreservation, cells were treated as for passaging (described in Section 2.3.3), but instead of being resuspended in cell culture media, cells were resuspended at a concentration between $5x10^5$ and $1x10^6$ cells per ml in cryopreservation medium prepared from 90% FCS, 10% dimethyl sulphoxide (v/v; DMSO; Sigma Aldrich, Dorset, UK). In case of HDMEC, cells were resuspended in Freezing Medium Cryo-SFM (PromoCell, Heidelberg, Germany). Cells were aliquoted into 1 ml cryovials and placed in Mr Frosty™ containers at -80ºC to allow the samples to freeze at a rate of -1ºC per min. After 24 hrs vials were transferred to liquid nitrogen at -196ºC.

To thaw cells, vials were removed from the liquid nitrogen and placed immediately into a water bath at 37ºC. Once the cell solution was thawed, appropriate cell culture medium was added and then centrifuged at 150 g for 5 min. Supernatant was discarded and cells were re-suspended in the desired volume of appropriate cell culture medium to continue culture. Medium was changed 24 hrs after seeding the cells and cultured until they reached 80% confluency.

2.3.5 Adipose tissue processing

Adipose tissue was donated by patients undergoing routine surgery (NHS research ethics 15/YH/0177). Patients gave written informed consent for their tissues to be used for research proposes. Adipose tissue samples were processed in biological safety cabinets and in sterile conditions. As a common first step adipose tissue was mechanically minced manually using a scalpel and tweezers. Around 20 ml of tissue were placed into a 90mm Petri dish for mincing until no big fragments were seen and the tissue had the appearance and consistency of lipoaspirate (Figure 2.1). The tissue was then processed using a variety of protocols, as described below.

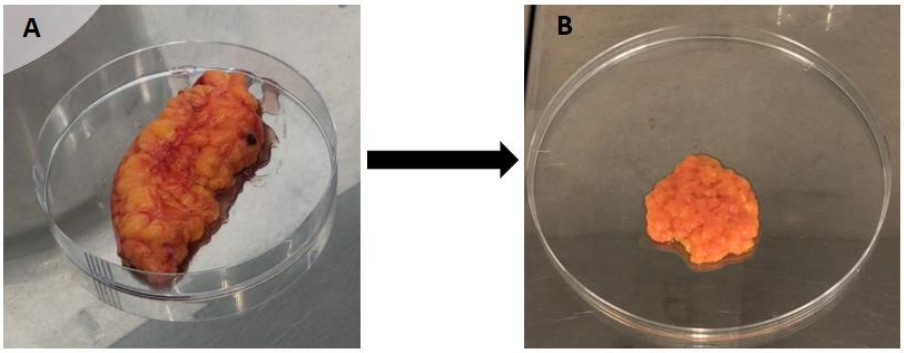

Figure 2.1 Photographs showing adipose tissue processing for conditioned media where the whole tissue (A) is minced mechanically (B).

2.3.6 Emulsified fat protocol

Minced adipose tissue (10 ml) was placed into a 20 ml Luer-Lock syringe and 5 ml of PBS was added to wash/lubricate the tissue. After two phases were formed, the PBS phase was discarded, and the syringe connected to another one by a female-to-female Luer-Lock connector (4 mm interior diameter) (Thermofisher, Loughborough, UK). The tissue was transferred between the two syringes 100 times.

Figure 2.2 Photographs showing how to produce emulsified fat from minced adipose tissue (A). Tissue is passed 100 times between two syringes (B) to produce emulsified fat (C).

2.3.7 SVF-gel protocol

To produce the SVF-gel, emulsified fat was first produced, as described in Section 2.3.6. After filtering using a 500 μm strainer (PluriSelect, Cambridge, UK) the product

was centrifuged at 2,000 g for 3 min. The oil phase was discarded, and the remainder used as SVF-gel.

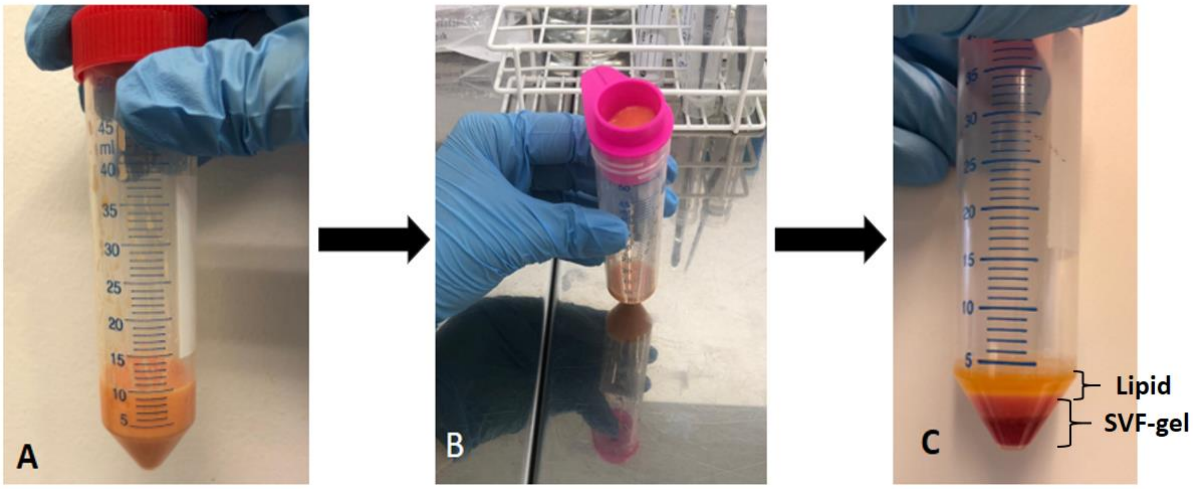

Figure 2.3 Photographs illustrating protocol to produce SVF-gel from emulsified fat (A). First emulsified fat is filtered (B) and then centrifuged to obtain the SVF-gel and a lipid layer that is removed (C).

2.3.8 ADSC isolation from adipose tissue

Minced adipose tissue was subsequently enzymatically digested. Hanks Balanced Buffer Solution (HBSS; Sigma-Aldrich, Dorset, UK) was supplemented with 1% collagenase type A (Roche Diagnostic GmbH, Mannhein, Germany), 1% bovine serum albumin (BSA; Sigma-Aldrich, Dorset, UK), and 1% antibiotic (500 i.u./ml penicillin and 500 µg/ml streptomycin). Samples were incubated for the enzymatic digestion for 40 mins at 37ºC with agitation every 10 min. The digested tissue was filtered using a metallic strainer to remove larger fragments of connective tissue, this facilitated a second filtration through a 100 µm pore size cell strainer (Falcon, Fisher Scientific, UK). The sample was then centrifuged at 150 g for 8 mins before discarding the supernatant and adding erythrocyte lysis buffer (1 ml for every $1x10^7$ cells) (BioLegend, London, UK). After 10 mins incubation at room temperature, the sample was centrifuged again at 150 g for 8 mins. The supernatant was discarded and the SVF suspended in supplemented MesenPRO RS™ with glutamine (as described in

Table 2.1) and seeded in a T75 to isolate ADSC by their capability to adhere to plastic. Cell cultures were kept at 37ºC with 5% CO_2.

2.3.9 Experimental design and samples

Different patient samples were used for the different assays throughout this thesis. As mentioned previously, adipose tissue was donated by patients undergoing routine surgeries at the NHS. This means that tissue was available when routine surgeries were programmed, and patients consented that their tissue could be used for medical research. As part of the NHS research ethics 15/YH/0177, samples were labelled by a batch number to protect patient's personal information.

Two of the major limitations of this research were the irregular supply of tissue and the amount of donated tissue. For the first issue, it was decided that data from lipoaspirate and minced adipose tissue (from sub-cutaneous fat) were combined to facilitate experiments to continue. Characterisation of lipoaspirate and minced adipose tissue were compared to determine differences in their structure and composition. Secondly, tissue was used as effectively as possible in order to guarantee that it was used and processed to obtain as many samples as possible for different experiments. However, there were occasions in which the volume of tissue was not enough to be processed in all the different formulations to compare the same batch in a specific assay, and different patients' samples had to be used. In Table 2.5, the different tissue batches used in each of the experiments in this chapter is described in detail. As has been previously reported and as expected there was a large degree of patient to patient variability in the tissues obtained. Our ethics approval did not allow for any information about the patient to be collected for his research.

Table 2.5 Tissue and formulation batches used in the different experiments.

Experiment	Sample	Rep 1	Rep 2	Rep 3	Rep 4
Flow cytomety	ADSC	415	426	430	
DNA isolation using Qiazol	ADSC	388	402	405	409
	Lipoaspirate	408	411		
	Adipose tissue	409	412	413	415
	Emulsified fat	409	411	412	413
	SVF-gel	409			
DNA isolation using NucleoSpin columns	ADSC	419			
	Adipose tissue	447	464	466	
	Emulsified fat	447	464	466	
	SVF-gel	447	464	466	
Correlation weight vs.volume	Lipoaspirate	408			
	Adipose tissue	409			
	Emulsified fat	411			
	SVF-gel	409			
Lightsheet imaging	ADSC	430			
	Lipoaspirate	440			
	Adipose tissue	437	441		
	Emulsified fat	441			
	SVF-gel	441			
Confocal Imaging	Adipose tissue	451	452	455	462
	Emulsified fat	451	452	455	462
	SVF-gel	451	452	455	462
Live/dead imaging	Lipoaspirate	450			
	Adipose tissue	451			
	Emulsified fat	451			
	SVF-gel	451			

2.3.10 Flow cytometry on ADSC

ADSC at passage 5 from three different patients were harvested at confluence using trypsin-EDTA digestion (see Section 2.3.2). Cells were washed twice with 1% Bovine Serum Albumin (BSA; Sigma-Aldrich, Dorset, UK) in PBS at 150 g for 5 min and resuspended in 1% BSA in PBS. Cells were counted and $5x10^5$ cells were retained as an unstained control. To the remaining cells Fixable Viability Dye (FVD; eBioscience, ThermoFisher, Loughborough, UK) was added and incubated for 30 min at room temperature protected from light. Afterwards, the sample was washed twice with Flow

Cytometry Buffer Solution (FCBS; eBioscience, ThermoFisher, Loughborough, UK) and spun at 150 g for 5 min. Cells were resuspended in FCBS with Human Fc Receptor Binding Inhibitor (RBI; eBioscience, ThermoFisher, Loughborough, UK) and incubated for 20 min at 4ºC. Then, samples were centrifuged at 150 g for 5 min and resuspended in the appropriate volume of FCBS for each 50 µl aliquot of this cell solution to contain $5x10^6$ cells. Seven different antibodies were used to characterise ADSC (Table 2.6). Different fluorophores, with different excitation wavelength, were used for each of the CD markers (see Appendix 1).

Table 2.6 Fluorophores used for the seven different CD markers used for ADSC characterisation

CD Marker	Fluorophore	Concentration	Supplier
CD31	APC eFluor® 780	0.1% (v/v)	eBioscience, Altrincham, UK
CD34	PE	0.1% (v/v)	eBioscience, Altrincham, UK
CD45	eFluor® 450	0.1% (v/v)	eBioscience, Altrincham, UK
CD73	PE-Cy7	0.1% (v/v)	eBioscience, Altrincham, UK
CD90	PerCP eFluor® 710	0.1% (v/v)	eBioscience, Altrincham, UK
CD105	APC	0.1% (v/v)	eBioscience, Altrincham, UK
CD146	FITC	0.1% (v/v)	eBioscience, Altrincham, UK
FVD	eFluor® 506	0.1% (v/v)	eBioscience, Altrincham, UK

Cells samples were incubated with the antibodies for 30 min at 4°C according to manufacturer's instructions. Then, samples were washed twice with FCBS, before fixing them using 0.5 ml of 4% paraformaldehyde. BD LSR II flow cytometry equipment (BD Biosciences, Oxford, UK) was used to analyse the samples, and Flowing Software 2.5.1 (Turku Centre of Biotechnology, Turku, Finland) was used to analyse the data. This analysis was performed in collaboration with my colleague Samuel Higginbotham. The position of the gates for each CD marker were set according to their fluorescence minus one control respectively. Then, samples were run into the system and their histograms were overlapped with the negative controls. To identify the cells side scatter area (SSC-A) vs forward scatter area (FSC-A) was used, while forward scatter area (FSC-A) vs forward scatter high (FSC-H) was used to exclude doubles.

2.3.11 QIAzol DNA isolation from adipose tissue, emulsified fat, SVF-gel, and ADSC

To prepare the samples, around 50 mg of adipose tissue, emulsified fat, SVF-gel, SVF and lipoaspirate samples were placed in 1.5 ml Eppendorf tubes. In case of ADSC, cell pellets were weighed after counting the cell number in the sample using a Neubauer chamber (see Section 2.3.3). Then 1 ml of QIAzol lysis reagent (QIAGEN, Manchester, UK) was added to each sample after which they were disrupted with a tissue disruptor until a homogenous sample was obtained, then samples were left at room temperature for 5 min. Afterwards, chloroform was added to each sample and shaken vigorously for 15 sec. After 2-3 min, during which the samples were left at room temperature, the samples were centrifuged at 12,000 g for 15 min. Three phases were formed: the upper, aqueous phase containing RNA was discarded, to conserve the interphase with the DNA and lower organic phase containing the proteins. Then, 0.3 ml of 100% ethanol was added to the interphase and to the organic phase with mixing by inversion. After 3 min of incubation at room temperature, the samples were centrifuged at 2,000 g for 2 min and the supernatant containing the protein fraction was discarded. The DNA pellet was washed twice using 1 ml of sodium citrate (0.1 M sodium citrate in 10% ethanol) and incubated at room temperature for 30 min with mixing by inversion every 5 min. To remove the sodium citrate, the sample was centrifuged at 2,000 g for 5 min. Then, 1 ml of 75% ethanol was added to the DNA pellet. After 20 min of incubation at room temperature with mixing by inversion every 5 min, the samples were centrifuged at 2,000 g for 5 min. After removing the supernatant, the pellet was left to air-dry for 5-15 min. The pellet was re-dissolved in 300 µl of 8 mM NaOH and centrifuged at 13,000 g for 10 min to precipitate any insoluble material. The supernatant was collected in a new tube and analysed using NanoDrop (Thermofisher, Loughborough, UK) and PicoGreen assay (see Section 2.3.12).

2.3.12 Macherey-Nagel NucleoSpin DNA isolation from ADSC

Macherey-Nagel NucleoSpin DNA Lipid Tissue kits (Thermofisher, Loughborough, UK) were used to process ADSC samples. Three different cell densities (10,000, 30,000, and 50,000 ADSC) were counted using a Neubauer chamber (see Section 2.3.3). Lipoaspirate and SVF-gel samples were processed in collaboration with Dr. Victoria Workman. In both cases around 0.03 grams of tissue were weighed in 1.5 ml Eppendorf tubes. For the case of SVF-gel three samples were processed without modification, and termed “unwashed” samples. In addition, another three samples of SVF-gel were placed on cell strainers (10 µm) (PluriSelect, Cambridge, UK) and washed several times with PBS. The mesh of the cell strainer was then cut from the plastic housing and was processed for DNA extraction[1]. All samples were then placed into NucleoSpin Bead tube with 100 µl of Elution Buffer, 40 µl Buffer LT, and 10 µl Proteinase K. Then samples were lysed by agitation on a Vortex-Genie 2 (Fisher Scientific, Leicestershire, UK) with a frequency of 30 Hertz for 5 min. Afterwards, tubes were centrifuged for 30 sec at 11,000 g to collect the sample and clean the lids. Next, 600 µl of Buffer LT was added for a second centrifugation at 10,000 g for 30 sec. The liquid supernatant was transferred to NucleoSpin columns that were placed in a 2 ml collection tube. Columns were centrifuged for 3 min at 11,000 g then transferred to a new collection tube. To wash the columns 500 µl of Buffer BW was added, then centrifuged for 30 sec at 11,000 g thus discarding the liquid collected in the collection tubes. A second wash was carried out by adding 500 µl Buffer B5 to the columns and spinning them for 30 sec at 11,000 g and discarding the flow-through. Afterwards, the columns were centrifuged for 30 sec at 11,000 g to dry the silica membranes in the columns. Finally, columns were placed into 1.5 ml Eppendorf tubes and DNA was eluted using 100 µl Buffer BE. After 1 min incubation at room temperature the columns were spun down in the Eppendorf tubes for 30 sec at 11,000 g.

[1] Due to Covid-19 lockdown it was not possible to analyse all the studied groups using NucleoSpin columns.

2.3.13 DNA quantification

The Quant-it PicoGreen dsDNA Kit (Thermofisher, Loughborough, UK) was used to quantify DNA obtained from adipose tissue, emulsified fat, lipoaspirate, SVF-gel, SVF and ADSC as described in Section 2.3.11 and 2.3.12. TE buffer (700 µl; 10 mM Tris-HCL, 1 mM EDTA) was added to all the samples to make the volume 1 ml. Then, 1 ml of the PicoGreen reagent (200-fold dilution of the concentrated PicoGreen reagent in TE buffer) was added to the samples, which were then incubated for 2 to 5 min at room temperature in darkness. Fluorescence of the samples was then measured using a spectrophotometer (excitation ~480 nm, emission ~520 nm; Bio-Tek, County, UK). A calibration curve was made between 0 to 20 ng/ml from dsDNA that was included in the PicoGreen kit.

2.3.14 Correlation between weight-volume for each sample

Different volumes of tissue were measured by pipetting (1ml micropipette) the tissue into 1.5ml Eppendorf tubes. To measure adipose tissue, it had to be minced (as described in Section 2.3.5) to be able to pipette and measure its exact volume. Afterwards, all samples were weighed, and volume vs weight plots were generated.

2.3.15 Lightsheet imaging of adipose tissue, emulsified fat, SVF-gel, and ADSC

Adipose tissue, emulsified fat, SVF-gel, and ADSC (see protocols in Sections 2.3.5, 2.3.6, 2.3.7 respectively) were stained using 1.3 µg/ml Isolectin IB_4 Alexa Fluor 488 dye conjugate (Thermofisher, Loughborough, UK) (514 nm laser used) in PBS, 6.6 µM BODIPY 558/568 C12 (Thermofisher, Loughborough, UK) (561 nm laser used), 1.66 µg/ml Hoechst 33342 (Thermofisher, Loughborough, UK) (405 nm laser used), and CellMask deep red plasma membrane stain (0.5X final working solution) (Thermofisher, Loughborough, UK) in PBS. Samples were covered with the dye solution and incubated for 30 min at room temperature protected from light. Afterwards, samples were washed twice with PBS to remove the excess dye. Samples were encapsulated in 0.8% low gelling temperature agarose (Sigma Aldrich, Dorset,

UK) and images were captured using a Lightsheet microscope (10x objective) using Zen Black 2014 software (Zeiss, Cambridge, UK). For Isolectin 514 nm laser was used. For Bo

2.3.16 Confocal imaging of adipose tissue, emulsified fat, SVF-gel and ADSC

Around 150 mg of adipose tissue, emulsified fat, and SVF-gel (see protocols in Sections 2.3.5, 2.3.6, 2.3.7 respectively) were placed into 1.5 ml Eppendorf tubes with 300 µl of 1X pre-stain buffer (Biotium, Cambridge, UK) in HBSS. Samples were incubated for 5 min at 37ºC. Then, tubes were centrifuged for 2 min at 11,000 rpm and pre-stain was removed carefully so as not to disturb the tissue in the supernatant or the pellet. MemBrite™ Fix 640/660 dye (Biotium, Cambridge, UK) (300 µl) 1X in HBSS was added and incubated for 5 min at 37ºC. After the incubation time, tubes were centrifuged for 2 min at 11,000 rpm and the MemBrite™ Fix dye was removed. BODIPY 558/568 C12 (0.1 M) and DAPI (1:1000 in PBS) (300 µl) were added to the samples and incubated for 30 min at room temperature protected from light. To wash the samples, tubes were centrifuged for 2 min at 11,000 rpm to discard the dye solution and 300 µl of PBS were added. After 5 min incubation at room temperature, tubes were centrifuged for 2 min at 11,000 rpm and PBS was removed. To fix the samples 300 µl of paraformaldehyde (3.7%) (Sigma-Aldrich, Dorset, UK) were added to each of the samples and incubated for 30 min at room temperature protected from light. Finally, samples were centrifuged at 11,000 rpm for 2 min and paraformaldehyde was discarded. Samples were placed into µ-slides (8-well, Ibidi, Thistle, Glasgow, UK) and mounted using 1% agarose to avoid the sample moving during imaging. Two or three drops of agarose were placed on top of the tissue samples and the slide placed on top of an ice bag to let it set. Slides with tissue samples were kept at 4ºC until confocal imaging using Zeiss LSM880 AiryScan Confocal microscope using using Zen Black 2014 software (Zeiss, Cambridge, UK). A UV laser (405 nm) was used for DAPI, while two VIS lasers (633 nm, and 543 nm) were used for MemBrite™ and BODIPY respectively.

2.3.17 Live/dead imaging of adipose tissue, emulsified fat, SVF-gel, and ADSC

Adipose tissue, emulsified fat, SVF-gel, and ADSC (see protocols in Sections 2.3.5, 2.3.6, 2.3.7 respectively) were stained using 2 µM Calcein AM (Thermofisher, Loughborough, UK) in PBS, 3 µM Ethidium homodimer-1 (EthD-1) (Thermofisher, Loughborough, UK) in PBS. Samples were covered with live/dead solution in a 24 well plate and incubated for 1 hour at room temperature protected from light. Images from each sample were taken using an inverted epifluorescent microscope (4X objective) (Leica Microsystems, Milton Keynes, UK). This microscope has wLS LED illumination in which 488 nm and 540 nm excitation wavelengths were used to image Calcein AM and EthD-1 respectively.

2.4 Results

2.4.1 Tissue processing

Figure 2.4 shows the macroscopic appearance of the different formulations after adipose tissue processing. Most of the adipose tissue samples provided for this research were obtained by tissue excision rather than liposuction. This meant that samples were whole adipose tissue rather than lipoaspirate. Whole adipose tissue has a yellow colour with some blood around from the blood vessels that were broken during surgery. The tissue is formed by lumps that attach together by connective tissue. The general consistency of the tissue is soft and gelatinous (Figure 2.4A). Lipoaspirate is composed by detached lumps of adipose tissue in a more liquid form since big percentage of the ECM was broken and removed during liposuction (Figure 2.4B). The first step made to process the tissue is to mechanically break it by mincing it. By doing this, it was possible to take whole adipose tissue closer to lipoaspirate that is used clinically. The minced tissue was in small lumps with a yellow-reddish colour (Figure 2.4C). Free lipid is generated during the mincing process. Afterwards, tissue was emulsified by passing it between two syringes. The result is a viscous liquid with some residues of connective tissue. Emulsified fat changes in colour from yellow to orange-yellow similar in colour and consistency to a mango smoothie (Figure 2.4D). Finally,

when emulsified fat was filtered, centrifuged and the top lipid is removed, the rest of the layers were mixed to generate SVF-Gel which had a reddish liquid with no large fragments of connective tissue (Figure 2.4E). It is important to mention that 10 ml of minced adipose tissue produced around 4 ml of SVF-gel. Also, as the tissue was more processed and broken up, it was easier to handle and to measure its volume since it became easier to pipette it.

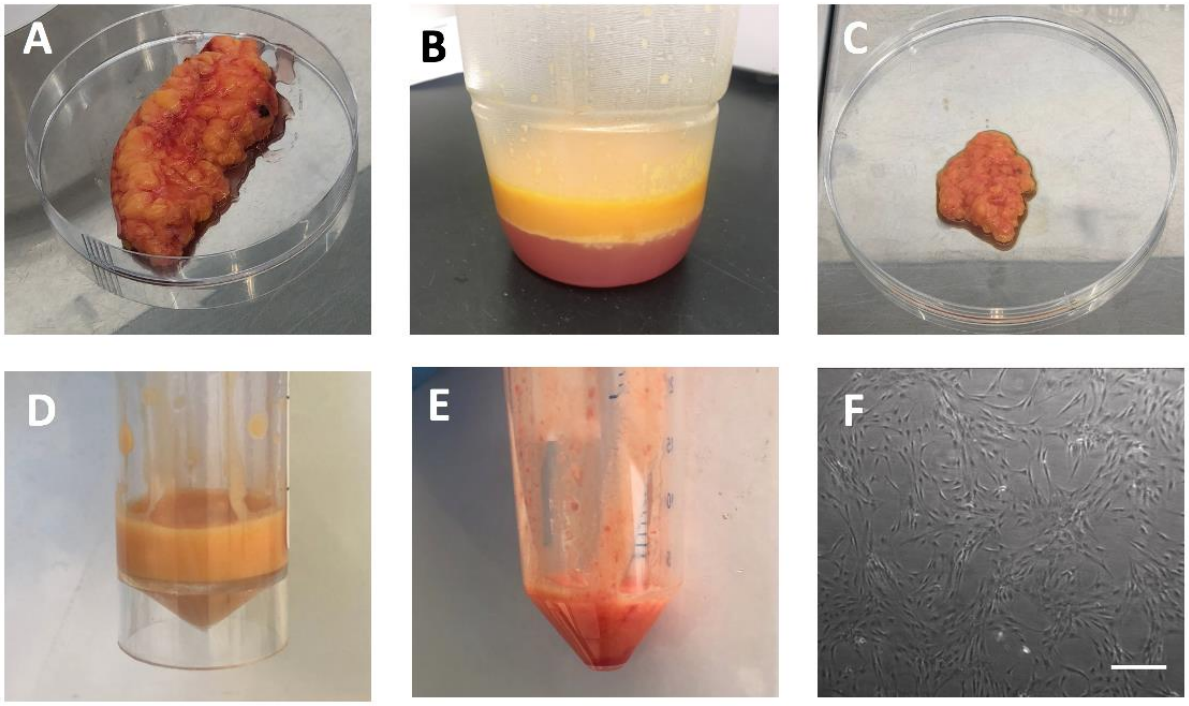

Figure 2.4 Images of whole adipose tissue (A), lipoaspirate (B), minced adipose tissue (C), emulsified fat (D), SVF-gel (E), and cultured ADSC (F). Scale bar = 500 µm.

2.4.2 ADSC characterisation

In order to study how adipose tissue compared to cultured ADSCs were also prepared from the same adipose tissue used to produce emulsified fat and SVF-gel. The ADSC protocol used was the well-established protocol from (Efimenko *et al.*, 2014; Roman *et al.*, 2014), however, it is important to confirm that the isolated cells had the phenotype of stromal cells. Three different batches of ADSC from different donors were analysed using flow cytometry. Figure 2.5A shows the histograms for ADSCs stained with CD31, CD34, CD45, CD73, CD90, CD105, and CD146, alongside unstained controls. In this case, it is possible to identify that the cell population isolated

from patient's adipose tissue was positive for the markers CD73, CD90, and CD105, and was negative for the markers CD31, CD45, CD146. In the case of CD34, most of the cells were negative for this marker. There was variation in the percentage of cells with the CD34 marker between the three different batches with 7.2, 5.1, and 22.7% of cells positive for CD34 from the total cells analysed (might be handy to put the number here). Once the data was further analysed, it was possible to identify the percentage of cells that were positive for each cell marker (Figure 2.5B). For the markers CD31, CD45, and CD146 less than 1% of the cell population were positive. On the other hand, 98.5% cells were positive for CD73, 98.9% for CD90, and 94.9% for CD105.

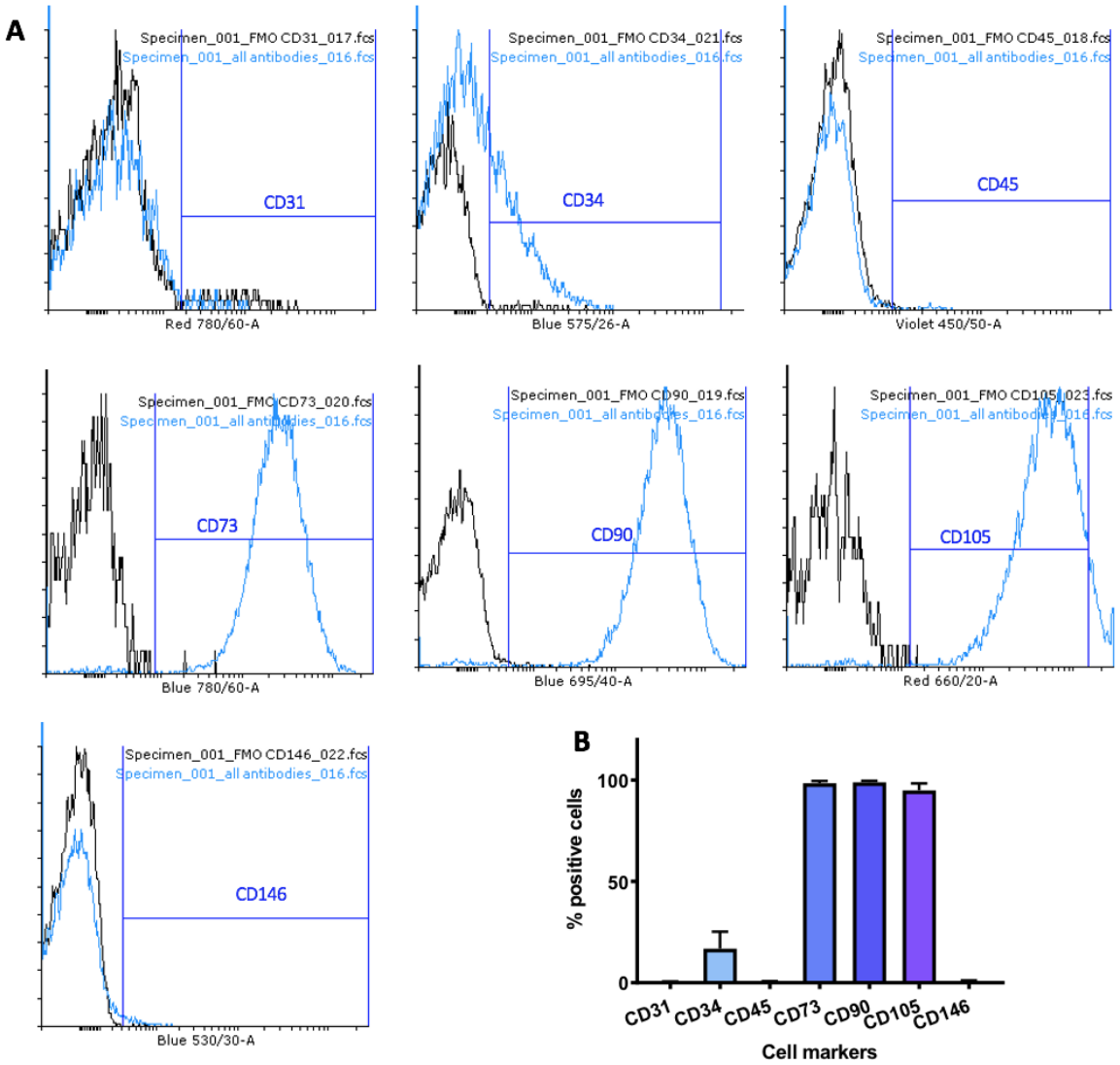

Figure 2.5 Flow cytometry histograms (A) illustrating analysis carried out using different cell markers. Isotype control peaks are in black, while ADSC sample intensity is in blue. Flow cytometry analysis showing the percentage of positive cells for each marker (B). N=3 n=1

Forward scatter area (FSC-A) vs side scatter (SSC) (Figure 2.6A) was used to identify the stromal cell population based on the size and granularity. While forward scatter height (FSC-H) vs FSC-A plot (Figure 2.6B) was used to exclude doublets. The cells that were included in both delimited areas mentioned before were further analysed for their CD markers. Most of the cells were double positive for CD90 and CD73 (Figure 2.6C), positive for CD105 and negative for CD34 (Figure 2.6D), double negative for

CD45 and CD73 (Figure 2.6E), and positive for CD90 and negative for 146 (Figure 2.6F).

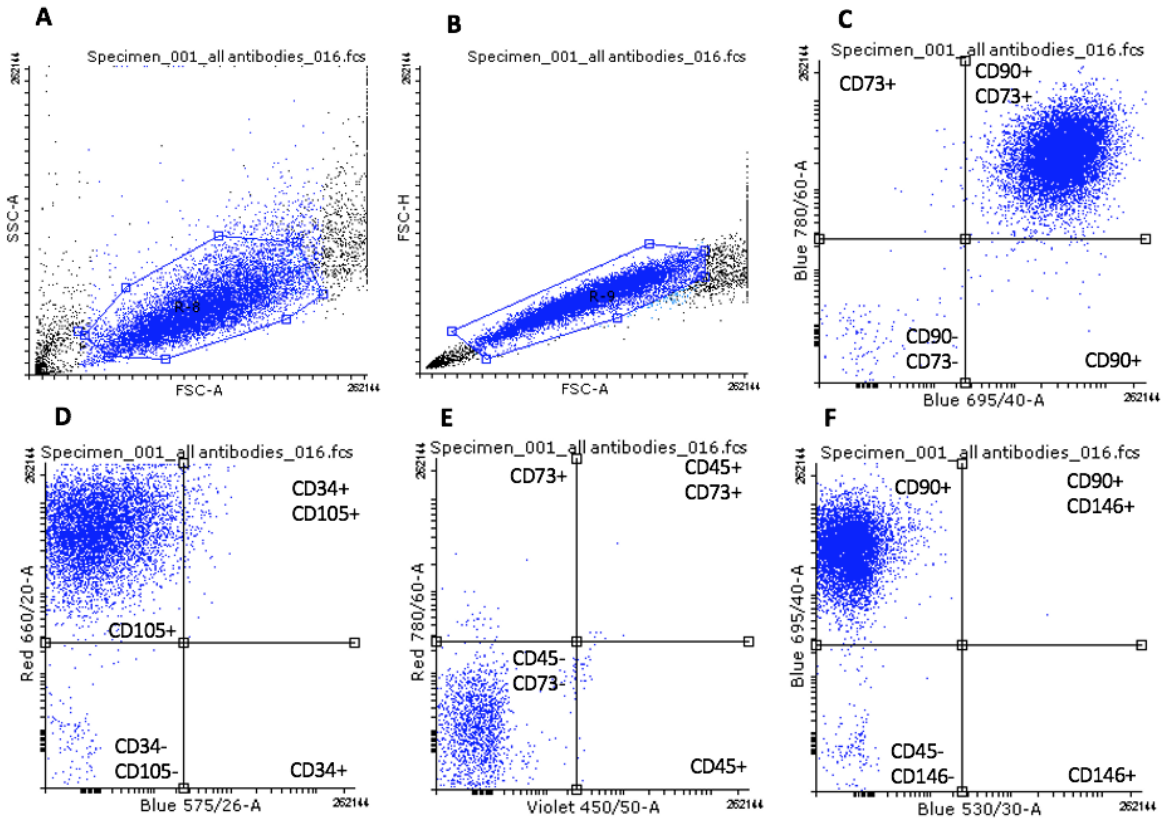

Figure 2.6 Cells side scatter area (SSC-A) vs forward scatter area (FSC-A) (A), and forward scatter area (FSC-A) vs forward scatter high (FSC-H) (B). Two parameter density plots for different markers to identify ADSC population using CD73 vs CD 90 (C), CD34 vs CD105 (D), CD45 vs CD73 (E), and CD146 vs CD90 (F). N=3

2.4.3 DNA isolation and quantification using QIAzol

After confirming that cells isolated and cultured on plastic from the adipose tissue were ADSC, it was important to characterise the adipose tissue, emulsified fat and SVF-gel. Since adipose tissue, emulsified fat, and SVF-gel are complete tissues, while ADSC are cells, it was more difficult to correlate how much tissue is equal to a certain number of cells. As part of the characterisation for each group, we attempted to use DNA quantification to deduce how many cells were present in each sample and to understand how dense or concentrated they were. QIAzol was used to lyse all the samples since it is widely used to prepare fatty tissues (Paradis *et al.*, 2006). Once

isolated, DNA was purified with a sequence of multiple washes (Section 2.3.11). Initially, NanoDrop was used to measure the DNA concentration. However, NanoDrop readings showed that the samples were not completely pure, and RNA and proteins were interfering with the instrument readings. PicoGreen was used as an alternative to quantify DNA in the samples (Section 2.3.13). As it is specific for double stranded DNA any interference from impurities was avoided.

After analysing three different samples from five different patient samples, we obtained the results shown in Figure 2.7. As it is expected the ADSC have the highest average µg of DNA per gram of sample with a value of 284 µg DNA/g sample. The adipose tissue and the lipoaspirate had the lowest with 68 and 30 µg of DNA per gram of sample respectively. While emulsified fat and SVF-gel have 84 and 66 µg of DNA per gram of sample respectively. Combining data from 4 different batches of ADSC in which the number of cells in each sample were counted before the DNA isolation, the amount of DNA per cell according to our data is 0.212 picograms.

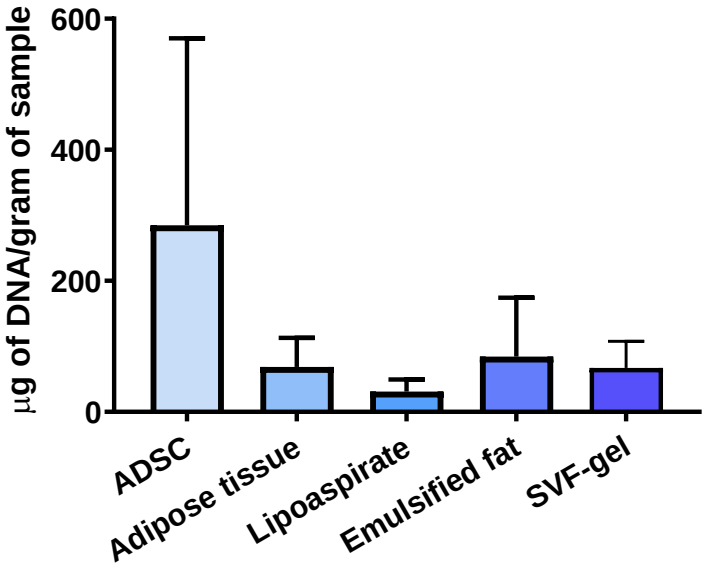

Figure 2.7 DNA quantification in µg of DNA per gram of sample of ADSC, adipose tissue, lipoaspirate, emulsified fat, and SVF-gel. DNA isolation and purification were performed using QIAzol and phenol chloroform method and quantified using PicoGreen. Mean with error bars showing standard deviation. N=5, n=3.

2.4.4 DNA isolation and quantification using NucleoSpin columns

Since the isolation from the QIAzol method had a lot of variation and the amount of DNA extracted and quantified per cell was much lower than the one reports in the literature, NucleoSpin DNA Lipid Tissue kit was tested as an alternative. In order to determine whether this method was more accurate, different concentrations of ADSC were tested. Ten thousand, three thousand and five thousand ADSC were counted using a hemocytometer prior the DNA isolation. Afterwards, samples were processed using NucleoSpin columns to isolate the DNA (Section 2.3.12) and quantified by PicoGreen. In Figure 2.8A the correlation between number of cells and the isolated amount of DNA is directly proportional. Also, it is possible to identify that there is not much variation between samples. After analysing the data, the amount of DNA per cell according to this method was calculated as 10.51 pg. Preliminary data was produced using lipoaspirate and SVF-gel (Figure 2.8B). Lipoaspirate contains double the quantity of DNA compared to unwashed SVF-gel indicating a higher number of cells per gram of sample. SVF-samples were washed to remove DNA from lysed cells to enable us to measure DNA from intact cells only. Washed SVF-gel contained a third of DNA compared to unwashed SVF-gel, after the series of PBS washes.

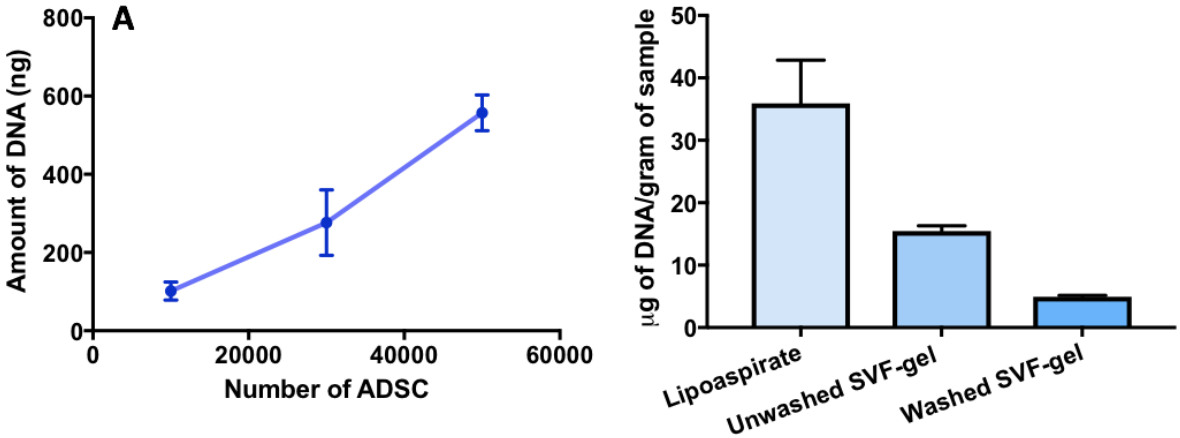

Figure 2.8 DNA quantification from 10,000, 30,000, and 50,000 ADSC using NucleoSpin DNA Lipid Tissue kit (A). DNA quantification in µg of DNA per gram of sample of lipoaspirate, unwashed SVF-gel and washed SVF-gel (B). N=1, n=3. Mean with error bars showing standard deviation.

2.4.5 Correlation between weight-volume for each sample

A correlation between weight and volume (Figure 2.9) of SVF-gel, emulsified fat, adipose tissue and lipoaspirate was obtained to enable comparisons between samples to be made (Section 2.3.14). It is easier to measure volumes of SVF-gel and emulsified fat as these can be pipetted while cell pellets and whole adipose tissue were weighed. Figure 2.9 shows a good correlation between weight and volume for all samples.

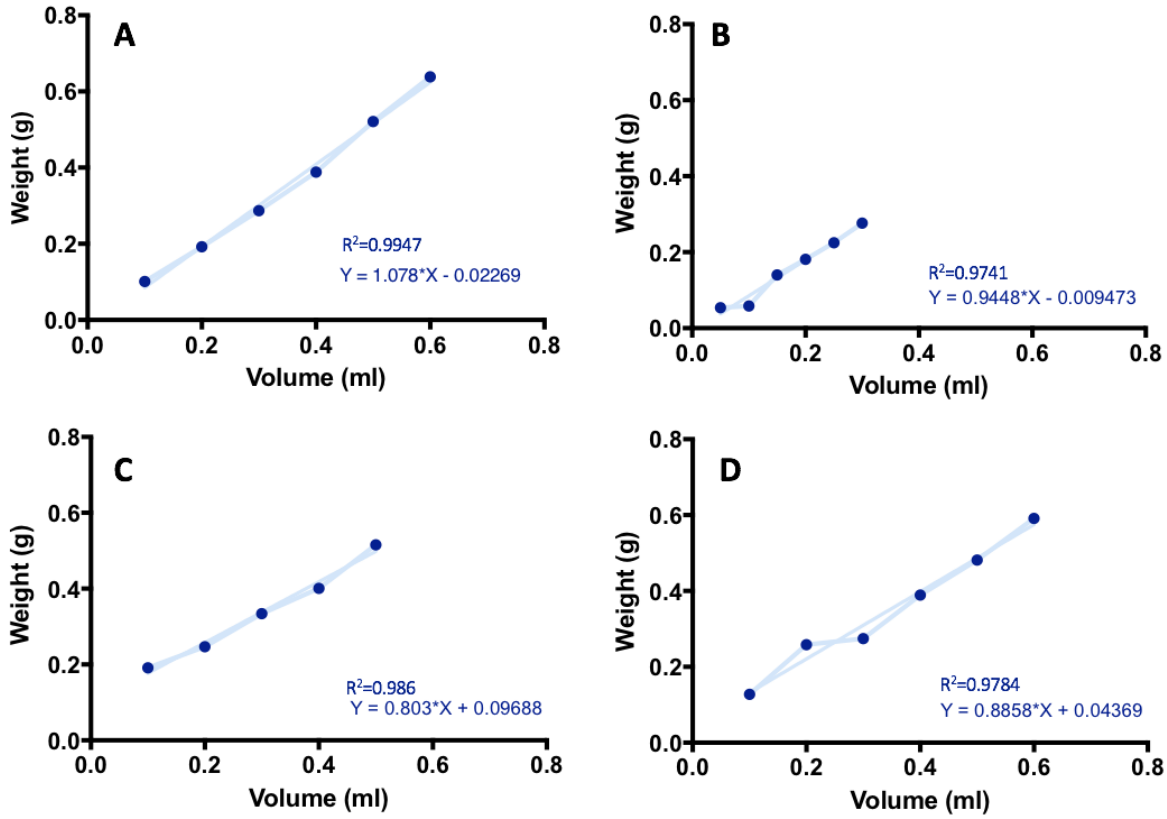

Figure 2.9 Correlation between weight and volume for adipose tissue (A), lipoaspirate (B), emulsified fat (C), and SVF-gel (D).

2.4.6 LightSheet imaging

Structure of the tissue is also important for tissue characterisation since it can show how the different isolation protocols affect the integrity of the adipose tissue. Different stains were used to study a variety of structures of the tissue. To study the integrity of the adipocytes BODIPY (lipids) and CellMask (plasma cell membrane) were used. Isolectin and Hoechst were used to visualise the endothelial cells and nuclei

respectively (Section 2.3.15). When the different stains were applied at the same time to stain resuspended ADSC or adipose tissue, it was not possible to detect the CellMask in any of the samples (Figure 2.10A). However, when resuspended ADSC and adipose tissue were stained only with CellMask, it was possible to detect the plasma membrane of the cells (Figure 2.10B).

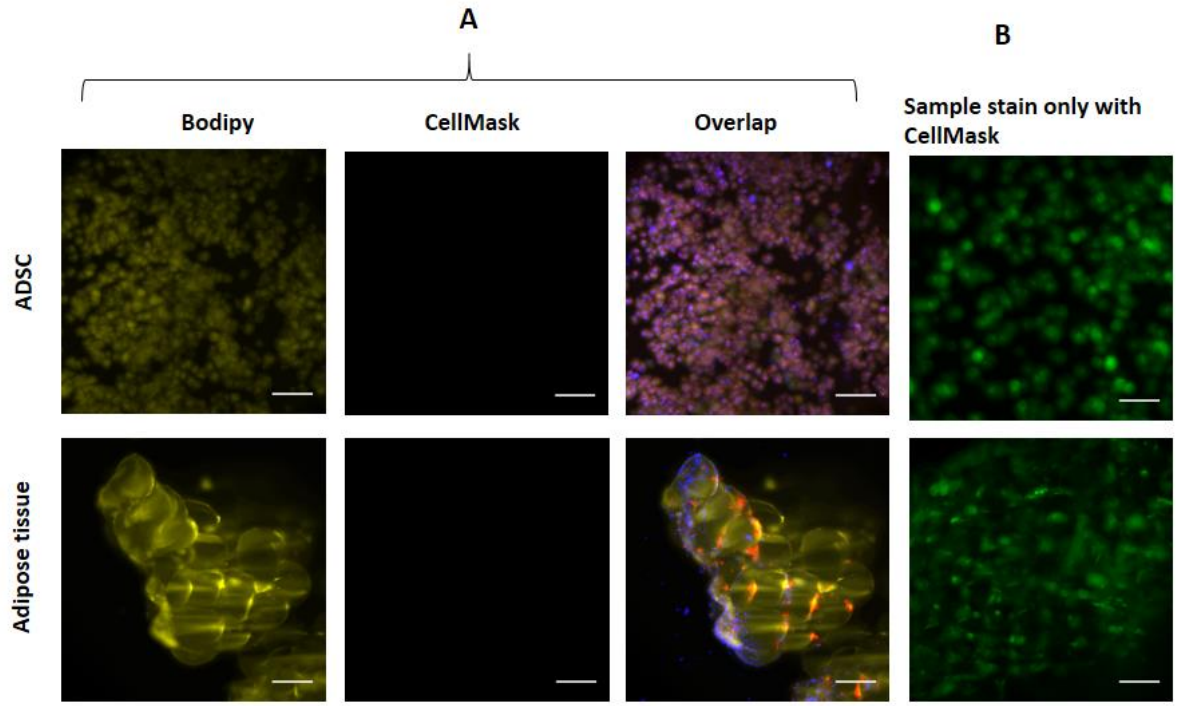

Figure 2.10 ADSC and adipose tissue imaged using BODIPY (yellow), CellMask (green), Hoechst (blue) and Isolectin stains (red) (A) compared to samples stained only with CellMask (B). Scale bar = 100 µm.

This result suggested that the BODIPY didn't bind specifically to the lipids inside the cells, but also has the ability to bind to the phospholipids present in the plasma membrane. As a result, BODIPY competes with CellMask to stain the plasma membrane. Since it was not possible to obtain any information from the CellMask, the stains used to study the structure of adipose tissue before and after processing were BODIPY, Isolectin, and Hoechst.

Samples of ADSC, adipose tissue, lipoaspirate, emulsified fat, and SVF-gel were stained and LightSheet microscopy was used to capture images (Figure 2.11). Resuspended ADSC were seen to be rounded in shape since they were not attached

to a surface, where normally they would have a spindle shape (Li *et al.*, 2014) as observed in Figure 2.4F. All samples except the ADSCs showed positive staining for all of the dyes used, including Isolectin, which stains for endothelial cells, thus resulting in nonspecific staining.

The structures of whole adipose tissue and lipoaspirate at this scale were seen to be similar even though lipoaspirate was more liquid, while whole tissue was dense and completely solid (Figure 2.11). In both cases the adipocytes appeared to be intact and some blood vessels could be identified. Moreover, after processing the tissue to obtain emulsified fat, the tissue appeared disorganised. Some intact adipocytes remained in the emulsified fat, but in parts of the sample free oil was present giving a blurry appearance to the image. Similarly, SVF-gel appeared to contain some intact adipocytes. Nevertheless, large areas appeared disordered with some smaller lipid droplets. Imaging each of the different tissues showed the structural integrity of the adipose tissue before and after processing.

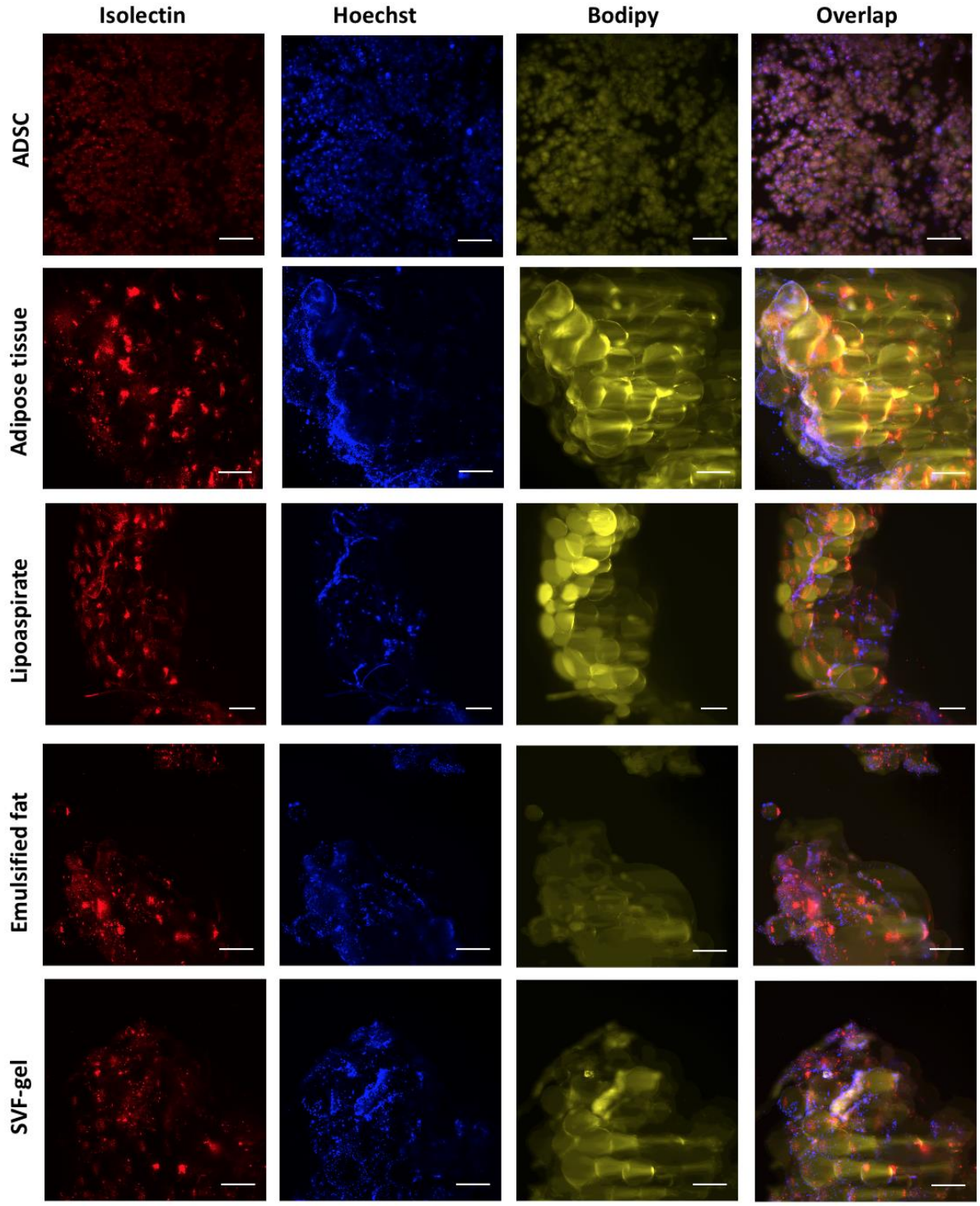

Figure 2.11 ASDC, adipose tissue, lipoaspirate, emulsified fat, and SVF-gel stained using Isolectin (endothelial cells in red), Hoechst (nuclei in blue), and BODIPY (fatty acids in yellow). Images taken using LightSheet microscopy. Scale bar = 100 µm.

2.4.7 Confocal imaging

LightSheet images gave an overview of the structure of the different formulations; however, the images are not completely clear and small details are difficult to distinguish. As an alternative, confocal imaging was used to provide higher quality, more detailed images (Figure 2.12). Capturing the integrity of the adipocytes provides valuable information on how processing the tissue affects its structure. In particular it is important to determine whether the emulsification protocol successfully lysed the adipocytes. A stain specific for cell surface proteins (MemBrite™) was used to stain adipocyte cell membranes as an alternative to the CellMask (lipid bi-layer stain) used previously, while BODIPY was used to stain lipids. Finally, DAPI was used to stain cell nuclei. In the case of adipose tissue, most of the adipocytes were intact with a well-defined membrane (Figure 2.12A). Emulsified fat shows a similar structure to the minced adipose tissue, however, large lipid droplets without a cell membrane are also visible and there is a clear disruption on the tissue (Figure 2.12B). This indicated that emulsification of the tissue does lyse some of the adipocytes however some appear intact. It is also possible to distinguish some blood vessel fragments around the adipocytes in the emulsified fat samples. Finally, SVF-gel presented large lipid droplets with tissue fragments present with cells attached. Surprisingly, small numbers adipocytes were still detectable in SVF-gel with an intact cell membrane (Figure 2.12C).

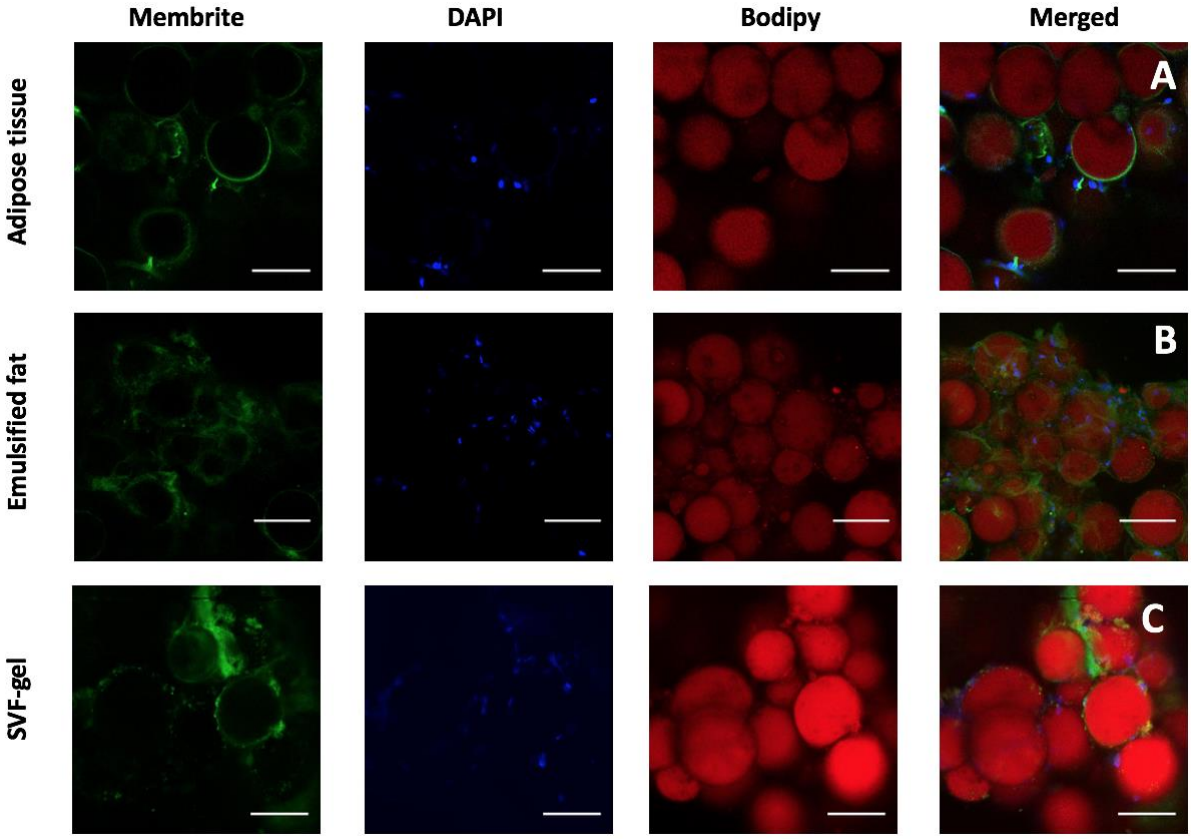

Figure 2.12 Confocal imaging of adipose tissue (A), emulsified fat (B), and SVF-gel (C) using MemBrite™ Fix dye (cell membrane in green), DAPI (nuclei in blue), and BODIPY (fatty acids in red). Scale bar = 100 µm.

To study SVF-gel in more detail three different images were taken (Figure 2.13). The first shows the mix of all the layers that compose the SVF (pellet, aqueous phase and fat layer) (Figure 2.13B). It is still possible to distinguish a few adipocytes in whole SVF-gel due to the presence of cell membranes. Nevertheless, are more lipid droplets are present than adipocytes. Also, small fragments of blood vessels are visible. The second image of the SVF-gel (Figure 2.13C) presents only the yellow layer that is formed under the lipid layer after centrifugation of the tissue. This layer has a similar appearance to the complete SVF-gel. A few adipocytes can be seen, with lipid droplets. Lastly, the SVF-gel pellet was imaged to show the presence of the SVF cells which were isolated during the centrifugation (Figure 2.13D). Interestingly it was still possible to distinguish some small lipid droplets around a highly concentrated cellular fraction.

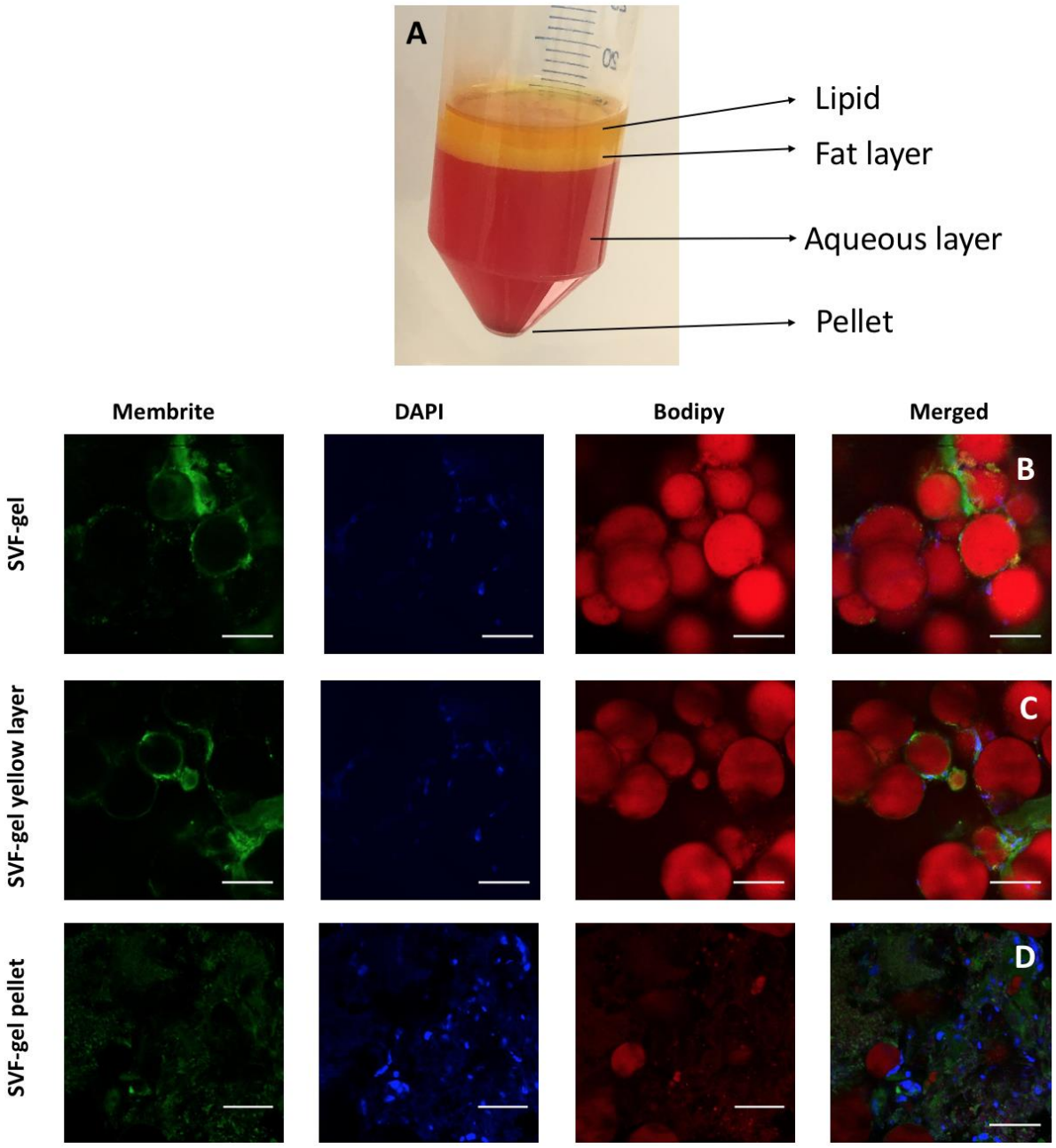

Figure 2.13 Image of SVF-gel showing the different layers formed after centrifugation (A). Confocal imaging of whole SVF-gel (B), SVF-gel yellow layer or fat layer (C), and SVF-gel pellet (D). Samples were stained with MemBrite™ Fix dye (cells membrane in green), DAPI (nuclei in blue), and BODIPY (fatty acids in red). Scale bar = 100 µm.

2.4.8 Live/Dead imaging

Since adipose tissue has been processed using different protocols, it is important to measuring how the different protocols affect the tissue viability. A Fluorescent

live/dead stains were used to detect the live and dead cell population in the tissue before and after processing (Figure 2.14). Live cells are stained by Calcein AM showing a green fluorescence, while dead cells are stained by EthD-1 with a red fluorescence. A visualise large percentage of cells within the whole adipose tissue were viable, with some spots in red representing dead cells (Figure 2.14A). Similarly, lipoaspirate has a major population of viable cells with some dead cells around the tissue (Figure 2.14B). In both cases the integrity of the tissue is conserved and blood vessels going through can be distinguished. On the other hand, when adipose tissue is processed to generate emulsified fat, the structure of the tissue is disrupted and the number of dead cells increases (Figure 2.14C). It is impossible to identify any remaining structure in the SVF-gel and the stains are mixed with all the lysed cells making it difficult to identify cells from the background (Figure 2.14D). Also, there are some red spots that could be caused by light refraction in the lipid droplets. Finally, to identify the autofluorescence of adipose tissue, an unstained sample was imaged (Figure 2.14D).

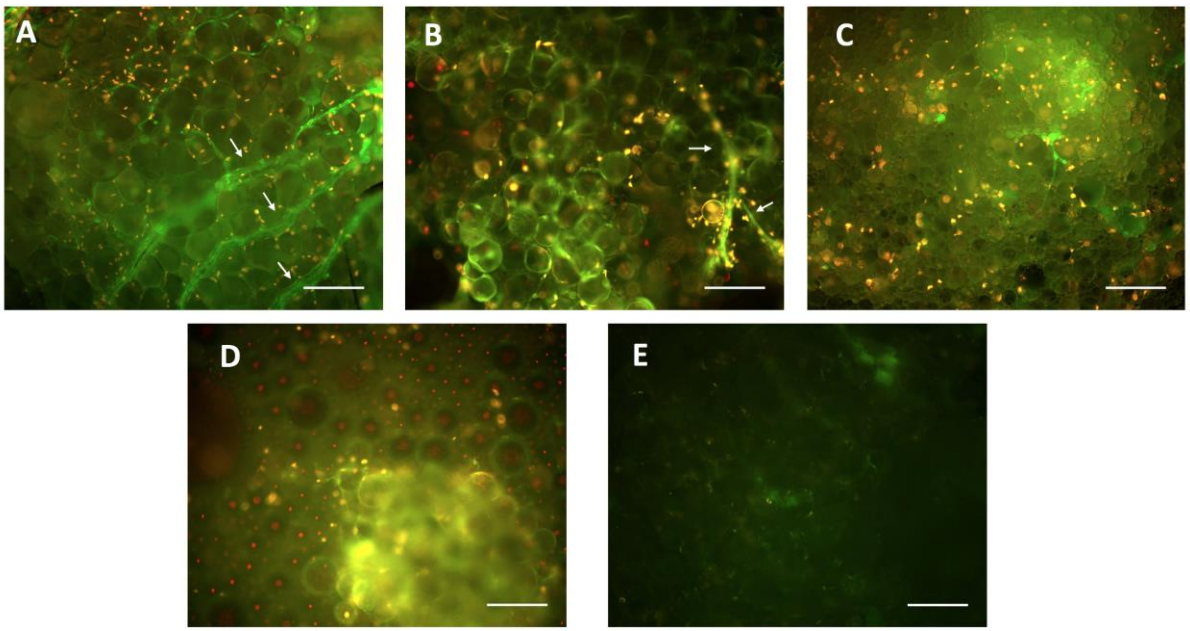

Figure 2.14 Live/dead imaging of adipose tissue (A), lipoaspirate (B), emulsified fat (C), SVF-gel (D), and unstained adipose tissue (E). Live cells are stained in green with Calcein, while dead cells are in red stained with EthD-1. Arrows: blood vessels. Scale bar= 200 µm.

2.5 Discussion

The aim of this chapter is to compare the structure of adipose tissue, emulsified fat, SVF, and ADSC. All these formulations have been used and have great potential to be used for clinical treatments. However, there are still some obstacles to overcome in adipose tissue related treatments. First, it is important to understand how adipose tissue exerts its regenerative properties in order to enhance and utilise them effectively. Also, process standardisation and dosage are still uncertain. Knowing the composition of each of the formulations is essential to set a starting point to overcome these obstacles.

First, characterisation of the cells isolated from adipose tissue is important to corroborate that the cells present have a stromal cell phenotype. ADSC were isolated using enzymatic digestion of adipose tissue. After 5 passages, three different batches of cells (see Table 2.5) were analysed using flow cytometry. It has been reported that phenotype for stromal cells in the literature is $CD31^-$, $CD45^-$, $CD90^+$, $CD105^-$, $CD146^-$ (Tsuji, Rubin and Marra, 2014). Cells were positive for CD73, CD90, CD105, while negative for CD31, CD45, and CD146 indicating that they have the phenotype of stromal cells and fit the classification for ADSC (Tsuji, Rubin and Marra, 2014). In addition, some of the cells were positive for the CD34 marker (Figure 2.5B). It has been reported that freshly isolated ADSC are more likely to be positive for CD34, while cultured ADSC tend to lose expression of this marker through passaging (Kilinc *et al.*, 2018). The cells tested here were passage 5 which explains the low expression of this marker (only 17% were positive for this marker). It is important to consider that during the isolation a low percentage of the isolated cells are fibroblasts (Baaße *et al.*, 2018). This is one of the reasons it is important to use the cells on a low passaging to guarantee that most of the cultured cells are healthy ADSC.

Figure 2.6E shows that most of the cells were negative for both CD45 and CD73 indicating the absence of endothelial cells since both of these markers are present in endothelial cells (Kilinc *et al.*, 2018). On the other hand, CD90 is a marker expressed in stromal cells as well as in pericytes, while CD146 is a marker expressed in pericytes cells (Efimenko *et al.*, 2014). In this case, the majority of the cells are positive for CD90,

but negative for CD146 (Figure 2.6G). In this way, we can confirm that the cells isolated and cultured from the adipose tissue are ADSC with relative no presence of endothelial cells nor pericytes.

Adipose tissue has been processed using different protocols that have previously been used in clinics to treat different skin wounds and reconstructive procedures (Tiryaki, Findikli and Tiryaki, 2011; Yao *et al.*, 2017). Clinically, it has been seen that adipose tissue, emulsified fat, and SVF-gel have regenerative properties. However, the mechanism of this action is not yet known, and there are very few comparisons, from clinical or *in vitro* data, to understand which of them has the greatest regenerative potential. As a result, it is important to study each of them side-by-side to know how the different protocols affect the tissue. Processing adipose tissue resulted in different formulations with very different compositions and appearances. In order to carry out a comparison between formulations we looked for a parameter which could be used to quantify the number of cells in each of them.

DNA quantification was used to attempt to measure the number of cells in our samples and to standardise the concentration of each sample between each other and between groups. Quantifying the amount of DNA per sample is also useful in clinical treatment as it is important to know the number of transplanted cells in order to determine the optimum doses (Hasegawa and Ikeda, 2015). Initially QIAzol was used since it is one of the few reagents reported to lyse cells in fatty samples (Khudyakov *et al.*, 2018). We were able to measure the DNA content however large variability and inaccuracies were present. The accuracy of this method was a concern as the amount of DNA per cell obtained from ADSC data (0.212 pg per cell) was much lower than in the literature (6 pg per cell) (Russo *et al.*, 2014). The QIAzol protocol to isolate the DNA contains a long sequence of washes in which small amounts of DNA could be lost each time. In addition, we had concerns about the complete lysis of the cells and tissues which could have led to variability between samples seen in our results.

Sesé *et al*., (2019) isolated DNA from adipose tissue, emulsified fat and SVF-gel using the E.Z.N.A. Tissue DNA Kit from Omega. Using this kit, it was reported that adipose tissue had 10.5 million cells per gram, lipoaspirate had 9.2 million cells per gram, and

emulsified fat had 7.3 million cells per gram (Sesé *et al.*, 2019). Using the reported value of 6 pg of DNA per cell we could estimate the number of cells per gram of tissue from our data in Figure 2.7. Using the QIAzol method our data suggests there were 1,020 cells per gram of adipose tissue, 87,000 cells per gram of lipoaspirate, 1,300 cells per gram of emulsified fat, and 1,900 cells per gram of SVF-gel. These values are significantly lower than the data from Sesé *et al*. (2019). The number of cells per gram of sample we obtained are considerably lower, supporting the theory that DNA was not effectively isolated or was lost during the process of purifying using the QIAzol protocol.

Sesé *et al*., (2019) used two standard curves, obtained by analysing two different amounts of SVF cells to process the data. Even though these two curves present a strong linear regression (R^2=0.9958 and R^2=0.9968), the gradient between them differed considerably. In addition, when they compared these standard curves to the theorical standard curve calculated from the literature value of amount of DNA per cell (6 pg), the gradients of the standard curves were far from the expected values. These observations suggest the E.Z.N.A method was also not accurate for DNA isolation and quantification from adipose tissue.

Additionally, it is important to mention that E.Z.N.A. Tissue DNA Kit from Omega is not specific for fatty tissues. This could affect the isolation process since adipose tissue lipid could interfere with the efficacy of the kit. E.Z.N.A. protocol suggests to lyse the studied tissue by freezing it in liquid nitrogen and then pulverising, instead of mechanical homogenisation to improve the DNA isolation (Omega Bio-Tek, 2019). DNA isolation by this method relies on HiBind matrix columns to which DNA binds. Then, a series for washing steps (6 in total) and one elution step, after which DNA can be analysed. In the kit manual, they recommend to use this method to isolate DNA for PCR, sequencing, southern blot analysis, and restriction digestion (Omega Bio-Tek, 2019). The fact that DNA quantification is not suggested by the manufacturing company could suggest that this method is not accurate for DNA extraction to quantify cell number.

An alternative method to isolate DNA from adipose tissue is the Macherey-Nagel Nucleo Spin lipid tissue kit. This kit is specifically designed for fatty-rich tissues from humans and animals and it uses enzymatic (proteinase k) and bead disruption to achieve efficient tissue lysis. Also, this kit is supplied with a specific buffer to remove lipid from the samples which does not interfere with the efficacy of the other buffers used for the isolation (Macherey-Nagel, 2016). To determine whether this method was accurate for DNA isolation for quantification of cell number, three different amounts of ADSC (10,000, 30,000, and 50,000 cells) were processed. The variation between samples was low (Figure 2.8A) and the quantity of DNA is proportional to the number of cells. The most important result, is that according to this result, the amount of DNA per cell is 10.51 pg. This value is considerably closer to the literature value, 6 pg per cell, indicating that this technique could give a close approximation of number of cells in adipose tissue, emulsified fat and SVF-gel samples. Preliminary data was obtained for lipoaspirate and SVF-gel. Lipoaspirate has 2- and 7-fold the amount of DNA per grams of sample than unwashed and washed SVF-gel respectively (Figure 2.8B). Adding the washing step for SVF-gel certainly removed a large amount of DNA from lysed cells and allowing to quantify only those cells that are intact/viable. This allows us to take into account only intact cells that can have an active role in tissue regeneration processes.[2] This is an effective method for DNA purification from adipose tissue and could provide valuable information that could help in determining dosage of adipose tissue for treatments. However, it is important to consider that there are some obstacles regarding this technique.

It is well known that there is variability between patients in cell density in adipose tissue (Maclean *et al.*, 2015). This can be seen in the different values for number of cells in the adipose tissue reported above (Table 1.2). Adipose tissue volume is composed mainly of the volume of adipocytes, which varies depending upon the fat percentage of an individual (Maclean *et al.*, 2015). Although the number of adipocytes in a healthy

[2] Due to Covid-19 lockdown it was not possible to analyse all the studied groups using NucleoSpin columns.

adult remain constant through adulthood, adipocyte size varies according to weight gain and weight loss with adipocytes becoming larger with weight gain and smaller when weight is lost (Maclean *et al.*, 2015). This affects the structure of the tissue and cell density in a specific tissue volume. Because of this inconsistency it has been difficult to accurately isolate DNA from adipose tissue samples, not only due to the fatty nature of the tissue, but also due to the large variability between patients. Therefore, it was decided that a comparison of DNA between formulations could have some value in determining how each processing method concentrated the cells but that other characterisation methods were needed to more clearly understand how processing affects the cells present.

Each of the adipose tissue formulations was imaged to determine how processing affected the tissue structure and cell integrity. Changes in the integrity of the tissue could affect the regenerative properties of the adipose tissue since it can generate stress in the cells, can lyse cells and may affect the release of cytokines. LightSheet and confocal microscopy were used to create 3D images from ADSC, adipose tissue, lipoaspirate, emulsified fat and SVF-gel.

For LightSheet imaging, four different dyes were used to study the structure of the adipose tissue. Isolectin IB_4 is a protein isolated from an African plant, *Griffonia simplicifolia,* which has been found to bind to terminal a-D-galactosyl residues of glycoproteins of erythrocytes, perivascular cells, and endothelial cells (Ernst and Christie, 2006). Hoechst 33342 is widely used for DNA staining since it binds to AT-rich sequences in double-stranded DNA (Lin and Goodell, 2011). One of the advantages of Hoechst over DAPI is that it is cell permeant and allows cell staining without fixation and permeabilisation processes. This is important since emulsified fat and SVF-gel are samples that can dissolve in liquids, so sample loss is expected with washing the samples. BODIPY 558/568 C12 is a fatty acid analogue with a tail composed of 12 carbons that binds covalently to the hydrophobic end of lipids and has been used to track lipid droplets in different cell types (Targett-Adams *et al.*, 2003; Rambold, Cohen and Lippincott-Schwartz, 2015). Finally, Deep Red CellMask was initially used to try to analyse the integrity of the adipocytes in the different samples.

CellMask Deep Red is a lipophilic fluorophore that is widely used for staining cellular plasma membrane (Mönkemöller *et al.*, 2012).

ADSC were used as a specificity control for the different stains. When all four stains were used together, the CellMask was not detectable (Figure 2.10A). However, when the cells or tissue were stained only with the CellMask, it was possible to see the cell membrane of cells. Images taken with the CellMask appeared very similar to the structures seen using the BODIPY (Figure 2.10B), suggesting that both stains compete to bind to the different lipids present in the cells including the ones in the plasma membrane. In previous studies, it was seen that BODIPY not only stains lipid droplets in adipocytes, but also cell membranes including the ones of SVF cells (Hagberg *et al.*, 2018). The ADSC showed some staining with BODIPY (most likely due to the cell membranes) however the distribution and appearance of the BODIPY staining was very different in the samples which contained adipocytes where the BODIPY predominantly stained the fatty droplets within cells. Finally, Isolectin B4 was used to stain endothelial cells, but the data presented here indicated some low-level background staining in the ADSC sample (Figure 2.11). As a result, for the rest of the images obtained by LightSheet only BODIPY, Isolectin and Hoechst were used with the knowledge that Isolectin may have some cross reactivity with ADSCs as well as endothelial cells (Figure 2.11).

LightSheet images provided an overview of the structure of the different studied formulations; however, the resolution of the images was not high enough to study small details. As a result, confocal imaging was used to obtain higher resolution images. In this case instead of using CellMask, a protein-specific membrane stain, MemBrite™, was used to stain the membrane of the adipocytes and to determine whether the adipocytes were intact following processing. MemBrite™ Fix dye binds covalently to cell surface membrane proteins (Biotium, 2020). The difference between CellMask and MemBrite™ Fix dye is that the CellMask stains all lipid, while the MemBrite™ binds to wide range of cells membrane proteins (Biotium, 2020). The advantage of MemBrite™ Fix dye is that it would not overlap with BODIPY, allowing us to study the integrity of the adipocytes.

Adipose tissue structure is characterised by lobules of adipocytes supported by a well-organised ECM and capillaries running alongside them (Volz, Huber and Kluger, 2016). Wittman *et al*., (2015), Mashiko *et al*., (2017) and Yao *et al*., (2017) have previously used confocal imaging on adipose tissue with BODIPY, Isolectin and Hoechst. In these three studies, whole adipose tissue presented a compact structure with the round-shaped adipocytes and smaller cells types located along the capillary network that runs through the adipocyte lobules.

In this study, we have shown that minced adipose tissue and lipoaspirate have comparable structures indicating that liposuction does not affect the majority of cellular integrity of the tissue. It is also possible to visualise blood vessels within the lipoaspirate and some Isolectin stained cells in both cases, which could be the perivascular ADSC niches (Figure 2.11) (Lin *et al.*, 2008). In the confocal images it is also possible to observe some vessels running through the adipocyte lobules (Figure 2.12). In this case, MemBrite™ Fix dye shows the BODIPY stained lipid droplets surrounded by membrane stain, indicating the adipocytes remain intact in the whole adipose tissue sample. Nevertheless, there are some free lipid droplets that could be a result of the lysis of some adipocytes during the harvesting or preparation processes.

In contrast, when the emulsified adipose tissue was imaged using LightSheet and confocal images (Figure 2.11 and Figure 2.12) after the emulsification process the adipose tissue structure was disrupted and there was free lipid present in the sample. On the confocal images, there are some adipocytes with an intact cell membrane in the emulsified fat samples. These adipocytes remain agglomerated surrounded by free lipid droplets. In contrast, Mashinko *et al.,* (2017) studied emulsified fat using perilipin to stain adipocytes, lectin to stain capillaries and Hoechst for the nuclei. They describe that emulsified has irregular-sized and/or shaped adipocytes suggesting that these are damaged or dead (Mashiko *et al.*, 2017). Similarly, Sesé *et al*. (2019) used histological analysis of emulsified fat to show that it was composed of broken mature adipocyte membranes with a high concentration of stromal cells. In both cases mentioned, after transferring the adipose tissue multiple times between syringes, the tissue was filtered using a mesh that may have broken or removed the remaining adipocytes in the samples. It has been reported before that fragmentation level of the

ECM of the adipose tissue increases as the tissue is processed more (Yao *et al.*, 2017). While lysis of adipocytes is expected after emulsification, it is possible that different protocols (for example, different number of passes between syringes) to obtain emulsified fat affects the integrity of the tissue in different ways.

Finally, on the LightSheet images the SVF-gel appears to have more concentrated on cell content with very few adipocytes and some free lipid. Similarly, confocal images show that SVF-gel contains few adipocytes with an intact cell membrane surrounded by free lipid droplets with smaller cells around. Since SVF-gel is composed of different layers (pellet, aqueous layer and ECM layer) after the centrifugation step in the protocol (see Section 2.3.7 for further detail), it is important to identify which components are in each layer (Figure 2.13). In the ECM layer or yellow layer, there are some adipocytes remaining, remaining of tissue with SVF cells attached, and some free lipid. Even though the lipid layer was removed to obtain SVF-gel, these images demonstrate that the free lipid and adipocytes are not completely removed. Similarly, there are small lipid droplets in the SVF-pellet around the concentrated cellular and remaining's of tissue mixture.

Yao *et al*., (2017) studied the structure of adipose tissue before and after processing to obtain SVF-gel by confocal microscopy using Hoechst to stain the nuclei, lectin for vascular endothelial cells, and BODIPY for adipocytes. They reported that in their SVF-gel most of the lipid droplets were removed by the centrifugation step leaving a small number of flat shaped adipocytes (Yao *et al.*, 2017). Similarly, Zhang *et al.,* (2018) studied SVF-gel structure by histology. They describe that SVF-gel contained a concentrated number of small-sized cells with multiple intracellular lipid droplets (Zhang *et al.*, 2018). These studies support our result that even when most of the free lipids are removed, SVF-gel contains some adipocytes and lipid droplets. Nevertheless, it is clear that SVF cells are concentrated within a disrupted tissue fragments with this processing method.

All the changes in structure of the adipose tissue present valuable information about how the different processes impact structure, especially how the presence and integrity of adipocytes is modified. This change in structure could affect the tissue's

regenerative properties, and how the host responds once each formulation is implanted. One hypothesis is that the absence of adipocytes in emulsified fat and SVF-gel could reduce the resorption of the adipose tissues therefore enhancing the regenerative potential. It has been shown that terminally differentiated adipocytes are unlikely to survive post lipotransfer as these cells require a high nutrient supply (not present initially) and these cells are less resilient compared to ADSCs (Dong *et al.*, 2013; Volz, Huber and Kluger, 2016; Zhang *et al.*, 2018).

Knowing the viability of cells before and after processing the tissue is important, since only viable cells will contribute to the regenerative process for wound healing. Live/dead assays were used to stain adipose tissue before and after processing to study the viability of the cells in each sample. In Figure 2.14, live cells are stained in green using Calcein AM that penetrates live-cell membranes and stain their cytoplasm, while dead cells are stain in red by EthD-1 since the cell membranes are disrupted allowing this stain to bind to the DNA (Molecular Probes Inc., 2005).

Our results show live adipocytes in the whole adipose tissue with some green-stained cells of the blood vessels running through it (Figure 2.14A). Around the adipocytes some dead cells were identified. Lipoaspirate had a similar structure and cell viability as the adipose tissue. This could be a result of harvesting procedures and tissue handling. Also, the time in which the tissue is collected from the theatre and transported to the lab could produce some dehydration affecting the viability of the cells.

Once the tissue was processed to emulsified fat, most of its structure was lost and the proportion of cells stained red increased meaning that more dead cells were present. These dead cells may be the lysed adipocytes, supported by the appearance of more free lipid within the sample. Tonnard *et al*. (2013) also imaged emulsified fat using live/dead staining and found that adipose tissue after emulsification was completely disrupted leaving an oily emulsion with no viable adipocytes. One limitation of the live/dead assay is it cannot distinguish between different cell types and we cannot determine how many of the dead cells were adipocytes and how many were from the stromal vascular fraction.

In the same way, the process to create SVF-gel damaged the adipose tissue structure so much that it is just possible to identify a small lump of tissue surrounded by a mix of stains. A greater proportion of dead cells can be seen in the SVF-gel than in the emulsified fat. In contrast to the images collected using the LightSheet and confocal microscopes, emulsified fat and SVF-gel appeared different in structure. In the LightSheet images the tissue is not well defined as a consequence of the free lipid around the samples. This could be as a result of the washing steps to prepare the samples for imaging, the Live/dead staining protocol did not require a wash step. These extra washing steps could have removed some of the free oil of the samples leaving only small fragments of the remaining adipose tissue. These remaining pieces are more likely to have structures similar to the un-processed adipose tissue than the tissue which was washed away. This again indicated the challenges associated with handling and characterising adipose tissue. Even when there are small fragments in the emulsified fat and SVF-gel, it is clear that most of the tissue has been disrupted from the amount of lipid released from lysed adipocytes in the live/dead images. It would be expected that emulsified fat contains more lipid droplets than SVF-gel, since the main purpose of the SVF-gel protocol is to remove the free lipid. Nevertheless, the amount of lipid removed from SVF-gel is highly variable between batches. This could be a result of the amount of lipid in the adipocytes that varies according to the fat percentage of each individual.

Adipose tissue has been used clinically mainly for lipofilling tissues that need volume reconstruction. In the past few years, different protocols to process adipose tissue have been developed to enhance the regenerative properties of adipose tissue (emulsified fat, SVF-gel, and ADSC) and make easier to handle and re-inject into patients. As a result, different inquiries have emerged including the mechanism behind their regenerative properties. In order to understand this, it is important to know how the different protocols affect the structure and viability of the tissue. Many articles in the literature speculate how each processing method affects the adipose tissue structure and composition but quantitative data and direct comparisons from the same samples of adipose tissue are lacking. In order to fulfill this gap, the aim of this chapter

was to characterize the structure, cellular composition and viability of adipose tissue, emulsified fat, and SVF-gel. In summary we have shown that:

- ADSC isolated and cultured from adipose tissue have the phenotype of stromal cells.
- Minced adipose tissue and lipoaspirate appear morphologically similar indicating the clinical relevance of studying minced adipose tissue and supports the decision to combine these samples in analysis where needed.
- Emulsification lyses the majority of the adipocytes leaving a considerable amount of free lipid within the sample.
- Filtering and removing the lipid layer from emulsified fat leaves a concentrated SVF-gel with SVF cells with some remaining adipocytes.
- As adipose tissue is processed, it loses its structure and cell viability decreases.

Using this knowledge of how adipose tissue processing affects tissue composition and structure we will next compare the angiogenic properties of ADSC, adipose tissue, emulsified fat and SVF-gel.

Chapter 3 Study of conditioned media from adipose tissue and derivatives in 2D models of angiogenesis

3.1 Aim

To compare the pro-angiogenic properties of conditioned media from adipose tissue, emulsified fat, SVF-gel, and ADSC on 2D endothelial cell cultures.

3.2 Introduction

It is believed that the regenerative properties of adipose tissue derive from the growth factors that it releases. However, the mechanisms underlying these regenerative properties are not well understood. Conditioned media is a novel approach for non-cellular therapies that contains the growth factors, miRNA and mRNA, and proteins from the cells of tissues it was produced from. All these components in the conditioned media have a similar regenerative effect as a transplant of tissue or cells with a lower risk of rejection from the host body (Locke *et al*., 2015). Various trials have been carried out using conditioned media from ADSC for treatment of kidney, lung, and liver injuries, cardiovascular disease, cartilage and bone regeneration, and wound healing (Pawitan, 2014). However, although there are some studies into soft wound vascularisation using conditioned media from ADSC or SVF, there are no studies which compare ADSC conditioned media with whole adipose tissue or conditioned media made from its derivatives.

Conditioned media is a recently introduced approach for cell free therapies that can deliver growth factors released from cells and tissue with the same positive effect as cell therapies (Locke, Feisst and Meidinger, 2015). Conditioned media can deliver the secreted factors of the source cells and tissue without the risk of poor survival after transplantation into the wounded area (Kwon *et al.*, 2015). Since conditioned media do not contain cells, there is no need to match cells used for its production with the patient. (Pawitan, 2014). Tumorigenic risk related to stromal cells is avoided, plus conditioned media can be standardised reducing variability of patient to patient cell

therapies (Cai *et al.*, 2019). In addition, it can be produced, frozen, freeze-dried, packaged, and easily transported as an off-the-shelf product (Pawitan, 2014).

Finally, in a laboratory setting, the fact that conditioned media can be frozen and stored helps with experimental planning. For this research this is the main advantage of using conditioned media. Due to the Human Tissue Act human and ethically approved protocols tissue could only remain for one week in our laboratory (NHS research ethics 15/YH/0177). This is a small window of time to run all the necessary experiments and rely on a regular supply of waste tissues. In addition, one of the main limitations of this research was the inconsistency of tissue supply. Conditioned media allowed us to obtain a considerable amount of samples per patient that could be stored until required and used for different types of assays used on this thesis.

Comparing the effects of conditioned media from adipose tissue, emulsified fat, and SVF-gel to those observed with ADSC is important since these studied groups are currently used clinically. Using conditioned media allows us to estimate the importance of the growth factors released by the cells and tissue in vascularisation and how this could help the wound healing process. In addition, it could provide some insights into the mechanisms of wound healing properties of the adipose tissue before and after processing. In this chapter, conditioned media with different seeding densities and amounts of tissue were produced and tested on endothelial cells (for further details see 1.11.3) to determine the optimal conditions for vascularisation.

3.3 Methods

3.3.1 *Conditioned media*

To produce conditioned media from the different groups, cells and different formulations of fat were cultured in 6 well plates with 3 ml of media per well and incubated for 3 days. The type of media that was used depended on the cell type used for the experiments (see Section 2.3). As the adipose tissue is further processed, cells are more concentrated within the tissue, as a result higher volume of adipose tissue were used compared to emulsified fat and SVF-gel. In addition, there are no studies

to this date in which they compare side by side adipose tissue with emulsified fat and SVF-gel, making it hard to approximate the amount of tissue/number of cells require to have an effect on endothelial cells. For this reason, a range of weight/volume of each sample and number of cells were selected to produce conditioned media, which are specified in Table 3.1. After 3 days of cultivation, the media was removed carefully and centrifuged for 5 min at 112 g. In the case of the emulsified fat the media was also filtered using cell strainers (100 μm pore size) to remove any tissue residual in the media. Then, the media were aliquoted into 5 ml tubes and frozen at -80ºC for further use. For lipid controls, lipid extracted from adipose tissue during its processing was added to MV medium without supplements in 10, 20, and 30% of volume.

Table 3.1 Cell and tissue quantities used for conditioned media

Group to study	Cultures for conditioned media						
	1	**2**	**3**	**4**	**5**	**6**	**7**
ADSCs (cells/cm^2)	1,500	10,000	30,000	40,000	50,000	60,000	70,000
Adipose tissue (g fat/ml media)	0.035 +/- 0.03	0.6 +/- 0.03	0.8 +/- 0.03	0.1 +/- 0.03	0.13 +/- 0.03	0.15 +/- 0.03	
Emulsified fat (ml emulsified fat/ml media)	0.06	0.83	0.1	0.13	0.16		
SVF-gel (ml SVF-gel/ml media)	0.006	0.01	0.016	0.023	0.026	0.03	0.036

3.3.2 Experimental design and samples

As it was mentioned before conditioned media from adipose tissue and its derivatives was used in this research in order to help experiment planning. Using conditioned media allowed us to freeze samples that could be used when required. This was crucial for this research because tissue donations were not regular and the amount, we obtain from batch to batch was highly variable. As a result, conditioned media allowed us to constantly run experiments, especially during those long periods of times (weeks, or even months) without tissue. Every batch of tissue was processed and cultured within 24 hours after it was donated to warranty a high viability. Different batches were used for each of the repeats of the experiments listed on Table 3.2.

Table 3.2 Tissue and formulation batches used in the different experiments.

Experiment	Sample	Rep 1	Rep 2	Rep 3
LDH in conditioned media	ADSC	398		
	Adipose tissue	404	408	
	Emulsified fat	402		
	SVF-gel	404		
LDH in conditioned media with migration and metabolic assays	Adipose tissue	411		
	Emulsified fat	413		
HMEC-1 migration assay	ADSC	399	398	402
	Adipose tissue	390	393	404
	Emulsified fat	402	404	409
	SVF-gel	402	404	409
HMEC-1 metabolic actibity	ADSC	399	398	402
	Adipose tissue	390	393	404
	Emulsified fat	402	404	409
	SVF-gel	402	404	409
HDMEC migration assay	ADSC	419	420	429
	Adipose tissue	421	422	430
	Emulsified fat	421	422	430
	SVF-gel	433	434	441
HDMEC metabolic activity	ADSC	419	420	429
	Adipose tissue	421	422	430
	Emulsified fat	421	422	430
	SVF-gel	433	434	441
Lipid effect on HDMEC	Lipid	433	434	441

3.3.3 LDH assay

Lactate dehydrogenase (LDH) in the conditioned media was measured using an LDH Cytotoxicity Assay kit (Thermofisher, Loughborough, UK). First, 50 μl of conditioned media from ADSC, SVF-gel, emulsified fat or fat were transferred in triplicate into a 96 well plate. DMEM media was used as negative control, while the positive control from the kit was used by diluting 1μl of 0.1μg/ml LDH solution included in the kit in 10 ml of 1% BSA in PBS. The reaction mixture was prepared by dissolving a vial of Substrate Mix (lyophilised) in 11.4 ml of deionised water and adding a vial of assay buffer (0.6 ml). Once all the samples were in the 96 well plate, 50 μl of reaction mixture was added to each of the samples and they were incubated for 30 min in darkness and room

temperature. After the incubation time, 50 μl of the stop solution was added to each sample and absorbance was measured at 490 nm and 680 nm using a spectrophotometer (Bio-Tek, Swindon, UK).

3.3.4 Endothelial migration assay

To study endothelial cell migration, silicone stoppers (Enzo, Exeter, UK) were used to create an exclusion zone of 2 mm diameter in endothelial cell cultures. Sterile stoppers were placed into 96 well plates and pushed to the bottom of the wells to seal them and create an exclusion zone in each well. Human microvascular endothelial cells-1 (HMEC-1) or human dermal microvascular endothelial cells (HDMEC; Promocell, Heidelberg, Germany), were seeded carefully around the stoppers at a density of 25,000 cells/well with 0.1 ml of media according to each cell type (see Section 3.3.1). After 24 hours, the stoppers were removed, and media was changed for conditioned media from ADSC, adipose tissue, emulsified fat or SVF-gel (collected as described in Section 3.3.1). Vascular endothelial growth factor (VEGF) and fibroblast growth factor (FGF) were used as positive controls at a concentration of 50 ng/ml for HMEC-1. In the case of HDMEC, 20 ng/ml VEGF and 10 ng/ml FGF with 2% serum in media was used as recommended from Promocell. Images were acquired at 0, and 24 hours after media change using an inverted light microscope and Moticam 2 software (Motic, Barcelona, Spain). Images were analysed using ImageJ to measure the area of the exclusion zone (Figure 3.1). Then, data was normalised to the non-conditioned media to generate a graph for data analysis.

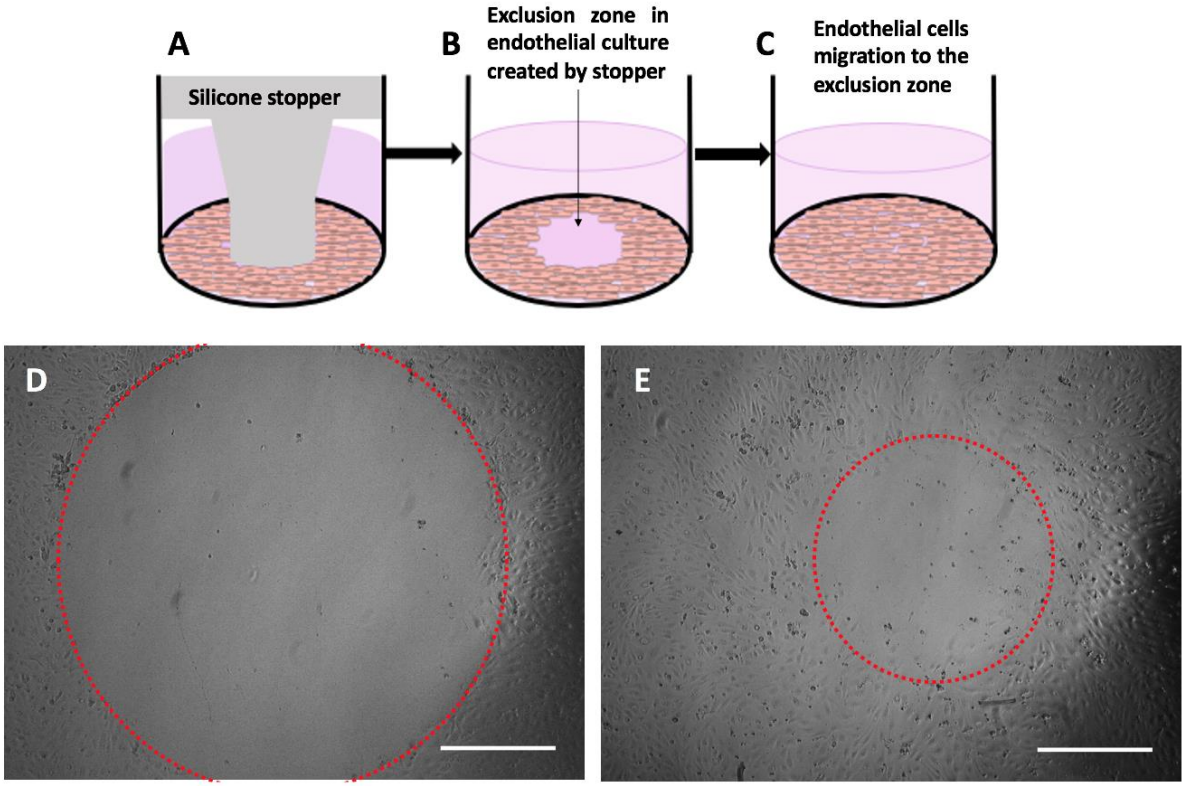

Figure 3.1 Schematic diagram illustrating endothelial migration assay using silicone stoppers (A) to create an exclusion zone during 24 hrs of initial culture. Then the stoppers are removed (B) to allow the cells to migrate to the exclusion zone (C). Image analysis for migration assay at time 0 (D) and after 24 hrs (E) measuring the exclusion area highlighted by the red circles. Scale bar = 0.5 mm

3.3.5 Endothelial metabolic activity assay

Human microvascular endothelial cells, HMEC-1 or HDMEC, were seeded at 10,000 cells/well in 24 well plates with 0.5 ml of appropriate media. In case of the HDMEC, the media used for seeding the cells did not contain any serum. After 24 hrs, media was changed for conditioned media and cells cultured for an additional 48 hrs. Afterwards, MTT (3-(4,5-dimethylthiazol-2-yl)-2,5-diphenyltetrazolium bromide; (Sigma Aldrich, Dorset, UK) was used to measure metabolic cell activity (Figure 3.2). Conditioned media was removed from each well and cells were washed using modified PBS without calcium chloride and magnesium chloride (Sigma Aldrich, Dorset, UK). Subsequently, MTT reagent was added using a concentration of 0.5 mg of MTT per ml of modified PBS to each well (0.5 ml per well). After 60 min of incubation, MTT reagent was removed and the colourant was released using acidified isopropanol (128

μM HCL in isopropanol). After 10 min of incubation at room temperature, absorbance was read at 570 nm using a spectrophotometer (Bio-Tek, Swindon, UK). Data was normalised to non-conditioned media for analysis.

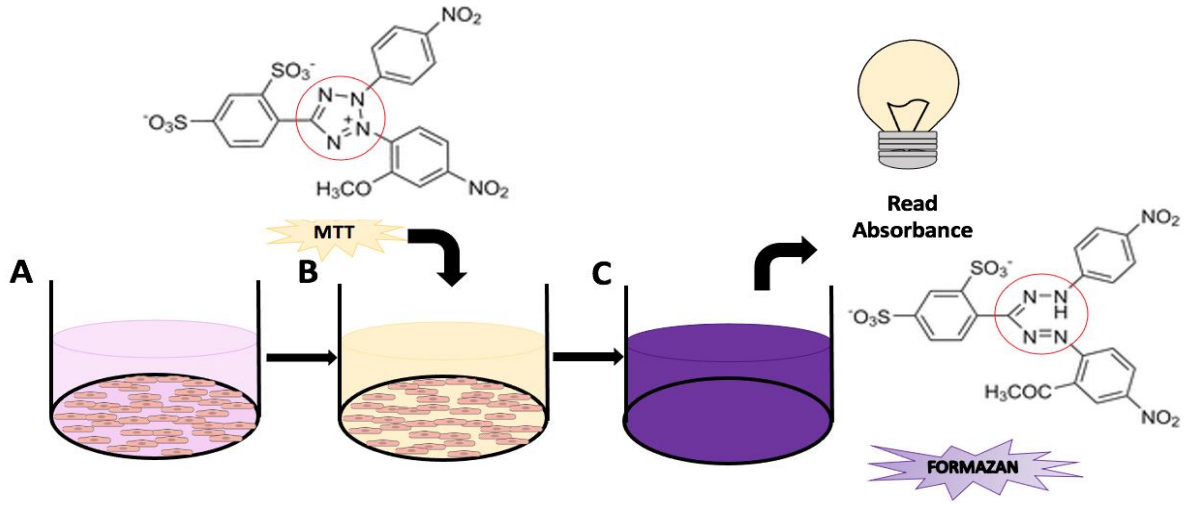

Figure 3.2 Schematic diagram illustrating MTT assay of endothelial cells after 48 hr of culture in conditioned media (A). Media is removed, cells are washed with PBS and MTT reagent is added (B). After 1 hr incubation MTT is removed and acidified isopropanol is added to measure the absorbance of the released colorant using a spectrophotometer.

3.3.6 Free lipid effect on endothelial cells

Free lipid from adipose tissue was obtained during the last step of SVF-gel preparation (see Section 2.3.7 for further details). This free lipid was added to MV medium (without any additional supplements) at 10, 20 or 30% (v/v). HDMEC migration and metabolic activity were analysed using the protocols in Sections 3.3.4 and 3.3.5 using this MV medium supplemented with free lipid instead of conditioned media. MV media without supplements was used as a negative control.

3.3.7 Statistical analysis

Data from experiments, excluding the LDH cytotoxicity assay, was normalised in relation to the negative control before running statistical analysis. Statistical analysis was made using GraphPad Prism 7 programme. One-way ANOVA was applied to compare each group to the negative control using Dunnett's multiple comparison test. All values are presented with mean ± standard deviation and differences were taken to be significant for $p<0.05$.

3.4 Results

3.4.1 Generation of conditioned media

Initially, the effect of using different quantities of adipose tissue, emulsified fat, SVF-gel or ADSCs to condition the media were investigated (Figure 3.3 and Table 3.1). The media conditioned from fat-derived tissue or cells were added to endothelial cells and the metabolic and migratory activities were measured. The aim was to find the optimal quantity of each formulation to invoke an increase in cell response.

ADSC conditioned media (not shown in image) remained clear and was the easiest to collect with any remaining cell debris removed by centrifugation. Adipose tissue floated on the medium and some lipid droplets were visible (Figure 3.3A). Collecting this conditioned media was not complicated since the tissue is easily removed. However, some lipid droplets and small tissue pieces remained in the conditioned media even after centrifugation. Then, emulsified fat dissolved in the media creating a cloudy media with lipid layer mainly on the top and some remaining fragments of tissue were visible (Figure 3.3B). Collecting media from emulsified fat was the most complicated one from all the studied ones. Spinning it down and filtering it helped to separate a medium layer from the free lipids. Nevertheless, the conditioned media remained cloudy with some lipid and tissue within it. Finally, SVF-gel gel conditioned medium looked clearer with a small amount of lipid on top (Figure 3.3C), that was easily removed after centrifugation.

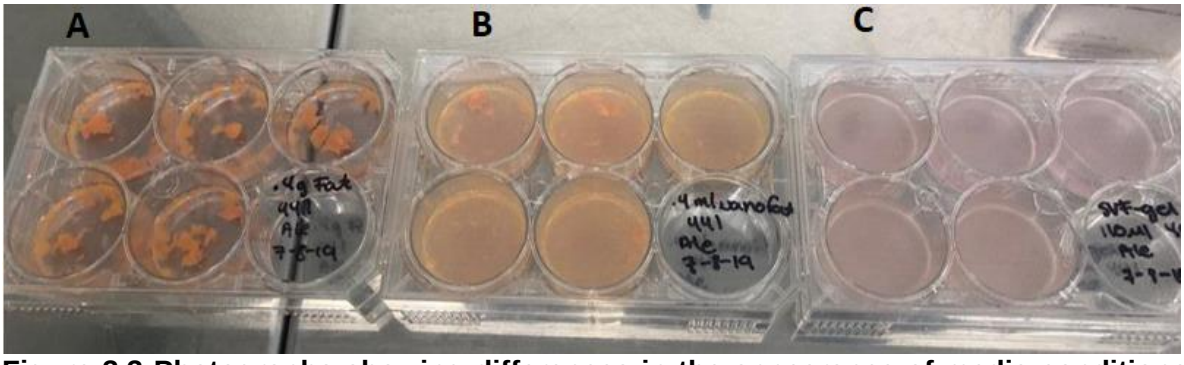

Figure 3.3 Photographs showing differences in the appearance of media conditioned using 0.13 g adipose tissue per ml of media (A), 0.13 ml of emulsified fat per ml of media (B), and 0.036 ml of SVF-gel per ml of media (C).

3.4.2 LDH cytotoxicity assay

Lactate dehydrogenase (LDH) was measured in conditioned media from ADSC, SVF-gel, adipose tissue, and emulsified fat (Figure 3.4A) to measure the cell death rate in conditioned media. The conditioned media from ADSC presented the lowest LDH readings of all the groups with a value of 15%. Then, the SVF-gel provided measurement of 126% higher than the positive control. In contrast, adipose tissue and emulsified fat reached values 5.5 and 3 times higher than positive control respectively indicating that in these cases there is a very high number of dead cells present in the samples obtained from processed adipose tissue.

To measure how the levels of LDH change over culture time, three different quantities of adipose tissue were cultured and after 1, 4, 24, 48, 72 and 168 hrs the media was collected to measure LDH levels (Figure 3.4B). A similar trend was observed in all samples. The highest LDH level released into the media was within the first hour; this was expected due to the stress the tissue is exposed to before being cultured. After that, the levels of LDH in media were detected but not as elevated as in the first hour of culture.

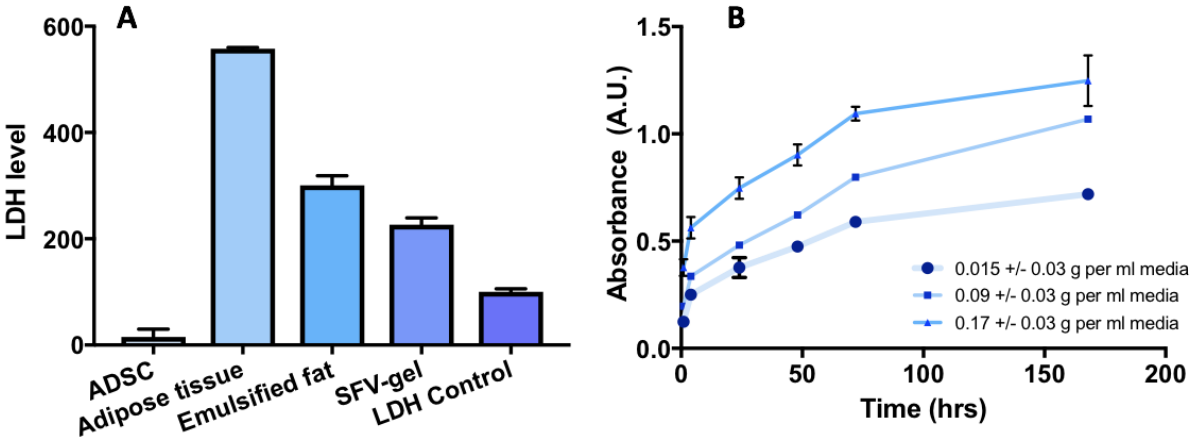

Figure 3.4 Lactate dehydrogenase (LDH) content of conditioned media from ADSC (50,000 cells/cm^2), adipose tissue (0.1 g/ml media), emulsified fat (0.13 ml/ml media), SVF-gel (0.03 ml/ml media) after 3 days of co-culture (A), and LDH accumulation over time with three different concentrations of adipose tissue in conditioned media (B). LDH positive control 0.1μg/ml LDH. Mean with error bars showing standard deviation. N=1 n=3.

Four different adipose tissue and emulsified fat cultures were used to investigate whether changing the media after one hour of incubation, to remove dead cells and their metabolites, could increase the metabolic activity and migration of the endothelial cells on treatment with these samples. For adipose tissue conditioned media 0.1 g of tissue per ml media was used to produce all the conditioned media, and for the emulsified fat 0.13 ml of tissue per ml media were cultivated. For two of the samples in each case, media was changed after one hour of culture to remove all the cellular debris formed during culture preparation. Then, the conditioned media was collected after 24 and 72 hrs to compare the LDH levels and effects analysed on endothelial cells (Figure 3.5A). In both tissues, treatment of endothelial cells with the media that was changed after one hour resulted in significantly lower LDH levels than those samples with media collected from time 0. The metabolic activity of the endothelial cells exhibited values close to the non-conditioned media (control) in both tissues' media and were similar between every sample (Figure 3.5B). However, cell migration was non-significantly increased for the conditioned media from adipose tissue cultured from 0-24 hrs. However, in the rest of the samples the migration was comparable to the negative control (Figure 3.5C).

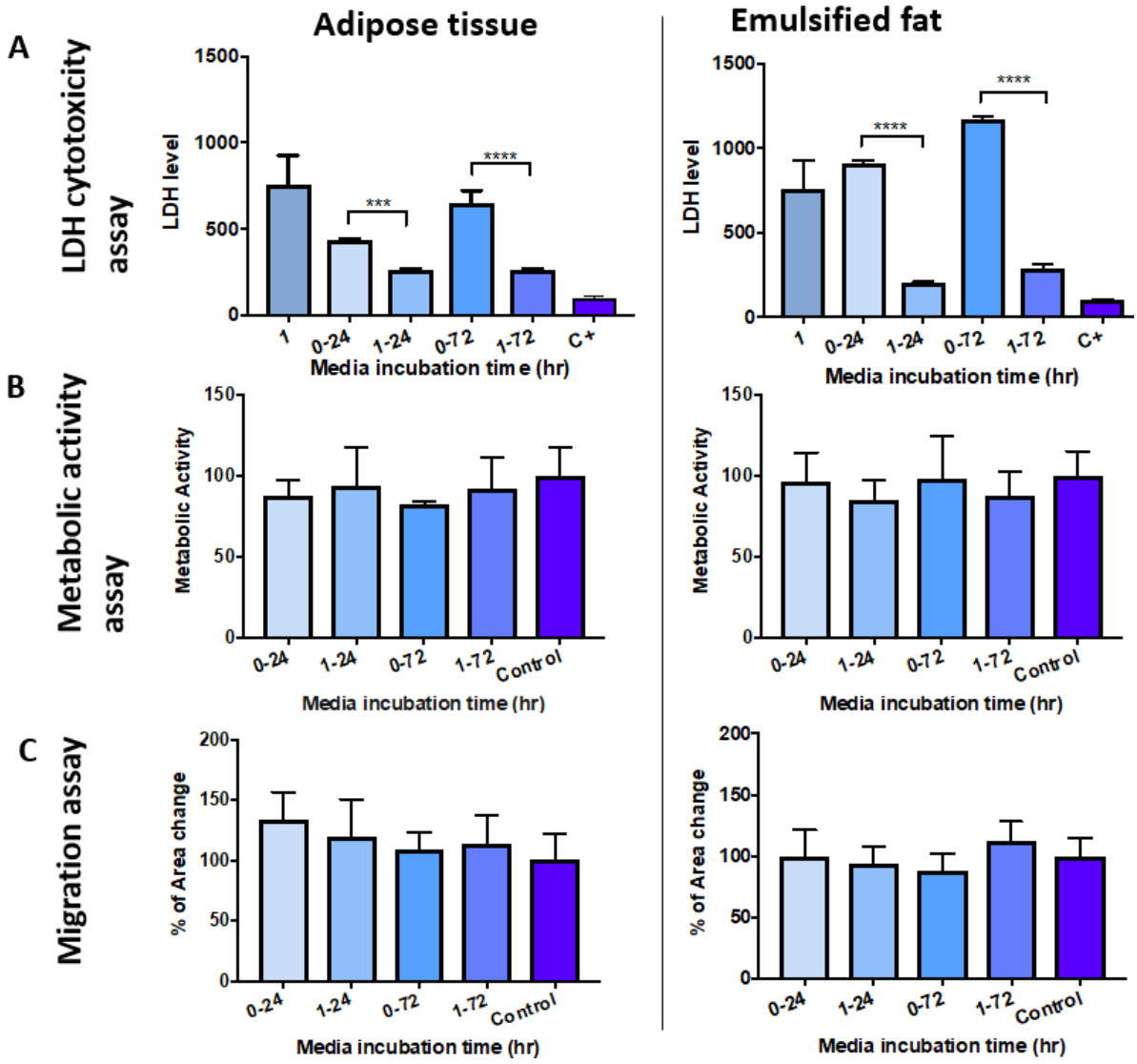

Figure 3.5 LDH analysis of media conditioned with adipose tissue or emulsified fat for different incubation times (A). Metabolic activity (B) and migration (C) of endothelial cells (HMEC-1) using the conditioned media from adipose tissue and emulsified-fat with a change of media after 1 hr of culture or without any media change. LDH positive control 0.1µg/ml LDH. Control for endothelial metabolic activity and migration was serum free non-conditioned media. Mean with error bars showing standard deviation. N=1, n=3 *p<0.05, **p<0.01, ***p<0.001, ****p<0.0001.

3.4.3 Endothelial (HMEC-1) migration assay

Human endothelial microvascular endothelial cells (HMEC-1) were used to estimate the angiogenic potential of the conditioned media from the different studied groups since these cells form micro-vessels and are essential for the vascularisation process. Endothelial migration (Figure 3.6) and metabolic activity (Figure 3.7) on HMEC-1 were

used to study the angiogenic properties of media conditioned using ADSC, adipose tissue, emulsified fat, and SVF-gel. ADSC conditioned media enhanced cell migration with concentrations of 40,000 and 50,000 ADSC per cm^2 with an increase of 35 and 41% compared to the negative control respectively (Figure 3.6A). Whilst a trend, this was not statistically significant. On the other hand, adipose tissue conditioned media did not stimulate cell migration compared to the negative control reaching the highest value of 111% with 0.08±0.03 grams of fat per ml of media (Figure 3.6B). The emulsified fat presented a similar trend on cell migration. As the quantity of emulsified fat increased in the conditioned media, cell migration increased also (Figure 3.6C). However, the highest value obtained with a concentration of 0.13 ml of emulsified fat per ml of media was 114% without a significant difference from the non-conditioned media. Lastly, SVF-gel conditioned media did not make a difference to cell migration since the degree of migration obtained with the different concentrations of SVF-gel were similar in value to non-conditioned media (Figure 3.6D). In this case, the positive control FGF promoted cell migration achieving a value of 158% of area change (not significant).

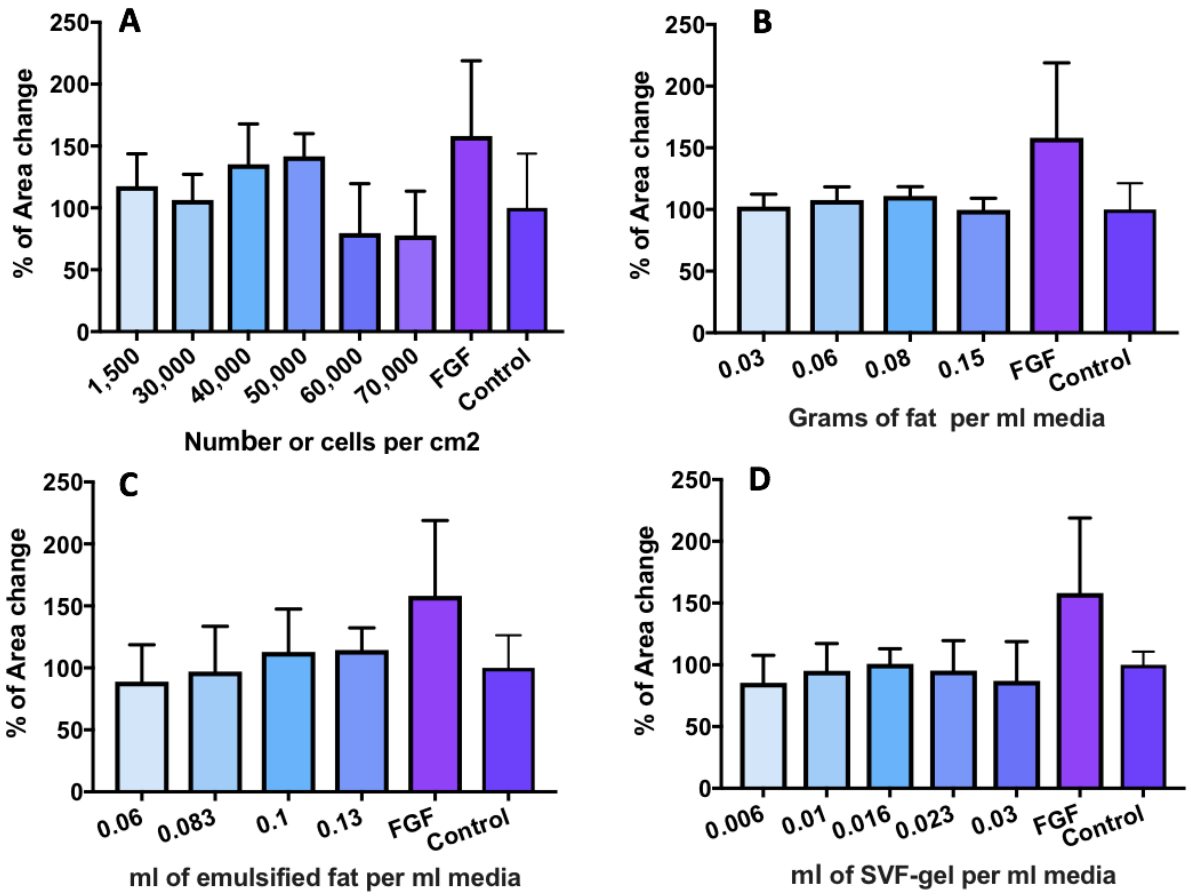

Figure 3.6 Migration of endothelial cells (HMEC-1) after 24 hrs cultivated in conditioned media from ADSC (A), adipose tissue (B), emulsified fat (C), and SVF-gel (D). Normal media, DMEM, was used as negative control; while 50 ng/ml of FGF were used as positive controls. Mean with error bars showing standard deviation. N=3, n=3.

3.4.4 Metabolic activity using MTT on HMEC-1

HMEC-1 were cultured at a density of 10,000 cells/well in 24 well plates with 0.5 ml of conditioned media. After two days of culture MTT assays were performed to measure the HMEC-1 metabolic activity. As the cell seeding of ADSC to produce the conditioned media increased, the metabolic activity of the endothelial cells rose without statistically significant difference reaching a maximum value of 121.94% with a seeding density of 60,000 cells per cm^2 (Figure 3.7A). However, above this seeding density, metabolic activity did not change compared to the negative control (normal media). In contrast, adipose tissue conditioned media (Figure 3.7B) showed a negative impact on endothelial cells in all the different culture densities, non-significantly

reducing their metabolic activity compared to the positive and negative controls. Comparably, emulsified fat conditioned media (Figure 3.7C) also reduced endothelial metabolic activity related to normal media. Nevertheless, there was a slight but not statistically significant increase in cell metabolic activity as the amount of emulsified fat increased in conditioned media. Finally, SVF-gel conditioned media (Figure 3.7D) did not significantly affect the endothelial proliferation. All the cell cultures with this type of conditioned media had a mean value of metabolic activity below the control but not statistically significant. The positive control used in these experiments was FGF (50 ng/ml), however in both cases HMEC-1 cells were not significantly stimulated presenting a value 5% higher than non-conditioned media.

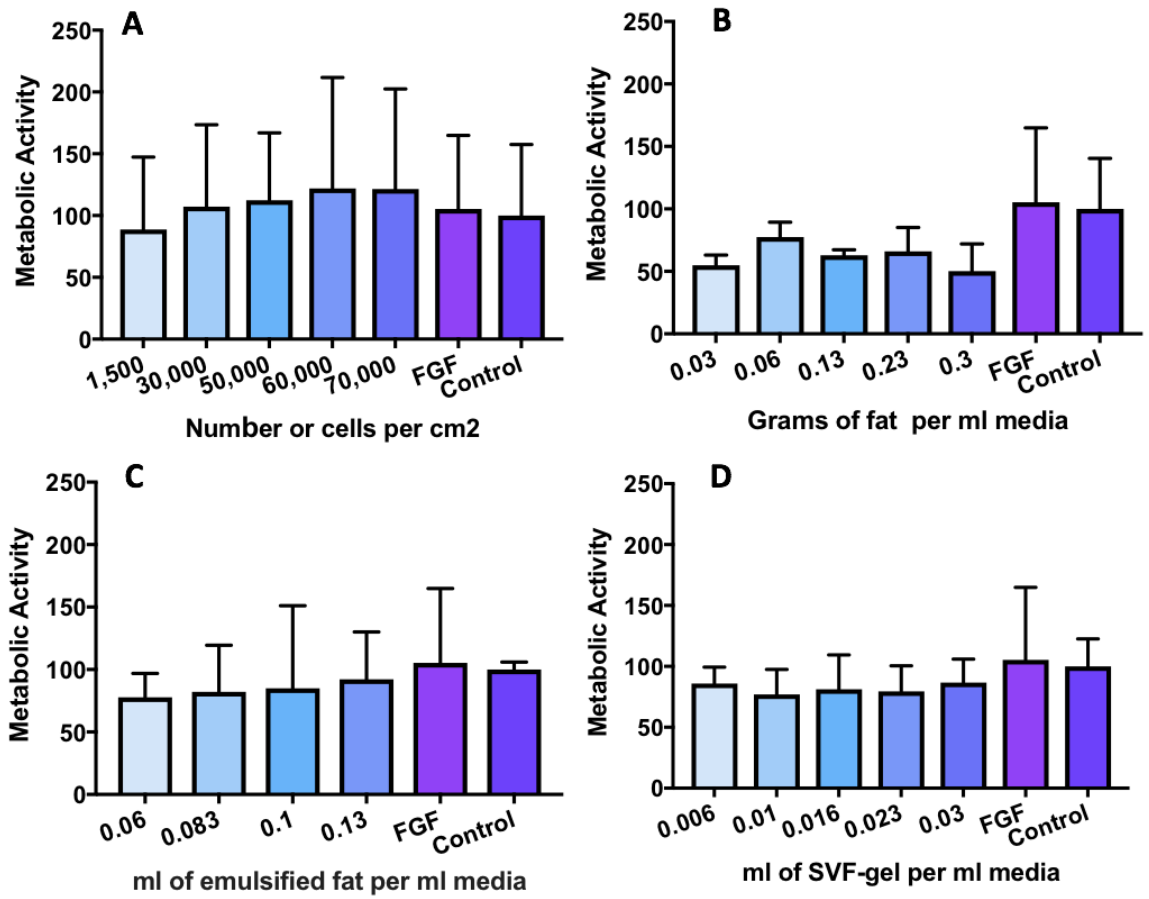

Figure 3.7 Metabolic activity of endothelial cells (HMEC-1) after 2 days cultivated in conditioned media from ADSC (A), adipose tissue (B), emulsified fat (C), and SVF-gel (D). Normal media, DMEM, was used as a negative control; while 50 ng/ml FGF were used as positive controls. Mean with error bars showing standard deviation. N=3, n=3, $p<0.05$.

3.4.5 Endothelial (HDMEC) migration assay

Since HMEC-1 were not stimulated with the conditioned media or FGF, HDMEC were chosen as an alternative to study the effect of conditioned media. HDMEC were used to test the conditioned media and analyse its effects on migration (Figure 3.8) and metabolic activity (Figure 3.9). ADSC conditioned media was able to increase HDMEC migration with no statistically significant difference when compared with normal media with a seeding density of 10,000 cells per cm^2 to produce the conditioned media (Figure 3.8A). When adipose tissue was used to condition the media, the migration was lower than the negative control with the lowest percentage of area change with 0.13 grams of tissue per ml media (Figure 3.8B). However, culturing with media conditioned with emulsified fat considerably decreased the migration of the cells with values lower than half of the percentage of area change obtained with normal media in most of the cases (Figure 3.8C). Finally, SVF-gel conditioned media did not increase endothelial cell migration since all the different densities of SVF-gel conditioned media showed values comparable to the negative control.

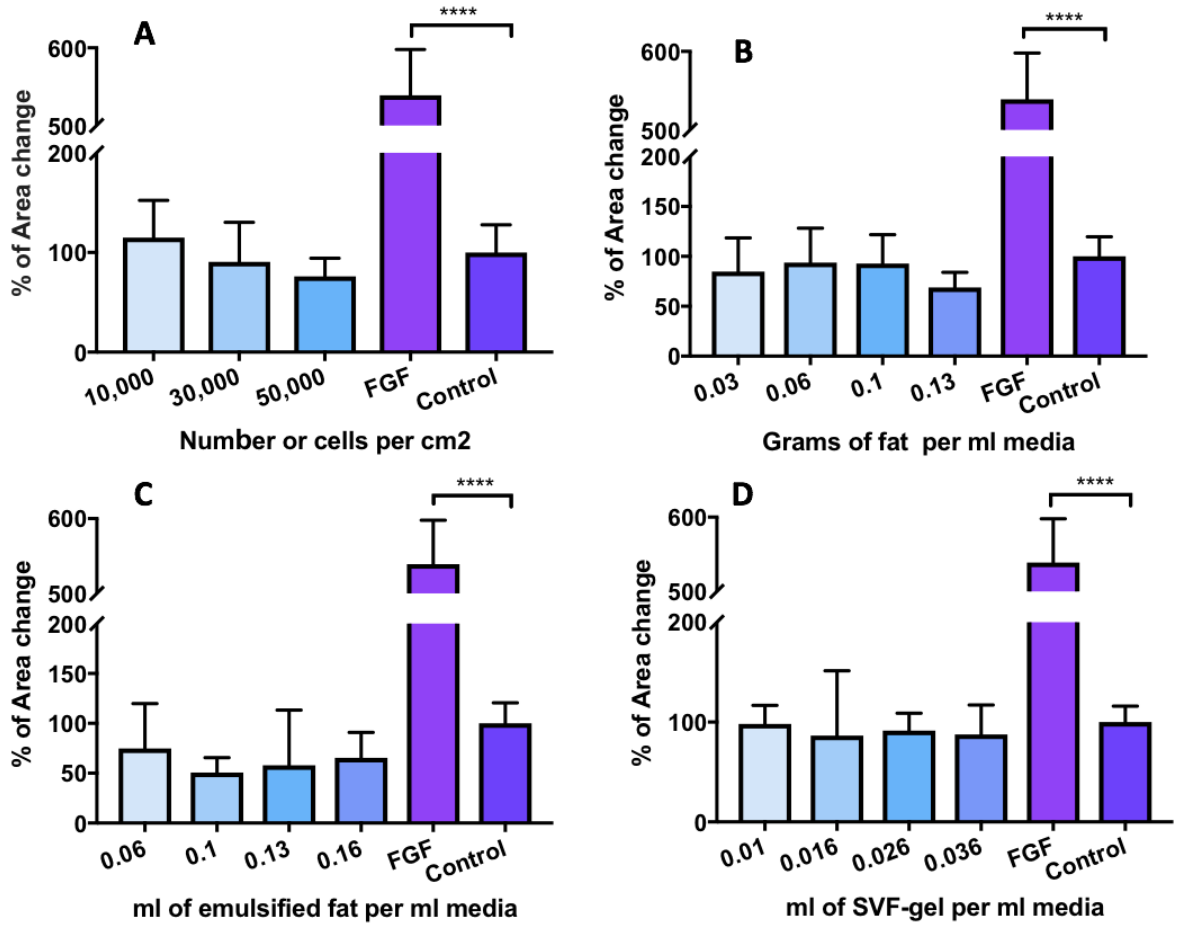

Figure 3.8 Migration of endothelial cells (HDMEC) after 24 hrs cultivation in conditioned media from ADSC (A), adipose tissue (B), emulsified fat (C), and SVF-gel (D). MV media without supplements, was used as negative control; while 10 ng/ml FGF was used as positive control. Mean with error bars showing standard deviation. N=3, n=3. ****p<0.0001.

3.4.6 Metabolic activity using MTT on HDMEC

In contrast with the results obtained from the migration assay, the ADSC conditioned media did not increase metabolic activity of HDMEC with any of the concentrations investigated (Figure 3.9A). Similar results were obtained from the adipose tissue conditioned media. In this case, lower metabolic activity was found compared to the negative control (Figure 3.9B); however, it was not as pronounced as the difference obtained in the experiments on HMEC-1. The emulsified fat conditioned media was able to maintain a metabolic activity close to the negative control (Figure 3.9C). This is quite different from the results from the HMEC-1 in which the metabolic activity was

considerably negatively affected by the conditioned media from emulsified fat. Similarly to the emulsified fat conditioned media, SVF-gel conditioned media maintained metabolic activity close to the negative controls (Figure 3.9D). Even though the conditioned media from the different groups did not considerably increase the HDMEC metabolic activity, the cells metabolic activity was increased non-significantly by FGF.

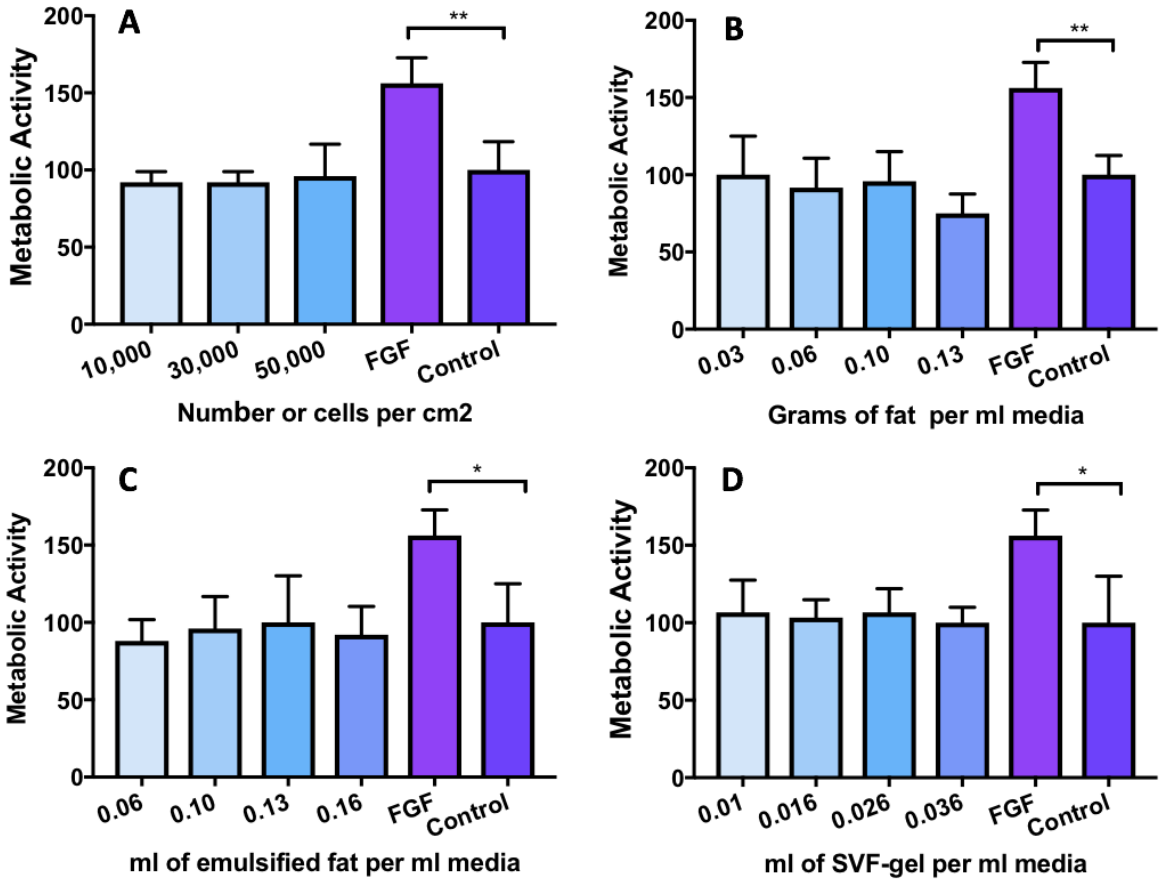

Figure 3.9 Metabolic activity of endothelial cells (HDMEC) after 2 days cultivation in conditioned media from ADSC (A), adipose tissue (B), emulsified fat (C), and SVF-gel (D). MV media without supplements, was used as a negative control; while 10 ng/ml FGF was used as positive control. Mean with error bars showing standard deviation. N=3, n=3. *p<0.05, **p<0.01.

3.4.7 Free lipid effect on endothelial cells

Different proportions of pure lipid extracted from the adipose tissue were added to MV media without supplements. HDMEC metabolic activity and migration were measured

to analyse whether lipids affected the endothelial cell development in the previous experiments (Figure 3.10). Endothelial cell migration was decreased non-statistically with a high percentage, 30%, of lipid in the media. However, the metabolic activity was not affected by the different percentages of lipids in the media presenting values similar to the negative control.

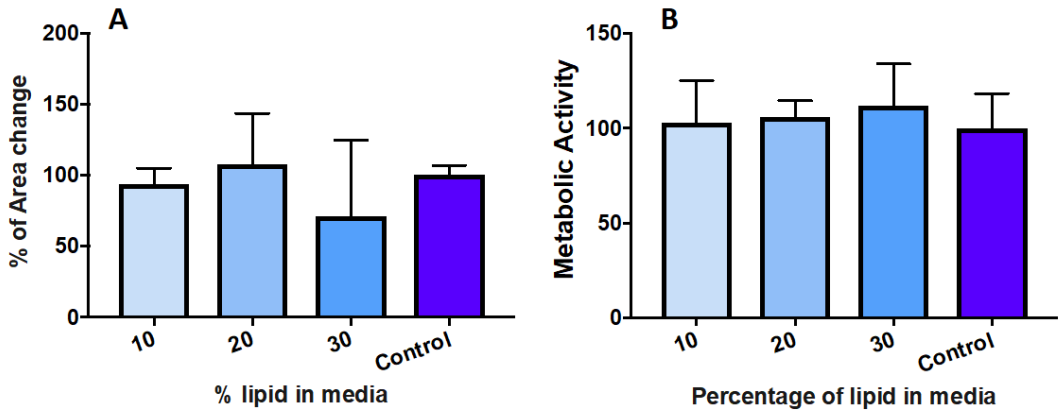

Figure 3.10 Effect of lipids in the media on migration (A) and metabolic activity (B) of HDMEC. Mv media without supplements was used as a negative control. Mean with error bars showing standard deviation. N=3, n=3.

3.5 Discussion

Using conditioned media from adipose tissue is a novel approach for adipose-supported treatments since tissue grafts are usually used in clinic. Different quantities of tissue and cell densities were tested in order to find the optimal culture density to produce conditioned media with enough growth factors to have an effect on the tested cells. A literature search (Table 1.3) identified different incubation periods that have been used to produce conditioned media. Overall, 2 to 5 days were the most commonly used incubation times, so 3 days was established as the incubation time used in this research.

In order to use conditioned media to study the angiogenic potential of the conditioned media it was important to verify that it did not have a negative effect on the endothelial cells. Tissue was processed using different protocols, in which media could be "contaminated" with dead cell bodies or metabolites that had a negative effect on the

endothelial cells. This could be a result of mincing the fat, and/or the remaining pieces of fat could be necrotic inside due to lack of nutrients and oxygen. To estimate the number of cells that lysed or were dead during production of conditioned media the LDH concentration was measured. Lactate dehydrogenase (LDH) is an intracellular enzyme that is present in all cell types, which catalyses the reversible reduction of pyruvate to lactate with the conversion of nicotinamide adenine dinucleotide (NADH) to NAD^+ (Bauhammer, Sacha and Haltner, 2019). The amount of LDH in the conditioned media is proportional to dead cell number and can be measured by the reduction of a tetrazolium salt (yellow colour) to a formazan salt (red colour), which can be quantified using photometry (Bauhammer, Sacha and Haltner, 2019).

First, the LDH levels in all the conditioned media were tested. LDH values in the conditioned media from adipose tissue and emulsified fat were extremely high. It has been reported before that there is an increase in LDH concentration in conditioned media as cultured cell density increases (Sukho *et al.*, 2017). In agreement with this finding, our data in Figure 3.4 shows that the LDH levels increased as the amount of adipose tissue increased in the conditioned media. Tissue is also exposed to harvesting, mincing, and emulsion (in case of the emulsified fat) processes before culturing them. All these processes increased cell lysis and death thereby increasing LDH levels. To further confirm this high LDH levels were detected during the first hour of culture suggesting that the high cell death is a result of tissue processing.

As a result, cultures of adipose tissue and emulsified fat were washed after one hour of culture to remove the metabolites of dead cells to try to avoid a negative effect on the HMEC-1. By doing this, the levels of LDH in the media were significantly reduced, confirming that the majority of the dead cells in the tissue are a result of the tissue processing previous to culturing it (Figure 3.5A). However, when the conditioned media was tested on HMEC-1, its metabolic activity and migration did not improve compared to the unwashed conditioned media. Concluding that even though changing the media after one hour of the conditioned media helps to reduce the dead cells and its metabolites, this does not impact the behaviour of HMEC-1. Since changing the media after one hour of culture did not make a significant difference on endothelial cell

metabolic activity, the conditioned media for future experiments was collected without any change of media.

In order to investigate whether the cytokines and growth factors in the conditioned media had angiogenic properties, the effects on migration and metabolic activity of cells after exposure to the conditioned media were measured. Cell migration is important in the angiogenesis process. It is believed that the pro-angiogenic properties of ADSCs or adipose tissue are a result of their potential ability to recruit different cell types for wound healing (Tobita, Orbay and Mizuno, 2011). In this study endothelial cells have been used as a simple 2D model to test the angiogenic properties of media conditioned with adipose tissue, emulsified fat, SVF-gel, and ADSC.

Initially, HMEC-1 were selected to study the angiogenic properties of the conditioned media in 2D assays. HMEC-1 is an endothelial cell line immortalised by the transfection of a tumour gene. It has been reported that after 95 passages these cells do not present signs of senescence thereby retaining their phenotype, morphological and functional characteristics similar to primary cells (Tat *et al.*, 2015). As a result, they have been used for long-term *in vitro* studies into angiogenesis.

Once the endothelial cell line was chosen, an important factor to consider is which media should be conditioned for further investigation. The ideal conditioned media should have low serum content to test only the growth factors released by the fat-derived tissue and ADSC into the media and not any already present. Also, the medium must sustain the tissue or cells used to produce the conditioned media, as well as the cells in which it is going to be tested. DMEM supplemented with 2.5% or 10% serum were used to cultivate ADSC for 3 days. At the end of that period of time the number (counted using a Neubauer haemocytometer as described in Section 2.3.3) and metabolic activity (using MTT) of the ADSC in the test wells was measured. The low serum medium decreased the metabolic activity and number of ADSC in the culture (Appendix 1). A significant decrease on the number of ADSC is not ideal since the conditioned media could not be rich enough in secreted growth factors. Due to this it was decided that 10% serum DMEM would be used to produce conditioned media to investigate HMEC-1 cells.

To test the efficacy of the assays, positive controls were used. VEGF and FGF were selected as the best growth factors to stimulate vascularisation of the endothelial cells used in this thesis. Both growth factors were assessed for their effect on the viability and migration of HMEC-1 at a concentration of 50 ng/ml. This concentration has previously been proven to stimulate cell proliferation and migration of this type of endothelial cells (Cartland *et al.*, 2016). For the case of HDMEC, it was recommended by the cell supplier (Promocell) in a later phase of this research to use 20 ng/ml VEGF and 10 ng/ml FGF with 2% serum in media. After testing both growth factors side-by-side, it was decided that FGF would be used as a positive control since it resulted in greater increases in cell proliferation and migration than VEGF (Appendix 2). This observation could be due to the VEGF purchased for use in this experiment being inactive (due to incorrect storage or being past it has expiry date), thus making it impossible to overstimulate the endothelial cells[3].

To investigate the effect of media conditioned with adipose tissue and its derivatives on cell migration an exclusion zone in a confluent layer of endothelial cells was created using rubber stoppers. Studying endothelial cell migration is important as this process is essential for angiogenesis since these cells are the ones that create the structure of new blood vessels (Ribatti *et al.*, 2001). The conditioned media did not make any statistically significant difference to HMEC-1 migration compared to normal media. Our positive control, FGF, increased the migration of the cells compared to normal media and conditioned media from all the studied groups. However, there was no statistically significant difference. Given HMEC-1 are an immortalised cell line our interpretation of these results was that these cells were difficult to stimulate.

MTT was used to test the metabolic activity of HMEC-1 cells after two days of culture with the conditioned media. In case of the ADSC and emulsified fat the conditioned media did not make any statistical difference to metabolic activity with any concentration compared with the negative control. On the other hand, the conditioned media from adipose tissue and SVF-gel had a statistically non-significant negative

[3] Due to Covid-19 lockdown it was not possible to investigate further.

effect on HMEC-1 metabolic activity. This result was hypothesised to be as a result of the high lipid concentration in the conditioned media. However, if the lipids affected the HMEC-1 cell viability, a similar result would be expected from the emulsified fat. The difference between emulsified fat and adipose tissue is that emulsified fat is in a more liquid state with more free lipids as a result of the lysed adipocytes. Another theory for the negative effect of adipose tissue and SVF-gel conditioned media on HMEC-1 metabolic activity, especially in the case of adipose tissue, was that some of the tissue cultured to produce conditioned media was not surviving.

In this study it appeared that HMEC-1 could not be stimulated to increase metabolic activity or migration even using growth factors (VEGF and FGF). The reason for this could be that HMEC-1 is a cell line that can grow perfectly under stress without affecting its growth rate making it harder to over stimulate them. On the other hand, HDMEC are primary cells that could be a better model to study angiogenic properties of the conditioned media since they are the cells responsible for skin wound vascularisation (Unger *et al.*, 2002; PromoCell, 2017).

First, metabolic activity of HDMEC cultured in DMEM media and MV media (recommended by the provider) was analysed to observe if DMEM could affect HDMEC viability. This was important because until this point conditioned media had been made using DMEM. DMEM statistically significantly decreased the metabolic activity of these endothelial cells suggesting that DMEM was not the best option to use for conditioning media (Appendix 3). As a result, MV medium without any supplements was chosen to collect conditioned media from ADSC, adipose tissue, emulsified fat, and SVF-gel to apply to HDMEC.

HDMEC migration was analysed using conditioned media from each group with different cell and tissue densities. Conditioned media from ADSC, 10,000 cells per cm^2, elicited a non-significant increase in HDMEC migration. In the same way, Kim *et al*., (2018) tested ADSC conditioned media on human dermal fibroblasts (HDF) and human keratinocytes (HaCaTs) using MTT and scratch assays to measure the effect of the conditioned media on cells' metabolic activity and migration. They found that conditioned media from ADSC increased the metabolic activity and migration in both

tested cell lines (Kim *et al.*, 2018). In case of the adipose conditioned media, it maintained similar levels of migration compared to the negative control at all concentrations; except for the highest concentration (0.13 grams of adipose tissue per ml of media) that was seen to have a non-statistically significant decrease compared to the control.

In contrast, the conditioned media from emulsified fat considerably (although not significantly) reduced the migration of the endothelial cells in all the different concentrations used to produce the conditioned media; while SVF-gel conditioned media did not affect HDMEC migration compared to the negative control. Deng *et al*., (2017) tested conditioned media from SVF, emulsified fat, and SVF-gel on fibroblasts and keratinocytes. They cultured conditioned media using $5x10^5$ cells [1.85 ml SVF-gel ($2.7x10^5$ cells/ml SVF-gel) and 5 ml adipose tissue ($9.9x10^4$ cells/ml tissue)] in 5 ml serum free DMEM for 24 hours (Deng *et al.*, 2017). They found that the conditioned media from the SVF-gel was the best to promote migration and cell proliferation in both cell lines. However, conditioned media from SVF and emulsified fat did positively stimulate the migration and proliferation of fibroblasts and keratinocytes (Deng *et al.*, 2017). The biggest difference between this study and ours is the amount of tissue used to produce conditioned media. They used at least 17-fold more SVF-gel and 12-fold more adipose tissue than we used. These high concentrations of tissue must increase considerably the growth factors secreted, and it is possible that the quantities used for this study are not enough to produce conditioned media rich enough to have a positive effect on the endothelial cells. Nevertheless, to obtain those high concentrations, especially for SVF-gel, would require extremely large amounts of adipose tissue, that in clinic application would not be viable especially for those patients with low body fat percentages. In addition, that they tested their conditioned media on fibroblasts and keratinocytes, while in this study endothelial cells were used.

The conditioned media were tested to investigate the effect on HDMEC metabolic activity. In contrast to the results from migration, the conditioned media from ADSC and adipose tissue did not increase the metabolic activity of HDMEC in any of the cell densities used to produce the conditioned media. However, it has been reported before by Nakagami *et al.,* (2005) that ADSC conditioned media increases viability of

human aortic endothelial cells (HAEC). They studied the effect of ADSC conditioned media on HAEC using another metabolic activity assay; MTS (3-(4,5-dumethylthiazol-2-yl)-5-(3-carboxymethoxyphenyl)-2-(4-sulfophenyl)-2H-tetrazolium) (Nakagami *et al.*, 2005). Unfortunately, no further detail on how they produced their conditioned media is given. This is an important point to consider, that there is significant variability in methods used to produce conditioned media between studies. Additionally, when donor variability is taken into account it is hard to compare the results between studies (Sagaradze *et al.*, 2019).

Chung *et al.,* (2015) used three different hydrogels (collagen, fibrin, and P-fibrin gels) to produce 3D ADSC cultures. Each hydrogel (0.5 ml) was seeded with 25,000 ADSCs and cultured in 12 well plates using Transwell inserts. Conditioned media was collected daily and concentrated 10-fold using a centrifugal filter unit (Chung *et al.*, 2015). HDMEC were treated with 500 µl of media that was obtained by combining 200 µl of 10% FBS media with 300 µl of conditioned media from the hydrogel cultures. After 48 hours, HDMEC metabolic activity was measured. HDMEC cultured with conditioned media from ADSC cultured in fibrin-based and P-fibrin hydrogels presented high metabolic activity, while conditioned media collected from ADSC cultured in collagen gels had a lower metabolic activity (Chung *et al.*, 2015). These results suggest that the environment in which the same number of cells is cultured could considerably affect their secreted growth factors. In addition, they used as a negative control serum free media and full FBS-containing media as a positive control. For their negative control, HDMEC did not survive when they were cultured in the serum free media. However, they showed the highest metabolic activity in the FBS-containing media (Chung *et al.*, 2015). In our study, conditioned media was produced using MV media without serum. While this is ideal to study only the secreted factors of adipose tissue and their derivatives, it is possible that the metabolic activity of HDMEC was a result of the lack of serum in the media and the secreted growth factors in all the studied groups were not enough to increase their metabolic activity.

Cai *et al.,* (2019) analysed the effect of the liquid fraction of SVF-gel or fat extract (FE) on HUVEC migration in a scratch assay. The liquid phase was obtained after centrifuging emulsified fat and discarding the lipid, cell/ECM fraction, and pellet.

According to the authors FE is rich in growth factors and is a potential cell-free therapy (Cai *et al.*, 2019). HUVEC were cultured with serum-free media supplemented with different percentages of FE (0%, 5%, 10% and 20%). It was reported that all the concentrations of FE stimulated HUVEC migration compared to serum-free media. Even though they did not compare FE properties to SVF-gel, they suggest that SVF-gel should have a better outcome than FE since SVF-gel has the presence of SVF and ECM to physically protect the cells (Cai *et al.*, 2019). Nevertheless, in our results SVF-gel did not increase HDMEC migration compared to non-conditioned media.

Even though HDMEC are primary cells, based on these experiments, it appears that it is difficult to over stimulate them. Our positive control, FGF, showed an increase in HDMEC migration; however, it was merely 16% higher than our negative control and not statistically significant. While addition of FGF gave a non-statistically significant difference of 32% higher than the negative control on the metabolic activity. Interestingly, in the previous studies by Cai *et al.,* (2019), Chung *et al.,* (2015), and Nakagami *et al.,* (2005), in which conditioned media or FE was tested on different endothelial cells, their positive controls were fully supplemented basal media. It is possible that, in order to stimulate HDMEC with FGF a minimum percentage of serum is required. This could also be a limitation for the conditioned media, in which ADSC and tissue are cultured in serum free media thereby affecting the secreted factors and the viability of HDMEC when cultured using this medium.

Overall, the results suggest that the conditioned media from adipose tissue and emulsified fat affect (not significantly) the metabolic activity, and in some cases, the endothelial cell migration. Looking closely at the difference between the conditioned media from adipose tissue and emulsified fat compared to ADSC and SVF-gel. The ADSC and SVF-gel media was clear, while the adipose tissue and emulsified fat media were cloudy due to small tissue fragments and lipids that were not possible to remove (Figure 3.3). Smaller filters could be used for this purpose, however using smaller meshes could remove molecules that could have a positive effect for wound healing removing healing properties from the conditioned media.

It is also possible that lipids present in the conditioned media could affect cell migration and proliferation by covering the tissue culture surface thereby affecting our results. Additionally, if a lipid layer formed on top of the media, oxygen exchange of the cell culture media could be affected thus decreasing both migration and metabolic activity. To ensure free lipid did not affect our measurements, different proportions of lipids were added to the medium (MV media without supplements) and metabolic activity and cell migration were analysed (Figure 3.10). When 30% of the total volume was lipid, the cell migration was considerably but non-significantly decreased. However, the metabolic activity remained stable and close to the values obtained for the negative control meaning that even 30% of lipid content in the media did not affect the growth of the cells. It is important to mention that in this experiment the lipid that was added to the media formed a layer on the surface, while in the case of the emulsified fat the tissue with its free lipid is suspended within the media. As a result, the free lipid is not only on the top of the media, but also in contact with the well and the cells creating a possible negative effect that was impossible to replicate.

Conditioned media is a non-cellular potential therapy with all the benefits of the growth factors that cells or tissue secrete but with a reduced immune rejection risk. Also, conditioned media can be produced and stored until it is needed as an off-the-shelf product. For this laboratory-based project, this is very important since it helps experimental planning especially during periods with low adipose tissue supply. Since one of the main obstacles for adipose tissue related therapies is dosage, it is essential to identify how many cells or tissue is required to produce conditioned media rich enough to have a positive regenerative effect. So far, different ADSC seeding densities and amount of adipose tissue, emulsified fat, and SVF-gel were used to produce conditioned media which were tested on two different endothelial cell types. In general, the conditioned media from any of the conditions studied did not stimulate cell migration or metabolic activity in either of the cell types used. In the case of adipose tissue and emulsified fat a reduction on the metabolic activity was observed. LDH assays confirmed in both cases there was an increased cell death rate as a result of the tissue processing. However, washing the tissue after one hour of culture and thus reducing the LDH concentration did not improve the metabolic activity of the

endothelial cells. Another theory for the observed decrease in metabolic activity was the lipid content in the media. Nevertheless, when lipid was added in different concentrations to the HDMEC cultures there was no effect on their metabolic activity. As a result, the 2D cell culture model was not suitable to study the effects of the conditioned media, given the challenges seen stimulating with the positive controls. HMEC-1 is a cell line that even when it has been used to study angiogenesis in previous studies, in this case it was very hard to overstimulate using FGF and VEGF. Changing to HDMEC made our model of study closer to in vivo conditions. Nevertheless, it was hard to overstimulate them with low serum media. It is possible that to study our conditioned media that has no serum, a support system for the cells is required. In addition, angiogenesis is a process that takes place three-dimensionally and involves different cell types. In this case, it is possible that more complex models with a matrix as support and that not only involve endothelial cells, such as endothelial tube formation, chick aortic ring and CAM assay, could have a better outcome compared to 2D endothelial cell cultures used so far.

Chapter 4 Study of conditioned media on endothelial tube formation assay, *ex vivo* and *ex ovo* models

4.1 Aim

To analyse the angiogenic properties of conditioned media from adipose tissue, emulsified fat, SVF-gel, or adipose derived-stromal cells (ADSC) by their ability to promote endothelial cells to form tubular structures in 3D cultures, and new vessels in *ex vivo* and *ex ovo* models.

4.2 Introduction

Conditioned media collected from varying cell densities and amounts of tissue of ADSC, adipose tissue, emulsified fat, or SVF-gel have been tested on two different endothelial cell lines on 2D assays (Chapter 3). However, none of the conditioned media were able to significantly stimulate either migration or metabolic activity in the endothelial cells. Vascularisation is a complex process that requires a variety of cytokines to stimulate different cell types to work together to expand the blood vessel network. Endothelial cell migration and viability assays (as in Chapter 3) can give us an idea of the angiogenic potential of adipose tissue and its derivatives. However, it is important to use more complex models to obtain a closer environment to physiological tissues. In order to accomplish this, it is important to give the cells a 3D support, especially when the studied process outcome is to create tubular structures.

Endothelial tubular formation assay is a simple and quick method in which Matrigel or collagen coated wells give 3D support to endothelial cells to create tubular structures within 24 hrs of culture (see Section 1.11.3.3 for further details). Testing the angiogenic properties in assays that involve different cell types is important since *ex vivo* vascularisation depends on a variety of cell types interacting throughout this process. Aortic ring assays and CAM assays not present in these models, include all cells

involved in the tubular development process, making these models closer to the *in vivo* situation.

The chick aortic ring assay is an *ex vivo* assay in which the aortas from embryonic chickens are embedded in Matrigel to analyse the angiogenic potential of conditioned media by the sprouts (initiation of the formation of a new vessel by a tip cell around the aortic rings (see Section 1.11.4.1 for further details) (Chappell, Wiley and Bautch, 2011). This technique allows results to be obtained within 4 days in a complex environment. In the same way, the Chick Chorioallantoic Membrane (CAM) assay is an *ex ovo* assay in which effects of conditioned media can be tested in a living organism (see Section 1.11.2.1 for further details). Finally, understanding which cytokines are present in conditioned media will inform us about the differences in cytokine release from the different formulations and how they contribute to their regenerative potential. In addition, this will supplement our knowledge of how the different processing methods affect not only the structure of the tissue, but also the growth factors secreted.

4.3 Materials and Methods

4.3.1 Experimental design and samples

As it was mentioned before conditioned media from adipose tissue and its derivatives was used in this research in order to help experiment planning. Using conditioned media allowed us to freeze samples that could be used when required. This was crucial for this research because tissue donations were not regular and the amount, we obtain from batch to batch was highly variable. As a result, conditioned media allowed us to constantly run experiments, especially during those long periods of times (weeks, or even months) without tissue. Every batch of tissue was processed and cultured within 24 hours after it was donated to warranty a high viability. Different batches were used for each of the repeats of the experiments listed on Table 4.2.

Table 4.1 Tissue and formulation batches used in the different experiments.

Experiment	Sample	Rep 1	Rep 2	Rep 3	Rep 4
Endothelial tube formation	ADSC	419	429	430	
	Adipose tissue	433	434	441	
	Emulsified fat	433	434	441	
	SVF-gel	433	434	441	
Aortic ring assay	ADSC	419	419	429	430
	Adipose tissue	421	433	434	441
	Emulsified fat	421	433	434	441
	SVF-gel	433	433	434	441
Cam assay	ADSC	419	420	429	430
	Adipose tissue	421	433	434	441
	Emulsified fat	421	433	434	441
	SVF-gel	433	433	434	441
Cytokine array	ADSC	429	430	433	
	Adipose tissue	430	433	441	
	Emulsified fat	422	433	441	
	SVF-gel	433	434	441	

4.3.2 Endothelial tube formation

In a 96 well plate, 50 µl low growth factor Matrigel (Corning, Loughborough, UK) were added to each well avoiding any bubbles. Then, 20,000 cells/well of HDMEC were seeded on the Matrigel covered wells. Conditioned media (100 µl) were collected as described in Section 3.3.1 from adipose tissue, emulsified fat, SVF-gel, and ADSC and were added to each well. MV media without supplements and 100 ng/ml FGF was used as a positive control (Xue and Greisler, 2002) and MV media without supplements as a negative control. Samples were incubated at 37ºC with 5% CO_2 for 24 hrs. Afterwards, media was removed, and samples were fixed using 3.7% formaldehyde in PBS for 45 min at room temperature. Then, samples were washed with PBS three times and kept in PBS and images acquired using an IX73 Olympus microscope (Olympus, Essex, UK). Images were analysed using the ImageJ plug in "Angiogenesis Analyser" to count the number of tubes and total segment length as shown in Figure 4.1 (Yu *et al.*, 2018)

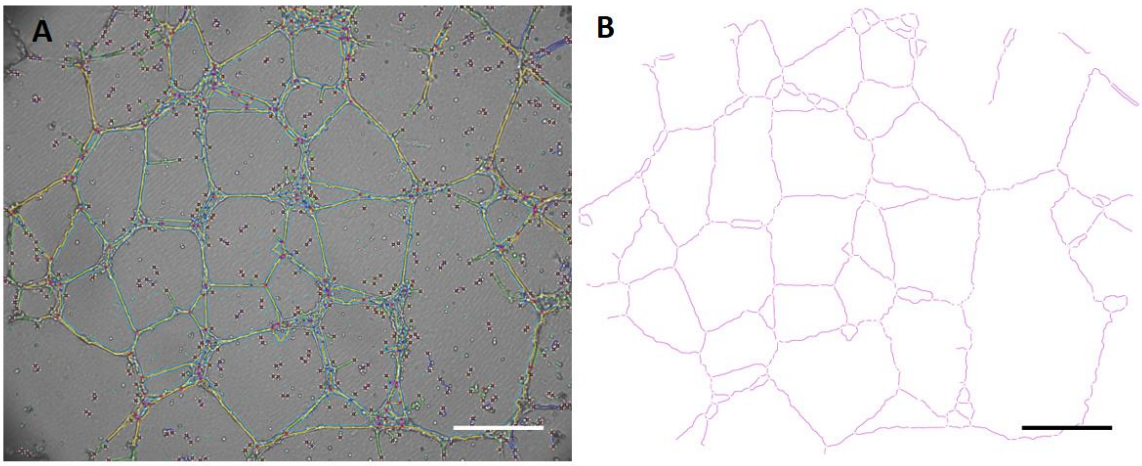

Figure 4.1 Light microscope image (A) showing HDMEC endothelial tube formation assay analysis using ImageJ to identify all the tubular structures in the image to produce the map of segments identified (B). Scale bar= 500 µm.

4.3.3 Chick aortic ring

Fertilised chicken eggs were incubated at 37.5ºC for 13 days post fertilisation (day eggs laid counted as day 0). The first three days of incubation eggs were in a Rcom King Suro Max-20 Incubator (Rcom, Beverley,UK) with rocking movement, then they were transferred to a cell culture incubator until day 13 when chicks were sacrificed by cutting their vitelline arteries. The chick chests were opened from the bottom of the thoracic box with scissors and the heart and aortas were removed and placed into a petri dish. Once the aortas were dissected from the heart, they were cleaned of the surrounding connective tissue using sterile forceps and scalpel. A M3Z microscope (Wild Heerbrugg, Switzerland) inside a laminar flow hood was used to remove the connective tissue from and cut aortas to keep the samples sterile. Then, 1 mm length rings were cut and placed on top of 50 µl low factor Matrigel (Corning Inc. Loughborough, UK). Then, aortic rings were encapsulated by adding another 30 µl low growth factor Matrigel in a 24 well plate. Once the Matrigel was set, 0.5 ml conditioned media collected from adipose tissue, emulsified fat SVF-gel, and ADSC (as described in Section 3.3.1) was added to each ring and incubated at 37ºC with 5% CO_2 for 4 days (diagram of the process Figure 1.14). Non-conditioned media was used as a negative control, while 100 ng/ml FGF (Sigma Aldrich, Dorset,

UK) was used as a positive control. Pictures were taken at day four by light microscopy (4X magnification) to record vessel growth and analysed using ImageJ. To analyse the tube outgrowth of the rings, freehand tool was used to obtain the sprout area around the rings as shown in Figure 4.2.

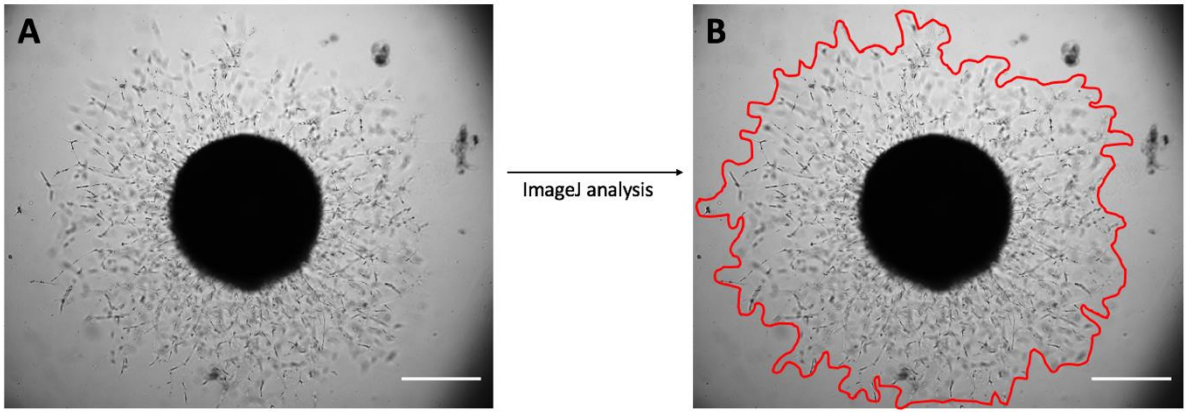

Figure 4.2 Light microscope image of vessels grown from chick aortic ring (A), and after measuring the branches area around the ring (in red) using ImageJ (B). Scale bar= 500 µm.

4.3.4 Chick Chorioallantoic Membrane (CAM) Assay

Fertilised chicken eggs were placed in a Rcom King Suro Max-20 Incubator at 37.5ºC with rocking movement 24 hours after lay day (lay day counted as day 0). On day 3 of incubation, eggs were cracked into a plastic weighing boat containing 2 ml of 1% penicillin in PBS. Then, the box containing the embryo was enclosed in a petri dish with 10 ml of water to maintain humidity during its incubation at 37ºC. On day 7 of incubation, sterilised 6 mm silicone rings were implanted on CAM using sterile forceps. Rings were placed in an area of the CAM with no large vessels nearby that could make it difficult to observe the new vessels developing. Conditioned media (50 µl) from adipose tissue, emulsified fat, SVF-gel or ADSC were added into the ring every two days. Conditioned media was collected as described in Section 3.3.1 and non-conditioned media was used as negative control, while 100 ng/ml FGF was used as a positive control. Pictures were taken inside the hood using Micro Capture 2.0 camera on days 7, 10 to track vascularisation around the samples. On day 14, embryos were sacrificed by cutting their vitelline arteries (Mangir *et al.*, 2019). ImageJ was used to analyse all the images by Vessel Analysis plugin (Figure 4.3F-H).

An area of 200 mm^2 around each ring was selected to measure the vascular area (Figure 4.3F-G). Cut images were split into main colour channels (red, green and blue) and the green channel was used to continue with the analysis as it gave the most accurate and detailed results for blood vessels (Figure 4.3H). The green channel image was then processed enhanced contrast, noise removal using Mexican hat plugin and converting the image to binary (Figure 4.3I). Finally, the vascularisation area was calculated and graphed by the plug in Vessel Analysis on ImageJ.

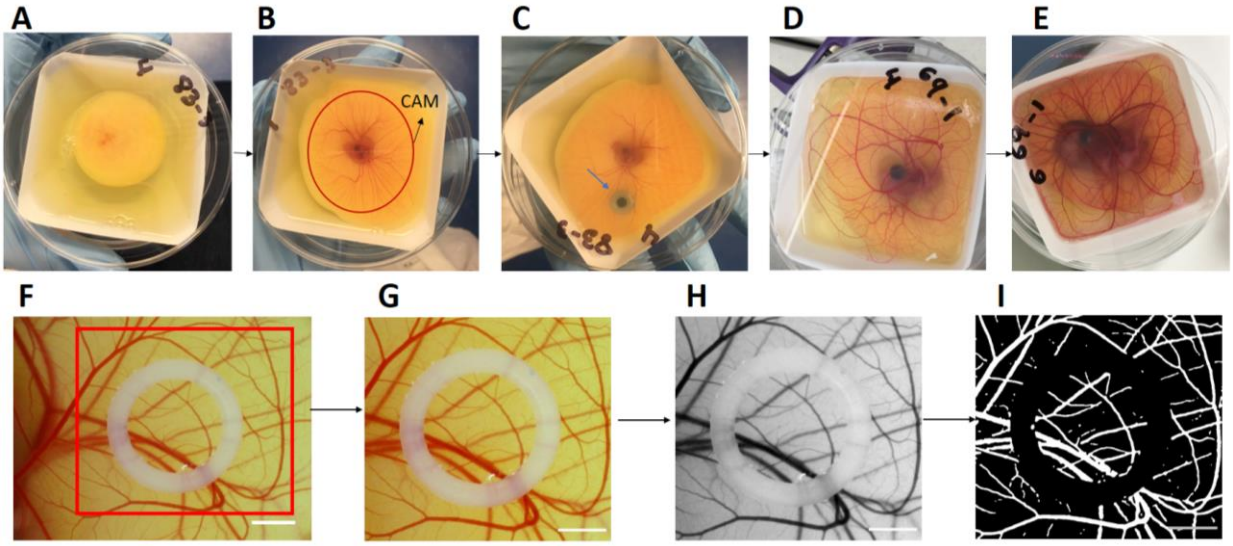

Figure 4.3 Images of the chicken embryo development (A-E). Starting on day 3 of incubation when eggs are cracked, and embryos transfer to a Petri dish (A). On day 7 (B), CAM is visible and silicone rings were implanted adding conditioned media (represented with blue coloured water) (C). Chicken embryos at day 10 (D) in which pictures of the silicone rings were taken. At day 13 (E) embryos were sacrificed. Finally, CAM assay image analysis using ImageJ (F-H). Coloured images (F-H) were cut 200 mm^2 around the rings. Then images were split to colour channels keeping the green channel adjusting its contrast and removing of noise by applying Mexican hat plugin (H). Finally, images were converted to binary in which the vessels are detected and highlighted on white in a black background (I). The Vessel Analysis plugin analyses the percentage of vessel area of the image to complete the image analysis. Scale bar= 3 mm.

4.3.5 Human angiogenesis antibody array

The different cytokines present in the conditioned media were analysed using Human Angiogenesis Array C1(8) (which includes all the reagents listed below) (RayBiotech, Cambridge, UK) according to manufacturer's instructions (Figure 4.4). Five different arrays were used for each of the four studied groups and MV without supplements as

background control. First, each of the membranes was placed printed side up into a well of the Incubation Tray (provided in the kit). Then, 2 ml of blocking buffer was added to each well for an incubation of 30 min at room temperature. After removing the blocking buffer, 1 ml of conditioned media was added to the different films and incubated overnight at 4ºC. Conditioned media from three different patient batches were pooled into one array. The conditioned media from the different groups was collected as indicated in Section 3.3.1 using Growth MV serum free media. Afterwards, each film was washed three times using Wash Buffer I for 5 min at room temperature. Then, two washes with Wash Buffer II were carried out, incubating films with the washing buffer for 5 mins at room temperature. Once samples were washed, 1 ml of Biotinylated Antibody Cocktail was added for an incubation overnight at 4ºC. Next, films were washed using Wash Buffers I and II as described above. Afterwards, 2 ml of HRP-Streptavidin reagent were added to each film and incubated for 2 hours at room temperature. A series of washes using Wash Buffers I and II were carried out as described above, before transferring the membranes, printed side up, to chromatography paper to remove the excess washing buffer. Then, membranes were transferred to a plastic sheet to add 500 µl of (1:1) Detection Buffer C and Detection Buffer D to each membrane. After 2 mins of incubation at room temperature, another plastic sheet was placed on top of the films. Bubbles were gently removed using a plastic roller to proceed to chemiluminescence analysis using a C-DiGit Blot Scanner (Li-Cor Biosciences, Cambridge, UK). Quantitative analysis of dot intensity in the arrays was performed using Image Studio 5.2 software. An intensity average of the two dots per cytokine was used for the analysis. Finally, data was normalised using negative control as a reference in order to plot the results.

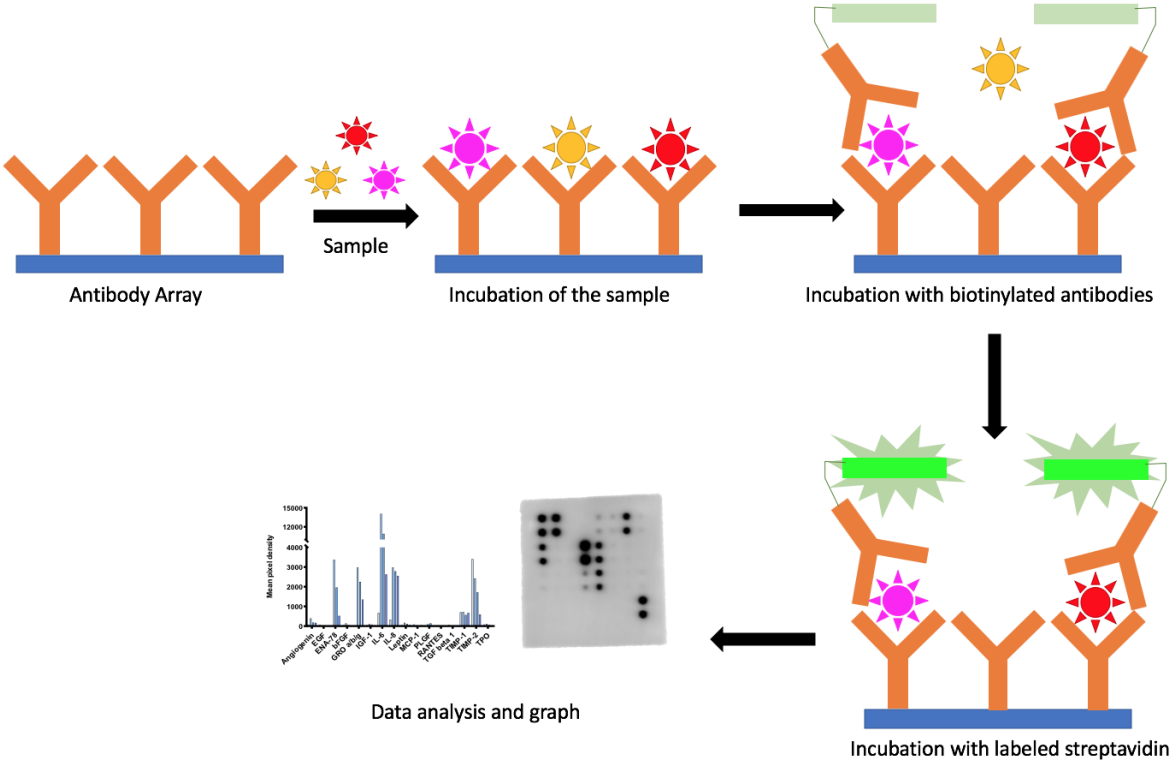

Figure 4.4 Schematic diagram illustrating how the angiogenesis cytokine array functions. Primary antibody is attached to a membrane. Conditioned media is added to the membrane and different growth factors bind to specific antibodies located in defined areas of the membrane (dots). Then secondary antibodies attached to a labelled streptavidin molecule are loaded to bind to those antibody-growth factor complexes. Using a chemiluminescent excitation system, a membrane image is obtained with different signal intensity in each dot representing different analysed growth factors.

4.3.6 Statistical analysis

Data from experiments was normalised in relation to the negative control before running statistical analysis. Statistical analysis was made using the GraphPad Prism 7. One-way ANOVA was applied to compare each group to the negative control, FGF and each of the other groups using Dunnett's multiple comparison test. All values are presented with mean ± standard deviation and differences were taken to be significant for $p<0.05$.

4.4 Results

4.4.1 Tube formation assay

The HDMEC tube formation assay (Section 4.3.2) was performed using conditioned media produced using different ADSC seeding densities and different amounts of tissue (Section 3.3.1). Two different parameters were used to analyse the images: total number of tubes and total length of segments (Figure 4.5 and Figure 4.6). Conditioned media from different densities of ADSCs were tested and it was observed that more tubes were formed in the conditioned media from a greater number of cells (Figure 4.5A). Adipose and emulsified fat conditioned media also showed a trend in which as the amount of tissue in the conditioned media increased, so did the number of tubes (Figure 4.5B and Figure 4.5C). In the case of the emulsified fat, conditioned media with the two highest concentrations of emulsified fat (0.13- and 0.16-ml emulsified fat/ ml media) statistically significantly increased the number of tubes. Finally, SVF-gel conditioned media showed a similar trend, but in this case the two higher concentrations, 0.026 and 0.036 ml of SVF-gel per ml of media, were significantly increased compared to the non-conditioned media (Figure 4.5D). In the case of the 0.036 ml SVF-gel/ml media, the formation of number of tubes was significantly higher than the two lower SVF-gel concentrations used. In all the cases, FGF was used as a positive control that was able to over stimulate the number of tubes formed compared to the non-conditioned media.

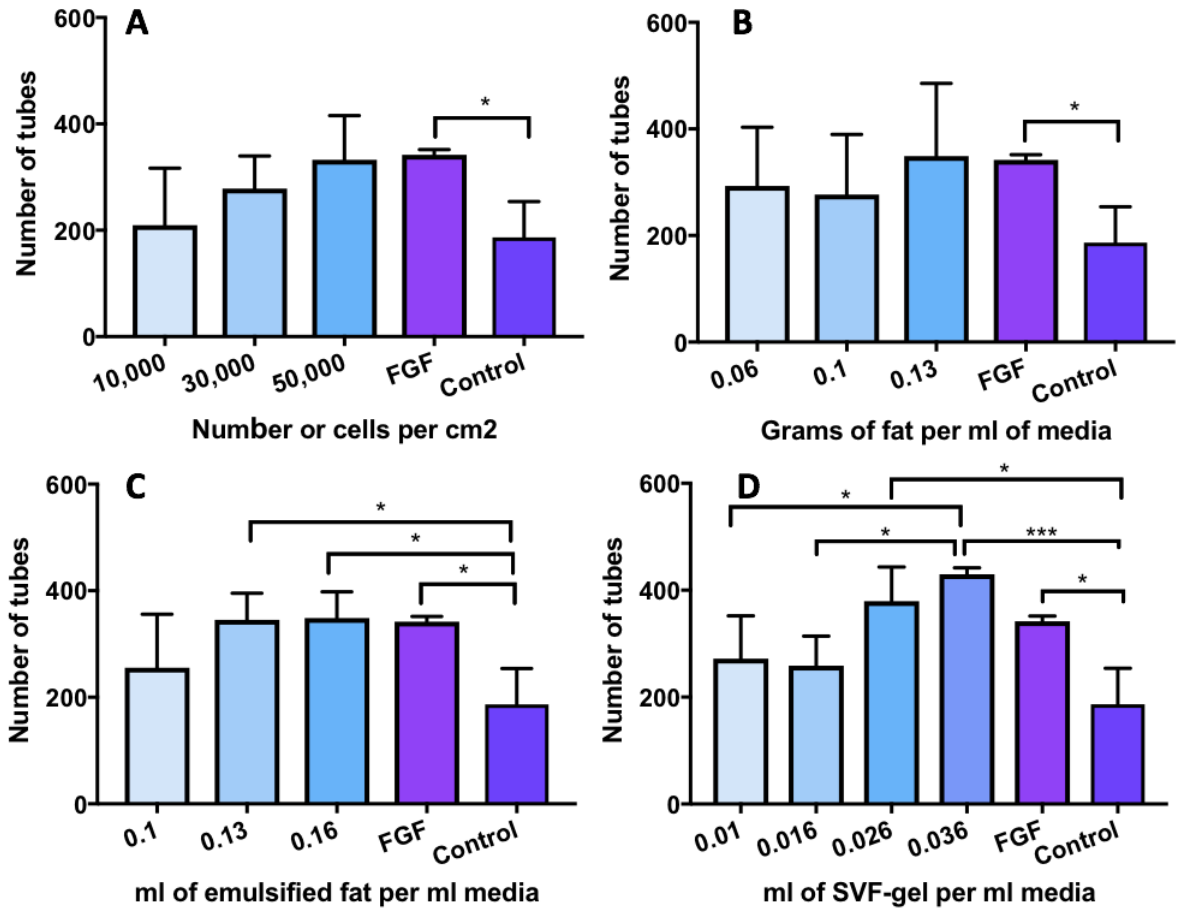

Figure 4.5 Number of tubes formed on endothelial tube formation assay using conditioned media from ADSC (A), adipose tissue (B), emulsified fat (C), and SVF-gel (D). FGF (100 ng/ml) was used as a positive control while MV media without supplements, was used as negative control. Mean with error bars showing standard deviation. N=3, n=3, *p<0.05, **p<0.01, ***p<0.001.

Another parameter used to evaluate the angiogenic properties of the conditioned media on the tube formation assay was the total segment length (Figure 4.6). In this case the conditioned media from ADSC showed the same trend as in the number of tubes formed. In both cases 50,000 cells/cm^2 conditioned media showed the highest potential to induce tube formation (Figure 4.6A). For the adipose tissue, the highest length was achieved with the 0.13 g tissue per ml of media, doubling the length compared to the non-conditioned media (Figure 4.6B). In contrast, emulsified fat showed the highest total length with the middle concentration used in this study, (0.13 ml of emulsified fat per ml media) (Figure 4.6C). Finally, SVF-gel conditioned media

significantly increased the total length of the tubes compared to non-conditioned media with the two highest concentrations used in this study (0.026 and 0.036 ml SVF-gel per ml media) (Figure 4.6D). FGF at a concentration of 100 ng/ml was used as a positive control (Xue and Greisler, 2002). In this case FGF promoted the endothelial cells to significantly increase the total length of the tubular structures compared to the negative control (non-conditioned media).

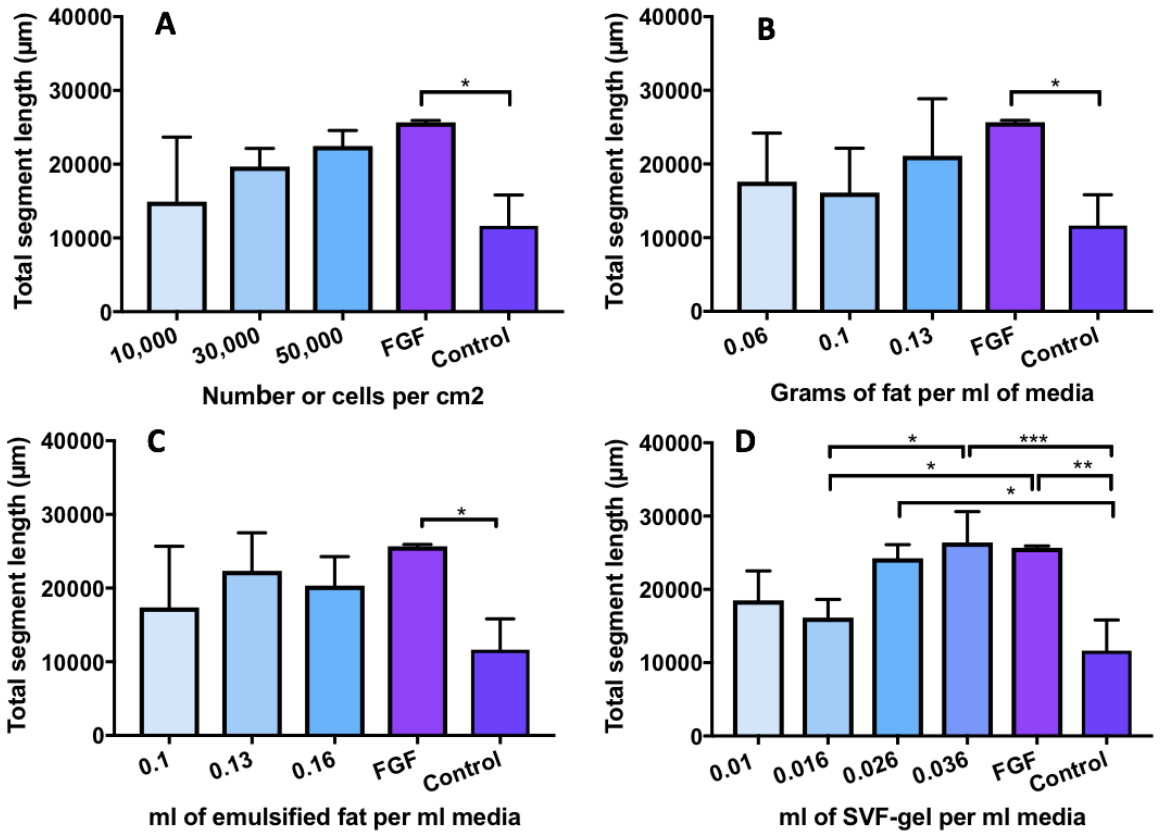

Figure 4.6 Total segment length on endothelial tube formation assay using ADSC (A), adipose tissue (B), emulsified fat (C), and SVF-gel (D) FGF (100 ng/ml) was used as a positive control while MV media without supplements, was used as negative control. Mean with error bars showing standard deviation. N=3, n=3, *p<0.05, **p<0.001, ***p<0.0001.

In Figure 4.7, representative images of tube formation by the HDMEC cultured with the different conditioned media are shown. As shown in Figure 4.5 and Figure 4.6, SVF-gel (0.036 ml/ml media) resulted in an increase of tube formation with a more interconnected tubular network compared to the other conditioned media and controls (Figure 4.7D). In the case of the negative control (media without serum), endothelial

cells did not form many tubular structures (Figure 4.7E); while FGF as a positive control did promote their formation (Figure 4.7F). In order to reduce the number of samples used in the experiments, the most effective concentrations of conditioned media according to the endothelial tube formation assay results were selected to continue with the *ex vivo* and *ex ovo* experiments. The final concentrations chosen for the conditioned media were as outlined in Table 4.2 (see Figure 2.9 for unit conversion between volume and weight of each sample).

Table 4.2 Conditions to produce conditioned media

Studied group	Conditioned media
ADSC	50,000 cells/cm^2
Adipose tissue	0.13 g/ml media
Emulsified fat	0.13 ml/ml media
SVF-gel	0.036 ml/ml media

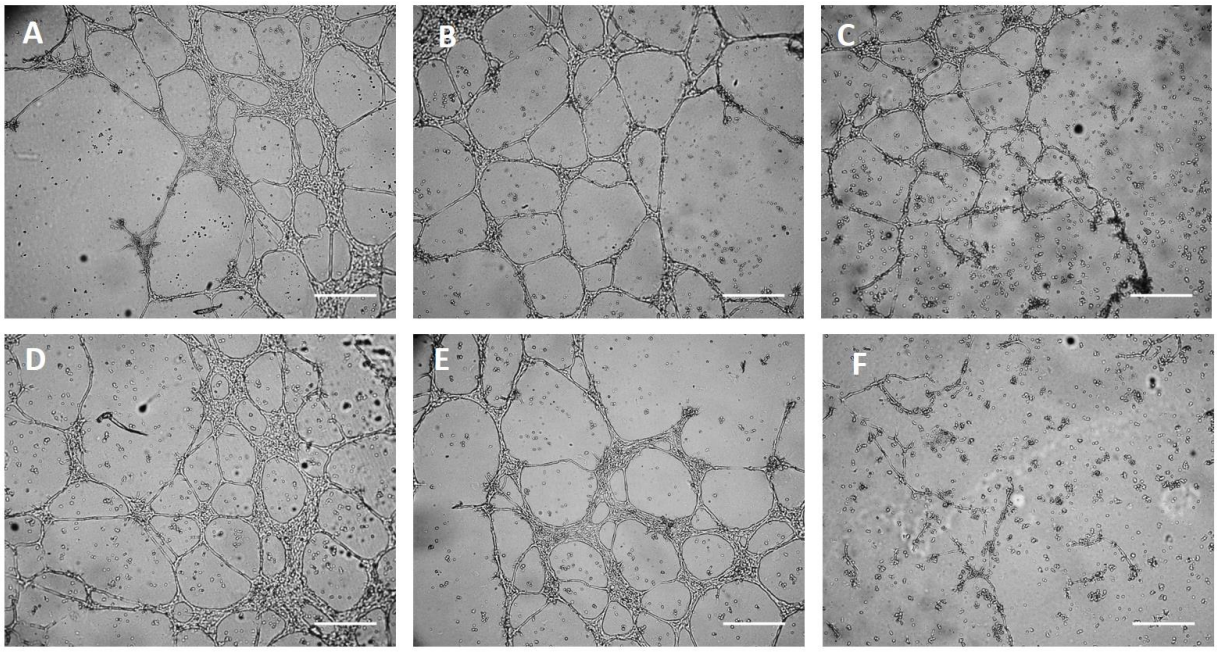

Figure 4.7 Images showing endothelial tube formation using conditioned media from ADSC (50,000 cells/cm^2) (A), adipose tissue (0.13 g/ml media) (B), emulsified fat (0.13 ml/ml media) (C), and SVF-gel (0.036 ml/ml media) (D) conditioned media. FGF (100 ng/ml) (E) was used as a positive control and MV media without supplements (F) as negative control. Scale bar = 500 µm.

4.4.2 Aortic ring assay

The conditioned media obtained as described in Table 4.2 were tested in the chick aortic ring assay (Figure 4.8). After four days of culture in conditioned media, images were acquired to analyse the sprouts from the rings. In case of the ADSC conditioned media, it was possible to identify homogenous dense tube growth around the ring (Figure 4.8A). On the other hand, adipose tissue promoted long sprouts around the ring, but they did not grow uniformly around the ring leaving some areas with short tubes and others with long ones (Figure 4.8B). The emulsified fat conditioned media did not promote tube growth around the aortic rings, resulting in a few short tubes around it (Figure 4.8C). In contrast, SVF-gel stimulated tube outgrowth around the rings in a uniform way all around the rings, but with a lower density than ADSC conditioned media (Figure 4.8D). FGF (100 ng/ml) was used as a positive control. Rings cultured with FGF created a dense tubular outgrowth around the rings (Figure 4.8E). Compared to the conditioned media from the different tested groups, FGF did not produced very long sprouts, but it seems to have promoted a higher number of sprouts around the ring. Finally, non-conditioned media was used as a negative control resulting in a few tube outgrowths around the rings (Figure 4.8F).

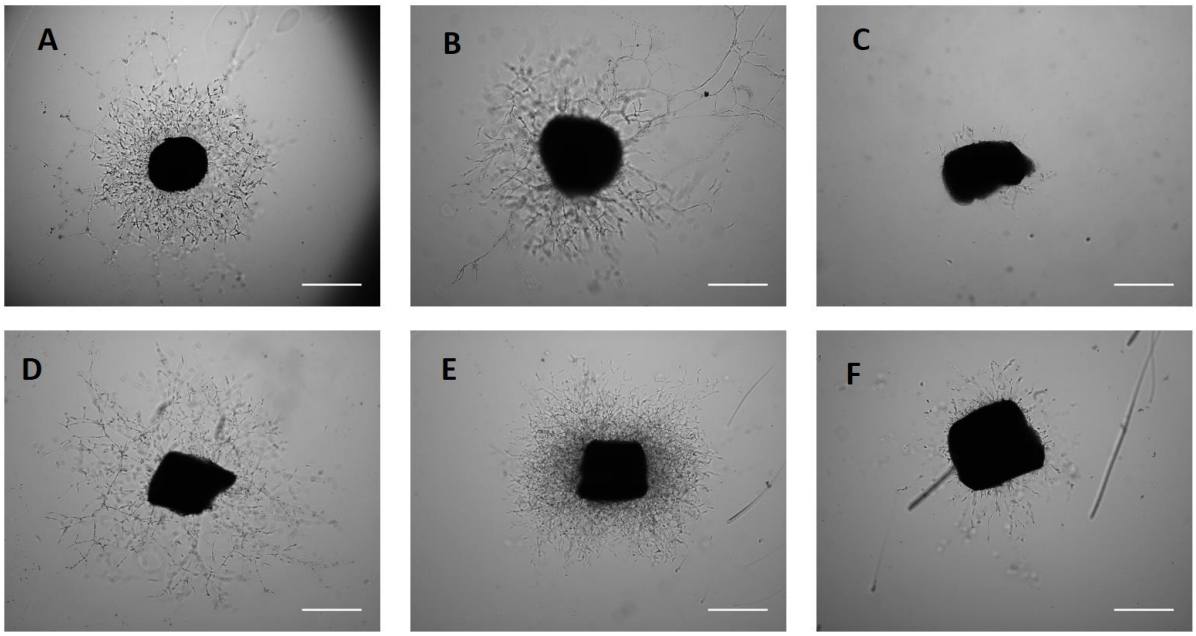

Figure 4.8 Chick aortic rings after 4 days culture using ADSC (50,000 cells/cm^2) (A), adipose tissue (0.13 g/ml media) (B), emulsified fat (0.13 ml/ml media) (C), and SVF-gel (0.036 ml/ml media) (D) conditioned media. FGF (100 ng/ml) (E) was used as a positive control and MV media without supplements (F) as negative control. Scale bar = 500 µm.

Aortic ring assay images were analysed by measuring the area of sprouts from each ring using the ImageJ “freehand” tool. The final mean sprout length is shown in Figure 4.9. ADSC conditioned media doubled the sprout area compared to the non-conditioned media. Adipose tissue conditioned media statistically significantly increased the sprout area compared to non-conditioned media with a value 3.5-fold higher. In contrast, conditioned media from emulsified fat promoted higher area of tubes than non-conditioned media. SVF-gel conditioned media statistically significantly increased the mean sprout area in aortic rings compare to the non-conditioned media. FGF (100 ng/ml) was used as a positive control and although the mean area of the tubes around the rings increased, it was not statistically significant compared to the non-conditioned media, negative control.

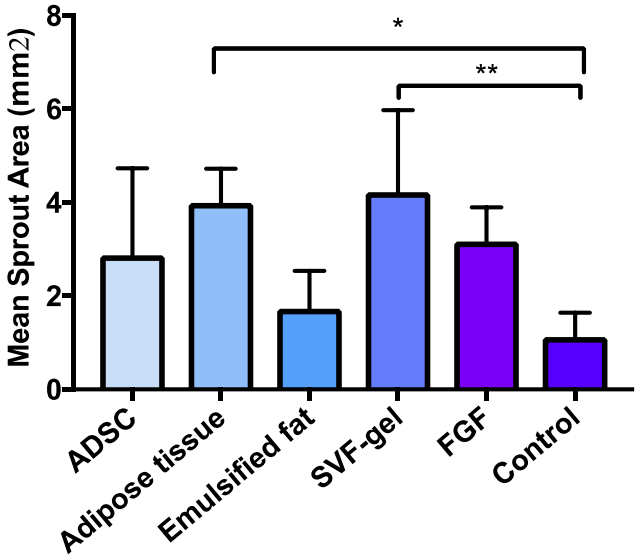

Figure 4.9 Average sprout area on chick aortic ring assay using ADSC (50,000 cells/cm^2), adipose tissue (0.13 g/ml media), emulsified fat (0.13 ml/ml media), and SVF-gel (0.036 ml/ml media) conditioned media. FGF (100 ng/ml) was used as a positive control and MV media without supplement as negative control. Mean with error bars showing standard deviation. N=4, n=3, *p<0.05, **p<0.01.

4.4.3 CAM assay

To analyse the conditioned media on the CAM assay, silicone rings were used to track the place in which the samples were added every two days. New blood vessels were counted at day 7 when the samples were added for the first time, until day 13. FGF (100ng/ml) as a positive control statistically significantly doubled the vascular area on the CAM compared to non-conditioned media. ADSC conditioned media did not increase the vascular area with a similar area to nonconditioned media. On the other hand, adipose tissue, emulsified fat and SVF-gel conditioned media slightly increased the number of new blood vessels compared to the negative control however these did not reach statistical significance. There is high variability between the samples since it is an *ex ovo* assay. As a result an increased number of repeats and samples were necessary to reduce inconsistencies.

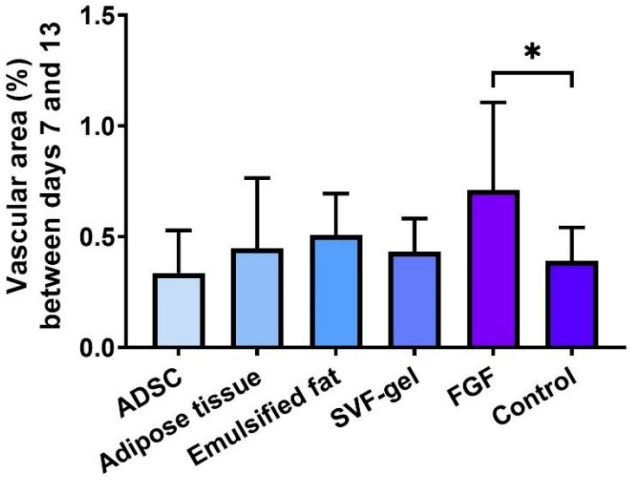

Figure 4.10 Vascular area change on CAM between day 7 and 13 of culture. Mean with error bars showing standard deviation. N=4, n=4, *p<0.05.

Throughout this research different angiogenic assays were used to study the angiogenic properties of conditioned media from ADSC, adipose tissue, emulsified fat, and SVF-gel. Table 4.3 shows a summary of the results from each of the assays in this chapter. In the endothelial tube formation assay emulsified fat and SVF-gel conditioned media were able to stimulate the tube formation. In this case the best outcomes were produced by SVF-gel conditioned media, followed by emulsified fat. Likewise, on the aortic ring adipose tissue and SVF-gel conditioned medium stimulated sprouts around the aortic rings. In these assays SVF-gel had the best outcomes, followed by adipose tissue. FGF was used as a positive control and was shown to produce statistically significant positive results in all the different assays except, the aortic ring assay it was not possible to stimulate.

Table 4.3 Summary of results obtained from different angiogenic assays on this chapter using conditioned media from ADSC, adipose tissue, emulsified fat, and SVF-gel. ↔ = no increased outcome, ↑ = increased outcome. *p<0.05, **p<0.01, ***p<0.0001.

Assay	Endothelial Cell type	ADSC	Fat	Emulsified fat	SVF-gel	FGF
Endothelial Tube formation (Number of tubes)	HDMEC	↔	↔	↑*	↑***	↑*
Endothelial Tube formation (Total tubes length)	HDMEC	↔	↔	↔	↑***	↑*
Aortic ring assay	--	↔	↑*	↔	↑**	↔
CAM assay	--	↔	↔	↔	↔	↑*

4.4.4 Cytokine array

Studying the growth factors in the conditioned media is essential to understand how the different protocols to process the adipose tissue could affect its angiogenic properties. An angiogenic cytokine array was carried out on the conditioned media of ADSC, adipose tissue, emulsified fat, SVF-gel, and non-conditioned media (Figure 4.11A). Between each array there are differences not only in the intensity of the dots, but also in the different cytokines detected acording to the array map on Figure 4.11B. In general the media conditioned with ADCS had lowest cytokine expression with a lower intensity than media conditioned with derivatives of adipose tissue. Also, media conditioned with adipose tissue and emulsified fat presented a similar cytokine secretion profile. While media conditioned with SVF-gel showed some similarities to adipose tissue and emulsified fat, the overall intensity of the cytokines is much lower than those present in conditioned media from adipose tissue and emulsified fat.

Once the data was processed, the mean pixel density for each growth factor of each studied group was plotted (Figure 4.11C) (for further detail on each growth factor see Appendix 4). Cytokines that presented the higest pixel density were Epithelial neutrophil activating peptide (ENA-78 or CXCL5), chemokine (CXX motif) ligand 1 (GRO a/b/c), interleukin 6 and 8 (IL-6 and IL-8), and tissue inhibitor of metalloproteinase 1 and 2 (TIMP-1 and TIMP-2). Interestingly, the cytokines that were not detected in any of the groups were interferon gamma (IFN-ɣ), platelet-derived growth factor –BB (PDGF-BB), RANTES, and vascular endothelial growth factor –A and –B (VEGF-A and VEGF-B). All these cytokines are well known to have pro-angiogenic properties, however adipose tissue or its derivates did not produce them in this study.

A

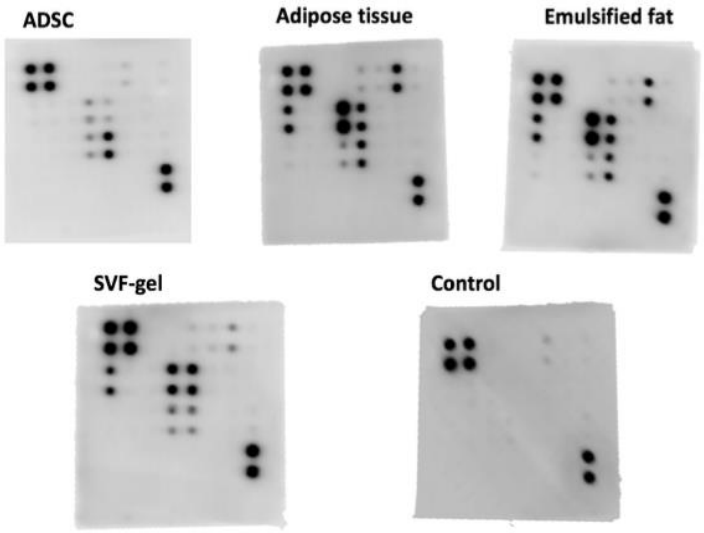

B

Pos	Pos	NEG	NEG	Angiogenin	EGF	ENA-78 (CXCL5)	bFGF
Pos	Pos	NEG	NEG	Angiogenin	EGF	ENA-78 (CXCL5)	bFGF
GRO a/b/c	IFN-γ	IGF-1	IL-6	IL-8 (CXXL8)	Leptin	MPC-1 (CCL2)	PDGF-BB
GRO a/b/c	IFN-γ	IGF-1	IL-6	IL-8 (CXXL8)	Leptin	MPC-1 (CCL2)	PDGF-BB
PLGF	RANTES (CCL5)	TGF β1	TIMP-1	TIMP-2	TPO	VEGF-A	VEGF-D
PLGF	RANTES (CCL5)	TGF β1	TIMP-1	TIMP-2	TPO	VEGF-A	VEGF-D
Blank	Blank	Blank	Blank	Blank	Blank	Neg	Pos
Blank	Blank	Blank	Blank	Blank	Blank	Neg	Pos

C

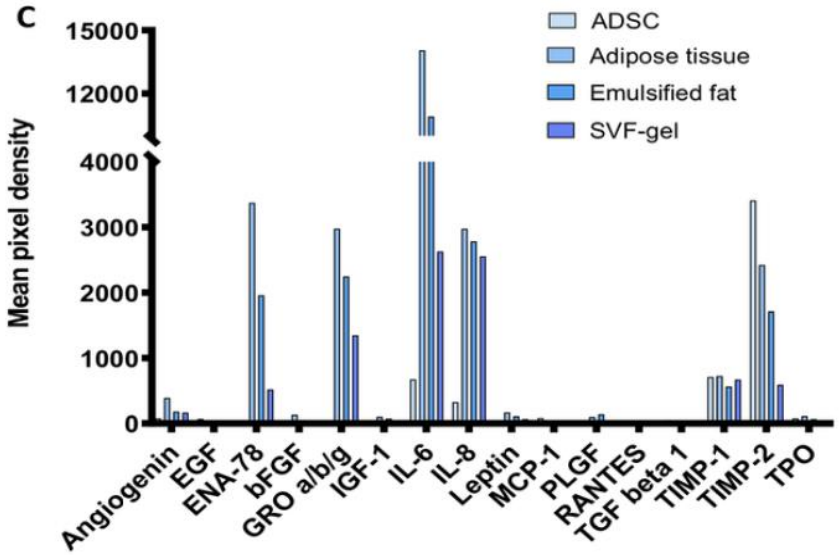

Figure 4.11 Angiogenic cytokine array after incubation with conditioned media from ADSC, adipose tissue, emulsified fat, SVF-gel, and non-conditioned media (A). Map of the different cytokines studied on the array (B), and analysis of mean pixel density for all the samples (C).

Angiogenin, IL-6, TIMP-2, basic fibroblast growth factor (bFGF), and placental growth factor (PLGF) were selected to be analysed in more detail for their relevance to vascularisation (Figure 4.12). Angiogenin was detected in all the conditioned media. In the same way, IL-6 expresion was easily detectable in adipose tissue and emulsified fat conditioned medias. However, SVF-gel and ADSC produced barely detectable levels of this growth factor. In contrast, TIMP-2 was detected in all groups of conditioned media. In the case of bFGF, adipose tissue, ADSC and emulsified fat contined easily detectable values of FGF, however SVF-gel had barely detectable levels. Finally, PLGF was only detected in media conditioned with adipose tissue and emulsified fat.

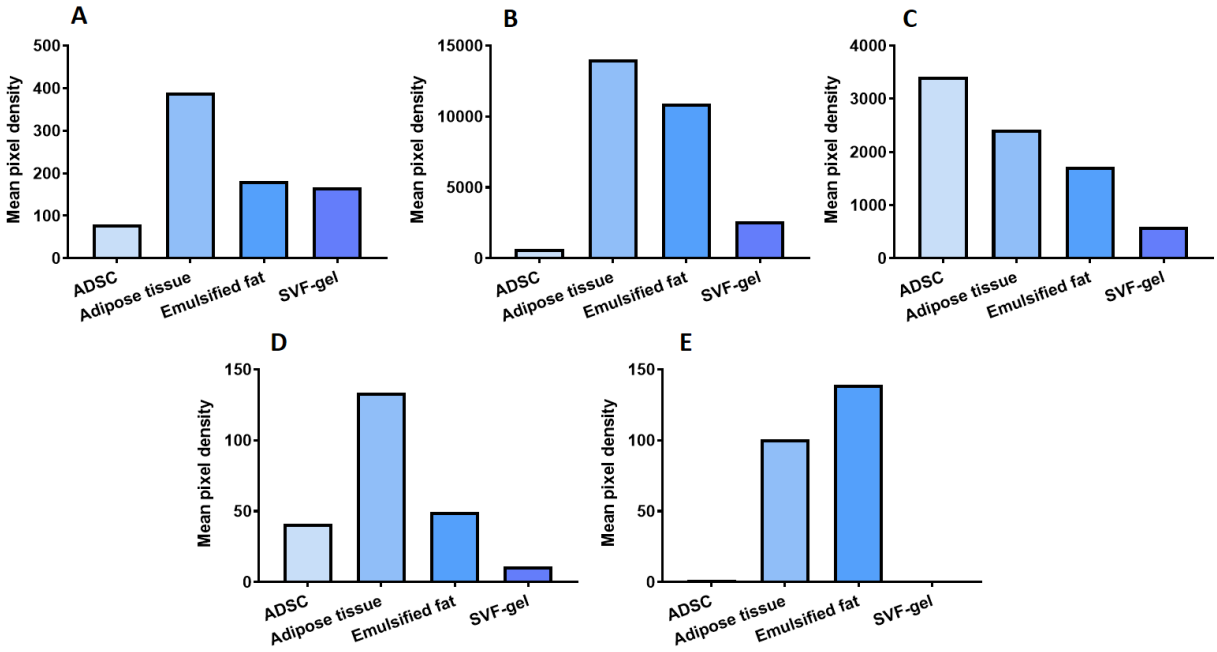

Figure 4.12 Relative expression levels (A) angiogenin, (B) IL-6, (C) TIMP-2, (D) bFGF, and (E) PLGF in conditioned media from ADSC, adipose tissue, emulsified fat, and SVF-gel.

4.5 Discussion

Previously, conditioned media from ADSC, adipose tissue, emulsified fat and SVF-gel were tested on endothelial cells to ascertain whether the angiogenic properties of the cells and tissues could stimulate endothelial cell migration and proliferation. There are trends that indicate that as the number of cells and quantity of tissue is increased to produce the conditioned media, the migration and proliferation of endothelial cells is increased. However, it was not statistically different compared to non-conditioned media (Chapter 3). It is vital to take into account that vascularisation is a complex process that takes place in a 3D environment, enrols different types of cells, and a variety of cytokines and growth factors regulate this process (Laschke *et al.*, 2006; Yu *et al.*, 2018). As a result, it is important to test the angiogenic properties of the conditioned media in more complex assays.

Endothelial tubular assays give a 3D environment to cells in which they can form tubular structures, getting closer to an *in vivo* model (see Section 1.11.3.3 for further details). The most used matrix for this is Matrigel (Adair and Montani, 2010). Matrigel is a basement membrane matrix extracted from mouse sarcoma rich in laminin, collagen IV, heparin sulphate proteoglycans, elastin, and some growth factors that allow endothelial cells to migrate, proliferate and create tubular-like structures (Corning, 2013; Zakhari *et al.*, 2018). For this thesis it was important to use a Matrigel reduced in growth factors to avoid stimulation of the endothelial cells from Matrigel itself.

In this study, ADSC conditioned media was able to stimulate tube formation in a dose dependent way (Figure 4.5 and Figure 4.6). However, even at the highest concentration of 50,000 cells/cm^{2,} the conditioned media did not significantly increase the number of tubes or their length compared to the negative control. In comparison, Pu *et al*., (2017) tested conditioned media from ADSC (22,000 cells/cm^2 cultured for 28 hrs) on endothelial cells (HUVECs) and reported that the conditioned media significantly increased the tubular structure formation compared to serum free media. Similarly to our study, Nakagami *et al*., (2005) tested ADSC conditioned media on human aortic endothelial cells (HAECs) in tube formation assays. The conditioned

media was able to non-significantly increase the length of the tubular structures (Nakagami *et al.*, 2005). In this case no details were given about the conditioned media preparation. It is possible the different outcomes on endothelial tubular formation between studies is a result of variation in the protocols to produce the conditioned media, or in patient to patient variability from isolated ADSC.

In contrast to ADSC conditioned media, SVF-gel conditioned media in the two highest concentrations did increase significantly the number and length of tubular structures. Similarly, Sun *et al*., (2017) cultured HUVEC with SVF-gel conditioned media obtained after 7 days of culture. The SVF-gel conditioned media induced HUVEC to form tubular interconnected structures, while HUVECs treated with non-conditioned media were unable to form a tubular network (Sun *et al.*, 2017). Interestingly, there are different studies analysing the angiogenic properties of the aqueous layer of the SVF-gel as a non-cellular treatment alternative. This aqueous layer forms after centrifuging emulsified fat to obtain four different layers: the top oil layer, a fatty second layer, a third aqueous layer, and a cellular pellet (Yu *et al.*, 2018; Cai *et al.*, 2019). Cai *et al*., (2019) refers to this aqueous layer as cell-free fat extract (FE) and they used it to enhance HUVEC tube formation. They tested different percentages of FE (0%, 5%, 10%, and 20%) on the endothelial cell cultures and they reported that FE is able to stimulate HUVEC cell proliferation and tube formation in a dose dependent manner (Yu *et al.*, 2018; Cai *et al.*, 2019). It is suggested that the proangiogenic properties of FE comes from the fact that emulsified fat is rich in growth factors not only produced by the presence of ADSC or SVF, but also during the process of emulsification (Cai *et al.*, 2019).

Nevertheless, our results show that emulsified fat has similar angiogenic properties to adipose tissue in the different assays performed to this point (endothelial cell migration, metabolic activity and HDMEC tube formation). This suggest that the emulsification stress induces cells present in the emulsified fat to produce higher levels of growth factors, or the growth factors could be released by the cell lysis during this process. In any of those cases, these did not enhance an angiogenic response on endothelial cells. Cai *et al*., (2019) also speculate that SVF-gel should have better angiogenic properties than just FE since the presence of cells could enhance even

more the presence of growth factors. This could explain results, in which SVF-gel showed higher number of tubular structures formed with its conditioned media compared to the other studied groups.

Comparable to the work done by Cai *et al*., He *et al*., (2019) worked with the liquid portion of the adipose tissue that they called Adipose Liquid Extract (ALE). In the protocol to produce the emulsified fat to extract ALE, they added an equal portion of PBS to the tissue. After the emulsification, they centrifuged the diluted emulsified fat at 2,000 g for 5 min to extract the third aqueous fraction. It is important to highlight that in this protocol the PBS added to the tissue is not removed before passing the sample between the syringes. As a result, it was easier to obtain a more defined liquid proportion, than with the method used in Cai *et al*., (2019) or in this thesis. However, their results are comparable to the FE because ALE was able to induce tubular structure formation on HUVEC in the similar way to VEGF and bFGF. They indicate that ALE is so rich in growth factors since the emulsification process releases bioactive molecules that are normally stored in cells and ECM (He *et al.*, 2019).

Compared to these results, Figure 4.5 showed emulsified fat was able to stimulate tubular structures in a manner very similar to FGF. However adipose tissue also achieved this, meaning that the emulsification in this case did not enhance this process. It is also possible that the emulsification did enhanced the tube formation but the free lipids in the conditioned media impaired the positive effect.

In our study, adipose tissue conditioned media expressed most of the cytokines in the studied array similar to emulsified fat conditioned media. While He *et al*., (2019) detected greater levels of angiogenic growth factors in their ALE the same was not true in our conditioned media from SVF-gel or emulsified fat. It is possible that the process of emulsification enhances the amount of growth factors immediately after the process. However, after culturing the emulsified fat to produce conditioned media it is possible that some of these growth factors are degraded or used by the cells in culture to grow, thus reducing the final growth factor concentration in the conditioned media.

From the results obtained in the endothelial tube formation assay it was possible to select a number of cells or amount of tissue in each of the studied groups to continue

studying their angiogenic properties. The endothelial tube formation assay is a valuable *in vitro* assay to test angiogenic properties of the conditioned media, however, only endothelial cells are involved in creating the tubular structures, so it cannot be considered a true recapitulation of angiogenesis. It is better described as a representation of the vasculogenic process, in which tubular structures are formed by cellular components, missing the other phases of angiogenesis (Zakhari *et al.*, 2018). As a result, this study next went on to investigate the angiogenic potential of conditioned media from different adipose formulations with the chick aortic ring and CAM assays. These models involve a heterogeneous cell population, giving more physiologically relevant information similar to an *in vivo* angiogenic model (Baker *et al.*, 2012).

In the aortic ring assay conditioned media from 50,000 ADSC/cm^2 (450,000 cells/well) approximately tripled the mean area of the sprouts compared to the non-conditioned media. In a related study, Eke *et al*., (2017) tested hydrogels seeded with different number of ADSC on the chick aortic ring assay in a co-culture using a tissue culture insert to test their angiogenic potential. The two highest concentration of cells used for this study were 0.5 x10^6 and 1x10^6, which were able to double and triple sprout length respectively compared to their control showing the same trend as our result. To develop these hydrogels, two different polymers (hyaluronic acid and gelatin) were used and ADSC were added to the polymer solution before they were crosslinked in order to obtain a cell-containing hydrogel (Eke *et al.*, 2017). Eke *et al*., (2017) claim that the angiogenic properties of the ADSC hydrogels come from the paracrine action of ADSC and not the hydrogels, explaining the similarity between their results and the ones obtained in this thesis.

In contrast, Iqbal *et al*., (2017) developed an aortic ring co-culture assay in which rat aortic rings were cultured with first trimester human umbilical cord perivascular cells (FTM HUCPVCs) and human bone marrow mesenchymal cells (BMSC) within a basal membrane extract (BME). In order to achieve the co-culture, different stromal cells were added to the aortic ring model 48 hrs after embedding the ring to allow the endothelial network to start developing. After the cells were added to the model, it was cultured for at least another 5 days to allow the cells to have an effect on the sprouts

around the ring. FTM HUCPVCs co-cultures created a greater tubular network than the aortic ring itself (control); while the control had a more developed network than BMSC co-culture (Iqbal *et al.*, 2017). In both cell types the secreted growth factors were similar, but the cell presence along the co-culture differed suggesting that direct interaction between MSCs and endothelial cells plays a structural supportive role for the endothelial cells (Iqbal *et al.*, 2017). Even when FTM HUCPVCs were shown to support the sprouts around the rings, the cells were added once the tubular network was already developing and it would be interesting to measure the angiogenic properties from the beginning of the experiment. Moreover, their model of study suggests that the improvement observed in sprouting is a consequence of direct contact between the cells; while in this research the angiogenic molecules secreted by ADSC or adipose tissue and their derivatives were studied. Nevertheless, our result shows that ADSC paracrine effect increases the sprouts area around the aortic rings. It is important to take into consideration that in this study chick embryonic aortas were used, while Iqbal et al., (2017) used adult rat aortas. It has been reported before that chick embryonic aortas have higher cell division rate than rat adult aortas making it hard to compare between studies (Auerbach *et al.*, 2003).

In this thesis adipose tissue and SVF-gel conditioned media were able to statistically significantly increase the mean sprout area around the aortic rings. On the other hand, emulsified fat conditioned media was the conditioned media with the lowest mean sprout area. This could be as a result of the free lipids in the media that could have a negative effect on the rings. To our knowledge, there have not been any attempts to study the angiogenic properties of adipose tissue, emulsified fat and SVF-gel using the aortic ring assay. Rojas-Rodriguez *et al*., (2014) developed an assay to study angiogenesis from adipose tissue fragments. This method is derived from the aortic ring assay, however they embedded small fragments of adipose tissue (1 mm^2) instead of the aortic rings and analysed the capillary sprouts around them. They reported that after day 5 of culture capillary sprouts were observed, and after day 11 the growth was greatly increased. In addition, around the sample it was possible to visualise fibroblast cells adhering to the surface of the well (Rojas-Rodriguez *et al.*, 2014). This assay is very interesting to study how adipose cells migrate from the

tissue, giving information as to how this may happen in patients when adipose tissue transplantation is performed. Nevertheless, it doesn't allow the paracrine properties of the tissue to be studied as in the aortic ring assay.

Conditioned media tested on the aortic ring was also tested on the CAM assay. CAM assays allow the study of the angiogenic properties of a tissue, cell or material in a live model in which different cells participate in the angiogenic process. In order to track the place where samples were loaded into the CAM silicone rings were used. This also facilitated the analysis of the vessels around the rings. ADSC conditioned media did not increased the number of blood vessels around the silicone rings compared to non-conditioned media (Figure 4.10). On the contrary, Eke *et al*., (2017) tested ADSC hydrogels on the CAM obtaining a positive effect on vascularisation. They report that hydrogels containing ADSC moderately increased the number of vessels, while hydrogels containing VEGF significantly increased the number of vessels (Eke *et al.*, 2017). Likewise, Shafaat *et al.*, (2018) tested spun polyurethane scaffolds with or without 17-β-estradiol seeded with $2.5x10^5$ ADSC into the CAM to observe their angiogenic potential. It was reported that the scaffolds with ADSC significantly increased the mean vessel count at the end of experimentation compared to the scaffold without cells (Shafaat *et al.*, 2018). Finally, Handel, *et al.,* (2013) tested a bio-glass based 3D scaffold seeded with ADSC on the CAM to see their angiogenic properties. In this study, the authors verified that the scaffold without cells did not promote vessel ingrowth, while the scaffolds with ADSC did induce angiogenesis within the scaffold structure. As a result, they suggest that angiogenic potential came from the cells and their secreted growth factors and not the scaffold alone (Handel *et al.*, 2013). Having ADSC on the CAM allows to have a constant realise of cytokines and 2 way communication with the surrounding cells enhancing their angiogenic properties.

To our knowledge, there are no other reports in which adipose tissue, emulsified fat and SVF-gel were studied on the CAM assay. In this thesis the conditioned media from adipose tissue, emulsified fat and SVF- gel promoted a slight (non-significant) increase in the vascular area around the silicone rings, while FGF, used as a positive control induced statistically significantly angiogenesis (Figure 4.10). Results from the

CAM assay present large variability in all the studied groups. This is caused by variation between embryos and the manipulation that embryos are exposed to that also leads to high mortality rate. As a result higher number of embryos are required to compensate for this (Naik, Brahma and Dixit, 2018). Nevertheless, this assay is a bridge between *in vitro* and *in vivo* assays and provided useful information.

In summary, on the CAM assay emulsified fat promoted the highest non-statistically significantly vascular area increased compared to non-conditioned media. While, in the aortic ring assay indicate that adipose tissue and SVF-gel conditioned media statistically significantly enhance angiogenesis. To understand why these groups have higher angiogenic potential, it is important to study the different cytokines secreted into the conditioned media. Different studies have suggested that the angiogenic potential of ADSC and adipose tissue and its derivatives is through their secreted factors (Handel *et al.*, 2013; Iqbal *et al.*, 2017). An angiogenesis cytokine array was used to obtain a general idea of the cytokines that are present in each conditioned media. There was a considerable variation between expression of growth factors and the level at which these are secreted depending on how the adipose tissue is processed (Figure 4.11). The stress to which the cells are exposed during the tissue processing, type, and number of cells cultured are presumably the reasons why each conditioned media has a different cytokine profile.

The cytokine array treated with ADSC conditioned media showed less variety of growth factors and in less intensity than the other conditioned media. Among the growth factors that were identified in this conditioned media were TIMP-2, EGF, monocyte chemoattractant protein-1 (MCP-1), and TGF- β. Previously, it has been shown ADSC conditioned media contains 19% angiogenic growth factors, 14% inflammatory growth factors, and the remaining cytokines are for other different cell functions (Xu *et al.*, 2016). Within the angiogenic growth factors were included PLGF, TGF-β, angiopoietin (Ang-1), bFGF and VEGF (Nakagami *et al.*, 2005; Pu *et al.*, 2017; Noverina *et al.*, 2019). There is a notable difference between our ADSC conditioned media growth factors and what has been reported before. It is likely that the media and incubation time to produce the conditioned media plays a key role for the cytokines

that are secreted by cells explaining this variation between the growth factor profiles. In addition to patient variability as these are primary cells.

On the other hand, of the cytokines secreted by adipose tissue, it has been reported that 50% are involved in immune respose and 25% in cell communication (Klimcakova *et al.*, 2007). The growth factors that have been detected and that are related with wound healing include IL-6, IL-8, TIMP-1, TIMP-2, bFGF, VEGF, and PDGF (Klimcakova *et al.*, 2007; Yu *et al.*, 2018). Coupled with our data, adipose tissue conditioned media also contains IL-6, IL-8, TIMP-1, TIMP-2, and bFGF. Klimacakova *et al.,* (2007) studied the RNA of some of the growth factors produced by different cell populations in adipose tissue. This analysis indicated that adiponectin and leptin are cytokines secreted by adipocytes; while IL-6, angiogenin, TIMP-1, and HGF are secreted by cells in the SVF (Klimcakova *et al.*, 2007). This could suggest that even when the SVF population is the main growth factor producer, the environment of the whole tissue induces the cells to secrete them; while as the tissue is further processed, cells are exposed to different stress and environment thereby reducing its expression. This can be verified as emulsified fat conditioned media presented the same growth factor profile as adipose tissue, but with slightly less intensity. This could be a result that all the cell populations in adipose tissue are still present on emulsified fat, however the emulsification process does affect the levels in which these factors are secreted. It has been indicated in previous studies that emulsified fat is rich in growth factors including VEGF, EGF, bFGF, BDNF, PDGF, IGF, and IL-6 (Xu *et al.*, 2018; Yu *et al.*, 2018; Cai *et al.*, 2019).

Finally, TIMP-1, IL-8, IL-6, GRO a/b/g, and Ang were present in SVF-gel conditioned media. Comparably, Yu *et al*., (2018) in preliminary results found that the growth factors present in the aqueous part of SVF-gel are similar to the molecules secreted by ADSC including bFGF, TGF- β1, EGF, VEGF, PDGF, and HGF. However, the levels in the FE were higher than the ones secreted by ADSC (Yu *et al.*, 2018). Similarly, Deng *et al*., (2017) reported that conditioned media from SVF-gel contained higher concentrations of bFGF, TGF-β, and EGF than conditioned media from ADSC and adipose tissue. The authors suggest that the shear forces used to produce SVF-gel could regulate the secretion of different growth factors, adding to the highly

concentrated cells and ECM making SVF-gel a better source of cytokines (Deng *et al.*, 2017). This is comparable to our results since SVF-gel conditioned media presented higher levels of IL-8, leptin, GRO a/b/g, and Ang than ADSC. These cytokines are pro-inflammatory and/or promote angiogenesis in wound healing.

As it has been mentioned before SVF-gel is cell dense including ADSC with the protection of extracellular matrix, which not only plays a support for cells, but also it creates a dynamic microenvironment that regulates cell behaviours and functions enhancing its angiogenic properties (Sun *et al.*, 2017). This could also explain why SVF-gel conditioned media had better angiogenic results on endothelial tube formation, and aortic ring. It is important to mention that the shear forces to produce SVF-gel are also part of the protocol to produce emulsified fat. Nevertheless, emulsified fat did not have the same angiogenic response as SVF-gel in the different assays used in this research. An explanation for this could be that most of the free lipids present on emulsified fat are removed on SVF-gel. This free lipid in emulsified fat conditioned media are mixed in the media, which could have a negative effect on the endothelial cells. This negative effect would not be expected in *in vivo* models, like CAM assay, where there are natural mechanisms to remove the lipids, allowing the angiogenic potential of emulsified fat be higher.

Comparing our results with these previous studies, the main difference is the absence of VEGF from all of our conditioned media. VEGF is the gold-standard pro-angiogenic cytokine due to its major regulator function in neovascularisation in different tissues (Nomi *et al.*, 2002). However, as in this study, Park *et al.,* (2013) also found that monolayer ADSC cultures did not secrete VEGF. Nevertheless, in most studies it has been reported that conditioned media from ADSC, emulsified fat and lipoaspirate did contain VEGF (Edwards *et al.*, 2014; Deng *et al.*, 2017; Yu *et al.*, 2018; Sagaradze *et al.*, 2019). It has been reported before that the soluble form of VEGF undergoes rapid diffusion and degradation with a half-life of 50 min (Guex *et al.*, 2014). It is possible that if VEGF was secreted into the conditioned media, it was already degraded by the time it was analysed on the cytokine array. This could be a limiting factor for our study, not only for the cytokine detection, but also for the other angiogenic assays that were performed. In order to avoid this limitation, conditioned media would have to be

analysed immediately after it is collected to avoid any loss of the cytokines. In addition, it would be interesting how the cytokine profile of each of the studied groups change during the cultivation time.

In addition, there are a several of differences (media, time, number of cells or amount of tissue, etc) as to how to produce conditioned media in each study. The conditions in which the conditioned media is produced has a direct impact on the growth factors secreted (Sukho *et al.*, 2017; Sagaradze *et al.*, 2019). Sagaradze *et al.*, (2019) tested two different media, DMEM low glucose and NutriStem, without serum or supplement to produce conditioned media from mesenchymal stromal cells. They measured the concentration of different growth factors after 7 days of culture and discovered that each media induced cells to secrete different levels of growth factors (Sagaradze *et al.*, 2019). In this study, MV media without supplements was used to produce the conditioned media. This media was selected since HDMEC grow much better in this media than DMEM (see Appendix 4) and the lack of supplements helped to avoid any noise from serum proteins and allows analysis of the growth factors secreted by the cells and tissue. However, it is important to consider that the lack of serum could stress the cells/tissue by itself changing the cytokine profile as if they were cultured on a low/complemented serum medium. Also, another factor that can impact considerably on the growth factors and their concentration in the conditioned media is the seeding density.

For example, Sukho *et al.* (2017), found that the levels of secreted VEGF and FGF increased as the seeding density of ADSC increased. In both cases they reported that the highest concentration of these growth factors in ADSC conditioned media were produced by 400,000 cells/cm^2 cultures. They suggest that this is a result of the hypoxic stress that is generated due to the high cell density (Sukho *et al.*, 2017). In addition, it has been reported that a hypoxic environment stimulates the production of growth factors including VEGF (Park *et al.*, 2013). It is important to consider that media and seeding density are not the only factors that can affect the secreted cytokines since cells that have been cultured for longer presented lower angiogenesis activity compared to newly isolated ADSC (Noverina *et al.*, 2019). Additionally, the production

of pro-angiogenic growth factors from ADSC decreases in aged patients (Efimenko *et al.*, 2014).

The donors of the tissue used in this research vary and their health status is not known. Unfortunately, the research ethics used for this research does not allow us to access this information. However, this could have an impact on our results since it has been reported before that age, BMI, and physiological condition of the patients could affect the angiogenic capacity of the adipose tissue and ADSC (Aust *et al.*, 2004; Efimenko *et al.*, 2014; Rojas-Rodriguez *et al.*, 2014). Efimenko *et al*., (2014) studied the effect of patients age on the regenerative potential of their ADSC. Three different age ranges were used with an average age of 7, 45 and 64 years in each of them. ADSC were isolated from harvested tissue and conditioned media was collected after 48 hrs of 70-80% confluent cultures. Endothelial cells cultured on Matrigel with the conditioned media were able to stimulate capillary-like structures. However, the quantity of tubular structures decreased in correlation with the patient age (Efimenko *et al.*, 2014). This might also apply to adipose tissue, emulsified fat and SVF-gel. It is important to highlight that this not only affected the cytokine array, but also all the angiogenic assays performed in this thesis. As a result, it is essential that conditioned media from ADSC, adipose tissue, emulsified fat or SVF-gel is standardised for clinical application.

Another limitation for this thesis is that angiogenic cytokines were studied from the conditioned media, when it has been established in other studies that conditioned media does not only contain cytokines, but also other types of molecules that regulate the healing process such as extracellular vesicles and mRNA. Extracellular vesicles are nanoparticles that can vary in size and shapes. They are formed by a bilayer lipid membrane with some integrated proteins and receptors. Researchers use different names for extracellular vesicles according to its characteristics such as size. Some of the names used for extracellular vesicles are: exosomes, ectosomes, microvesicles, microparticles, promininosomes, migrasomes texosomes (Konoshenko *et al.*, 2018). These vesicles are lateral communication between cells to transfer biological active molecules including soluble proteins, lipids, ribonucleic acids (mRNA, microRNA, tRNA, rRNA, etc), and are produced by all types of tissues in the body (Locke, Feisst and Meidinger, 2015; Konoshenko *et al.*, 2018). Depending on their content, vesicles

could have a variety of regulatory effects on the target cells (Konoshenko *et al.*, 2018). In previous studies, it has been shown vesicles in conditioned media can improve vascularisation and healing processes (Locke, Feisst and Meidinger, 2015; Konoshenko *et al.*, 2018). It was not possible within the constraints of this project to study further the cytokines, extracellular vesicles or mRNA secreted by the different groups studied.

Five relevant growth factors were chosen to study in more detail according to their relevance to this research. First, angiogenin is a complex with actin that promotes endothelial cell migration and proliferation (Efimenko *et al.*, 2014). Adipose tissue conditioned media predominately expressed this growth factor compared to ADSC, emulsified fat, and SVF-gel (Figure 4.12A). Nevertheless, adipose tissue conditioned media did not increase endothelial migration and metabolic activity (see Table 4.3). However, this conditioned media promoted the highest number of sprouts on the aortic ring and the highest number of new vessels around the silicone rings on the CAM assay. In addition, angiogenin concentration is positively associated with levels IL-6 and TNF-α (Klimcakova *et al.*, 2007), suggesting that its presence in conditioned media from adipose tissue are correlated with the high levels of IL-6 in this conditioned media (Figure 4.12B).

IL-6 is a broad-spectrum pro-inflammatory cytokine that participates in wound healing process and angiogenesis (Klimcakova *et al.*, 2007; Pu *et al.*, 2017). Pu *et al*., (2017) studied the effect of this molecule on endothelial cells. They describe that IL-6 increased endothelial tube formation in a dose dependent manner and tube formation was considerably reduced when IL-6 was knocked out in interfering RNA-transfected ADSC (Pu *et al.*, 2017). However, in order to have an effect on endothelial cells this cytokine needed to be present in concentrations higher than 75 pg/ml (Pu *et al.*, 2017). Compared to this study, ADSC conditioned media had IL-6 levels barely detectable, while this cytokine was more highly expressed by adipose tissue, emulsified fat, and SVF-gel. Nevertheless, the number and length of tubes on the endothelial tube formation assay was approximately the same for each of them, with the exception of SVF-gel which presented a much higher outcome. Similar to our results, Klimcakova

et al., (2007) reported that IL-6 was the cytokine secreted in highest quantities of all studied secreted protiens in adipose tissue.

TIMP-2 is a cytokine that is involved in vessel maturation and stabilisation during the angiogenesis process. TIMPS are the main inhibitor of metalloproteinases (MMP). ECM degradation by MMPs is a crucial step to allow cells to migrate and form tubular vessels (Stratman *et al.*, 2009). At the end of the angiogenic process it is important to stop matrix degradation to allow vessel maturation by pericytes (Stratman *et al.*, 2009). TIMP-2 regulates the activity of some specific pro-MMP and it can inhibit angiogenesis by decreasing endothelial cell proliferation (Fernández *et al.*, 2003; Grainger, 2012). Fernandez *et al.,* (2003) and Seo *et al.,* (2003) suggest that the TIMP-2 inhibition ability of endothelial cell proliferation is independent of the ability to regulate MMP activity. As a result TIMP-2 has two inhibitory activities that reduce angiogenesis *in vitro* and *in vivo* (Fernández *et al.*, 2003; Seo *et al.*, 2003). TIMP-2 was highly detected in all the studied groups conditioned medias, especially on ADSC conditioned media. Since TIMP-2 inhibits endothelial proliferation, adding the fact that the rest of the angiogenic cytokines were expressed in lower quantities than the other groups, this could explain why ADSC did not show high angiogenic potential in this research.

Since bFGF was used as a positive control during this thesis, it is noteworthy to study if FGF was secreted into the conditioned media of the different groups. FGF is a growth factor family that promotes migration and proliferation of fibroblasts and keratinocytes, and it induces fibroblasts to produce collagen (Deng *et al.*, 2017; Noverina *et al.*, 2019). bFGF or FGF-2 is essential for mesenchymal cell expansion and viability and it promotes MSC differentiation into adipocytes, chondrocytes and osteocytes (Noverina *et al.*, 2019). Our cytokine array shows that adipose tissue conditioned predominately had FGF, while it was also detected in ADSC and emulsified fat in a lower intensity. While media conditioned with SVF-gel presented a very low value barely detectable (Figure 4.12D). On the contrary, Noverina *et al.,* (2019) analysed the cytokine profile of ADSC in conditioned media from different passages. bFGF was the growth factor secreted in highest concentrations from the studied cytokines in all different ADSC passages (Noverina *et al.*, 2019).

It has been reported before that the levels of bFGF in conditioned media are related to endothelial cell migration velocity (Sagaradze *et al.*, 2019). Interestingly, adipose tissue conditioned media significantly promoted the longest sprouts around the aortic rings and the highest number of new vessels on CAM assay. This could be a result of the high levels of angiogenin, IL-6 and bFGF found in its conditioned media. On the other hand, Deng *et al*., (2017) reported that conditioned media from SVF-gel had higher concentrations of bFGF, TGF-β, and EGF than conditioned media from adipose tissue. However, in our study, SVF-gel had barely detectable expression for many of the studied cytokines. Nevertheless, media conditioned with SVF-gel showed better angiogenic potential on endothelial tube formation assay, and aortic ring assay than ADSC and emulsified fat conditioned media.

Finally, PLGF or PGF is part of the VEGF family. This growth factor is highly expressed in the placenta during gestation. However, it is also expressed in normal physiological conditions in some tissues such as adipose tissue, heart, lungs and skeletal muscle (De Falco, 2012). The role of PLGF in angiogenesis is through promoting survival, proliferation and migration of endothelial cells particularly in a hypoxic environment (De Falco, 2012). It has been reported that in adipose tissue PLGF is expressed in adipocytes and SVF cells (Lijnen *et al.*, 2006). In this study PLGF was found in the conditioned media of adipose tissue and emulsified fat. This could suggest that the presence of adipocytes is necessary for this growth factor to be secreted; while in the SVF-gel and ADSC where adipocytes are absent, its expression is also absent. Another explanation could be that adipose tissue and emulsified fat cultures are more hypoxic as a result of the lipid layer formed on top inducing the production of PLGF in these two conditioned medias.

In summary, conditioned media from ADSC, adipose tissue, emulsified fat, and SVF-gel was tested on HDMEC tube formation assay. In contrast to 2D endothelial cultures (Chapter 2), the different conditioned media were able to stimulate the endothelial cells on the tube formation assay. SVF-gel conditioned media was the formulation that promoted the highest number and longest tubes. Also, this assay allowed us to pick one seeding density and amount of tissue for each group to produce conditioned media for the rest of the experiments. Interestingly, chick aortic ring results showed

that SVF-gel followed by adipose tissue conditioned media have the highest angiogenic properties, followed by SVF-gel conditioned media. These results indicate that the way adipose tissue is processed affects the growth factors secreted into the conditioned media. CAM assay did not show any statistically significantly result for any of the conditioned medias. A cytokine array was carried out in order to study a variety of cytokines that are related to the angiogenesis process. This array showed interesting differences in relative expression of growth factors in the conditioned media studied. Adipose tissue had the highest relative expression of most of the growth factors, specifically those pro-inflammatory signals such as IL-6 and IL-8. Emulsified fat secreted a similar cytokine profile to adipose tissue. Nevertheless, their relative expression of growth factors was lower than the adipose tissue. ADSC secreted growth factors related to tissue remodelling like TGF-β, EGF, and TIMP-2. Finally, SVF-gel showed a low relative secretion of most of the studied growth factors. However, this conditioned media was able to promote a positive angiogenic response in 3D endothelial cell culture, *ex vivo,* and ex *ovo* assays. In general, SVF-gel showed the highest pro-angiogenic properties of all the studied groups. It is possible that the shear forces used during tissue processing and the elimination of the lipids enhance the angiogenic properties of adipose tissue. Further investigation is needed to understand which factors or combination of factors in the SVF-gel and conditioned media are responsible for these observed differences.

Chapter 5 Conclusions and Future work

In recent years adipose tissue has called the attention of clinicians due to its regenerative properties. Along with the application of adipose tissue in clinics for lipofilling, new protocols to process the tissue were created to enable its application with small needles subcutaneously for aesthetic proposes such as removing wrinkles. Emulsified fat, stromal vascular fraction (SVF) -gel, and adipose derived stromal cells (ADCS) have proven to have similar regenerative properties similar to whole adipose tissue. However, the mechanisms behind how adipose tissue supports skin wound healing are not yet fully understood. Adipose tissue regenerative properties may come from its secreted cytokines and their ability to promote vascularisation but there has not been any study in which the vascularisation properties of emulsified fat, SVF-gel and ADSCs have been studied side-by- side. Such a study would reveal how as the tissue is processed, its regenerative properties change, and to determine formulation is best for clinical purposes. This thesis addressed this issue by studying the ability of adipose tissue, emulsified fat, SVF-gel and ADSC conditioned media to promote vascularisation in different angiogenic assays. The hypothesis of this study was that factors secreted by adipose tissue and formulations of adipose tissue can promote angiogenesis *in vitro* and *ex vivo*.

Another crucial step for adipose tissue related treatments is dosage. It is very important to know how many ADSC, or the amount of tissue is necessary to create a positive effect on *in vivo* wound healing. For this, characterisation of adipose tissue, emulsified fat, and SVF-gel plays a fundamental role. It is a requirement to know its composition, which and how many cells are in each formulation to create a dose dependent treatment and to understand how processing affects tissue morphology. Therefore, in this thesis, adipose tissue, emulsified fat, SVF-gel, and ADSC were characterised and using imaging, flow cytometry and DNA analysis.

First, LightSheet and confocal imaging showed the structure of the adipose tissue, and how, as it was processed, the presence of adipocytes reduced while free lipid increased. The reduction in adipocyte number in the emulsified fat and SVF-gel is a result of the emulsification process in which cells are lysed. Nevertheless, it was still

possible to identify some intact adipocytes in the emulsified fat and SVF-gel. Moreover, SVF-gel contained a considerable amount of free lipid that was mixed with the ECM layer after the centrifugation step. Since adipocyte density varies in each of the formulations, it was expected that cell density would increase from adipose tissue to SVF-gel. In order to confirm this, DNA isolation and quantification for each of the samples were used on this study. NucleoSpin columns were found to be an effective method for DNA isolation. Preliminary data was obtained on DNA isolation and quantification confirming that as the adipose tissue is processed, cell density decreases. This supports part of our hypothesis, as adipose tissue is processed, its structure is disrupted, and its cell content is reduced. Being able to estimate the number of cells per ml or g of tissue is essential to establish a dosage. This thesis provides a benchmark that can be used when considering data from further different patients samples.

One of the main limitations of this research was the inconsistency and sporadic tissue supply. As a result, experiment planning was a challenge, especially for those experiments in which fresh tissue was required, such as DNA isolation and tissue imaging. In order to help experiment planning, conditioned media was collected from tissue and stored frozen. Conditioned media was used to study the angiogenic properties of adipose tissue, emulsified fat, SVF-gel, and ADCS. Conditioned media has the property that it can be collected and frozen, helping experiment logistic. In addition, it could be an off-the-shelf product that can be standardised. Its availability would not be an issue especially for those patients that urgently need be treated such as patients with extensive burns. Additionally, conditioned media does not contain any cells, reducing considerably the risk of an immune response. At the moment, different studies use different amounts of tissue and number of cells combined with a variety of incubations times and media to produce conditioned media. As a result, to produce conditioned media from ADSC or adipose tissue, a range of number of cells and amount of tissue were used (Table 3.1). It is important to note that not having a standard procedure to produce conditioned media makes it difficult for researchers to compare results between studies.

Two different endothelial cells lines, human endothelial microvascular cells (HMEC-1) and human dermal microvascular endothelial cells (HDMEC), were used to test the conditioned media in 2D models. Our results on both cell types did not show any change on metabolic activity or migration with the conditioned media compared to our negative control (non-conditioned media). In addition, the amount of lipid or the concentration of LDH in the conditioned media did not show a significant effect on the endothelial cells. It is possible that the number of ADSC or amount of tissue used to produce the conditioned media were not high enough to have a positive effect on the endothelial cells. It is possible that the low serum medium could have affected the growth and migration of the endothelial cells. This is a limitation of this study since serum free media was selected in order to study only those cytokines secreted by the cells and tissue. As a result, using more complex models was another approach to study the angiogenic properties of conditioned media.

The endothelial tube formation assay proved a more physiologically relevant to test the conditioned media effect on angiogenesis. Media conditioned with SVF-gel induced the highest number of tubes and highest total segment length. However, in all the studied groups the number and length of tubes increased as the number of cells or amount of tissue was increased. This allowed us to choose the optimal concentration of conditioned media for each group to continue on their analysis on chick aortic ring assay and CAM assay. Both of these assays involve heterogeneous cell types in a 3D environment resulting in a model to study the angiogenic properties of adipose tissue and its cells, which is closer to the *in vivo* situation.

On the aortic ring assay, adipose tissue and SVF-gel conditioned media showed the best outcomes compared to the other studied groups and non-conditioned media. While on CAM assay, emulsified fat showed higher angiogenic properties compared to the other groups. It can be seen from these results that the protocols to process the adipose tissue affect the angiogenic properties of each formulation. This is a result of the variation of the cytokine profile of each conditioned media. The cytokine array showed that most expressed growth factors between the groups were ENA-78, GRO a/b/c, IL-6, IL-8, and TIMP2. Interestingly, most of these molecules are involved in inflammation process, and promotion of cell survival. Adipose tissue and emulsified

fat had similar cytokine expression with high relative expression of IL-6 and IL-8. While ADSC conditioned media contained TGF-β, EGF, and TIMP-2 that are part of ECM remodelling. Interestingly, SVF-gel had the lowest relative expression for most of the cytokines. However, it showed higher angiogenic properties than ADSC and emulsified fat. These data suggest that part of the hypothesis is rejected since the level of disruption on emulsified fat and SVF-gel does not affects negatively the production of pro-angiogenic cytokines compared to adipose tissue. A limitation of this research is that only a semi-quantitative cytokine profile was produced, while there are other molecules in the conditioned media that also have an angiogenic effect including extracellular vesicles, mRNA, etc.

Further research is needed to study the concentrations of different molecules in the conditioned media using quantitative methods (for example ELISA). Also, studying the effect of individual cytokines on the angiogenic assays performed in this research would provide useful information to understand the mechanism behind adipose tissue regenerative properties. Another significant aspect to study would be the angiogenic properties using of tissue itself instead of conditioned media. Interaction between endothelial cells and cells present in the tissue or ADSC could enhance their angiogenic properties or lead to differences in outcomes here. This study focussed on conditioned media as promising non-cellular off -the-shelf product that could be applied in clinics without as many regulations as a tissue/cell-based therapy. It is also important to study the angiogenic properties of conditioned media and adipose formulations on 3D skin wound models. These models can provide more information of a possible outcome from the conditioned media, tissue and cells when they are applied into patients.

ADSC, adipose tissue, emulsified fat, and SVF-gel are a promising tool for wound healing. Based on the preliminary findings presented here, conditioned media from SVF-gel showed the greatest potential, with adipose tissue also demonstrating a positive effect. This data suggests the heterogeneous uncultured cell population found in the SVF has more regenerative capabilities compared to ADSC alone. The positive effect of paracrine secretions on angiogenesis could not be confirmed in 2D experiments. However, in the 3D assays of chapter 4 we were able to demonstrate

that SVF-gel did produce pro-angiogenic effects in some assays which were not observed with media conditioned from ADSCs alone. However, further research is still required to properly estimate effective doses of paracrine secretion from each studied group. Once a standard procedure to obtain conditioned media has been established new technologies to deliver the tissue, cells, or their conditioned media into different types of skin wounds will need to be developed. This research has increased our fundamental understanding of the role of paracrine secretions from adipose tissues and their role in angiogenesis which will influence development of future treatments that will improve patients healing processes and lives after an injury.

Chapter 6 Appendix

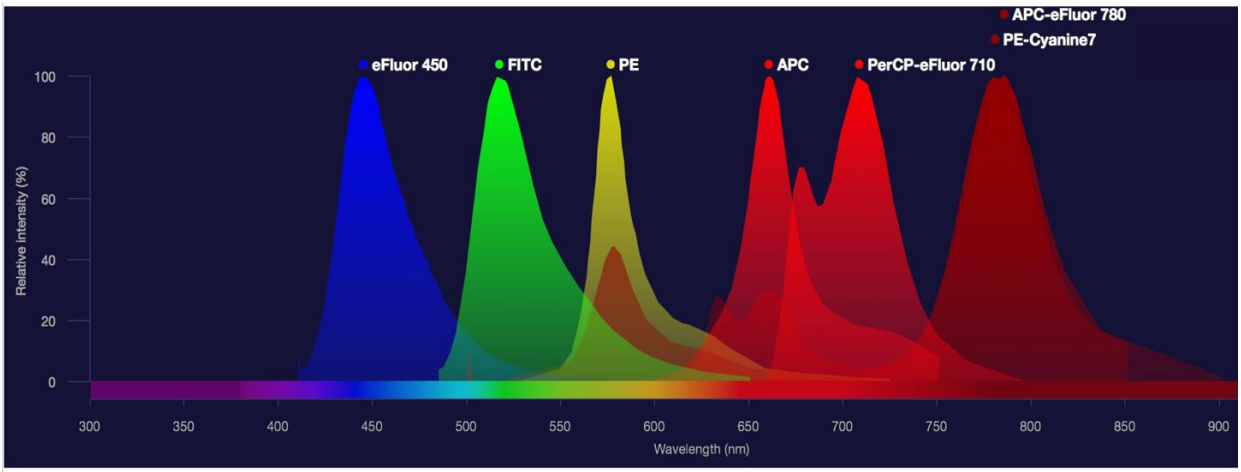

Appendix 1 Excitation wavelength for each of the fluorophores used for flow cytometry. In the case of APC-efluor 780 and PE-C7 two different lasers were used in order to avoid crossed signals. APC-efluor 780 was excited with 645nm laser, while PE-C7 was excited by 565nm laser. Diagram obtained from www.thermofisher.com.

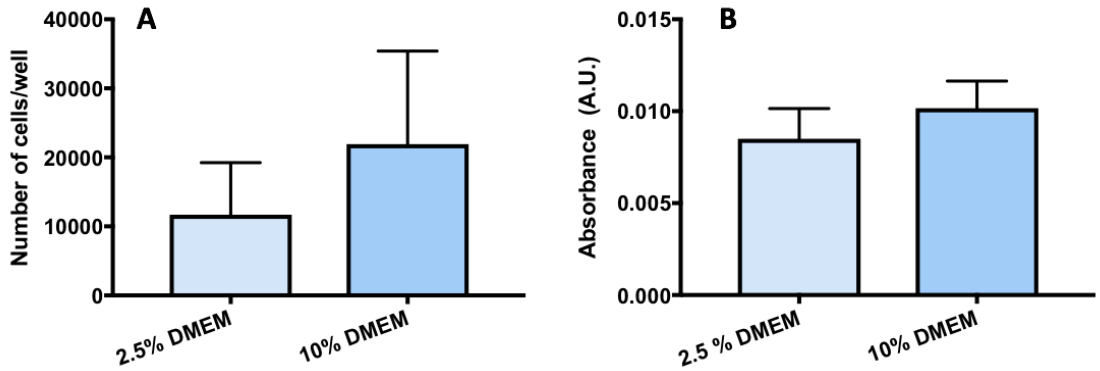

Appendix 2 Effect of 2.5% and 10% FBS supplemented DMEM on ADSC culture. Cell count (A) and metabolic activity (B) after 3 days' incubation with both serum concentrations. Mean with error bars showing standard deviation. N=3, n=3.

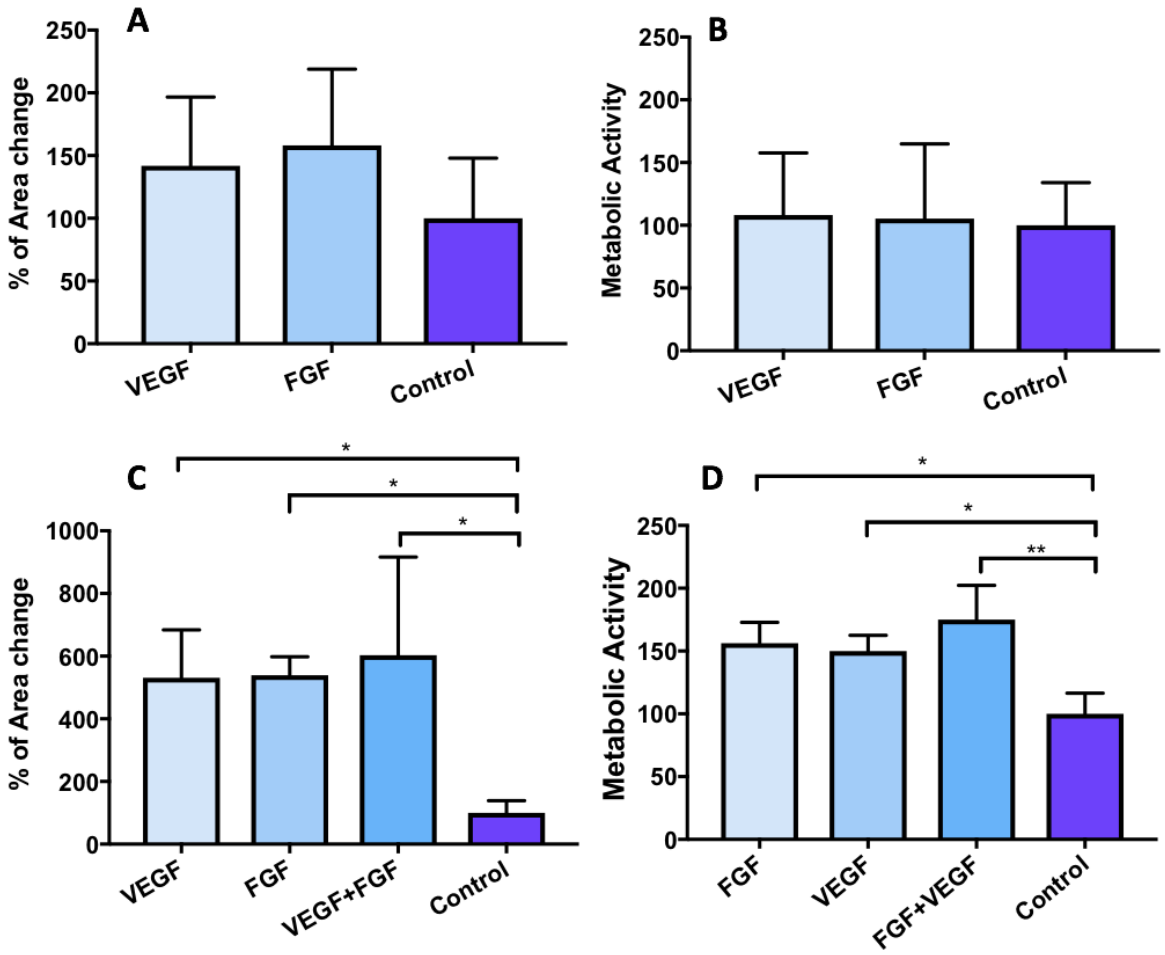

Appendix 3 Effect of 50ng/ml VEGF, FGF or both on percentage migration (A and C) or metabolic activity (B and D) using HMEC-1 (A and B), or HDMEC (C and D). Mean with error bars showing standard deviation. N=3, n=3. *p<0.05, **p<0.01.

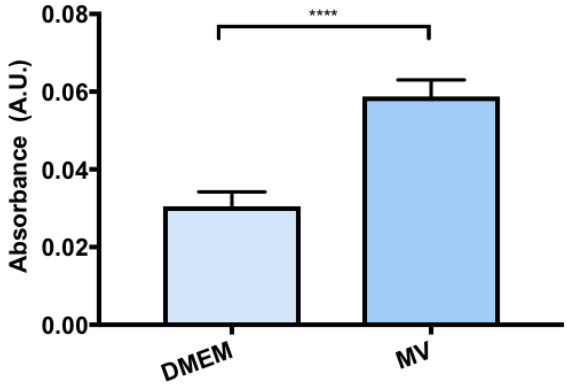

Appendix 4 Metabolic activity measured using MTT of HDMEC using 10% FBS supplemented DMEM or MV medium without supplements after 3 days of culture. Mean with error bars showing standard deviation. N=3, n=3. ****p<0.0001.

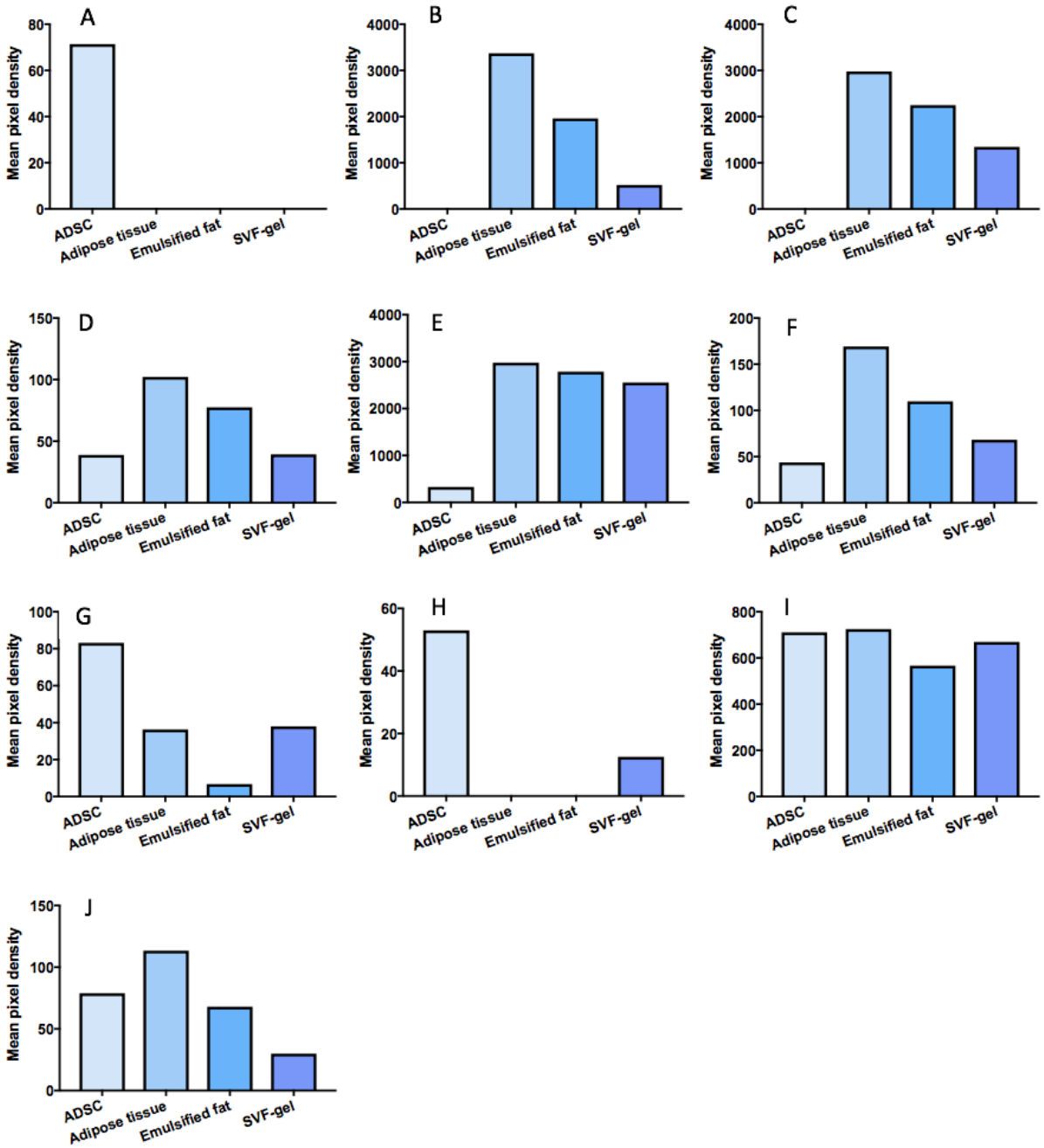

Appendix 5 Relative expression levels (A) EGF, (B) ENA-78, (C) GRO a/b/g, (D) IGF-1, and (E) IL-8, (F) Leptin, (G) MCP-1, (H) TGF-ß1, (I) TIMP-1, (J) TPO in conditioned media from ADSC, adipose tissue, emulsified fat, and SVF-gel.

Chapter 7 References

Adair, T. and Montani (2010) 'Chapter 2 Angiogenesis Assays', *Angiogenesis. San Rafael (CA): Morgan & Claypool Life Sciences*.

Alexander, R. W. (2016) 'Understanding Mechanical Emulsification (Nanofat) Versus Enzymatic Isolation of Tissue Stromal Vascular Fraction (tSVF) Cells from Adipose Tissue : Potential Uses in Biocellular Regenerative Medicine', *Journal of Prolotherapy*, 8, pp. 947–960.

Atalay, S., Coruh, A. and Deniz, K. (2014) 'Stromal vascular fraction improves deep partial thickness burn wound healing', *Burns*, 40(7), pp. 1375–1383. doi: 10.1016/j.burns.2014.01.023.

Auerbach, R. *et al.* (2003a) 'Angiogenesis assays: a critical overview.', *Clinical chemistry*, 49(1), pp. 32–40. doi: 10.1373/49.1.32.

Auerbach, R. *et al.* (2003b) 'Angiogenesis assays: A critical overview', *Clinical Chemistry*, 49(1), pp. 32–40. doi: 10.1373/49.1.32.

Aust, L. *et al.* (2004) 'Yield of human adipose-derived adult stem cells from liposuction aspirates', *Cytotherapy*. doi: 10.1080/14653240310004539.

Baaße, A. *et al.* (2018) 'Radiation sensitivity of adipose-derived stem cells isolated from breast tissue', *International Journal of Molecular Sciences*, 19(7). doi: 10.3390/ijms19071988.

Baer, P. C. and Geiger, H. (2012) 'Adipose-derived mesenchymal stromal/stem cells: Tissue localization, characterization, and heterogeneity', *Stem Cells International*, p. 11. doi: 10.1155/2012/812693.

Bai, Y. *et al.* (2018) 'Sequential delivery of VEGF, FGF-2 and PDGF from the polymeric system enhance HUVECs angiogenesis in vitro and CAM angiogenesis', *Cellular Immunology*, 323(October 2017), pp. 19–32. doi: 10.1016/j.cellimm.2017.10.008.

Baker, M. *et al.* (2012) 'Use of the mouse aortic ring assay to study angiogenesis', *Nature Protocols*, 7(1), pp. 89–104. doi: 10.1038/nprot.2011.435.

Bateman, M. E. *et al.* (2018) 'Using Fat to Fight Disease: A Systematic Review of Non-Homologous Adipose-Derived Stromal/Stem Cell Therapies', *Stem cells*. doi: 10.1002/stem.2847.

Bauhammer, I., Sacha, M. and Haltner, E. (2019) 'Establishment of a novel in vitro viable human skin model as a basis for the treatment of human and veterinary chronic skin diseases', *Journal of Drug Delivery Science and Technology*, 51(December 2018), pp. 695–699. doi: 10.1016/j.jddst.2019.04.008.

Bi, H. *et al.* (2019) 'Stromal vascular fraction promotes migration of fibroblasts and angiogenesis through regulation of extracellular matrix in the skin wound healing process', *Stem Cell Research and Therapy*, 10(1), pp. 1–21. doi: 10.1186/s13287-019-1415-6.

Biotium (2020) *MemBrite™ Fix Cell Surface Staining Kits*.

Braza, M. E. and Fahrenkof, M. P. (2020) *Split-Thickness Skin Grafts*, *StatPearls*. Available at: https://www.ncbi.nlm.nih.gov/books/NBK551561/ (Accessed: 17 June 2020).

Bunnell, B. A. *et al.* (2008) 'Adipose-derived Stem Cells: Isolation, Expansion and Differentiation', *Methods*, 45(2), pp. 115–120. doi: 10.1016/j.ymeth.2008.03.006.Adipose-derived.

Cai, Y. *et al.* (2019) 'Fat Extract Improves Random Pattern Skin Flap Survival in a Rat Model', *Aesthetic surgery journal*, 39(12), pp. NP504–NP514. doi: 10.1093/asj/sjz112.

Cartland, S. P. *et al.* (2016) 'Comparative Evaluation of Trial, FGF-2 and VEGF-A-Indiced Angiogenesis In Vitro and In Vivo', *International Journal of Molecular Sciences*, 17. doi: 10.3390.

Chadwick, P. *et al.* (2013) 'BEST PRACTICE GUIDELINES : WOUND MANAGEMENT IN', *Wound International*, pp. 1–27. Available at: www. woundsinternational.com.

Chae, D. S. *et al.* (2017) 'Stromal vascular fraction shows robust wound healing through high chemotactic and epithelialization property', *Cytotherapy*, 19(4), pp. 543–554. doi: 10.1016/j.jcyt.2017.01.006.

Chappell, J. C., Wiley, D. M. and Bautch, V. L. (2011) 'Regulation of Blood Vessel Sprouting', *Seminars in Cell & Developmental Biology*, 22(9), pp. 1005–1011. doi: 10.1016/j.semcdb.2011.10.006.

Chung, E. *et al.* (2015) 'Acta Biomaterialia Fibrin-based 3D matrices induce angiogenic behavior of adipose-derived stem cells', *Acta Biomaterialia*, 17, pp. 78–88. doi: 10.1016/j.actbio.2015.01.012.

CORNING (2013) *Corning® Matrigel® Growth Factor Reduced (GFR) Basement Membrane Matrix, LDEV-free, 10 mL*. Available at: https://certs-ecatalog.corning.com/life-sciences/product-descriptions/354230.pdf (Accessed: 20 September 2018).

Costa, M. *et al.* (2017) 'Cell Sheet Engineering Using the Stromal Vascular Fraction of Adipose Tissue as a Vascularization Strategy', *Acta Biomaterialia*. doi: 10.1016/j.actbio.2017.03.034.

DeCicco-Skinner, K. L. *et al.* (2014) 'Endothelial cell tube formation assay for the in vitro study of angiogenesis', *Journal of Visualized Experiments*, 10(91), pp. 1–8. doi: 10.3791/51312.

Deng, C. *et al.* (2017) 'Extracellular matrix/stromal vascular fraction gel conditioned medium accelerates wound healing in a murine model', *Wound Repair and Regeneration*, 25(6), pp. 923–932. doi: 10.1111/wrr.12602.

Dennis L. Kasper, Anthony S. Fauci, Stephen L. Hauser, Dan L. Longo, J. Larry Jameson, J. L. (2016) *Harriso's Manual of Medicine*. 19th edn. Mc Graw Hill.

Distler, J. W. *et al.* (2003) 'Angiogenic and angiostatic factors in the molecular control of angiogenesis', *The Quarterly Journal of Nuclear Medicine*, 47(3), pp. 149–161.

Dong, Z. *et al.* (2013) 'The survival condition and immunoregulatory function of adipose stromal vascular fraction (SVF) in the early stage of nonvascularized adipose transplantation', *PLoS ONE*, 8(11), pp. 1–11. doi: 10.1371/journal.pone.0080364.

Druecke, D. *et al.* (2004) 'Neovascularization of poly(ether ester) block-copolymer scaffoldsin vivo: Long-term investigations using intravital fluorescent microscopy', *Journal of Biomedical Materials Research*. doi: 10.1002/jbm.a.20016.

Edwards, S. S. *et al.* (2014) 'Functional analysis reveals angiogenic potential of human mesenchymal stem cells from Wharton's jelly in dermal regeneration', *Angiogenesis*, 17, pp. 851–866. doi: 10.1007/s10456-014-9432-7.

Efimenko, A. *et al.* (2014) 'Tissue-Specific Progenitor and Stem Cells Adipose-Derived Mesenchymal Stromal Cells From Aged Patients With Coronary Artery Disease Keep Mesenchymal Stromal Cell Properties but Exhibit Characteristics of Aging and Have Impaired Angiogenic Potential', *Stem Cell Translational Medicine*, 3, pp. 32–41. doi: 10.5966/sctm.2013-0014.

Eke, G. *et al.* (2017) 'Development of a UV crosslinked biodegradable hydrogel containing adipose derived stem cells to promote vascularization for skin wounds and tissue engineering', *Biomaterials*. doi: 10.1016/j.biomaterials.2017.03.021.

Ernst, C. and Christie, B. R. (2006) 'Isolectin-IB4 as a vascular stain for the study of adult neurogenesis', *Journal of Neuroscience Methods*, 150(1), pp. 138–142. doi: 10.1016/j.jneumeth.2005.06.018.

De Falco, S. (2012) 'The discovery of placenta growth factor and its biological activity', *Experimental and Molecular Medicine*, 44(1), pp. 1–9. doi: 10.3858/emm.2012.44.1.025.

Fernández, C. A. *et al.* (2003) 'Structural and functional uncoupling of the enzymatic and angiogenic inhibitory activities of tissue inhibitor of metalloproteinase-2 (TIMP-2): Loop 6 is a novel angiogenesis inhibitor', *Journal of Biological Chemistry*, 278(42), pp. 40989–40995. doi: 10.1074/jbc.M306176200.

Flanagan, M. (2013) *Wound Healing and Skin Integrity : Principles and Practice*. Edited by John Wiley and Sons. Hertfordshire: Wiley-Blackwell.

Frueh, F. S. *et al.* (2016) 'Current and emerging vascularization strategies in skin tissue engineering.', *Critical reviews in biotechnology*, 37(5), pp. 613–625. doi: 10.1080/07388551.2016.1209157.

Frykberg, R. G. and Banks, J. (2015) 'Challenges in the Treatment of Chronic Wounds', *Advances in Wound Care*, 4(9), pp. 560–582. doi: 10.1089/wound.2015.0635.

Gebremeskel, S. *et al.* (2019) 'Promotion of Primary Murine Breast Cancer Growth and Metastasis by Adipose-Derived Stem Cells Is Reduced in the Presence of Autologous Fat Graft', *Plastic and reconstructive surgery*, 143(1), pp. 137–147. doi: 10.1097/PRS.0000000000005142.

Gilbert, D. F. and Friedrich, O. (2017) *Cell Viability Assays ,Methods and Protocols*. Hatfield: Humana Press. doi: 10.1007/978-1-4939-6960-9.

Grainger, S. J. (2012) 'Engineering Functional Capillary Networks', *ProQuest Dissertations and Theses*, p. 169. Available at: http://proxy.lib.chalmers.se/login?url=http://search.proquest.com/docview/1029869488?accountid=10041%5Cnhttp://link.lib.chalmers.se/link.php?url_ver=Z39.88-

2004&rft_val_fmt=info:ofi/fmt:kev:mtx:dissertation&genre=dissertations+%26+theses&sid=ProQ:ProQuest.

Guex, A. G. *et al.* (2014) 'Covalent immobilisation of VEGF on plasma-coated electrospun scaffolds for tissue engineering applications', *Colloids and Surfaces B: Biointerfaces*, 123, pp. 724–733. doi: 10.1016/j.colsurfb.2014.10.016.

Hagberg, C. E. *et al.* (2018) 'Flow Cytometry of Mouse and Human Adipocytes for the Analysis of Browning and Cellular Heterogeneity', *Cell Reports*, 24(10), pp. 2746-2756.e5. doi: 10.1016/j.celrep.2018.08.006.

Handel, M. *et al.* (2013) '45S5-bioglass®-Based 3D-scaffolds seeded with human adipose tissue-derived stem cells induce in vivo vascularization in the CAM angiogenesis assay', *Tissue Engineering - Part A*, 19(23–24), pp. 2703–2712. doi: 10.1089/ten.tea.2012.0707.

Hasegawa, T. and Ikeda, S. (2015) 'Adipose-derived stromal / stem cells as a potential source of skin regeneration', *Stem Cell & Translational Investigation 2015*, 2, pp. 4–7. doi: 10.14800/scti.787.

He, Y. *et al.* (2019) 'Human adipose liquid extract induces angiogenesis and adipogenesis: A novel cell-free therapeutic agent', *Stem Cell Research and Therapy*, 10(1), pp. 1–14. doi: 10.1186/s13287-019-1356-0.

Health and Social Care Information Centre (2016) 'National Diabetes Foot Care Audit Report', *National Diabetes Foot Care Audit Report* , 1, p. 63.

Hirota, K. and Semenza, G. L. (2006) 'Regulation of angiogenesis by hypoxia-inducible factor 1', *Critical Reviews in Oncology/Hematology*, 59(1), pp. 15–26. doi: 10.1016/j.critrevonc.2005.12.003.

Huang, H. *et al.* (2017) 'Preferred M2 Polarization by ASC-Based Hydrogel Accelerated Angiogenesis and Myogenesis in Volumetric Muscle Loss Rats', *Stem Cells International*. doi: 10.1155/2017/2896874.

Human Tissue Authority (2020) *Regulation of stem cell lines*.

Hutmacher, D. *et al.* (2009) 'Characterization and culturing of adipose-derived precursor cells', *Emerging Technology Platforms for stem cells*.

Iqbal, F. *et al.* (2017) 'The aortic ring co-culture assay: A convenient tool to assess the angiogenic potential of mesenchymal stromal cells in vitro', *Journal of Visualized Experiments*, 2017(127), pp. 1–12. doi: 10.3791/56083.

Jeffrey E., J. and Bridget, H. (2014) 'Wound healing: Part I. Basic Science', *Plastic and Reconstructive Surgery*, 133(2), pp. 199–207. doi: 10.1016/j.jcma.2017.11.002.

Jiménez, B. *et al.* (2000) 'Signals leading to apoptosis-dependent inhibition of neovascularization by thrombospondin-1', *Nature Medicine*. doi: 10.1038/71517.

Jin, E. *et al.* (2017) 'Angiogenic characteristics of human stromal vascular fraction in ischemic hindlimb', *International Journal of Cardiology*, 234, pp. 38–47. doi: 10.1016/j.ijcard.2017.02.080.

Kamalov, A. A. *et al.* (2017) 'The application of a novel biomaterial based on the secreted products of human mesenchymal stem cells and collagen for spermatogenesis restoration in the model of experimental cryptorchidism', *Research Journal of Pharmaceutical, Biological and Chemical Sciences*, 8(1).

Kang, J. H., Gimble, J. M. and Kaplan, D. L. (2009) ' In Vitro 3D Model for Human Vascularized Adipose Tissue ', *Tissue Engineering Part A*, 15(8), pp. 2227–2236. doi: 10.1089/ten.tea.2008.0469.

Khudyakov, J. I. *et al.* (2018) 'A sample preparation workflow for adipose tissue shotgun proteomics and proteogenomics', *The Company of Biology*, 7(11), pp. 1–8. doi: 10.1242/bio.036731.

Kilinc, M. O. *et al.* (2018) 'The ratio of ADSCs to HSC-progenitors in adipose tissue derived SVF may provide the key to predict the outcome of stem-cell therapy', *Clinical and Translational Medicine*, 7(5). doi: 10.1186/s40169-018-0183-8.

Kim, M. H. *et al.* (2018) 'Galectin-1 from conditioned medium of three-dimensional culture of adipose-derived stem cells accelerates migration and proliferation of human keratinocytes and fibroblasts', *Wound Repair and Regeneration*, 26, pp. S9–S18. doi: 10.1111/wrr.12579.

Kim, W. S. *et al.* (2007) 'Wound healing effect of adipose-derived stem cells: A critical role of secretory factors on human dermal fibroblasts', *Journal of Dermatological Science*, 48, pp. 15–24. doi: 10.1016/j.jdermsci.2007.05.018.

Klar, A. S. *et al.* (2014) 'Tissue-engineered dermo-epidermal skin grafts prevascularized with adipose-derived cells', *Biomaterials*, 35(19), pp. 5065–5078. doi: 10.1016/j.biomaterials.2014.02.049.

Klar, A. S., Zimoch, J. and Biedermann, T. (2017) 'Skin Tissue Engineering: Application of Adipose-Derived Stem Cells', *BioMed Research International*, 2017, pp. 1–12. doi: 10.1155/2017/9747010.

Klimcakova, E. *et al.* (2007) 'Profiling of adipokines secreted from human subcutaneous adipose tissue in response to PPAR agonists', *Biochemical and Biophysical Research Communications*, 358(3), pp. 897–902. doi: 10.1016/j.bbrc.2007.05.012.

Konoshenko, M. Y. *et al.* (2018) 'Isolation of Extracellular Vesicles: General Methodologies and Latest Trends', *BioMed Research International*. doi: 10.1155/2018/8545347.

Korrapati, P. S. *et al.* (2016) 'Recent advancements in nanotechnological strategies in selection , design and delivery of biomolecules for skin regeneration', *Materials Science & Engineering C*, 67, pp. 747–765. doi: 10.1016/j.msec.2016.05.074.

Krapohl, D. J. and Shaw, P. K. (2015) 'Chapter 2- Anatomy and physiology for polygraph examiners', in *Fundamentals of Polygraph Practice*, pp. 29–60. doi: 10.1016/B978-0-12-802924-4.00002-5.

Kue, C. S. *et al.* (2014) 'Chick embryo chorioallantoic membrane (CAM): An alternative predictive model in acute toxicological studies for anti-cancer drugs', *Experimental Animals*, 64(2), pp. 129–138. doi: 10.1538/expanim.14-0059.

Kwon, S. H. *et al.* (2015) 'Conditioned medium of adipose-derived stromal cell culture in three-dimensional bioreactors for enhanced wound healing', *Journal of Surgical Research*. doi: 10.1016/j.jss.2014.10.053.

Laschke, M. W. *et al.* (2006) 'Angiogenesis in Tissue Engineering : Breathing Life into Constructed Tissue Substitutes', *Tissue Engineering*, 12(8), pp. 2093–2104.

Li, Q. *et al.* (2014) 'EGF Enhances ADSCs Secretion via ERK and JNK Pathways', *Cell Biochemistry and Biophysics*, 69, pp. 189–196. doi: 10.1007/s12013-013-9769-3.

Lijnen, H. R. *et al.* (2006) 'Impaired adipose tissue development in mice with inactivation of placental growth factor function', *Diabetes*, 55(10), pp. 2698–2704. doi: 10.2337/db06-0526.

Lin, G. *et al.* (2008) 'Defining stem and progenitor cells within adipose tissue', *Stem Cells and Development*, 17, pp. 1053–1063. doi: 10.1089/scd.2008.0117.

Lin, K. K. and Goodell, M. A. (2011) 'Recent Advances in Cytometry, Part B - Advances in Applications', *Methods in cell biology*, 103, pp. 221–66. doi: 10.1016/B978-0-12-385493-3.00010-3.

Locke, M., Feisst, V. and Meidinger, S. (2015) 'From bench to bedside: use of human adipose-derived stem cells', *Stem Cells and Cloning: Advances and Applications*, 8, p. 149. doi: 10.2147/SCCAA.S64373.

Lyons, F. and Ousley, L. (2014) *Dermatology for the Advanced Practice Nurse*. Edited by M. Zuccarini. New York: Springer Publising Company.

MacDonald, N. J. *et al.* (2001) 'Endostatin binds tropomyosin: A potential modulator of the antitumor activity of endostatin', *Journal of Biological Chemistry*. doi: 10.1074/jbc.M100743200.

Macherey-Nagel (2016) 'Genomic DNA from Tissue, User manual, NucleoSpin®Tissue', (June), p. 40.

Maclean, P. S. *et al.* (2015) 'The role for adipose tissue in weight regain after weight loss', *Obesity Reviews*, 16(S1), pp. 45–54. doi: 10.1111/obr.12255.

MacNeil, S. (2008) 'Biomaterials for tissue engineering of skin', *Materials Today*, 11(5), pp. 26–35. doi: 10.1016/S1369-7021(08)70087-7.

Maijub, J. G. *et al.* (2015) 'Concentration-Dependent Vascularization of Adipose Stromal Vascular Fraction Cells', *Cell Transplantation*, 24, pp. 2029–2039. doi: http://dx.doi.org/10.3727/096368914X685401.

Maione, L., Memeo, A., *et al.* (2014) 'Autologous fat graft as treatment of post short stature surgical correction scars', *Injury*, 45(S6), pp. S126–S132. doi: 10.1016/j.injury.2014.10.036.

Maione, L., Vinci, V., *et al.* (2014) 'Autologous fat graft in postmastectomy pain syndrome following breast conservative surgery and radiotherapy', *Aesthetic Plastic Surgery*, 38(3), pp. 528–532. doi: 10.1007/s00266-014-0311-9.

Mangir, N. *et al.* (2019) 'Using ex Ovo Chick Chorioallantoic Membrane (CAM) Assay to

Evaluate the Biocompatibility and Angiogenic Response to Biomaterials', *ACS Biomaterials Science and Engineering*, 5(7), pp. 3190–3200. doi: 10.1021/acsbiomaterials.9b00172.

Mashiko, T. *et al.* (2017) 'Mechanical Micronization of Lipoaspirates: Squeeze and Emulsification Techniques', *Plastic and Reconstructive Surgery*, 139(79), pp. 79–90. doi: 10.1097/PRS.0000000000002920.

McDaniel, J. C. and Browning, K. K. (2014) 'Smoking, Chronic Wound Healing, and Implications for Evidence-Based Practice', *Journal of Wound, Ostomy and Continence Nursing*, 41(5), pp. 415–423. doi: 10.1097/WON.0000000000000057.

Miana, V. V. and Prieto González, E. A. (2018) 'Adipose tissue stem cells in regenerative medicine', *Ecancermedicalscience*, 12, pp. 1–14. doi: 10.3332/ecancer.2018.822.

Molecular Probes Inc. (2005) *LIVE/DEAD™ Viability/Cytotoxicity Kit, for mammalian cells*. Available at: https://assets.thermofisher.com/TFS-Assets/LSG/manuals/mp03224.pdf (Accessed: 28 November 2019).

Mönkemöller, V. *et al.* (2012) 'Imaging fenestrations in liver sinusoidal endothelial cells by optical localization microscopy Viola', *The Royal Society of Chemestry*, pp. 7634–7639. doi: 10.1039/x0xx00000x.

Morgan, T. (2015) 'Are your wound management choices costing you money?', *Journal of Community Nursing*, 29(4), pp. 17–20.

Naik, M., Brahma, P. and Dixit, M. (2018) 'A Cost-Effective and Efficient Chick Ex-Ovo CAM Assay Protocol to Assess Angiogenesis', *Methods and Protocols*, 1(2), p. 19. doi: 10.3390/mps1020019.

Nakagami, H. *et al.* (2005) 'Novel autologous cell therapy in ischemic limb disease through growth factor secretion by cultured adipose tissue-derived stromal cells', *Arteriosclerosis, Thrombosis, and Vascular Biology*, 25(12), pp. 2542–2547. doi: 10.1161/01.ATV.0000190701.92007.6d.

Natesan, S. *et al.* (2011) 'Debrided skin as a source of autologous stem cells for wound repair', *Stem Cells*, 29(8), pp. 1219–1230. doi: 10.1002/stem.677.

National Burn Care Review Committee (2001) 'Standards and Strategy for Burn Care', *National Burn Care Review*, pp. 1–82. Available at: http://www.britishburnassociation.org/downloads/NBCR2001.pdf.

National Library of Medicien (2020) *Clini*. Available at: https://www.clinicaltrials.gov/ct2/home (Accessed: 21 March 2020).

Nishimura, S. *et al.* (2007) 'Adipogenesis in Obesity Requires Close Interplay', *Diabetes*, 56(June), pp. 1517–1526. doi: 10.2337/db06-1749.Additional.

Nomi, M. *et al.* (2002) 'Principals of neovascularization for tissue engineering', *Molecular Aspects of Medicine*, 23(6), pp. 463–483. doi: 10.1016/S0098-2997(02)00008-0.

Noverina, R. *et al.* (2019) 'Growth factors profile in conditioned medium human adipose tissue-derived mesenchymal stem cells (CM-hATMSCs)', *Clinical Nutrition Experimental*, 24, pp. 34–

44. doi: 10.1016/j.yclnex.2019.01.002.

Nowak-Sliwinska, P. *et al.* (2018) *Consensus guidelines for the use and interpretation of angiogenesis assays*, *Angiogenesis*. Springer Netherlands. doi: 10.1007/s10456-018-9613-x.

Omega Bio-Tek (2019) 'EZNA Tissue DNA Kit Quick Guide'. Omega Bio-Tek, pp. 1–32.

Opneja, A., Kapoor, S. and Stavrou, E. X. (2019) 'Contribution of platelets, the coagulation and fibrinolytic systems to cutaneous wound healing', *Thrombosis Research*, 179(March), pp. 56–63. doi: 10.1016/j.thromres.2019.05.001.

Padgett, M. E. *et al.* (2016) 'Methods for Acute and Subacute Murine Hindlimb Ischemia', *Journal of Visualized Experiments*, (112), pp. 1–8. doi: 10.3791/54166.

Papuga, A. Y. and Lukash, L. L. (2015) 'Different types of biotechnological wound coverages created with the application of alive human cells', *Biopolymers and Cell*, 31(2), pp. 83–96. doi: 10.7124/bc.0008D1.

Paradis, M. E. *et al.* (2006) 'Visceral adiposity and endothelial lipase', *Journal of Clinical Endocrinology and Metabolism*, 91(9), pp. 3538–3543. doi: 10.1210/jc.2006-0766.

Park, I. N. S. U. *et al.* (2013) 'Endothelial Differentiation and Vasculogenesis Induced by Three- Dimensional Adipose-Derived Stem Cells', *The Anatomical Record*, 296(August 2012), pp. 168–177. doi: 10.1002/ar.22606.

Pawitan, J. A. (2014) 'Prospect of Stem Cell Conditioned Medium in', *BioMed Research International*, 2014, pp. 1–14. doi: 10.1155/2014/965849.

Pill, K. *et al.* (2015) 'Vascularization mediated by mesenchymal stem cells from bone marrow and adipose tissue: A comparison', *Cell Regeneration*, 4(8). doi: 10.1186/s13619-015-0025-8.

Polzer, H. *et al.* (2014) 'Comparison of Different Strategies for In Vivo Seeding of Prevascularized Scaffolds', *Tissue Engineering Part C*, 20(1), pp. 11–18. doi: 10.1089/ten.tec.2012.0740.

Preisner, F. *et al.* (2017) 'Impact of Human Adipose Tissue-Derived Stem Cells on Malignant Melanoma Cells in An In Vitro Co-culture Model', *Stem Cell Reviews and Reports*. doi: 10.1007/s12015-017-9772-y.

PromoCell (2017) *The Right Choice of Endothelial Cells for Your Vascular Research*. Available at: https://www.promocell.com/cells-in-action/endothelial-cells-for-vascular-research/ (Accessed: 26 March 2020).

Pu, C. M. *et al.* (2017) 'Adipose-Derived Stem Cells Protect Skin Flaps against Ischemia/Reperfusion Injury via IL-6 Expression', *Journal of Investigative Dermatology*, 137(6), pp. 1353–1362. doi: 10.1016/j.jid.2016.12.030.

Rambold, A. S., Cohen, S. and Lippincott-Schwartz, J. (2015) 'Fatty acid trafficking in starved cells: regulation by lipid droplet lipolysis, autophagy and mitochondrial fusion dynamics', *HHS Public Access*, 176(6), pp. 678–692. doi: 10.1016/j.devcel.2015.01.029.

Ribatti, D. *et al.* (2001) 'Postnatal vasculogenesis', *Mechanisms of Development*, 100(2), pp. 157–163. doi: 10.1016/S0925-4773(00)00522-0.

Richardson, T. P. *et al.* (2001) 'Polymeric system for dual growth factor delivery', *Nature Biotechnology*, 19, pp. 1029–1034.

Riss, T. L. *et al.* (2004) 'Cell Viability Assays', *Assay Guidance Manual*, (Md), pp. 1–25. Available at: http://www.ncbi.nlm.nih.gov/pubmed/23805433.

Rojas-Rodriguez, R. *et al.* (2014) 'Adipose Tissue Angiogenesis Assay Raziel', *Methods Enzymol*, 537. doi: 10.1002/jcp.24872.The.

Roman, S. *et al.* (2014) 'Developing a Tissue Engineered Repair Material for Treatment of Stress Urinary Incontinence and Pelvic Organ Prolapse—Which Cell Source?', *Neurourology and Urodynamics*, 33, pp. 531–537. doi: 10.1002/nau.

Rouwkema, J., Rivron, N. C. and van Blitterswijk, C. A. (2008) 'Vascularization in tissue engineering', *Trends in Biotechnology*, 26(8), pp. 434–441. doi: 10.1016/j.tibtech.2008.04.009.

Rowan, M. P. *et al.* (2015) 'Burn wound healing and treatment : review and advancements', *Critical Care*, pp. 1–12. doi: 10.1186/s13054-015-0961-2.

Russo, J. *et al.* (2014) 'Methodology for Studying the Compartments of the Human Breast. In: Techniques and Methodological Approaches in Breast Cancer Research.' doi: https://doi.org/10.1007/978-1-4939-0718-2_3.

Sagaradze, G. *et al.* (2019) 'Conditioned medium from human mesenchymal stromal cells: Towards the clinical translation', *International Journal of Molecular Sciences*, 20(7), pp. 1–16. doi: 10.3390/ijms20071656.

Segura, I. *et al.* (2017) 'Inhibition of programmed cell death impairs in vitro vascular-like structure formation and reduces in vivo angiogenesis', *The FASEB Journal*, 16(8), pp. 833–841. doi: 10.1096/fj.01-0819com.

Sen, C. K. *et al.* (2010) 'Health and the Economy', 17(6), pp. 763–771. doi: 10.1111/j.1524-475X.2009.00543.x.Human.

Seo, D.-W. *et al.* (2003) 'TIMP-2 Mediated Inhibition of Angiogenesis: An MMP-Independent Mechanism', *Cell Press*, 114, pp. 171–180. doi: 10.1517/14712598.5.3.359.

Sesé, B. *et al.* (2019) 'Nanofat Cell Aggregates: A Near Constitutive Stromal Cell Inoculum For Regenerative Site-Specific Therapies', *Plastic and Rreconstructive Surgery*. doi: 10.1097/PRS.0000000000006155.

Shafaat, S. *et al.* (2018) 'Demonstration of improved tissue integration and angiogenesis with an elastic, estradiol releasing polyurethane material designed for use in pelvic floor repair', *Neurourology and Urodynamics*, 37, pp. 716–725. doi: 10.1002/nau.23510.

Shepherd, B. R. *et al.* (2006) 'Vascularization and engraftment of a human skin substitute using circulating progenitor cell-derived endothelial cells', *The FASEB Journal*, 20(10), pp. 1739–1741. doi: 10.1096/fj.05-5682fje.

Shukla, L., Morrison, W. A. and Shayan, R. (2015) 'Adipose-derived stem cells in radiotherapy injury : a new frontier', *Frontiers in Surgery*, 2(January), pp. 10–13. doi: 10.3389/fsurg.2015.00001.

Spiekman, M. *et al.* (2017) 'The power of fat and its adipose-derived stromal cells: emerging concepts for fibrotic scar treatment', *Tissue Engineering and Regenerative Medicine*, pp. 1–16. doi: 10.1002/term.2213.

Staton, C. A. *et al.* (2004) 'Current methods for assaying angiogenesis in vitro and in vivo', *International Journal of Experimental Pathology*, 85, pp. 233–248. doi: 10.1111/j.0959-9673.2004.00396.x.

Stratman, A. N. *et al.* (2009) 'Endothelial cell lumen and vascular guidance tunnel formation requires MT1-MMP-dependent proteolysis in 3-dimensional collagen matrices', *Blood*, 114(2), pp. 237–247. doi: 10.1182/blood-2008-12-196451.

Sukho, P. *et al.* (2017) 'Effect of Cell Seeding Density and Inflammatory Cytokines on Adipose Tissue-Derived Stem Cells: an in Vitro Study', *Stem Cell Reviews and Reports*, 13(2), pp. 267–277. doi: 10.1007/s12015-017-9719-3.

Sun, M. *et al.* (2017) 'Adipose Extracellular Matrix/Stromal Vascular Fraction Gel Secretes Angiogenic Factors and Enhances Skin Wound Healing in a Murine Model', *BioMed Research International*, 2017. doi: 10.1155/2017/3105780.

Tahergorabi, Z. and Khazaei, M. (2012) 'A review on angiogenesis and its assays', *Iranian Journal of Basic Medical Sciences*, 15(6), pp. 1110–1126. doi: 10.3791/51766.

Targett-Adams, P. *et al.* (2003) 'Live cell analysis and targeting of the lipid droplet-binding adipocyte differentiation-related protein', *Journal of Biological Chemistry*, 278(18), pp. 15998–16007. doi: 10.1074/jbc.M211289200.

Tat, C. N. *et al.* (2015) 'Comparison of invasion by human microvascular endothelial cell lines in response to vascular endothelial growth factor (VEGF) and basic fibroblast growth factor (bFGF) in a three-dimensional (3D) cell culture system', *3D Endothelial Cultures Systems*, 37(3), pp. 219–225.

The Regenerative Stem Cell Institute (2017) *STROMAL VASCULAR FRACTION CELL PROCEDURE*. Available at: https://stemcelldr.com/the-svf-procedure/.

Tiryaki, T., Findikli, N. and Tiryaki, D. (2011) 'Staged stem cell-enriched tissue (SET) injections for soft tissue augmentation in hostile recipient areas: A preliminary report', *Aesthetic Plastic Surgery*. doi: 10.1007/s00266-011-9716-x.

Tissue), (Advanced (2018) *Open Wound 101: Understanding the Types and Treatments*. Available at: https://advancedtissue.com/2018/09/open-wound-101-understanding-the-types-and-treatments/ (Accessed: 17 June 2019).

Tobita, M., Orbay, H. and Mizuno, H. (2011) 'Adipose-derived Stem Cells : Current Findings and Future', *Discovery Medicine*, 5, pp. 1–20.

Tomaszewski, C. E. *et al.* (2019) 'Adipose-derived stem cell-secreted factors promote early stage follicle development in a biomimetic matrix', *Biomaterials Science*, 7(2), pp. 571–580.

doi: 10.1039/c8bm01253a.

Tonnard, P. *et al.* (2013) 'Nanofat Grafting: Basic Research and Clinical Applications', *Plastic and Reconstructive Surgery*, 132(4), pp. 1017–1026. doi: 10.1097/prs.0b013e31829fe1b0.

Tsuji, W., Rubin, J. P. and Marra, K. G. (2014) 'Adipose-derived stem cells: Implications in tissue regeneration.', *World journal of stem cells*, 6(3), pp. 312–21. doi: 10.4252/wjsc.v6.i3.312.

Unger, R. E. *et al.* (2002) 'In vitro expression of the endothelial phenotype: Comparative study of primary isolated cells and cell lines, including the novel cell line HPMEC-ST1.6R', *Microvascular Research*, 64(3), pp. 384–397. doi: 10.1006/mvre.2002.2434.

Volz, A. C., Huber, B. and Kluger, P. J. (2016) 'Adipose-derived stem cell differentiation as a basic tool for vascularized adipose tissue engineering', *Differentiation*, 92, pp. 52–64. doi: 10.1016/j.diff.2016.02.003.

Wittmann, K. *et al.* (2015) 'Engineering Vascularized Adipose Tissue Using the Stromal-Vascular Fraction and Fibrin Hydrogels', *Tissue Engineering: Part A*, 21(7–8), pp. 1343–1353. doi: 10.1089/ten.tea.2014.0299.

Wood, S., Bellis, M. A. and Atherton, J. (2010) *Burns, a review of evidence for prevention*. Liverpool.

Wu, Y.-C. *et al.* (2019) 'Differential Response of Non-cancerous and Malignant Breast Cancer Cells to Conditioned Medium of Adipose tissue-derived Stromal Cells (ASCs)', *International Journal of Medical Sciences*, 16(6), pp. 893–901. doi: 10.7150/ijms.27125.

Xie, H. *et al.* (2018) '3D- cultured adipose tissue-derived stem cells inhibit liver cancer cell migration and invasion through suppressing epithelial-mesenchymal transition', *International Journal of Molecular Medicine*, 41, pp. 1385–1396. doi: 10.3892/ijmm.2017.3336.

Xu, P. *et al.* (2018) 'Nanofat Increases Dermis Thickness and Neovascularization in Photoaged Nude Mouse Skin', *Aesthetic Plastic Surgery*, 42(2), pp. 343–351. doi: 10.1007/s00266-018-1091-4.

Xu, Y. *et al.* (2016) 'The Comparison of Adipose Stem Cell and Placental Stem Cell in Secretion Characteristics and in Facial Antiaging', *Stem Cells International*, 2016. doi: 10.1155/2016/7315830.

Xue, L. and Greisler, H. P. (2002) 'Angiogenic effect of fibroblast growth factor-1 and vascular endothelial growth factor and their synergism in a novel in vitro quantitative fibrin-based 3-dimensional angiogenesis system', *Surgery*, 132(2), pp. 259–267. doi: 10.1067/msy.2002.125720.

Yang, S. *et al.* (2015) 'Oriented cell division: new roles in guiding skin wound repair and regeneration', *Bioscience Reports*, 35(6), pp. 1–11. doi: 10.1042/bsr20150225.

Yao, Y. *et al.* (2017) 'Adipose Extracellular Matrix/Stromal Vascular Fraction Gel: A Novel Adipose Tissue-Derived Injectable for Stem Cell Therapy', *Plastic and Reconstructive Surgery*, 139(4), pp. 867–879. doi: 10.1097/PRS.0000000000003214.

Yoshimura, K., Sato, K., Aoi, N., Kurita, M., Hirohi, T., *et al.* (2008) 'Cell-assisted lipotransfer for cosmetic breast augmentation: Supportive use of adipose-derived stem/stromal cells', *Aesthetic Plastic Surgery*, 32(1), pp. 48–55. doi: 10.1007/s00266-007-9019-4.

Yoshimura, K., Sato, K., Aoi, N., Kurita, M., Inoue, K., *et al.* (2008) 'Cell-assisted lipotransfer for facial lipoatrophy: Efficacy of clinical use of adipose-derived stem cells', *Dermatologic Surgery*, 34(9), pp. 1178–1185. doi: 10.1111/j.1524-4725.2008.34256.x.

Yu, Z. *et al.* (2018) 'Fat extract promotes angiogenesis in a murine model of limb ischemia: a novel cell-free therapeutic strategy', *Stem cell research & therapy*, 9(1), p. 294. doi: 10.1186/s13287-018-1014-y.

Zakhari, J. S. *et al.* (2018) 'Vasculogenic and angiogenic potential of adipose stromal vascular fraction cell populations in vitro', *In Vitro Cellular and Developmental Biology - Animal*, 54(1), pp. 32–40. doi: 10.1007/s11626-017-0213-7.

Zhang, G. and Suggs, L. J. (2007) 'Matrices and scaffolds for drug delivery in vascular tissue engineering', *Advanced Drug Delivery Reviews*, 59, pp. 360–373. doi: 10.1016/j.addr.2007.03.018.

Zhang, Y. *et al.* (2018) 'Improved Long-term Volume Retention of SVF-gel Grafting with Enhanced Angiogenesis and Adipogenesis', *Plastic and Reconstructive Surgery*. doi: 10.1097/PRS.0000000000004312.